THE INFLUENCE OF EXTRACELLULAR–ORIGINATING SIGNALS ON THE mTOR/mTORC1 SIGNALLING PATHWAY TO AUTOPHAGY INDUCTION IN HOSCC

Ari Nathan Nerwich

A dissertation submitted to the Faculty of Science, University of the Witwatersrand, Johannesburg, in fulfilment of the requirements for the degree of Master of Science.

Johannesburg, 2012

DECLARATION

I declare that this dissertation is my own, unaided work. It is being submitted for the Degree of Master of Science at the University of the Witwatersrand, Johannesburg. It has not been submitted before for any degree or examination at any other university.

Ari Nathan Nerwich

28th day of September 2012 in Johannesburg

"...the key to every biological problem must finally be sought in the cell, for every living organism is, or at sometime has been, a cell."

Edmund B. Wilson

The Cell in Development and Heredity

ABSTRACT

Cell-extracellular matrix (ECM) detachment triggers a cell survival mechanism known as autophagy. A link between attachment and autophagy suggests a form of adhesion-based regulation, involving mechanotransduction of extracellular-originating signals to the cellular machinery controlling autophagy induction. This implies a role for integrin-linked kinase (ILK), which transmits mechanical stimuli to the mammalian target of rapamycin (mTOR) signalling pathway. Cells with a propensity for metastasis may negate these adhesive signals, inducing autophagy inappropriately. Metastasis is a hallmark of transformation frequently associated with human oesophageal squamous cell carcinoma (HOSCC). Additionally, hyperactive mTOR/mTORC1 signalling correlates increasingly with HOSCC. Therefore, the protein expression of significant signal transduction pathway intermediates was investigated in response to both soluble and ECM-originating stimuli. Measurements by SDS-PAGE and western-blotting coupled to semi-quantitative densitometry, during standard tissue culture conditions, revealed that HOSCC's expressed moderate-to-high levels of mTOR, p-RPS6$^{(Ser\ 235/236)}$ and mATG-13; indicating elevated levels of autophagy induction despite aberrant signalling through mTOR/mTORC1. Additionally, an 80 kDa mTORβ isoform was identified in HOSCC cells with lower mTOR abundance, presumably to maintain aberrant mTORC1 signalling. A canonical role for the PI3K/PKB pathway was also identified; where autophagy induction accompanied diminished mTORC1 signalling in response to specific PI3K inhibition with LY294002 and serum withdrawal. However, autophagy induction varied in response to a dose-dependent decrease in mTORC1 signalling after exposure of HOSCC cells to rapamycin. Moreover, specific inhibition of p90RSK with BI-D1870, suggests that mTORC1 phosphorylates RPS6$^{(Ser\ 235/236)}$ in the absence of MAPK signals. Furthermore, ectopic ILK expression indicated an enhanced potential for adhesion-based signalling. Correspondingly, HOSCC cells commonly increased mTOR and p-RPS6$^{(Ser\ 235/236)}$ expression following growth on fibronectin or collagen. However, co-immunoprecipitation analysis revealed that signals transduction to mTOR precludes a direct interaction with ILK or FAK. Rather, ECM-modulation of mTOR occurs in a integrin-triggered, but PI3K-depedant manner; since specific inhibition of PI3K negated fibronectin-induced increases of mTOR concentration and RPS6$^{(Ser\ 235/236)}$ phosphorylation. Thus, these data strongly suggest mTOR is a target for adhesion-based signal transduction, where the ECM influences cell survival through mTORC1. Moreover, exploitation of autophagy induction post cell-ECM detachment in HOSCC may promote the survival of metastases during dissemination.

LIST OF ASSOCIATED PUBLICATIONS AND PRESENTATIONS

Original Publications

"Nerwich, A. N. and Veale, R. B. (2012) The mammalian target of rapamycin (mTOR) is a target for adhesion-based signal transduction, and influences autophagy induction through mTORC1 in a PI3K-dependant manner in HOSCC." In preparation for submission to *Cell Biology International*.

Local Conferences

Nerwich, A.N. and Veale, R.B. The Influence of Extracellular-originating Signals on the mTOR/mTORC1 Signalling Pathway to Autohagy Induction in HOSCC. Accepted for poster presentation at the 4th Cross-Faculty Graduate Symposium, University of the Witwatersrand, Johannesburg, 19 – 22 October 2012.

Nerwich, A.N. and Veale, R.B. ILK Modulation of the mTOR Signalling Pathway in HOSCC. Accepted for poster presentation at the *SASBMB-FASBMB XXVIth* Congress, Drakensburg. 29 January – 1 February 2012.

Nerwich, A.N. and Veale, R.B. ILK Modulation of the mTOR Signalling Pathway in HOSCC. Accepted for oral presentation at the Molecular Biosciences Research Thrust (MBRT) Research Day, WITS Personal Development Hub (WPDH), University of the Witwatersrand, Johannesburg, 7th December 2011.

ACKNOWLEDGEMENTS

I am greatly indebted towards the following people who helped me complete this Masters Research dissertation. First and foremost, I am grateful to my supervisor, Professor Rob Veale. Without his help, constructive criticism, creative input and sense of humour, this research would never have been achieved. I am sincerely appreciative and thankful for all your time, effort and enthusiasm.

Many thanks is owed to Mrs Elsabé Scott for ensuring that there was always a regular supply of cells, antibodies and reagents, as well as for teaching me the finésse of mammalian tissue culture. Thank you for all your assistance.

It is not possible to express the proper amount of thanks owed to my colleagues in the Cell Biology Research Laboratory – Nicolene Shaw, Yael Dahan, Stephanie Fanucchi, Sandile Buthulezi and Megan Kilroy. Without their help, understanding and support I would surely have struggled endlessly. Please know that all your help is greatly appreciated.

A special mention must also be made to my family. To my mother and father, Rolene and Raymond, thank you for the opportunity to study this far, catering to my every need and putting up with my ever-changing moods. Also, to my brothers, David and Gidon, thank you for all your support and kindness during these years of study.

Gratitude is also owed to Dr Sharoon Tooze, from Cancer Research UK (CRUK), for your gift of the mATG-13 antibody. Your contribution is very much appreciated and has contributed greatly to this work. Also, mention must be made to Dr James Hastie, from the Division of Signal Transduction Therapy at the University of Dundee. Thank you for your prompt correspondence and advice in dealing with the p90RSK-specific inhibitor BI-D1870.

I would also like to acknowledge the University of the Witwatersrand for the Postgraduate Merit Award (PMA) and Postgraduate Merit Scholarship Award (PMSA), the National Research Foundation (NRF) Prestigious and Equity Scholarship and ISOE/FoodBev-SETA Bursary for Unemployed Learners for all financial support. Without your funding this research would not have been possible.

TABLE OF CONTENTS

LIST OF FIGURES

LIST OF TABLES

LIST OF ABBREVIATIONS AND SYMBOLS

4E-BP1:	eIF4E binding protein 1
α:	Alpha
AMPK:	Mammalian adenosine monophosphate–activated protein kinase
ANK:	Ankyrin repeat
APS:	Ammonium persulphate
ATCC:	American Type Tissue Collection
ATG:	Autophagy-related gene product
ATP:	Adenosine triphosphate
β:	Beta
Bcl-2:	B cell lymphoma-2
BRRS:	Bannayan-Riley-Ruvalcaba syndrome
BSA:	Bovine serum albumin
CK 5/6:	Casein kinase 5 or 6
CN:	Collagen
Co-IP	Co-Immunoprecipitation analysis
COSMIC:	Catalogue for Somatic Mutations in Cancer
COx:	Carcinoma of the oesophagus (where x designates a particular cell line)
Cvt:	Cytoplasm-to-vacuole targeting
Deptor:	DEPDC6, DEP domain-containing protein 6
dH_2O:	Distilled water
DMEM:	Dulbecco's Modified Eagles Medium
DMSO:	Dimethyl sulfoxide
DNA:	Deoxyribonucleic acid
ECM:	Extracellular matrix

EDTA:	Ethylenediaminetetra-acetic acid
EGFR:	Epidermal growth factor receptor
eIF4E:	Eukaryotic translation initiation factor 4E
ERK:	Extracellular-signal regulated kinase
ESCC:	Esophageal squamous cell carcinoma (of Chinese origin)
Fab-region:	Fragment antigen-binding region
FAK:	Focal adhesion kinase
FAT:	Focal adhesion targeting (FAK-specific domain)
FAT:	FRAP, ATM, and TRRAP
FATC:	FAT carboxyterminal domain
Fc-region:	Fragment crystallizable region
FCS:	Foetal calf serum
FERM:	Erythrocyte band four.1exrin-radixin-moesin
FIP200:	Focal adhesion kinase family interacting protein of 200 kDa
FKBP12:	FK506 binding protein 1A of 12 kDa
FN:	Fibronectin
FRB:	FKBP12-rapamycin binding domain
GAP:	GTPase-activating protein
GPCR:	G-protein coupled receptors
GSK-3β:	Glycogen synthase kinase-3β
GTPase:	Enzyme capable of hydrolyzing guanidine triphosphate
HOSCC:	Human oesophageal squamous cell carcinoma
hr:	Hour
HRP:	Horseradish peroxidise
IB:	Immunoblot

iBMK:	Immortalized baby mouse kidney epithelial
ILK:	Integrin-linked kinase
IOD:	Integrated optical density
IP buffer:	Immunoprecipitation buffer
JNK:	c-Jun NH2-terminal kinase
kDa:	Kilodalton
LAM:	Lymphangioleiomyomatosis
LLB:	Laemmli double lysis buffer
MAPK:	Mitogen activated protein kinase
MAPKK:	Mitogen-activated protein kinase kinase
MAPKKK:	Mitogen-activated protein kinase kinase kinase
mATG-13:	Mammalian autophagy-related gene-13
MEKK:	MAP/ERK kinase kinase
min:	Minute/s
mLST8:	G-protein β-subunit-like protein, GβL (yeast homolog of LST8)
mSin1:	Mammalian stress-activated protein kinase interacting protein 1
mTOR:	Mammalian target of rapamycin
mTORC1:	mTOR-containing multi-protein complex 1
mTORC2:	mTOR-containing multi-protein complex 2
MWM:	Molecular weight marker
nM:	Nanomolar
NRP:	Normal renal parenchyma
p70S6K:	70 kDa ribosomal protein S6 kinase
p90RSK:	90 kDa ribosomal protein S6 kinase
PAGE:	Polyacrylamide gel electrophoresis

PARP:	Poly (ADP-ribose) polymerase
PBS:	Phosphate buffered saline
PCD Type-I:	Programmed cell death type-I
PCD Type-II:	Programmed cell death type-II
PDB:	Protein Data Bank
PH:	Pleckstrin homology
PI3K:	Phosphatidylinositol-3-kinase
PKB:	Protein kinase B
PKC:	Protein kinase C
PMSF:	Phenyl-methyl-sulphonyl fluoride
PP2C:	Protein phosphatase 2C
p-PBK$^{Ser\ 308}$:	Ser 308 phosphorylation of PKB
p-PBK$^{Ser\ 473}$:	Ser473 phosphorylation of PKB
PRAS40:	Proline-rich Akt substrate of 40 kDa
PRCC:	Primary renal cell carcinomas
p-RSP6$^{(Ser\ 235/236)}$:	Phosphorylation of Serine residues 235 and 236 of Ribosomal protein subunit 6
PTEN:	Phosphatase and tensin homologue deleted on chromosome
Rac:	A sub-family of the Rho GTPase
RAF:	A family of proto-oncogene serine/threonine-protein kinases
RagGTPase:	Ras homologue-related GTP-binding protein kinase
Raptor:	Regulatory associated protein of mTOR
RAS:	A protein family comprising small GTPases
RCSB:	Research Collaboratory for Structural Bioinformatics
Rheb:	Ras homologue enriched in brain

Rho:	Small family of GTPases belonging to the *Rho* subclass
Rictor:	Rapamycin insensitive companion of mTOR
RIPA:	Radioimmunoprecipitation assay
ROS:	Reactive oxygen species
RTKs:	Receptor tyrosine kinases
SCC:	Squamous cell carcinoma
SDS:	Sodium dodecyl sulphate
Ser:	Serine
SH2:	Src homology domain 2
T/E:	A mixture of Trypsin and EDTA
TBS:	Tris buffered saline
TCA:	Trichloroacetic acid
TEMED:	N,N,N',N'-Tetramethylethylenediamine
Thr:	Threonine
Tris:	Tris(hydroxymethyl)aminomethane
TSC1 and 2:	Tuberous Sclerosis Complex 1 and 2
μM:	Micromolar
ULK1:	UNC-51-like kinase
WHCO:	Wits Human Carcinoma of the Oesophagus

CHAPTER 1

1. GENERAL INTRODUCTION AND LITERATURE REVIEW

1.1. Regulation of intracellular communication at the cell-ECM interface

During development, highly coordinated signalling events guide the formation of coherent epithelial sheets into a functional, adult epithelium (Gumbiner, 1996). When the adult epithelium is formed properly, developmental signals are 'switched off' and morphogenetic information is no longer supplied (Gumbiner, 1996). The adult epithelium now conforms to a biologically-relevant structure that experiences different types of extracellular signalling events within all cell layers (Mammoto and Ingber, 2010). These new signals directly contribute towards the maintenance of tissue integrity, and therefore homeostasis.

Currently, extracellular-originating signals may influence tissue homeostasis through two known mechanisms (Asthagiri and Lauffenbburger, 2000; Mammoto and Ingber, 2010). The first mode is biochemical in origin; where signals are elicited in response to specialised cell membrane receptors that associate with soluble, cognate ligands; such as amino-acids, hormones and growth factors (Brunton *et al.*, 2004; Groves and Kuriyan, 2010). The second mode is mechanically-derived and rather involves signals elicited in response to a cell encountering a solid, matrix-like environment (Gao *et al.*, 2006; Mammoto and Ingber, 2010). Although these stimuli originate from different sources, the appropriate regulation of both types of signals is essential for the maintenance of healthy epithelial tissue.

A popular approach to addressing the basis to tumour development is to view it as a change in the molecular mechanisms regulating cell proliferation and survival signalling (Gray *et al.*, 2010; Hanahan and Weinberg, 2011). These mechanisms are seen to involve a corruption in sensing and transmitting the above stimuli. Since these signals are both numerous and varied, of particular interest to us is the influence of the immediate cellular environment on these signals, i.e. signals elicited from mechanical sources in response to cell-extracellular matrix (ECM) attachment. Adhesion-based signalling in this manner has been found to support inappropriate proliferative events; for example the aberrant activation of cell adhesion molecules (such as those forming part of the integrin adhesion system) are reported to delay

apoptotic cell death in squamous cell carcinoma (SCC) of the human oesophagus, allowing tumours to evade tissue-dependant survival restraints (Fanucchi and Veale, 2011). However, what remains to be understood in this regard is the influence of adhesion-based stimuli on a cellular process closely related to proliferation; such as the evolutionary conserved cell survival pathway known as autophagy (Meijer and Codogno, 2004).

In response to extensive biochemical and mechanical stimuli, epithelial cells may often utilize autophagy as a rehabilitation strategy (Cecconi and Levine, 2008; Eisenberg-Lerner *et al.*, 2009; Erol, 2011). Under conditions where autophagy is initiated, stressed cells are extended an opportunity for restoration before pro-death signals fully activate programmed cell death cascades, such as anoikis (Edinger and Thompson, 2004; Cecconi and Levine, 2008; Fung *et al.*, 2008; Lock and Debnath, 2008). In light of the above, we have identified major players that may contribute to epithelial transformation by dissecting the most likely route triggered by adhesion-based stimuli to the autophagy induction machinery. These include essential components of the integrin cell-extracellular matrix (ECM) adhesion system; namely integrin-linked kinase (ILK) - which is a major conduit for the transduction of adhesion-based signals (Clarke and Brugge, 1995); as well as the mammalian target of rapamycin (mTOR) signalling pathway - which is the main signal transduction pathway controlling extracellular-originating signals triggering autophagy induction (Schmelzle and Hall, 2000; Foster and Fingar, 2010). Therefore, in order to equip the reader with the relevant background and the current understanding of these cellular events, we begin with a brief discussion of the major players.

1.2. Integrin-mediated Cell-ECM Adhesion

Biochemical signal transduction is controlled by receptor tyrosine kinases (RTK's), which activate an array of intracellular protein kinase-mediated cascades. This type of signal transduction brings about a change in cell behaviour by influencing transcriptional events in the nucleus (Brunton *et al.*, 2004; Groves and Kuriyan, 2010). In contrast, mechanical signals are controlled by specialised biochemical entities forming part of the cell adhesion system (Gao *et al.*, 2006; Mammoto and Ingber, 2010). These are notably the integrins; transmembrane glycoproteins that adhere to an array of extracellular matrix (ECM) support structures and regulate cell-ECM interactions (Harburger and Calderwood, 2009). Integrins directly couple mechanical stimuli to biochemical signals through interactions with integrin-triggered protein kinases, thus influencing cell behaviour (Aplin *et al.*, 1998; Shwartz, 2001).

Clearly, both RTK's and integrin-mediated adhesion play an important role during the maintenance of homeostasis in epithelial tissue. However, while much is known concerning RTK-dependant biochemical signalling, comparatively less is known concerning the transduction of mechanical stimuli through integrins and the downstream effects on important cellular processes; such as proliferation or cell survival signalling. Moreover, understanding the impact of adhesion-based signalling schemes becomes complicated, as cells commonly integrate biochemical and mechanical signals to emphasise a particular behavioural response (Aplin *et al.*, 1998).

The integrin adhesion system is responsible for facilitating physical connections between a cell and ECM, as well as mediating the intracellular propagation of ECM-originating signals (Clark and Brugge, 1995). Structurally, integrins are heterodimeric, transmembrane glycoproteins composed of α and β subunits (Hynes, 1992; Rosales *et al.*, 1992); where each subunit possesses a protruding extracellular domain, a membrane spanning domain and a short cytoplasmic domain (Hynes, 1992; Rosales *et al.*, 1992). Integrins are capable of binding a variety of ECM proteins; for example fibronectin, collagen, laminin and vitronectin (Aplin *et al.*, 1998). This is a consequence of their immense ligand-binding ability, resulting from the numerous permutations possible between α and β integrin pairs (Aplin *et al.*, 1998).

The short cytoplasmic domains of α and β integrins do not possess any innate enzymatic activity (Harburger and Calderwood, 2009). Rather, they associate with a vast array of intracellular proteins that include both cytoskeletal and structurally-related components, and catalytic signalling proteins (Clark and Brugge, 1995). Structural proteins, such as α-catenin, talin, vinculin and tensin, commonly congregate to these sites, thereby linking integrin systems to the cytoskeleton. Additionally, co-localisation of specific protein kinases occurs; such as integrin-linked kinase (ILK), focal adhesion kinase (FAK) and phosphoinositol-3-kinase (PI3K) (Harburger and Calderwood, 2009), which are involved in signal transmission and will be discussed in more detail later in this chapter. Therefore, cytoplasmic regions of integrins are sites of multi-protein assemblies where structurally-related proteins play important roles in the stabilisation of cell adhesion, regulation of cell shape, morphology and mobility (Shwartz, 2001). The current model for integrin activation and focal adhesion formation was proposed by Legate *et al.* (2006). *Figure 1.1* on the next page visually demonstrates these important integrin structure-function relationships.

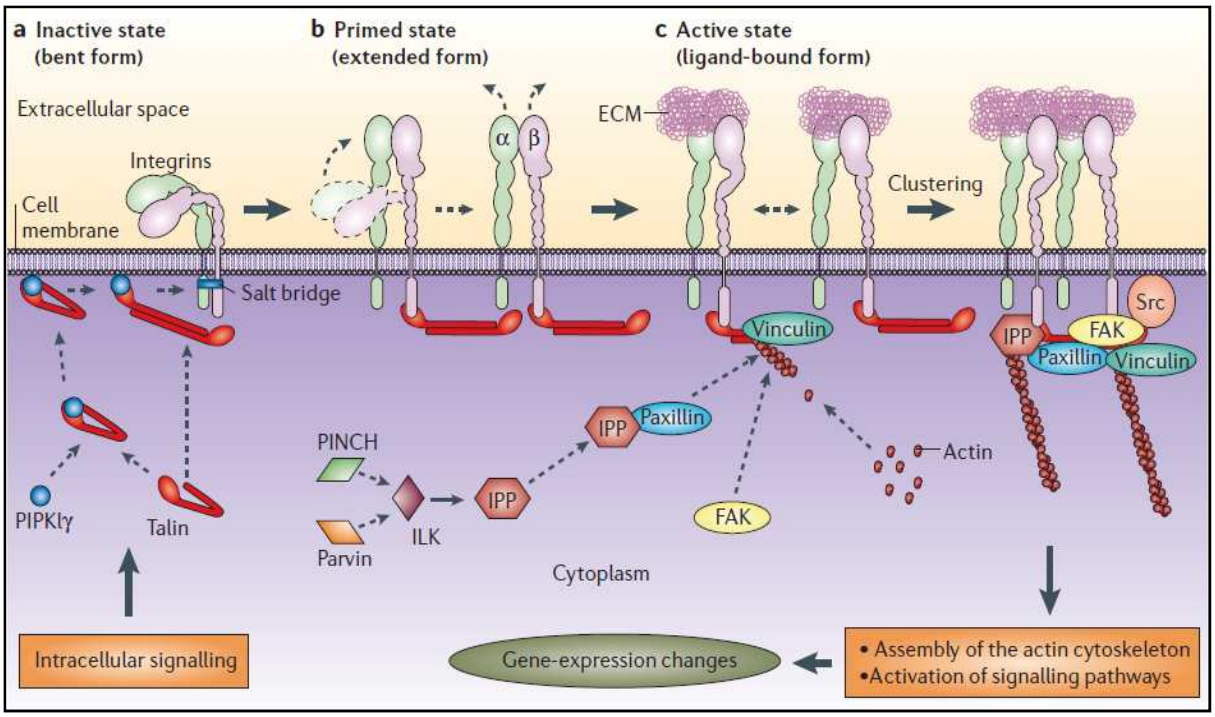

Figure 1.1: Model of integrin activation and focal adhesion formation. This schematic representation by Legate *et al.* (2006) demonstrates the molecular mechanisms pertaining to focal adhesion biogenesis upon contact with an ECM-like substrate. **(a)** When inactive, naturally occurring integrins within the cell membrane may be found in a 'bent' conformation. However, when structurally-related proteins, such as talin, are recruited to the plasma membrane, binding to cytoplasmic integrin tails occurs whereupon integrins adopt a 'primed' conformation **(b)**. Integrin extracellular domains extend and become unmasked, exposing sites with ligand-binding potential **(c)**. Depending on the integrin pair, these sites subsequently bind ECM components, inducing talin to act as a molecular platform for other focal-adhesion proteins; such as ILK, FAK, paxillin and PINCH. In this way, a fully mature focal adhesion develops and ultimately involves the clustering of numerous, ligand-interacting integrin α and β subunit pairs, which both tethers the actin cytoskeleton to the ECM and facilitates communication with related intracellular signalling pathways.

1.3. Sensing mechanical signals is necessary for the perception of the physical environment

Now that the role of integrin-mediated adhesion and signalling has been clarified, the purpose of mechanically-derived stimuli may be explored in context of the functional, adult epithelium. Under 'normal' physiological conditions, epithelial tissue functions as a biological interface protecting the internal milieus from environmental stresses (Junqueira and Carneiro, 2007; Young *et al.*, 2007). As a result, the cell layers comprising the epithelium of the gut and skin, for example, are constantly exposed to various types of physical and

chemical stimuli that may cause damage to the epithelium. Considering that physical and chemical damage elicit specific forms of mechanical signalling (Erol, 2011), the integrin adhesion system is primarily involved in sensing these stimuli (Jaalouk and Lammerding, 2009; Shwartz, 2010; Erol, 2011). Therefore, integrin-mediated cell adhesion allows for the intracellular propagation of these mechanical signals, which then bring about the appropriate biological response; such as the initiation of pro-death signals to destroy irreparably damaged cells, the initiation of pro-survival pathways to rehabilitate cells with reparable damage, or increase cell growth or proliferation to replace dying cells (Erol, 2011). However, a specific scheme of adhesion-based signal transduction must occur in order to trigger the correct cellular response.

1.3.1. Intracellular signal transduction of extracellular-originating stimuli

A relatively novel and exciting aspect of cell adhesion-related research is the concept of adhesion-based signalling, where conventional cell surface receptors function to intercept and relay extracellular-originating stimuli. Thus, external stimuli that are mechanical in nature may be sensed by the integrin adhesion system, and subsequently transmitted intracellularly by means of conformational changes to these receptors. These changes initiate a series of integrated signal transduction cascades that result in a change in gene expression, allowing for a regulated behavioural response (Aplin *et al.*, 1998; Shwartz, 2001).

In the past decade, an increasing amount of research has focussed on this aspect of integrin-mediated mechanotransduction. Integrins were shown to transmit biochemical signals into the cell (termed outside-in signalling), thus providing spatial information concerning the external environment, location and relative adhesive state (Harburger and Calderwood, 2009). In addition, it was discovered that integrins possess the ability to self-regulate affinity for extracellular ligands. This occurs by means of conformational changes in their extracellular domains in response to signals that impinge on the cytoplasmic tail (termed inside-out signalling) (Harburger and Calderwood, 2009). However, both outside-in and inside-out signalling requires spatially and temporally regulated multi-protein assemblies that form around the cytoplasmic tail of integrins (Aplin *et al.*, 1998; Shwartz, 2001). Therefore, these coordinated signalling processes function to determine cellular responses; such as migration, survival and differentiation, placing inputs received from growth factors and G-protein coupled receptors into context (Harburger and Calderwood, 2009).

Analysis of the biochemical events triggered by integrin engagement, as well as by the characterisation of proteins associated with focal adhesion complexes, has allowed the identification of a plethora of signalling events activated by the integrin adhesion system (Clark and Brugge, 1995). Protein phosphorylation was one of the earliest events detected in response to integrin stimulation; where focal adhesion kinase, or FAK (*Figure 1.2*, *A*), was identified as a phosphorylation-regulated signalling scaffold important for adhesion turnover, Rho-family GTPase activation, cell migration and cross-talk between growth-factor signalling and integrin adhesions (Mitra *et al.*, 2005).

Following this pattern of phosphorylation, a similar protein kinase was discovered, however, one pivotal in regulating cell adhesion, as well as anchorage-dependant growth (Persad and Dedhar, 2003). This key node vital to integrin signalling was termed integrin-linked kinase, or ILK. ILK is a 59 kDa, ubiquitously expressed serine/threonine protein kinase implicated in numerous signalling pathways; such as integrin-, growth factor- and Wnt signalling (Li *et al.*, 1999). Through a yeast two-hybrid screen, ILK was found to associate with the cytoplasmic domain of the integrin β1 subunit (Hannigan *et al.*, 1996). From this position, ILK primarily functions as a signalling scaffold at sites of integrin adhesion (Harburger and Calderwood, 2009), and ILK may therefore mediate a variety of downstream signal transduction cascades.

Structurally, ILK possesses three distinct regions, as seen in *Figure 1.2*, *B*. Four ankyrin (ANK) repeats lie at the N-terminal, a plekstrin homology (PH)-like motif and C-terminal that exhibits significant homology to other protein kinase catalytic domains (Wu and Dedhar, 2001). The ANK repeat domain of ILK allows for a variety of protein-protein interactions, where over nine binding partners have been established (Persad and Dedhar, 2003). This region also mediates interactions with Nck-2, a Src homology SH2 and SH3 domain-containing adapter protein. Nck-2 binds to a LIM domain-only adapter protein called PINCH (a cystein-rich motif first identified in *C. elegans*, *Lin-11*, *ISL-1* and *mec-3*), bridging the interaction between ILK and receptor tyrosine kinases (RTK's) (Wu and Dedhar, 2001; Persad and Dedhar, 2003).

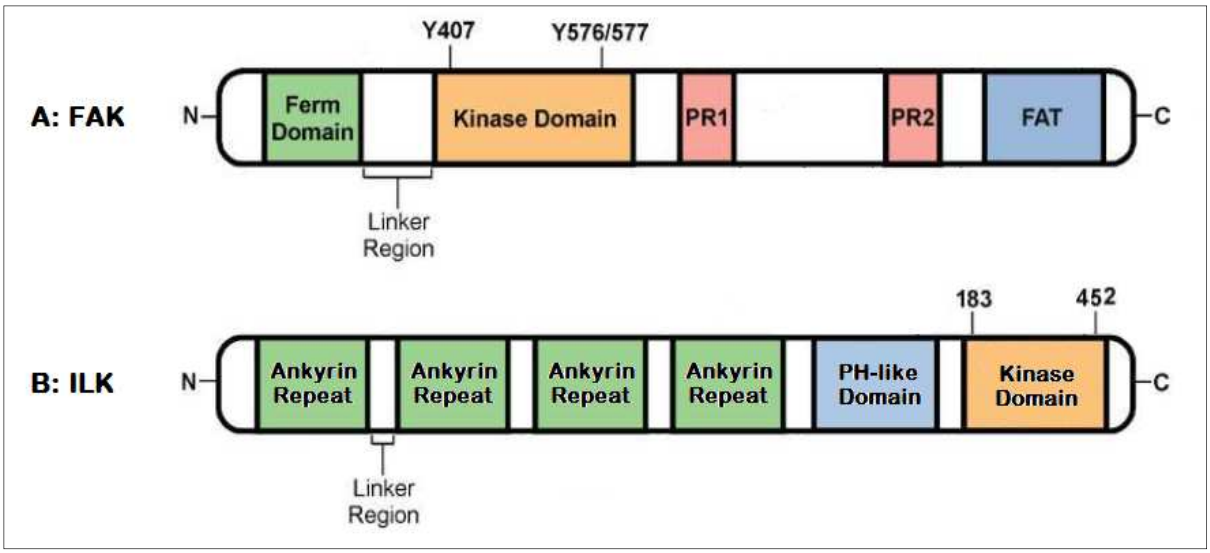

Figure 1.2: Comparative domain organization of focal adhesion kinase (FAK) and integrin-linked kinase (ILK). This schematic representation, adapted from Wu (2005) and Cox *et al.* (2006), demonstrates the relative position of functional domains in the commonly activated integrin-triggered protein kinases. FAK comprises a FERM and kinase domains towards the N-terminal as well as a FAT (or focal adhesion targeting) domain towards the C-terminus. ILK comprises an N-terminal ankyrin repeat domain, a PH-like motif and a C-terminal kinase domain. Both FAK and ILK are recruited to focal adhesions for the purposes of mechanotransduction, as well as a molecular scaffold for protein-protein interactions.

Since the functional plasticity of ILK involves both a molecular scaffold, as well as a protein kinase, ILK is capable of coupling signals captured by integrins and RTK's to downstream signalling pathways (Grashoff *et al.*, 2004). As such, ILK has been acknowledged as a component of numerous signalling pathways that control cell survival, differentiation, proliferation and gene expression in mammalian cells (Wu and Dedhar, 2001; Attwell *et al.*, 2003). A complete analysis of ILK's influence would require in depth discussion and vast detail. Therefore, to be as succinct as possible, we highlight the major roles of ILK during adhesion-based and intracellular signalling events.

1.3.2. ILK functions as a molecular conduit for adhesion-based signal transduction

ILK activity is regulated negatively by two protein phosphatases: namely PTEN and PP2C (Leung-Hagesteijn *et al.*, 2001). As a critical regulator of signal transduction, PTEN, a lipid phosphatase that dephosphorylates phosphatidylinositol-3,4,5-trisphosphate ($PI(3,4,5)P_3$) into a phosphatidylinositol-3,4-bisphosphate ($PI(3,4)P_2$) form (Morimoto *et al.*, 2000; Persad *et*

al., 2001). Interestingly, both $PI(3,4,5)P_3$ binding and ILK auto-phosphorylation are crucial for complete ILK activation, since mutations in the PH domain (Arg 211) or in the activation loop (Ser 343) render ILK inactive and unable to phosphorylate PKB; an important intracellular protein kinase (Persad *et al.*, 2001).

ILK may also associate with Raf, inducing MAPK activity in a FAK- and Ras-independant manner (Aplin *et al.*, 1998), depicted in *Figure 1.3*. In this way, ILK suppresses transcription factors required for myogenic differentiation (Huang *et al.*, 2000). Moreover, ILK interacts with members of the PI3K/PKB signalling pathway, where ILK phosphorylates $PKB^{(Ser\ 473)}$ consequently influencing cell growth and proliferation events (Wu and Dedhar, 2001). Furthermore, ILK may impinge on the Wnt signalling pathway by phosphorylating and inhibiting $GSK\text{-}3\beta^{(Ser\ 9)}$ by a similar mechanism (Persad and Dedhar, 2003). In this way, ILK may influence gene transcription (*Figure 1.3*) by stabilising the β-catenin-Tcf/Lef-1 transcription complex (Seidensticker and Behrens, 2000; Reya and Clevers, 2005). Also, a consequence of constitutive ILK activation or over-expression is the suppression of apoptosis and anoikis in mammalian cells (Attwell *et al.*, 2000; Persad *et al.*, 2000). Both of these effects involve ILK-mediated PKB activation and suppression of activated caspase-3 (Persad *et al.*, 2000). Consequently, ILK is major components of cell adhesion that facilitates mechanotransduction of extracellular-originating signals.

It is evident that signalling through integrin-triggered protein kinases, such as ILK, impacts cell behaviour. Therefore, one may gain an appreciation for the role mechanotransduction of extracellular-originating signals has on essential biological processes; such as anchorage-dependent growth, proliferation and pro-survival signalling. In light of this, it is conceivable that other important pro-survival pathways linked to the state of cell adhesion, such as autophagy (Fung *et al.*, 2008; Lock and Debnath, 2008; Chen and Debnath, 2010), may also contain an understated mechanotransduction component that has not, as of yet, been fully deciphered. Hence, a discussion concerning the mechanical regulation of pro-survival signalling and related pathways extends this idea further.

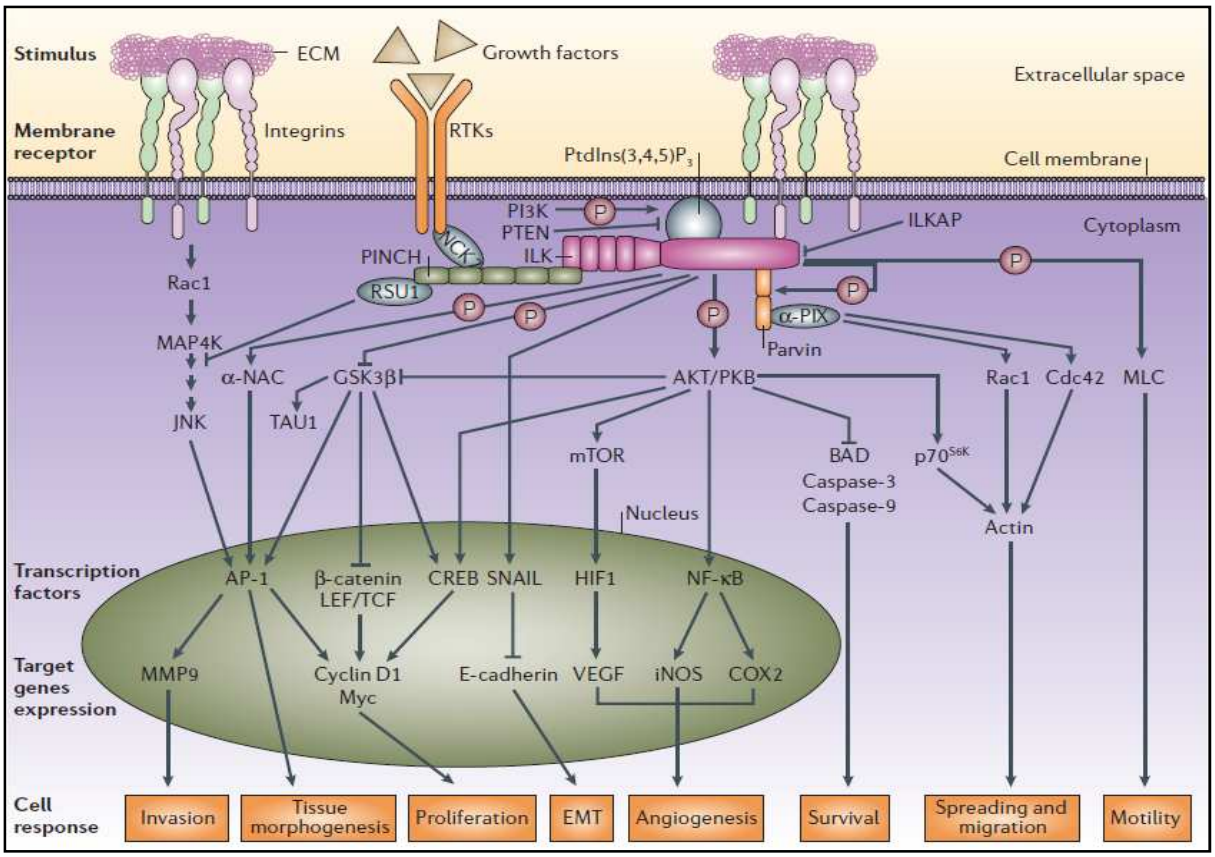

Figure 1.3: Mechanotransduction of extracellular-originating stimuli through integrin-mediated cell adhesion complexes. This model for mechanotransduction by Legate *et al.* (2006) demonstrates how extracellular-originating stimuli, derived from cell-ECM interactions, elicit intracellular signal transduction cascades that ultimately bring about a change in cell behaviour. Central to mechanotransduction is the influence of ILK; a focal adhesion-associated protein kinases that acts as a molecular conduit linking RTK and integrin receptor systems to downstream pro-survival pathways. The involvement of soluble factors eliciting biochemical signals, through RTK's, is also shown – since pathway integration is a common occurrence presumably to enhance a particular biological response.

1.4. Mechanical regulation of pro-survival signalling pathways

Autophagy serves as a catabolic strategy to recycle nutrients and provide energy for essential cellular processes during stressful environmental conditions (Cecconi and Levine, 2008; Eisenberg-Lerner *et al.*, 2009; Erol, 2011). Briefly, pro-survival signals induce the assembly of autophagosomes that sequester cytoplasmic constituents (Edinger and Thompson, 2004). However, if autophagy is allowed to continue unabated, total cell disassembly may occur (a 'so called' programmed cell death type II) (Edinger and Thompson, 2004). Consequently, if anoikis (the subset of apoptosis triggered upon loss of cell-ECM adhesion (Frisch and Francis, 1994), as well as autophagy are initiated in response to mechanically-derived stimuli,

the integrin adhesion system would be involved in sensing and relaying these signals (as discussed previously). Therefore, it follows that a molecular connection may exist between adhesion-based signalling events and the signalling machinery responsible for autophagy induction. By extension then, it is also conceivable that this relationship is somehow exploited in the transformed state to enhance tumour progression, since autophagy essentially functions as a cellular survival strategy and may be upregulated in solid tumours (Lock and Debnath, 2008).

In support of the above, seminal observations by Fung *et al.* (2008) and Lock and Debnath (2008) report that cell-ECM detachment (which usually triggers anoikis) may also trigger a concurrent anti-apoptotic signalling cascade inducing cellular autophagy. The activation of autophagy presumably delays the onset of anoikis and allows an opportunity for cell-ECM contacts to be re-established, promoting cell longevity and cell survival. Therefore, it is conceivable that a link exists between extracellular-originating signals and pro-survival signalling machinery which induces autophagy, allowing for cell survival during cell migration, necessary for migration and wound healing (Kim *et al.*, 2010). Conversely then, this link may be exploited in the tumourigenic sense, where abrogated mechanotransduction of extracellular-originating signals promotes the survival of transformed cells, thereby enhancing tumour progression, as well as the metastatic phenotype.

An example which may provide evidence for aberrant adhesion-based signalling promoting cell survival concerns a scenario where increased integrin signalling was found to promote cell survival by delaying anoikis. Enhanced activation of FAK through the β1 integrin subunit delays caspase-8 activation and subsequently promotes anoikis resistance (Fannuchi and Veale, 2011). From here we see that it is not enough for tumours to simply evade pro-death signals after cell detachment. Rather, tumours also require the co-activation of pro-survival pathways allowing for cell longevity during substrate-independent growth. Therefore, autophagy fills the criteria of a cellular processes allowing enhanced cell survival, triggered in parallel to cell death signals.

Considering the above, there is a reasonable basis to examine of the effect of extracellular-originating signals on the signalling machinery initiating cellular autophagy. In addition to constituting a novel aspect of adhesion-based signalling and autophagy-mediated cell survival research, such an examination would provide insight into a poorly understood

molecular mechanism enabling survival of detached cells during substrate-independent growth. However, it is necessary to stress that the primary focus of this investigation now shifts towards the signalling component of integrin-mediated cell-ECM interactions achieving this. Consequently, those initial signalling events (i.e. phosphorylation of autophagy-related proteins) controlling autophagy initiation – which are indicative of an activated pro-survival pathway – and not survival as a function of a completed autophagic process (i.e. autophagosome formation) is of specific concern. Therefore, it is prudent to elaborate on the mTOR signalling pathway: the foremost signal transduction pathway regulating cellular autophagy induction.

1.5. The mTOR signalling pathway is the main regulator of cellular autophagy

The mammalian target of rapamycin, commonly abbreviated mTOR, is a 220 kDa serine/threonine protein kinase belonging to the phosphatidylinositol 3-kinase (PI3K)-related kinase family (Hou *et al.*, 2007). Included in this family are other large proteins; such as ATM, ATR and DNA-dependant protein kinases, all of which possess a unique multi-domain structure (Abraham, 2004). As seen in *Figure 1.4*, towards the N-terminal are HEAT, FAT and FRB-binding domains, while the kinase, repressor and FATC domains are situated towards the C-terminal (Abraham, 2002; Fingar and Blenis, 2004). As a result of its appreciable length, mTOR exhibits extensive polypeptide folding (demonstrated in *Figure 1.5*), producing a large surface area enabling many opportunities to bind and phosphorylate downstream protein targets; such as Raptor, Rictor, p70S6K and 4EBP-1 (Sturgill and Hall, 2009).

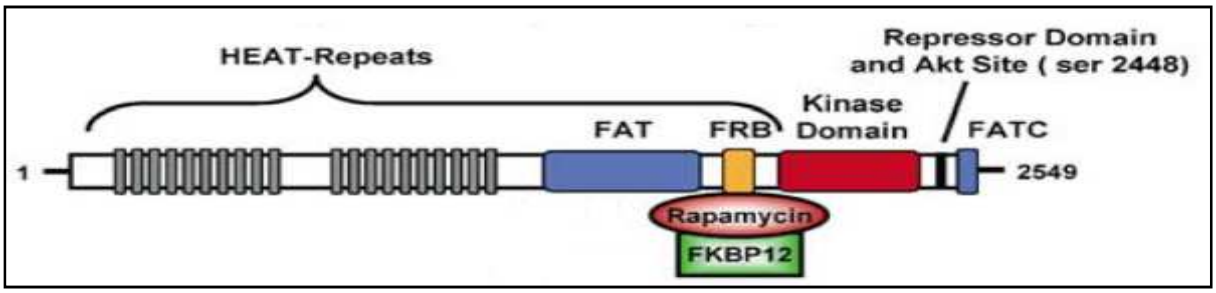

Figure 1.4: Schematic demonstrating the position of functional domains within the 220 kDa mTOR protein kinase. HEAT, FAT and FRB-binding (or rapamycin binding) domains are distributed towards the N-terminal half, while the kinase, repressor and FATC domains are situated towards the C-terminal half (adapted from Fingar and Blenis, 2004).

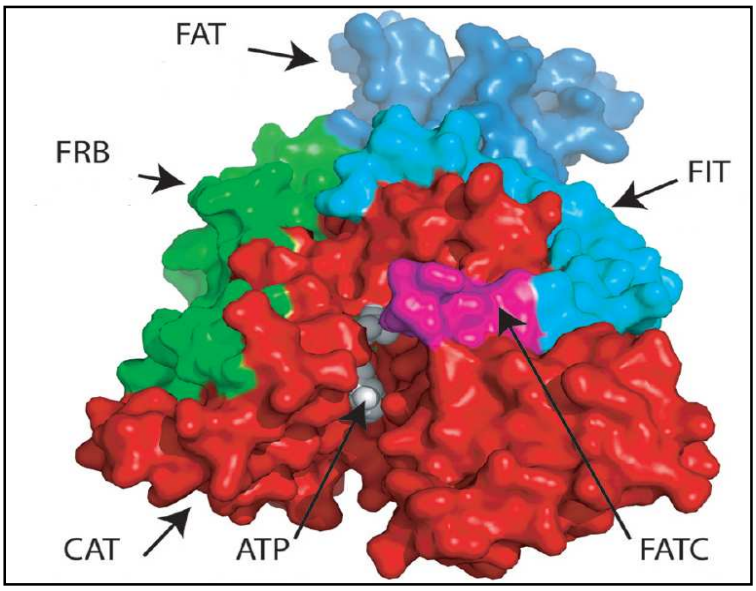

Figure 1.5: Predicted three-dimensional structure of mTOR. The three-dimensional structure of mTOR was generated by Sturgill and Hall (2009) using SWISS-MODEL software after a manual alignment of TOR with PI3KCγ (RCSB, PDB 1e8x). The model shows an inactive mTORC1 complex with ATP bound at the active site. From the model, it is evident that a large surface is available for protein interactions to occur, facilitating the inclusion of mTOR into multi-protein assemblies; such as mTORC1 and mTORC2.

In *Saccharomyces* cerevisiae and *Drosophila melanogaster* two different, but homologous, versions of the *TOR* gene are expressed: *TOR* (in yeast and *dTOR* in *Drosophila*). Subsequently, the expression of TOR forms two distinct multi-protein assemblies, with each complex possessing unique functions (Schmelzle and Hall, 2000; Caron *et al.*, 2010). In mammals however, one *mTOR* gene has been identified, which assemblies into two distinct multi-protein complexes; termed mTORC1 and mTORC2 (Fingar and Blenis, 2004). The distinction between mTORC1 and mTORC2 arises from the different protein binding partners found in each complex. The mTORC1 complex contains Raptor, mLST8, Deptor, FKBP38 and PRAS40, whereas the mTORC2 complex contains Rictor, mLST8, mSIN1, Deptor and Protor (Abraham, 2002; Zhou and Huang, 2010).

Through the action of these two complexes, mTOR is positioned at the nexus of numerous important intracellular signal transduction pathways and so ultimately controls an array of essential cellular functions. As a result of its influential position, the mTOR protein kinase has been termed a ‘master signal regulator’, ‘master switch’ and a ‘conductor of the cellular signalling symphony’ (Schmelzle and Hall, 2000; Caron *et al.*, 2010; Foster and Fingar, 2010; Dobashi *et al.*, 2011). These pseudonyms are an apt description because, to date,

mTOR is known to regulate mitochondrial metabolism, endocytosis, lipid synthesis, translation, ribosome biogenesis, nutrient uptake, cell survival, as well as autophagy (reviewed by Schmelzle and Hall, 2000; Foster and Fingar, 2010; Dobashi *et al.*, 2011).

1.5.1. mTOR regulates autophagy induction through phosphorylation of mATG-13

mTOR controls cellular autophagy through the action of mTORC1, which directly phosphorylates autophagy-related gene-13 (mATG-13 in mammals) (Hara *et al.*, 2008; Chan *et al.*, 2009; Yang and Klionsky, 2010). Phosphorylation of mATG-13 directly leads to the inhibition of autophagy induction (Hara *et al.*, 2008; Chan *et al.*, 2009). Therefore, mATG-13 is critical during autophagy initiation. When in complex with FIP200 and ULK-1, mATG-13 assembles into a 3 MDa multi-protein complex, the assembly of which signifies one of the earliest molecular events of autophagy activation (Chan *et al.*, 2009; Yang and Klionsky, 2010). It is important to note that the phosphorylation of mATG-13 by mTORC1 is an important, initial step in autophagy regulation (see *Figure 1.6*) because only mATG-13, in its dephosphorylated state, may fully initiate mature autophagosome formation (Meijer and Codogno, 2004; Hara *et al.*, 2008; Chan *et al.*, 2009; Yang and Klionsky, 2010).

The autophagic process is frequently deregulated in many cancers and is consequently implicated in supporting cancer progression (Brech *et al.*, 2009; Chen and Karantza-Wadsworth, 2009; Chen and Debnath, 2010). While deregulated autophagy may result from ectopic autophagy-related gene (ATG) expression and upstream regulators, such as PI3K, PTEN, PKB and mTOR (Brech *et al.*, 2009), aberrant integrin adhesion may also play a role considering the involvement of a potential underlying mechanical component (Fung *et al.*, 2008).

Indeed any alteration to the norm drastically affects the normal operating procedure of the integrin adhesion system. Deregulated cell adhesion and inappropriate mechanotransduction have been shown to support phenotypic transformation in epithelial tissue (Pantel *et al.*, 2008; Gray *et al.*, 2010; Hanahan and Weinberg, 2011). Therefore, since it has become increasingly apparent that altered cell-ECM adhesion events contribute towards epithelial transformation, a discussion concerning disease progression through aberrant regulation of cell adhesion events is prudent.

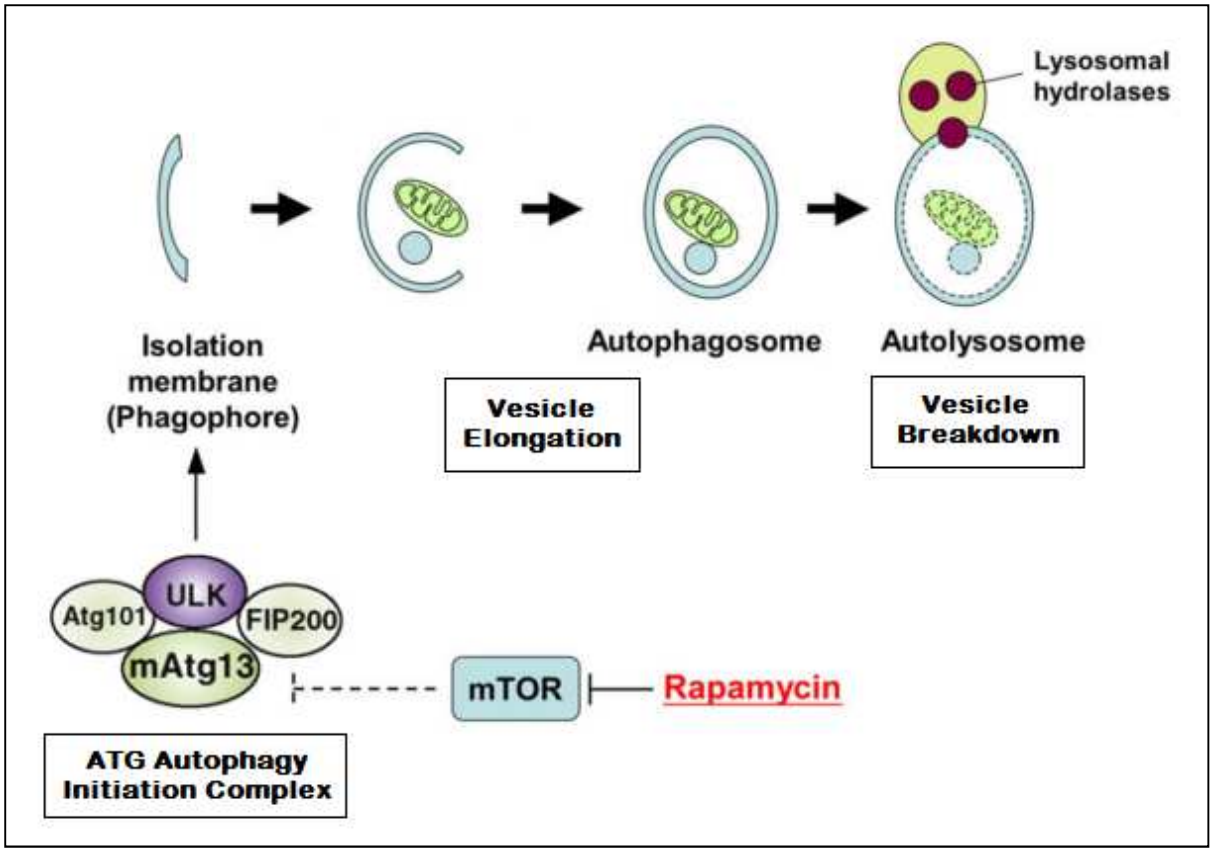

Figure 1.6: Signalling events giving rise to cellular autophagy induction. As the first step of autophagy, the isolation membrane (or phagophore) elongates and sequesters cytoplasmic constituents, non-specifically. Union of the phagophore edges results in the formation of an autophagosome. A lysosome (containing lysosomal hydrolases) fuses with the autophagosome, forming an autophagolysosome, which degrades captured components along with the inner autophagosome membrane. While autophagolysosome formation is important for the autophagic process, the appropriate temporal and spatial regulation of autophagy induction is just as vital. The mTOR signalling pathway is the principal regulator of autophagy initiation signals. mTORC1 phosphorylates and inhibits mATG-13 and ULK of the 3 MDa ATG complex, thus restraining autophagy induction signals – a process which is iteslf hindered by rapamycin or nutrient starvation (Adapted from Liang and Jung, 2009 and Tsuchihara *et al.*, 2009).

1.6. The aberrant regulation of adhesion-related events aids disease progression

A hallmark of both benign and malignant tumours is the capacity for deregulated cell growth and proliferative events (Hanahan and Weinberg, 2011). However, the invasive potential of a cell is exclusively associated with malignancy, and malignancy is directly associated with alterations in cell-cell and cell-ECM interactions (Behrens *et al.*, 1989). Therefore, the ectopic expression of cell adhesion molecules becomes significant when considering the

metastatic ability of transformed cells. Observations of rat colonic carcinomas induced with dimethylhydrazine exhibit dissociation of tubular structures, as well as the appearance of single cells at the invasion front (Gabbert, 1985; Gabbert *et al.*, 1985). This indicates that invasiveness correlates well with the degree of tumour dedifferentiation (Gabbert, 1985; Gabbert *et al.*, 1985). The release of carcinoma cells from the epithelia may therefore be a consequence of a breakdown in intercellular adhesion events, implicating oncogenic transformation as an instigator of metastatic potential.

A well known example epitomizing alterations in intercellular adhesion is squamous cell carcinoma affecting the human oesophagus, or HOSCC. Squamous cell carcinomas, like many other transformed epithelial cell types, display characteristic changes, or disease hallmarks, which underpin progression to the transformed state (Lam, 2000). One such change is the ectopic expression of integrin proteins as demonstrated by Miller and Veale (2001). Moreover, the inappropriate activation of integrin-triggered focal adhesion protein kinases (such as ILK or FAK) also contribute towards increased cell survival and tumourigenesis (Driver and Veale 2006; Fanucchi and Veale, 2011). These examples specifically communicate the ability of extracellular originating signals to support cell survival processes, especially under conditions where tumours exhibit a migratory phenotype.

1.7. Squamous cell carcinoma affecting the human oesophagus

1.7.1. Carcinomas result from the oncogenic transformation of epithelial tissue

‘Cancer’ is an umbrella term used to define any malignant tumour; however the term carcinoma specifically refers to malignant tumours arising from the epithelium (Young *et al.*, 2007). Further classification of carcinomas reveals the existence of adenocarcinomas, which arise from glandular epithelium, as well as squamous cell carcinomas, derived from stratified squamous epithelium (Young *et al.*, 2007).

Transition from a normal epithelium to the transformed carcinoma phenotype may be explained as a result of alterations within oncogenes, tumour suppressor genes and genes responsible for regulating homeostasis (Vogelstein and Kinzler, 2004). These alterations may be triggered by lifestyle, the environment or an inherent genetic predisposition (Scully and

Bagan, 2009). Therefore, no single genetic defect is likely to cause such a dramatic shift in cellular phenotype; rather it is the cumulative effect of multiple mutated genes and defective protein products that promote transition to the transformed state. Consequently, oncogenic transformation is a multistage process that involves the cumulative activation, mutation or loss of different genes (Behrens *et al.*, 1989). Thus, affected cells develop morphogenetic abnormalities that impinge on homeostatic feedback loops, ultimately affecting the control of growth and proliferation events (Hanahan and Weinberg, 2011). Furthermore, affected cells may acquire the potential to invade neighbouring tissue, as well as the potential to metastasize to distant sites by means of modified cell-cell and cell-ECM contacts (Bertram, 2001; Hanahan and Weinberg, 2011).

These changes within the epithelial phenotype may result in the formation of carcinomas, which comprise over 90 % of human malignant tumours (Behrens *et al.*, 1989). Carcinomas are aggressive epithelial cells capable of breaking through the basement membrane and invading the underlying mesochyme (Behrens *et al.*, 1989). This, together with a propensity for malignancy, accounts for the association of poor prognosis.

1.7.2. HOSCC is an appropriate model system

Cancer affecting the oesophagus is considered one of the most malignant gastrointestinal cancers affecting humans (Lehrbach *et al.*, 2003; Lam, 2000). Human oesophageal squamous cell carcinoma, or HOSCC, is currently rated the eighth most common cancer in the world and is responsible for approximately one sixth of all cancer related deaths worldwide (Scully and Bagan, 2009; Melhado *et al.*, 2010). Moreover, HOSCC possesses a variable geographical distribution; where the frequency of occurrence is reportedly high in Southern Africa and China, as well as Iran, Uruguay, France, Italy and Puerto Rico (Lam, 2000; Scully and Bagan, 2009). In South Africa, HOSCC occurs predominantly in the rural regions of the Transkei and Soweto (Hendricks and Parker, 2002).

Reports indicate a high incidence of HOSCC in individuals less than 40 years of age, where risk increases with each subsequent decade of life (Zhang *et al.*, 2004). Males are found to have a 3 - 4 times greater risk than females, while black males have a 5 times greater risk than their Caucasian counterparts (Walker *et al.*, 1984; Stoner *et al.*, 2007). While the

prognosis remains poor, a 50 % mortality rate is expected from all cases. Recent studies also show this rate to be 3.6 months for males and 4.2 months for females (Zhang *et al.*, 2004).

HOSCC possesses a multifactorial etiology; with environmental, dietary and genetic links (Stoner and Gupta, 2001). Tobacco derived carcinogens; such as polycyclic aromatic hydrocarbons, phenol and N-nitroso-containing compounds, are implicated as major contributors (Stoner and Gupta, 2001; Stoner *et al.*, 2007). In addition, excessive alcohol consumption may exacerbate this disease (Kato *et al.*, 2001). Recent studies also suggest salt-cured, salt-pickled and mouldy foods with N-nitrosamine carcinogen contamination or fungal toxin contamination (from *Fusarium verticillioides*) of home-brewed sorghum-based beers (popular in many townships throughout Sub-Saharan Africa) to play a role (Hendricks and Parker, 2002; Isaacson, 2005). However, the molecular mechanisms promoting HOSCC progression remain poorly understood.

1.7.3. Signal transduction through key pathway intermediates may provide this link

1.7.3.1. Alterations involving ILK

A review of recent proteomic data from 187 HOSCC-associated studies found that a total of 214 proteins were commonly altered in HOSCC (Lin *et al.*, 2009). Most candidate proteins commonly exhibited alterations in expression level, cellular localization or post-translational modification (Lin *et al.*, 2009). Additionally, while approximately 10 percent of aberrations contributed towards cell migration and cell adhesion events, over 50 percent of those proteins investigated were involved in signal transduction, cell cycle regulation, controlled transcription or translational processes, as well as apoptosis. *Figure 1.7* shows a breakdown of these commonly affected biological functions of deregulated proteins in HOSCC. The meta-analysis largely concluded that abnormalities affecting these aforementioned processes play the most vital role in HOSCC development.

At this time, the reader is reminded that ILK also plays a critical role in the regulation of these four processes. Consequently, the inappropriate regulation of ILK function may lead to the involvement of ILK in oncogenic transformation (Li *et al.*, 1999). Indeed, Wu *et al.* (1998) have shown that ILK over-expression in epithelial cells correlates with an increase in tumour formation *in vivo*, while studies using human tumour tissue revealed ILK to be constitutively over-expressed in Ewing's sarcoma and primitive nueroectodermal tumour

(Chung *et al.*, 1998). Consequently, ILK is used as a biomarker for these tumours. Furthermore, a previous member of the Cell Biology Laboratory at the University of the Witwatersrand established that a relationship exists between the integrins, ILK and human oesophageal squamous cell carcinomas; where ILK mediates integrin associated processes in WHCO cell lines which may contribute towards their cancerous phenotypes (Driver Ph.D. Thesis, 2007).

In antithesis, the contribution of mTOR was not included in the investigation conducted by Lin *et al.* (2009), despite mTOR acting as a critical upstream regulator for the majority of these biological processes. This is may be a result of the limited information available about the role played by mTOR within HOSCC-specific progression. In light of this, a discussion concerning aberrant mTOR function within other tumour systems may provide insight into possible roles of deregulated mTOR function within the HOSCC model system.

1.7.3.2. Alterations involving mTOR

The signalling components upstream and downstream of mTOR are frequently altered in a wide variety of human tumours; for example breast, renal cell carcinoma and non-small cell lung cancer (Rosner *et al.*, 2008). The fact that mTOR integrates signals from a variety of sources makes any point of incoming signal transduction cascades a possible target for aberration. In fact, this occurs frequently in tumour suppressor genes where mutations of TSC1, TSC2, LKB1, PTEN, VHL, NF1 and PKD-1 trigger the development of several diseases; including the hamartoma syndromes Tuberous Sclerosis, Peutz-Jeghers syndrome, Cowden syndrome, Bannayan-Riley-Ruvalcaba syndrome, Lhermitte-Duclos disease as well as von Hippel-Lindau disease (reviewed by Rosner *et al.*, 2008).

Considering that mTOR is a major influence during the progression of these diseases, mTOR was recently implicated as an attractive target for cancer therapy. This lead to the discovery that the mTOR signalling pathway is frequently activated in carcinomas; including HOSCC (Hou *et al.*, 2007; Hirashima *et al.*, 2012) – however these are the only known studies to demonstrate this in HOSCC specifically. Recently, there has been much interest in curbing mTOR-induced proliferation so as to stop tumourigenesis, as an increase in mTOR expression has been shown in advanced tumours (Villanueva *et al.*, 2008; Hirashima *et al.*, 2012). Also, increased levels of p-RPS6$^{(Ser\ 235/236)}$ (a direct downstream target of mTORC1) is

associated with moderately or poorly differentiated tumours (Villanueva *et al.*, 2008; Hirashima *et al.*, 2012).

Currently, there is a void in the scientific literature with respect to the influence of ILK on mTOR activity by way of ECM-signalling events. This is particularly appropriate in the case of HOSCC due to its highly metastatic nature. The immediate question therefore becomes: is mTOR a target of mechanotransduction through ILK? There is some evidence for the involvement of mTORC2 (McDonald *et al.*, 2008), but not mTORC1. Thus, there is a reasonable basis to investigate the link between extracellular-originating signals and their subsequent mechanotransduction through ILK to mTOR. Therefore, adhesion-based signaling in this manner may provide a regulatory element for inappropriate cell survival and autophagic processes in HOSCC.

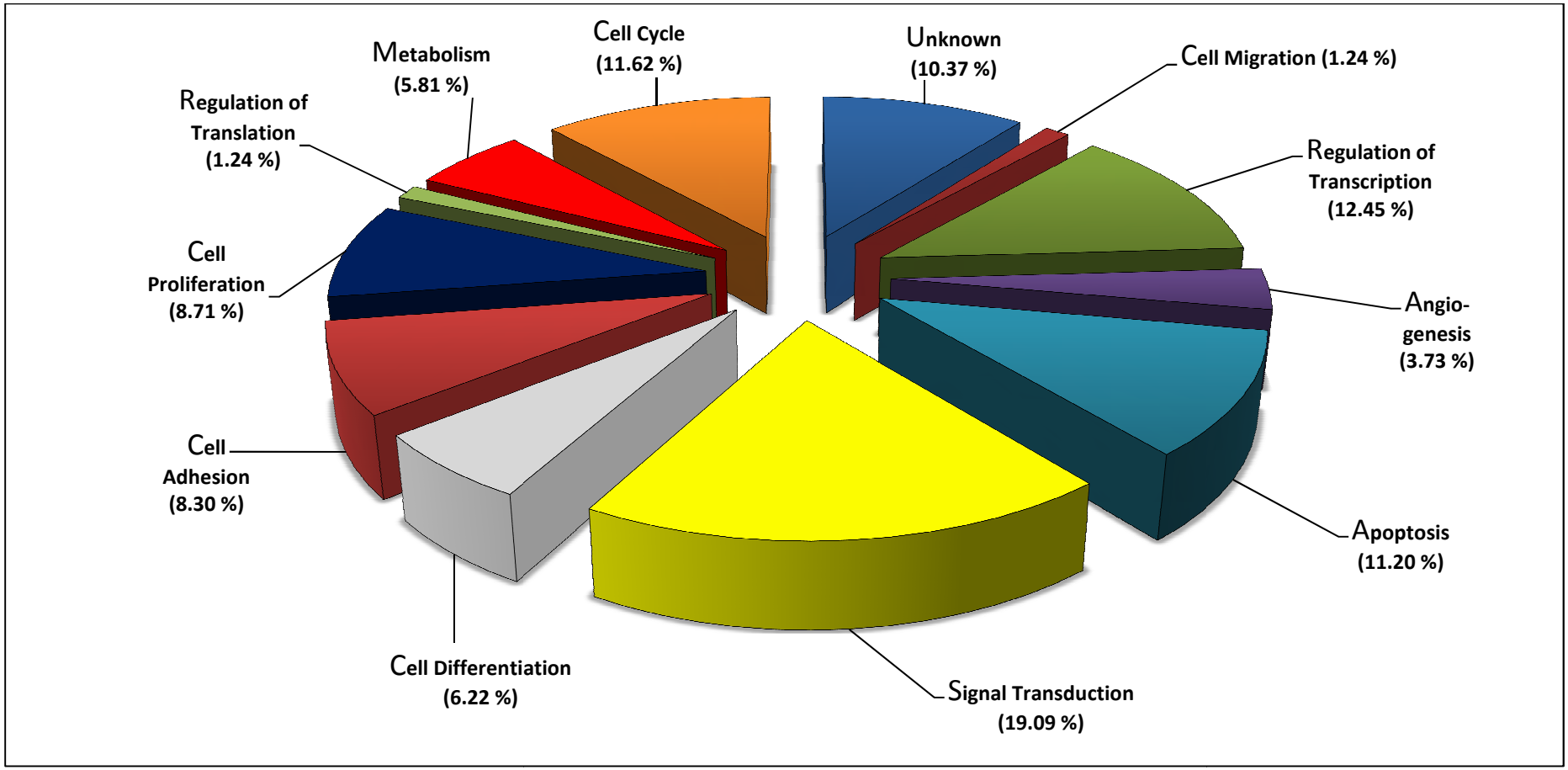

Figure 1.7: Commonly affected biological functions of deregulated proteins in HOSCC. Upon reviewing 187 HOSCC-associated studies, Lin *et al.* (2009) found that a total of 214 proteins were commonly altered in HOSCC. Over 50 % of these were found to be involved in signal transduction (19.09 %), regulation of transcription (12.45 %), cell cycle (11.62 %) or apoptosis (11.20 %), implicating that abnormalities within these four processes play the most vital role in HOSCC development.

1.8. Objective and Aims

In addition to its contribution to normal physiological homeostasis, aberrations involving the mTOR pathway are known to support tumour progression. An elevated instance of mTOR protein expression and hyper-activated mTOR signalling is associated with the transformed phenotype, as shown by studies using MCF-7 cells. Also, instances of elevated mTORC1 signalling are increasingly associated with pathology; in both metabolic diseases and cancer progression. Even though alterations within the mTOR pathway have been identified in the literature, a significant gap remains concerning the influence of extracellular-originating signals on mTOR signalling. This is particularly relevant considering the mTOR pathway controls autophagy initiation and a connection between autophagy and substrate dependence has recently been identified. This gap is what this research seeks to fill. Therefore, with the main objective being to investigate the influence of extracellular-originating signals on mTOR signalling in HOSCC, we sought to:

i. Monitor the protein expression of key mTOR signal transduction pathway intermediates responsible for autophagy induction using a system of moderately differentiated HOSCC cell lines.
ii. Investigate the response of these signalling networks to soluble stimuli.
iii. Determine the effect of extracellular-originating signals derived from cell-substrate interactions on the cellular concentration of mTOR and mTORC1 signalling.
iv. Characterise the possible route, or routes, of mechanotransduction from sites of cell-substrate contact to the mTOR/mTORC1 signalling pathway in HOSCC cells.

CHAPTER 2

2. EXAMINATION OF KEY SIGNAL TRANSDUCTION INTERMEDIATES REGULATING AUTOPHAGY INDUCTION IN HOSCC CELLS

2.1. Introduction

Autophagy is an evolutionary conserved cell survival mechanism responsible for the nonspecific bulk degradation of cellular proteins and organelles. Autophagy may be classified into two subtypes; namely constitutive autophagy and induced autophagy (Klionsky and Ohsumi, 1999). Constitutive autophagy refers to a basal rate of cellular autophagic processing, typified by the Cvt (cytoplasm-to-vacuole targeting) pathway in yeast, which mediates transport of aminopeptidase-1 (Ape-1) from the cytoplasm into the vacuole (Klionsky and Ohsumi, 1999). Induced autophagy refers to autophagic processing that is triggered in response to a particular cellular stress, such as nutrient starvation or exposure to rapamycin (He and Klionsky, 2009). In both cases, autophagy induction requires the involvement of the mammalian target of rapamycin (mTOR) signalling pathway, as mTOR mediates signal transduction to the cellular machinery controlling autophagy induction (Jung *et al.*, 2010; Neufeld, 2010; Yang and Klionsky, 2010). Therefore, monitoring the signalling potential of the mTOR pathway becomes the main focus of this investigation.

Transmission of intracellular signals through mTOR induces its translocation into one of two multi-protein complexes, known as mTORC1 and mTORC2. mTORC1 (mTOR-containing multi-protein complex 1) is sensitive to rapamycin treatment and is the primary mTOR complex involved during the regulation of cell growth, proliferation and autophagy (Jung *et al.*, 2010; Neufeld, 2010; Yang and Klionsky, 2010). mTORC2 (mTOR-containing multi-protein complex 2) is relatively rapamycin-insensitive and is rather involved during the regulation of actin cytoskeletal dynamics, survival and cellular metabolism (Loewith *et al.*, 2002; Jacinto *et al.*, 2004). Since mTORC1 is uniquely involved during the regulation of autophagy, we are particularly interested in signal transduction through the mTORC1 node of the mTOR pathway.

Signalling through mTORC1 requires the sequential activation of important upstream regulators, such as PI3K, PKB, Rheb-GTPases, Raptor and Rictor (Caron *et al.*, 2010; Schmelzle and Hall, 2000; Fingar and Blenis, 2004), as well as the functional inhibition of PTEN, AMPK, TSC1, TSC2 and Deptor (Schmelzle and Hall, 2000; Fingar and Blenis, 2004). Only once properly activated can mTORC1 regulate autophagy through inhibition of the ~ 3 MDa autophagy induction complex (Hosokawa *et al.*, 2009; Jung *et al.*, 2009). However, activated mTORC1 may also serve as a downstream branching point controlling protein synthesis and translation initiation through phosphorylation of p70S6K and 4E-BP1 (Schmelzle and Hall, 2000; Fingar and Blenis, 2004). Therefore, the mTOR signalling pathway is a multifaceted one containing a complex array of pathway intermediates required for the appropriate activation of mTORC1.

In mammalian cells, inhibition of autophagy correlates well with ribosomal protein S6 (RSP6) phosphorylation (Blommaart *et al.*, 1995). Since RPS6 phosphorylation is dependent on the activation of p-p70S6K by mTORC1, signal transduction to mTORC1 is critical (Brown *et al.*, 1995; Thomas and Hall, 1997). These findings suggest that one can effectively follow the earliest steps controlling the induction of autophagy by monitoring the activation of select signal transduction intermediates holding key positions within the mTOR pathway. Based on our understanding of mTOR/mTORC1 signalling dynamics, we also believe the mTOR pathway can be successfully reduced to a few major players, although based on two criteria: significance of activation, and relative position within the pathway. In doing so, we can distil the mTOR pathway into a set of measurable protein markers comprised of key pathway intermediates, which represent critical nodes during the course of mTOR/mTORC1 signalling. Our reduction of the mTOR pathway is illustrated in *Figure 2.1*; where we highlight major mTOR pathway intermediates we believe adequately fulfil this role.

Each molecular marker represents an important element of the mTOR signalling pathway and so conveys specific pathway information. As can be seen in *Figure 2.1*, the 220 kDa mTOR protein kinase (henceforth referred to as mTOR) is positioned immediately downstream of the PI3K/PKB pathway; an important signalling scheme maintaining cell survival and homeostasis (Foster *et al.*, 2003; Arcaro and Guerreiro, 2007; Duronio, 2008). mTOR is considered the principal conduit through which biochemical signals are propagated within the mTOR signalling pathway; owing to the presence of the C-terminal kinase domain (Foster and Fingar, 2010; Dobashi *et al.*, 2011). Therefore, by monitoring the protein expression of

mTOR, one may gain an understanding of how the central protein component of the mTOR signalling pathway responds to extracellular-originating stimuli.

Since it is well established that p70S6K is a downstream target of mTORC1 (Brown *et al.*, 1995; Thomas and Hall, 1997), the state of RPS6$^{(Ser\ 235/236)}$ phosphorylation is used extensively in the literature as a marker for active mTOR signalling (Sturgill and Wu, 1991; Dazert and Hall, 2011). In light of this, p-RPS6$^{(Ser\ 235/236)}$ is used to convey specific information pertaining to the signalling potential of mTORC1. This is ideal because, as will be elaborated on below, active signalling through mTORC1 is directly responsible for autophagy regulation as mTORC1 interacts with mATG-13 of the ~ 3 MDa autophagy induction complex.

mATG-13 (in its dephosphorylated state) forms a multi-protein autophagy induction complex together with ULK-1 and FIP200, which is an essential requirement for the development of functionally mature autophagosomes (Hara *et al.*, 2008; Chan *et al.*, 2009; Yang and Klionsky, 2010). mTORC1 regulates this process by directly phosphorylating mATG-13 during conditions where nutrient concentrations are not constrained, thereby inhibiting signals initiating autophagy induction (Chan *et al.*, 2009; Yang and Klionsky, 2010). Since the state of mATG-13 phosphorylation is a crucial regulatory step for autophagy to proceed, the presence of mATG-13 in its dephosphorylated form signifies an important, initial regulatory step for autophagy induction. For this reason, we believe mATG-13 serves as an informative pathway intermediate signifying mTORC1-dependent autophagy regulation.

It has been demonstrated, however, that extensive autophagy may result in cell death (Brech *et al.*, 2009; Tsuchihara *et al.*, 2009; Chen and Debnath, 2010). Therefore, it is necessary to differentiate between apoptosis, or programmed cell death-type I (PCD-Type I), and death as a result of excessive autophagy, or programmed cell death-type II (PCD-Type II), which may arise during the course of this investigation. Since the proteolytic cleavage of pro-caspase-3 into functionally-active fragments signifies apoptosis activation, the presence of cleaved caspase-3 is commonly used as a molecular marker indicating this early step (Thornberry and Lazebnik, 1998; Chowdhury *et al.*, 2008). Therefore, the presence of cleaved caspase-3 signifies that any observed cell death was a result of apoptosis, rather than autophagy, and so was regarded as an important signal transduction intermediate.

Lastly, since a component of this investigation is to explore the contribution of adhesion-based signalling to the autophagy induction process in HOSCC cells, a molecular connection mediating signal transmission from the ECM to the mTOR pathway is still required. Since ECM-originating signals are propagated in an integrin-mediated manner (Clarke and Brugge, 1995), an integrin-triggered focal adhesion protein kinase, such as ILK, would be the most likely conduit providing this molecular connection. Considering that autophagy occurs in an FAK-independent manner (Hara *et al.*, 2008), and ILK is a promiscuous protein kinase; functioning as both a molecular scaffold and signalling node at sites of focal adhesion, ILK and not FAK was chosen to represent signals arising from sites of cell-ECM adhesion.

By monitoring the protein expression of critical signal transduction pathway intermediates, we aim to establish an efficient system to monitor the mTOR signalling pathway. In selecting key elements of this pathway to act as molecular markers and monitoring them as a set under standard tissue culture conditions, we may also establish the normal operating procedure for signal transduction through mTORC1. Consequently, we may investigate the influence of such signalling to the autophagy induction machinery in a series of five moderately differentiated HOSCC cell lines.

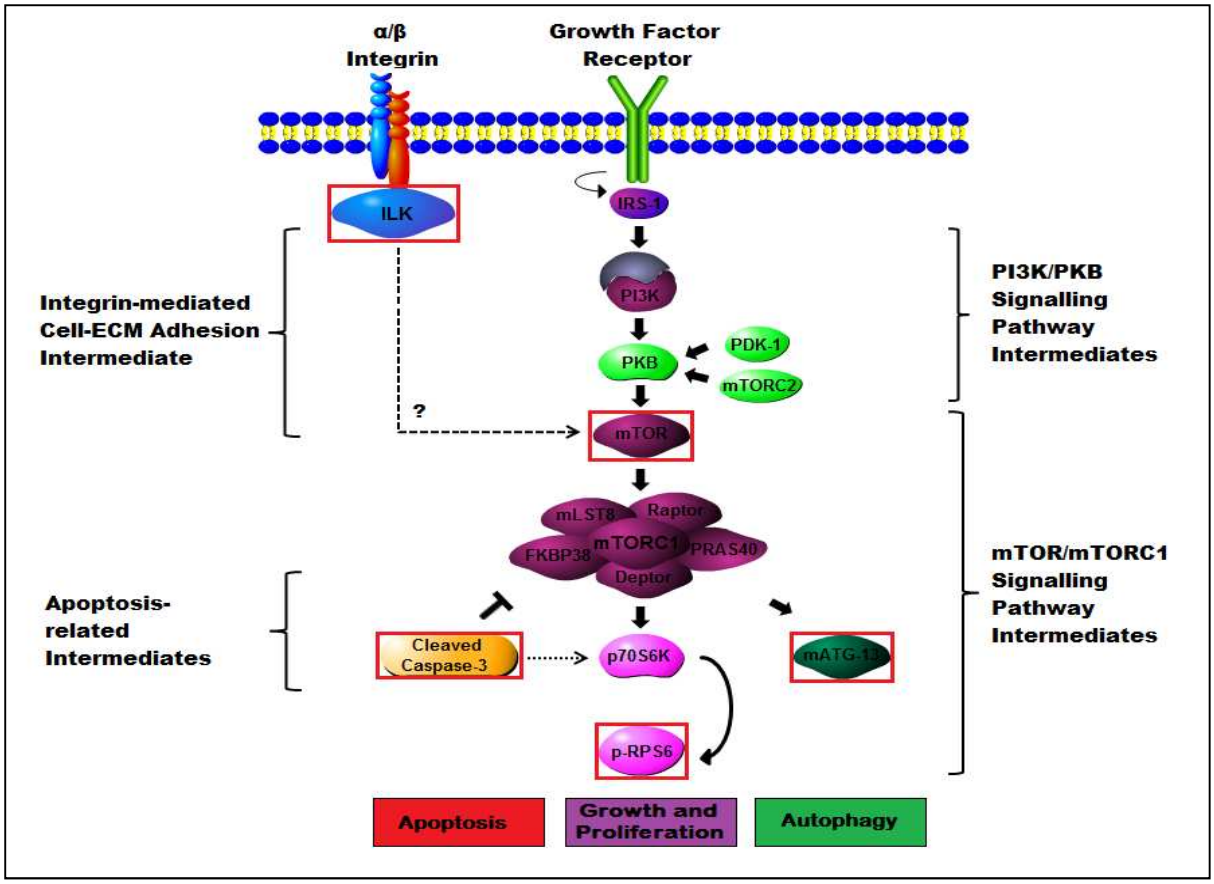

Figure 2.1: Illustration of a reduced mTOR/mTORC1 signalling pathway. By highlighting major players within the mTOR/mTORC1 signalling pathway, we emphasise the role and position of those cellular proteins included in the marker set. Consequently, by monitoring the protein expression of mTOR, p-RPS6$^{(Ser\ 235/236)}$, mATG-13, cleaved caspase-3 and ILK, we establish an efficient system conveying specific signalling information. This becomes an extremely practical method of investigating the mTOR pathway in response to factors influencing autophagy induction in HOSCC cell lines.

2.2. Materials and Methodology

2.2.1. Tissue Culture of WHCO, MCF-7 and HEK-293 Cell Lines

Five moderately differentiated human oesophageal squamous carcinoma (HOSCC) cell lines, of South African origin, were obtained from the Cell Biology Research Laboratory, University of the Witwatersrand, Johannesburg. Cell lines were designated WHCO1, WHCO3, WHCO5, WHCO6 (Veale and Thornley, 1989) and SNO (Bey *et al.*, 1976). Since physiologically 'normal' oesophageal cell lines are currently unavailable for comparative analysis (Jankowski *et al.*, 1995; Underwood *et al.*, 2010), the MCF-7 and HEK-293 cell lines were used as comparative controls. The SV40T-antigen (simian-virus-40 large T-antigen)-immortalized oesophageal squamous cell line, HET-1A, is incorrectly believed to be representative of truly untransformed oesophagus. This is because HET-1A cells do not display common characteristics of 'normal' oesophageal squamous cells; such as E-cadherin, casein kinase 5/6 (CK 5/6) or the stratified epithelial marker ΔNp63 (Underwood *et al.*, 2010). Therefore, the HET-1A cell line was not used for comparative purposes in this investigation.

The MCF-7 cell line, derived from a patient presenting with mammary adenocarcinoma pleural effusion (Soule *et al.*, 1973), and the HEK-293 cell line, established from human embryonic kidney cells and first described by Graham *et al.* (1977), were supplied by the America Type Culture Collection (ATCC). All cell lines were cultured in 10 cm tissue culture dishes (Corning) and maintained in 10 ml Dulbecco's Modified Eagles Medium (DMEM)/Hams F12 (3:1) (Appendix A, 1.2.1) supplemented with 10 % Foetal Calf Serum (FCS) (Highveld Biologicals), penicillin and streptomycin. Tissue cultures were incubated in a humid, 37 °C incubator with an atmosphere of 5 % CO_2 in air. Please note that all procedures for one set of experiments were performed using the same batch of FCS.

2.2.2. Sub-culture of WHCO, MCF-7 and HEK-293 Cell Lines

Cell cultures were allowed to proliferate until 10 cm dishes reached a confluence of approximately 80 %. Medium was then aspirated and cell monolayer washed twice with warm (37 °C) sterile phosphate buffered saline (PBS) (Appendix A, 1.1.1). Subsequently, 1ml Trypsin(Gibco BRL)/Ethylenediaminetetra-acetic acid (EDTA) (BDH Laboratory reagents) (Appendix A, 1.2.2) was added and the tissue culture dish placed into a 37 °C

incubator for 5 min, to augment cell-cell and cell-ECM detachment. Detachment was confirmed using a Leitz Watzlar Inverted Light Microscope. Subsequently, a fraction of the trypsinized cell-EDTA mixture was added to a new tissue culture dish with 10 ml fresh medium containing 10 % FCS. Tissue culture continued as previously described in 2.2.1.

2.2.3. Antibodies

Immunochemical analysis utilised an indirect antibody detection system requiring a range of specific primary antibodies to detect all proteins in the marker set. Since all primary antibodies were reared within rabbit hosts, only one type of polyclonal, goat-derived anti-rabbit secondary antibody was necessary. This secondary antibody was conjugated to a horseradish peroxidase (HRP) (Separations, SA), thus facilitating detection by chemiluminescence.

The mammalian target of rapamycin protein kinase (anti-mTOR) was detected with rabbit polyclonal antibodies obtained from Cell Signalling Technology®, USA. Phosphorylated ribosomal protein subunit 6 around Ser residues 235/236 (anti-p-RPS6$^{\text{Ser 235/236}}$) was detected with rabbit monoclonal antibodies obtained from Cell Signalling Technology®, USA. Mammalian autophagy related gene-product-13 (anti-mATG-13) was a gift from Dr Sharon Tooze from Cancer Research UK (CRUK). Since no commercial antibodies are available for mATG-13, Dr Tooze and colleagues generated polyclonal antibodies against human Atg-13 (designated KIAA0652) using the peptide sequence LAVHEKNVREFDAFVETLQ (Chan *et al.,* 2009). Furthermore, cleavage fragments of activated caspase-3 (anti-cleaved caspase-3) were detected using rabbit polyclonal antibodies obtained from Cell Signalling Technology®, USA. Integrin-linked kinase (anti-ILK) and anti-actin (β isoform) were detected with rabbit polyclonal antibodies obtained from Sigma-Aldrich®, USA.

2.2.5. Triton X-100-based Protein Extraction

The anionic detergent Triton X-100 is known to enrich the extraction of membrane and cytoplasmic associated proteins (Giancotti and Ruoslahti, 1990). Therefore, a protein extraction buffer containing Triton X-100 is appropriate for the extraction of various cellular proteins physically linked to integrin glycoproteins, as well as cytoplasmic signal transduction intermediates.

Cells were allowed to proliferate until a confluence of approximately 80 % was reached. Cells were washed twice with PBS, then 1 ml PBS containing a phenyl-methyl-sulphonyl fluoride (PMSF)/Aprotinin-based (Trasylol®, Bayer S.A.) protease inhibitor solution was added, into which cells were gently scraped off using a rubber policeman. The cell suspension was transferred to a sterile eppendorf and centrifuged in a TOMY HF-120 centrifuge (1 145 x g) for 5 min. The supernatant was removed and pellets re-suspended in 50 - 200 µl of a Tris-based 2 % (v/v) Triton X-100 (pH 7.2) protein extraction buffer (Appendix A, 1.3.1), then vortexed briefly and incubated for 3 hours on ice (with intermittent mixing by inversion). Thereafter, samples were centrifuged at 12 000 x g in a PRISM™ Refrigerated Microcentrifuge for 10 min at 4 °C. The supernatant containing total cellular protein was decanted into a sterile eppendorf. Subsequently, Laemmli double lysis buffer (Appendix A, 1.3.2) was added in a ratio of 1:1 to each sample, after which samples were boiled for 5 min, then centrifuged at 12 000 x g in a PRISM™ Refrigerated Microcentrifuge for 10 min at 4 °C. SDS-PAGE-ready samples were stored at – 20 °C.

2.2.6. Protein Estimation

To ensure that equivalent protein concentrations were loaded for all HOSCC cell lysates, an estimate of protein concentration within each sample was performed utilising the methodology proposed by Bramhall *et al.* (1969). Whatman® filter paper was first hydrated by washing in distilled water (dH_2O) for 20 min, then subjected to a series of dehydration steps; where 95 % ethanol, 100 % ethanol and 100 % acetone were applied in succession, each for 5 min (Appendix A, 1.4). Subsequently, the dehydrated filter paper was allowed to air-dry in a sterile fume hood. Protein standard concentrations were then prepared by solubilising Bovine Serum Albumin (BSA) (BDH Laboratory reagents) in Laemmli double lysis buffer (1µg/µl):2 % (v/v) Triton X-100 (pH 7.2) extraction buffer (1:1), and spotted onto the dry filter paper to create a curve possessing the following standards: 1 µg, 3 µg, 6 µg, 9 µg, 12 µg, 16 µg and 20 µg. In addition, 2 µl duplicates of each SDS-PAGE-ready sample were spotted onto the filter paper.

After spots were allowed to air-dry, the filter paper was placed in trichloroacetic acid (TCA) for 40 min (Appendix A, 1.4.2), in order to precipitate the proteins onto the filter paper medium. Excess TCA was removed by the addition of 0.25 % Coomassie Blue stain for 5 min (Appendix A, 1.4.3), which was then discarded. Thereafter, fresh 0.25 % Coomassie

Blue stain was applied for 45 min. The filter paper was then placed in a destain solution (Appendix A, 1.4.4) for approximately 1 hour until background stain was completely removed. Stained circles that remained were indicative of precipitated protein. These were then removed and placed, individually, into 5 ml elution solution (Appendix A, 1.4.5) in the dark for approximately 3 hours. Subsequently, the absorbance of each solution was determined at 596 nm using an Abbota SV1100 Spectrophotometer, with elution solution serving as a blank. A standard curve of absorbance (OD at 596 nm) versus protein concentration (µg/µl) was then constructed using the absorbance from the protein standards of known concentration (see Appendix B, *Figure B1* for sample standard curve). Therefore, protein concentration present in the unknown samples was determined using the standard curve, constructed using Microsoft® Excel 2007 (Version 12.0.6).

2.2.7. SDS-PAGE (Sodium Dodecyl Sulphate-Polyacrylamide Gel Electrophoresis)

Proteins present in each sample were resolved by either 10 % or 12 % (w/v) discontinuous SDS-PAGE, following the protocol proposed by Laemmli (1970). The Mighty Small™ SE245 Dual Gel Caster system (Hoefer Scientific) was used to construct all gels. Polyacrylamide gels containing sodium dodecyl sulphate (SDS) were prepared by pouring a 10 % or 12 % separating gel (Appendix A, 1.5.3.1) in between glass and silica plates, which were left to polymerise for approximately 30 min. Polymerisation was augmented by the addition of 200 µl 4 % SDS overlay solution (Appendix A, 1.5.3.3). SDS overlay was then removed and a 5 or 8 % stacking gel (Appendix A, 1.5.3.2) was poured above the separating gel. A comb possessing either 10 µl or 20 µl wells was placed into the stacking gel. The stacking gel layer was allowed to polymerise for approximately 20 min.

Once polymerized, the SDS-PAGE gel was placed in the Mighty Small™ Electrophoresis Unit containing electrophoresis running buffer (pH 8.3) (Appendix A, 1.5.2.1). After the comb was removed, the appropriate volume of each sample was loaded into the resulting wells. In addition, 2 µl of PageRuler™ Prestained Protein Ladder (Fermentas Life Sciences) was loaded into the first well of the gel. The bands in the molecular weight marker represented 170, 130, 100, 70, 55, 40, 35, 25, 15 and 10 kDa (clearly seen after separation in *Figure 2.2*). Thus, samples were resolved using a constant currant of 25 mA (~ 400 V) per gel for 1 hour, until the 10 kDa marker was 1 cm from the bottom of the separating gel. Resolved proteins were visualized by placing the gel into 0.25 % Coomassie Blue stain

(Appendix A, 1.5.3.5) for 1.5 hours and then placed in a destain solution (Appendix A, 1.5.3.6), overnight. The gel was subsequently digitized using a Hewlett Packard ScanJet G3110 desktop scanner.

2.2.8. Western Immunoblot Analysis

Western immunoblotting (immunodetection) is considered a reliable technique allowing for the detection and quantification of numerous polypeptide species. By exploiting the specific binding capabilities of monoclonal or polyclonal antibodies, specific polypeptides may be detected from a complex cellular mixture. In this investigation, immunodetection proceeded according to the protocol initially described by Towbin *et al.* (1979), later modified by Burnette (1981).

Western immunoblotting initially required sample resolution by 10 or 12 % (w/v) SDS-PAGE, as stated in 2.2.7. Subsequently, polyacrylamide gels were cut within the relevant range for each protein of interest, using the PageRuler™ Prestained Protein Ladder as a guide. Resolved proteins were then transferred onto Hybond™-C nitrocellulose membrane (Sartorius) using a Bio-Rad Criterion™ Blotter for 1.5 – 3 hours (depending on the requirements of individual proteins) in transfer buffer (pH 8.3; 4 °C) (Appendix A, 1.6.1.1) at a constant currant of 400 mA. The nitrocellulose membrane was then washed with the appropriate buffer (see Appendix B, *Table B1* for specific antibody requirements).

Nitrocellulose membranes were then placed in a casein-based blocking buffer solution (Blotto) (Appendix A, 1.6.1.2 or 1.6.1.3) for 1 hour at room temperature in order to block nonspecific binding sites. Thereafter, the membrane was rinsed with the appropriate buffer and incubated with the appropriate primary antibody (see Appendix B, *Table B1* for antibody dilutions and incubation conditions). Unbound antibody was removed by washing the membrane several times with the appropriate buffer (5 min per wash). Next, the membrane was incubated with a goat-anti-rabbit HRP-conjugated secondary antibody (see Appendix B, *Table B1* for antibody dilutions and incubation conditions). Unbound antibody was again removed by washing the membrane several times with the appropriate buffer (5 min per wash), after which the membrane was placed in a luminal:peroxide mixture (1:1) (SuperSignal® West Pico) for 5 min in the dark (Appendix A, 1.6.2). The membrane was subsequently wrapped in Versafilm® clear cling-wrap and exposed to clear-blue CL-XPosure™ X-ray film (Pierce) for 10 min in the dark. Immediately after, the film was placed

in a developer solution (Appendix A, 1.6.3), rinsed in water, placed in a fixer solution (Appendix A, 1.6.4) and rinsed in water.

2.2.9. Image Capturing

Images were digitized using a Hewlett Packard ScanJet G3110 desktop scanner. Magnification, contrast, brightness and cropping of all images were performed using Microsoft Paint® 2007 software (Version 6.1).

2.2.10. Laser Densitometry and Analysis of Relative Protein Expression

The Labworks™ Image Acquisition and Analysis software (Version 4.5) was used for densitometric analysis. This software allows for a semi-quantitative comparison of relative protein expression levels as determined by western immunoblotting. Protein expression levels are determined by analysing immunoblots, calculating band intensities and subtracting irrelevant background data, thus forming a calibration curve. The area under the curve is indicative of integrated optical density (IOD) or the amount of signal produced from HRP-dependant chemiluminescence. Subsequently, IOD was used to determine protein expression levels, described in more detail below.

Levels of relative protein expression were designated low (0 – 45 %), moderate (46 – 75 %) or high (76 – 100 % or above) based on the classification system originally set up by Hager *et al.* (2011) to analyse mTOR and p-RPS6 proteins in mammalian cells. This system was used during this investigation in order to compare protein expression across WHCO, MCF-7 and HEK-293 cell lines (see Appendix C, *Tables C1-C5* for densitometric data). IOD for each cell line was represented as a percentage of that recorded for the WHCO6 or MCF-7 cell line (unless otherwise indicated) using GraphPad Prism® software, Version 4.0 (GraphPad Software, Inc., San Diego, CA, USA).

2.2.11. Statistical Analysis

Results are expressed as the mean ± S.E. Statistical significance was determined by Student's *t*-test for comparative analysis (See Appendix D, *Table D1* and *Table D2*) using Sigma Plot®, Version 12.0 (SPSS Science, Chicago, Illinois USA), where $p < 0.05$ indicated statistical significance. All experiments were repeated at least three times, unless otherwise indicated.

2.3. Results

2.3.1. Extraction of cellular proteins from HOSCC cells

The successful separation of polypeptides by SDS-PAGE confirmed the efficacy of the protein extraction method used to acquire cellular proteins from HOSCC cell lysates (*Figure 2.2*). Since a similar banding pattern was also visible in all lanes of the SDS-PAGE gel (after polypeptides were stained with Coomassie Blue stain), this provided visual evidence supporting the accuracy of the protein estimation procedure. In addition, the clear separation of the molecular weight marker (MWM) in Lane 1 indicated that the blue-coloured polypeptide bands in Lanes 2 – 7 were also resolved by size. Since discreet polypeptide bands appear at the approximate molecular weight previously reported for proteins in the marker set (indicated by coloured arrows in *Figure 2.2*), this banding pattern signifies the potential presence of relevant mTOR pathway intermediates in HOSCC cells. Therefore, the presence of these bands supported proceeding to the next step of this investigation, which encompassed western immunoblot analysis for key mTOR pathway intermediates contained within the marker set.

2.3.2. HOSCC cells express the 220 kDa mTOR protein and the 80 kDa mTORβ splicing isoform

Analysis of a whole SDS-PAGE gel revealed the presence of two mTOR protein variants in HOSCC cells. Polypeptides corresponding to mTOR were detected at 220 and 80 kDa (*Figure 2.3*). Although the same amount of protein was loaded for each cell line (see *Appendix B, Figure B1* for standard curve based on the dilution of BSA), the 220 kDa mTOR isoform was dominantly expressed in WHCO5, WHCO6 and SNO cell lines. In comparison, mTOR (220 kDa) protein expression was visibly reduced in WHCO1 and WHCO3 cell lines. However, only the WHCO1 and WHCO3 cell lines expressed the 80kDa mTORβ splicing isoform.

Untransformed or physiologically ‘normal’ oesophageal cell lines are currently unavailable for comparative analysis with HOSCC cells (explained in Materials and Methodology, Section 2.2.1). Therefore, the breast adenocarcinoma cell line (MCF-7) and human embryonic kidney cell line (HEK-293) were used as controls in order to establish a relative

measure for mTOR expression in HOSCC cells. MCF-7 cells are known to over-express both mTOR and p-RPS6$^{(Ser\ 235/236)}$ (Hagner *et al.*, 2009), while HEK-293 cells are known to produce endogenous levels of mTORβ (Panasyuk *et al.*, 2009). Western blotting confirmed the expression of mTOR (220 kDa) polypeptide bands in MCF-7 and HEK-293 cells (*Figure 2.3*). Unexpectedly, mTORβ (80 kDa) expression was also observed in the MCF-7 cell line. An in depth analysis of the relevant literature revealed that this is the first observation of mTORβ in MCF-7 cells.

The specificity of the anti-mTOR antibody was also confirmed since there was no evidence of non-specific antibody binding in *Figure 2.3*. This observation indicates that the western blotting system used here is able to produce clear and reliable western blots. Therefore, this type of efficiency justifies trimming subsequent blots to conserve reagents, especially antibodies obtained as gifts.

2.3.3. Key mTOR pathway intermediates are expressed differentially by HOSCC cells

The expression of all relevant marker set proteins was confirmed in HOSCC cells by western blotting, under standard tissue culture conditions. Single polypeptides corresponding to mTOR (220 kDa), p-RPS6$^{(Ser\ 235/236)}$ (36 kDa), mATG-13 (72 kDa) and ILK (59 kDa) were detected in all HOSCC cell lines (*Figure 2.4*, *A*). β-actin (46 kDa) was also detected in HOSCC cells. The detection of β-actin was used as a visual demonstration of equal protein loading between cell lines (see *Appendix B, Figure* B1 for standard curve). However, polypeptide fragments indicative of cleaved caspase-3 (17 – 27 kDa) were not detected in any of the HOSCC cell lines (*Figure 2.4*, *B*).

Since cleaved caspase-3 is only expressed under circumstances of programmed cell death (Thornberry and Lazebnik, 1998; Chowdhury *et al.*, 2008), an appropriate panel of HOSCC cell line controls was required to confirm cleaved caspase-3 expression. Therefore, HOSCC cells from the WHCO6 cell line were used, where cells were starved of serum for either 0 or 24 hours. HOSCC cells serum-starved for 0 hours were used as a standard tissue culture control and designated 'Serum + (S+)', whereas HOSCC cells serum-starved for 24 hours were used as a serum-free control (SF/C).

Cells that became detached from the SF/C tissue culture substrate, as a result of apoptotic cell death, were collected from the media and used as an apoptotic control (A/C). Subsequently, cleaved caspase-3 expression was confirmed in A/C cells, only (*Figure 2.4, B*). Further analysis of the marker set in A/C cells by western blotting revealed a visible reduction in the polypeptides indicative of mTOR (220 kDa) and p-RPS6$^{(Ser\ 235/236)}$ (36 kDa) expression (*Figure 2.4, C*). However, polypeptides indicative of mATG-13 (72 kDa) and ILK (59 kDa) expression only appeared to be reduced to a small degree, while cleaved caspase-3 expression (17 – 27 kDa) was prominent in A/C cells under these conditions.

Semi-quantitative densitometric analysis of the marker set revealed different levels of protein expression between the WHCO series of cell lines (*Figure 2.5*). When expressed as a percentage of the MCF-7 control cell line, we observed that WHCO cell lines do not uniformly express all proteins in the marker set. Rather, protein expression was found to vary between low to high levels (see Materials and Methodology, Section 2.2.10, for a clear explanation of how we determined levels of protein expression). Noting this, we established that HOSCC cells conform to certain protein expression trends, that may or may not be shared by all WHCO cell lines (see *Table 2.1* for a detailed summary of these protein expression and cell line trends). This enabled the categorization of WHCO cell lines into groups, based on trend conformation, allowing the identification of an overriding protein expression trend for HOSCC cells.

HOSCC cells were therefore found to be high expressers of mTOR and low expressers of mTORβ. Analysis of the WHCO series revealed a high concentration of mTOR in WHCO1, WHCO5, WHCO6 and SNO cell lines. The WHCO3 cell line, however, was a low mTOR expresser; expressing significantly lower concentrations of mTOR compared to MCF-7 cells (*see Appendix D, Table D1* for a complete statistical analysis). However, only two of the five WHCO cell lines expressed the mTORβ splicing isoform. mTORβ was expressed at low levels within the WHCO1 and WHCO3 cell lines, only. In addition, the level of mTORβ expression was not significantly different to those endogenous levels found in HEK-293 cells (*see Appendix D, Table D2*).

HOSCC cells were also either moderate (WHCO1 and WHCO3) or high (WHCO5 and WHCO6) expressers of p-RSP6$^{(Ser\ 235/236)}$. The SNO cell line, however, was a low expresser of p-RSP6$^{(Ser\ 235/236)}$, expressing significantly lower concentrations when compared to MCF-7

cells (*see Appendix D, Table D1* for a complete statistical analysis). Since the WHCO series of cell lines (WHCO1, WHCO3, WHCO6 and SNO) were also high expressers of dephosphorylated mATG-13 (referred to henceforth as mATG-13), HOSCC cells were generally high expressers of mATG-13. However, the WHCO5 cell line was the exception in this case; expressing significantly lower concentrations of mATG-13 compared to MCF-7 cells (*see Appendix D, Table D1*). All WHCO cell lines were high expressers of ILK. Only, the WHCO6 and SNO cell lines were found to express significantly higher levels of ILK than MCF-7 cells (*see Appendix D, Table D1* for these statistical analyses).

Since cleaved caspase-3 was not detected in any of the WHCO cell lines, HOSCC cells were regarded as expressing low levels of cleaved caspase-3 under standard tissue culture conditions. However, analysis under apoptotic conditions revealed that HOSCC cells change these established trends and, not only increase cleaved caspase-3 expression, but decrease mTOR, p-RPS6$^{(\text{Ser } 235/236)}$ and mAG-13 protein expression to low levels. Only, ILK protein expression remained unaltered in HOSCC cells under apoptotic conditions.

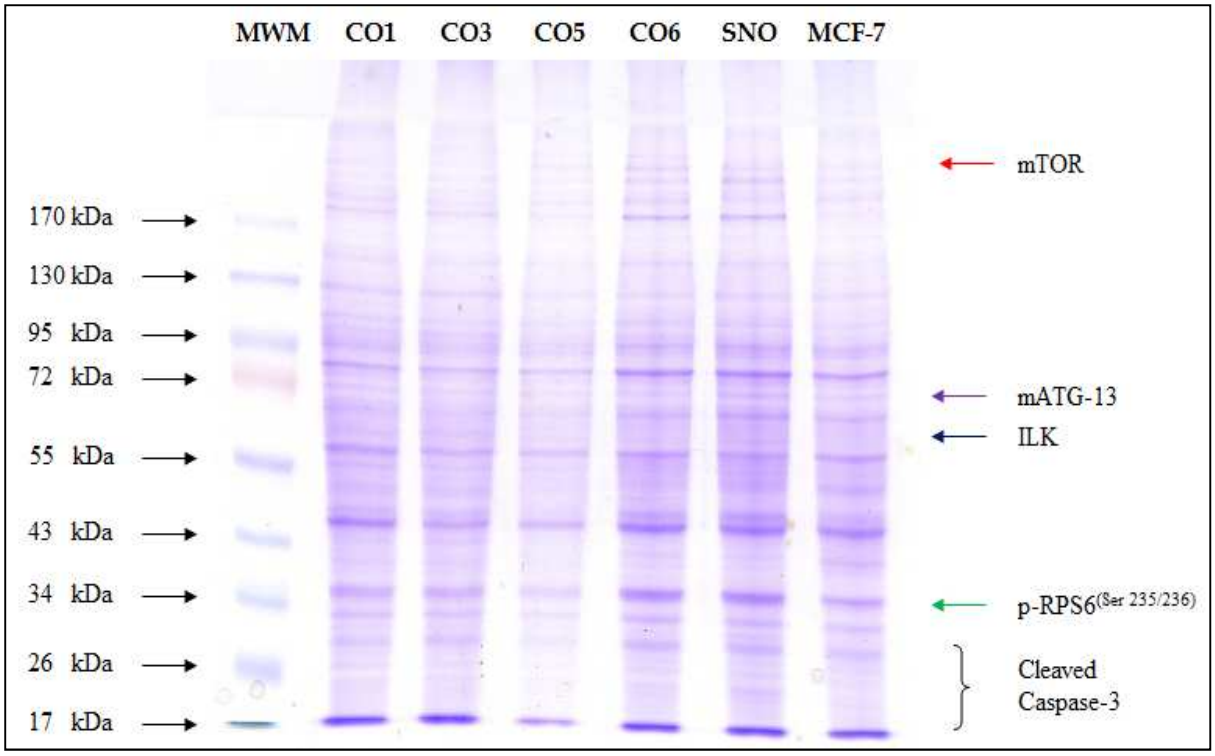

Figure 2.2: Separation of cellular proteins extracted from HOSCC cells. The presence of multiple polypeptide bands of similar staining intensity demonstrated that the extraction of cellular proteins from HOSCC cells was successful, and that the protein estimation was accurate. Staining with Coomassie blue visually confirmed the presence of discreet polypeptide bands at the approximate molecular weight expected for key mTOR pathway intermediates in the marker set. The relative position of these polypeptides is indicated by the coloured arrows, in relation to the molecular weight marker (MWM) in Lane 1. mTOR appears in red (220 kDa), mATG-13 in purple (72 kDa), ILK in blue (59 kDa), p-RS6$^{(Ser\ 235/236)}$) in green (36 kDa) and the cleavage products indicating activated caspase-3 in black brackets (17 – 28 kDa). (CO1 = WHCO1; CO3 = WHCO3; CO5 = WHCO5 and CO6 = WHCO6).

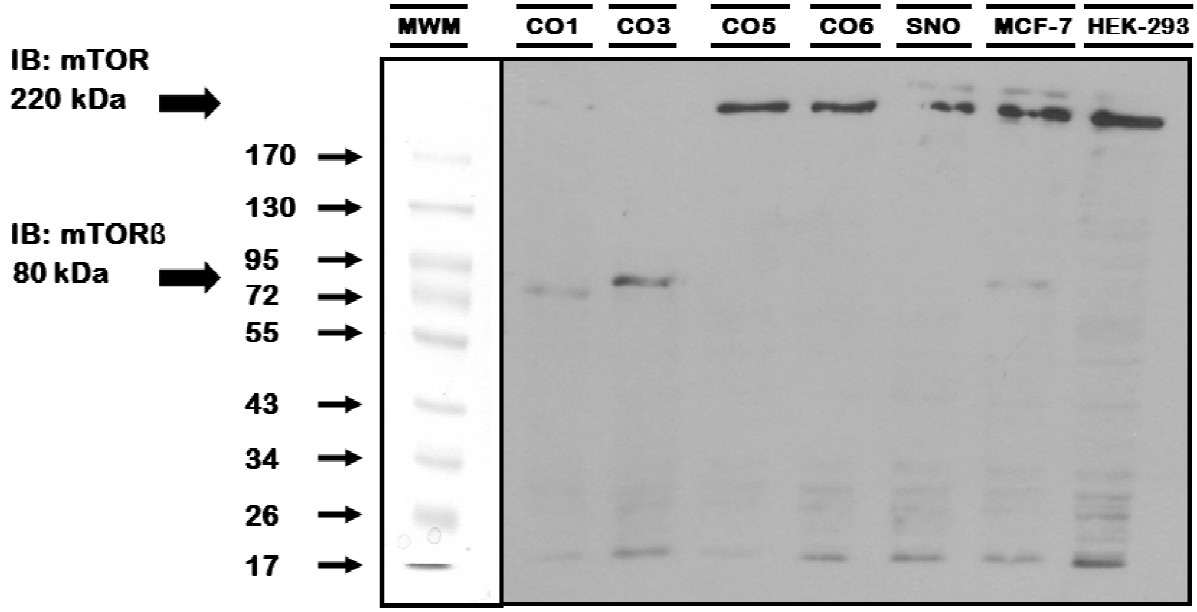

Figure 2.3: Immunodetection of mTOR and mTORβ using a full SDS-PAGE gel. Western blotting using a whole SDS-PAGE gel detected splice variants of the mTOR protein in HOSCC cells. Both the 220 kDa and 80 kDa version of mTOR is expressed by HOSCC cells; however visual assessment of polypeptide bands suggests that mTOR concentrations varies between HOSCC cell lines. WHCO5, WHCO6 and SNO cell lines express appreciably higher mTOR than WHCO1 and WHCO3, whereas WHCO1 and WHCO3 cell lines are the only HOSCC cells to express mTORβ. Immunodetection of discreet mTOR bands at only 220 kDa and 80 kDa also indicate the specificity of the anti-mTOR antibodies for the mTOR protein. This justifies the trimming of subsequent blots. (MWM= Molecular weight marker; CO1 = WHCO1; WHCO3 = WHCO3; CO5 = WHCO5; CO6 = WHCO6).

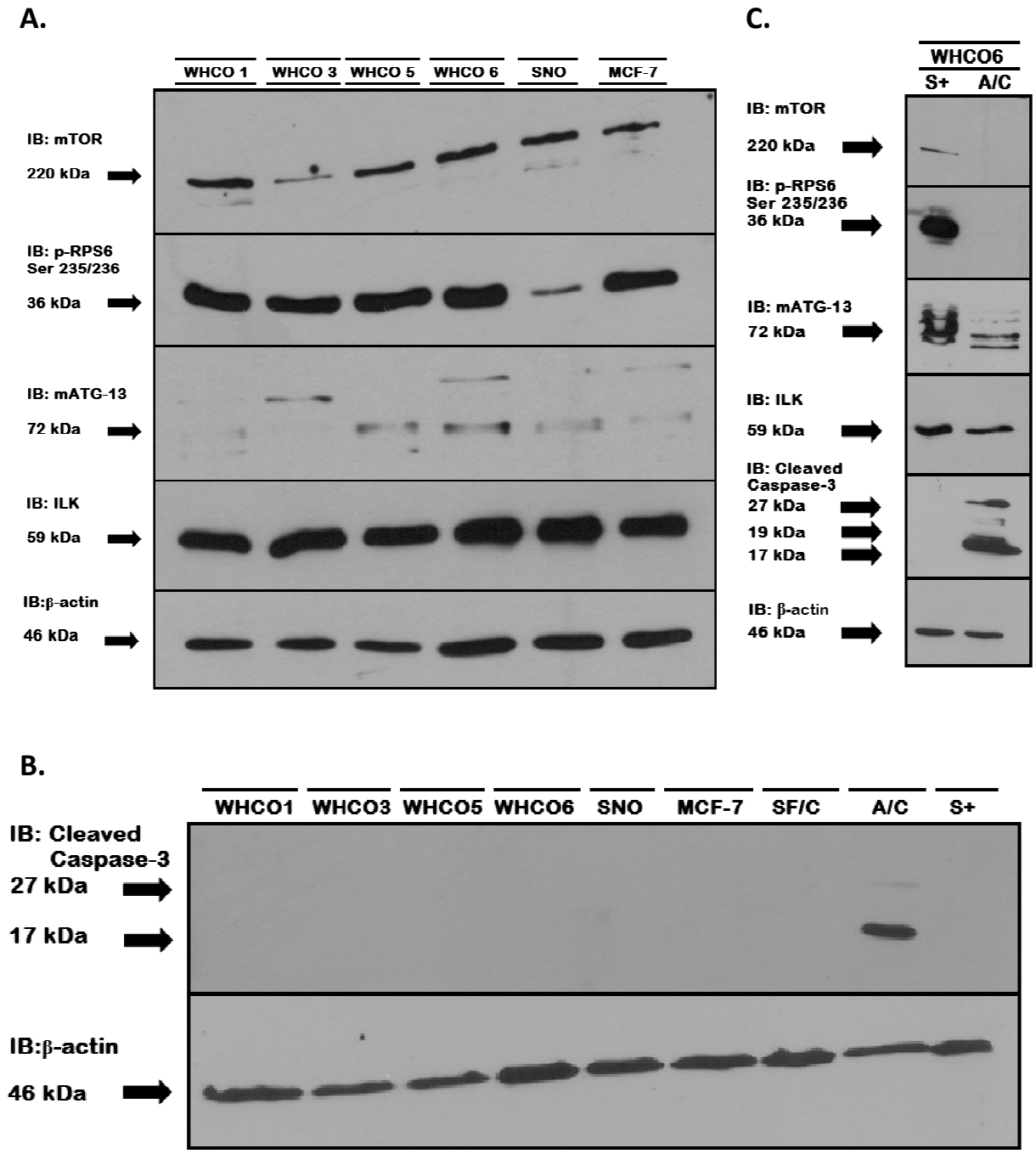

Figure 2.4: Detection of major protein markers identified for the mTOR/mTORC1 signalling pathway. A) mTOR, p-RPS6$^{(Ser\ 235/236)}$, mATG-13 and ILK were detected in the WHCO series, as well as in the MCF-7 control cell line, at 220 kDa, 36 kDa, 72 kDa and 59 kDa, respectively. Marker set proteins were detected under standard tissue culture conditions using monoclonal (anti-p-RPS6$^{(Ser\ 235/236)}$ and anti-mATG-13) or polyclonal (anti-mTOR, anti-ILK) antibodies. **B)** Cleavage fragments indicative of activated caspase-3 were only detected in the apoptotic control (AC) control at 17 and 27 kDa. **C)** Polypeptides corresponding to mTOR (80 kDa) and p-RPS6$^{(Ser\ 235/236)}$ (36 kDa) were not detected under apoptotic conditions, while mATG-13 (72 kDa), ILK (59 kDa) and cleaved caspase-3 (17 – 27 kDa) polypeptides were detected in the apoptotic control (A/C). β-actin was used to demonstrate equal protein loading of HOSCC cell lysates in all blots.

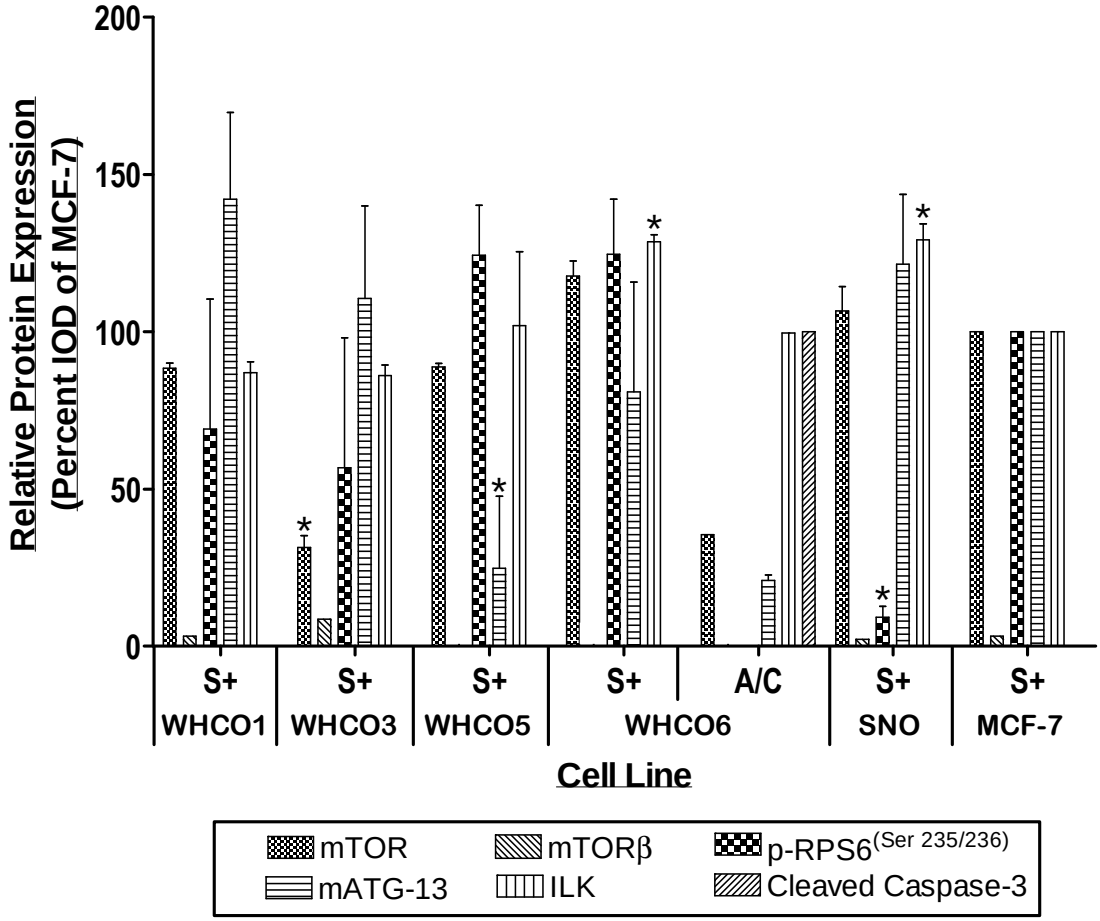

Figure 2.5: Relative expression of major protein markers identified for the mTOR/mTORC1 signalling pathway under standard tissue culture conditions (Serum +). Protein expression levels for marker set proteins were determined by semi-quantitative densitometric analysis, and expressed as a percentage of the MCF-7 cell line. The WHCO series was found to express differential levels of proteins contained in the marker set. As a general trend, HOSCC cells were high expressers of mTOR, mATG-13 and ILK, but either moderate or high expressers of p-RPS6$^{(Ser\ 235/236)}$. Under these conditions, HOSCC cells were also low expressers of mTORβ and cleaved caspase-3, but transitioned to high cleaved caspase-3 expressers under apoptotic conditions (as see in the A/C control). Apoptotic conditions also lead to a shift in the expression of other marker set proteins, where HOSCC cells became low expressers of mTOR, p-RPS6$^{(Ser\ 235/236)}$ and mATG-13, or high expressers of ILK. The presence of any significant difference is indicated graphically by the '*' symbol.

Table 2.1: Summary of protein expression levels and cell line trends for major mTOR pathway intermediates in HOSCC cells.

Protein	Molecular Weight (kDa)	Cell Line						
		WHCO1	WHCO3	WHCO5	WHCO6		SNO	MCF-7
		Serum +	Serum +	Serum +	Serum +	A/C	Serum +	Serum +
mTOR	220	High	* Low	High	High	Low	High	High
mTORβ	80	Low	Low	Not Present	Not Present	Not Present	Not Present	Low
p-RPS6 (Ser 235/236)	36	Med	Med	High	High	Low	* Low	High
mATG-13	72	High	High	* Low	High	Low	High	High
ILK	59	High	High	High	* High	High	* High	High
Cleaved Caspase-3	17 - 28	Low	Low	Low	Low	High	Low	Low

Key: Low = 0 – 45 %; Medium (Med) = 46 – 75 %; High = 76 – 100 % (and above). Protein expression levels are based on the Hager *et al.*, (2011) classification system for analyses of mTOR and p-RPS6 proteins (see Materials and Methodology, Section 2.2.10). The use of a star (*) symbol and red text represents a statistically significant difference, when compared to MCF-7 using a Student's t-test, where $p < 0.05$ (see Appendix D, *Table D1 and D2 for a complete statistical report*). (Serum + = standard tissue culture conditions; A/C = Apoptotic control).

2.4. Discussion

2.4.1. Elevated mTOR expression and enhanced mTORC1 signalling are common features of the mTOR pathway in HOSCC cells

The mTOR pathway forms part of a composite signalling network regulating essential cellular processes, such as metabolism, transcription, translation and autophagy induction, by integrating signalling information from numerous sources (Schmelzle and Hall, 2000). Through the action of mTORC1, mTOR regulates various signal transduction pathway intermediates controlling these processes (Foster and Fingar, 2010; Dobashi *et al.*, 2011). In order to delineate the route of signal transmission through the mTOR pathway and understand how those signals govern autophagy induction in HOSCC cells, it was necessary to monitor the protein expression of key pathway intermediates associated with both mTOR and autophagy induction (see *Figure 2.1.* for an illustration of these pathway intermediates). By monitoring these select cellular proteins, we established an information-rich reporter system conveying specific signalling information about the mTOR pathway and mTORC1-dependent autophagy regulation. Henceforth, we refer to this reporter system as a marker set of proteins.

All protein markers were detected in HOSCC cells under standard tissue culture conditions. This means that HOSCC cells express all relevant mTOR, autophagy and integrin-triggered signal transduction intermediates, as well as that the marker set can be detected efficiently under conditions that represent standard cell growth. Establishing the expression of major pathway intermediates under these conditions was an important prerequisite for later experiments in this investigation to proceed. This is because the protein expression levels detected here serve as a baseline of comparison for subsequent changes arising from any manipulation of standard tissue culture conditions. Furthermore, by establishing relative levels of HOSCC protein expression through comparison with the MCF-7 cell line (rather than to a continuous oesophageal cell line, such as HET-1A), we can find similarities within the corruption of the mTOR signalling pathway in solid epithelial carcinomas. We believed that the HET-1A cell line was not appropriate for comparative analysis during this investigation. This was because HET-1A cells do not truly represent untransformed or physiologically ‘normal’ oesophagus (Jankowski *et al.*, 1995; Underwood *et al.*, 2010), and

most importantly, the status of the mTOR pathway and mTOR protein expression is currently unknown in these cells.

The MCF-7 cell line therefore provides a more suitable comparison as MCF-7 cells are understood to over-express the mTOR protein kinase (Hagner *et al.*, 2009) and display elevated signalling through mTORC1. Alterations of the mTOR pathway in MCF-7 cells was found to be a consequence of an amplification in the *S6K1* gene (Bärlund *et al.*, 2000a; Bärlund *et al.*, 2000b), as well as a result of activating mutation affecting the p110 subunit of PI3K (Bachman *et al.*, 2004; deGraffenried *et al.*, 2004). Mutation of PI3K leads to a constitutively active PI3K/PKB signalling pathway. These alterations enhance mTOR signalling as the PI3K/PKB pathway is the canonical upstream regulator of the mTOR pathway, and p70S6K is a downstream target of mTORC1. Therefore, the MCF-7 cell line represents a more appropriate control cell line for comparative analysis.

Semi-quantitative densitometric analysis of marker set protein expression revealed HOSCC cells express similarly high levels of mTOR and mTORC1 signalling compared to MCF-7 cells (*Figure 2.5*). Ectopic mTOR expression and aberrant mTORC1 signalling has been reported in poorly- and well-differentiated ESCC cells of Chinese origin (Hou *et al.*, 2007; Hirashima *et al.*, 2012), where atypical functioning of the mTOR/mTORC1 signalling pathway is associated with the progression of solid tumours. Since HOSCC cells were found to parallel these findings, it is reasonable to suggest that aberrant mTOR/mTORC1 signalling plays a similar role in HOSCC of South African origin.

A high instance of mTORC1 signalling does not detract from HOSCC cells exhibiting a high basal rate of autophagy induction under standard tissue culture conditions. At first, this seems incongruous, since mTORC1 signalling typically inhibits autophagy; however autophagy is reported to be upregulated in many solid tumours, including EC9706 ESCC cells (Kondo *et al.*, 2005; Liu *et al.*, 2011). Enhanced autophagy induction is thought to provide a selective survival advantage by providing resistance to chemotherapeutic agents and increasing tumour aggressiveness through the provision of essential metabolites and energy under stress (Bursh *et al.*, 1996; Kanzawa *et al.*, 2004; Longo *et al.*, 2008). Considering that HOSCC cells display enhanced cell survival and anoikis resistance (Fanucchi and Veale, 2009; Fanucchi and Veale, 2011), increased basal autophagy may be another component facilitating these events.

HOSCC cells also exhibited increased potential for mechanotransduction through high expression of the promiscuous, integrin-triggered protein kinase; ILK. These findings were in agreement with data previously reported for HOSCC cells by Driver and Veale (2006). ILK is known to play a central role in numerous intracellular signalling pathways affecting mTOR/mTORC1 signalling, such as the PI3K/PKB and Wnt signalling pathways (Wu and Dedhar, 2001). Therefore, an increased propensity for ILK-based signalling combined with ectopic mTOR protein expression may contribute towards transformation and tumourigenesis in HOSCC cells, and provide a rational basis to consider the impact of adhesion-based signal transduction during mTORC1-dependent autophagy regulation.

2.4.2. Expression of the 80 kDa mTORβ splicing isoform in HOSCC may be one explanation for increased signalling through mTORC1

An 80 kDa splicing variant of mTOR, termed mTORβ by Panasyuk *et al.* (2009), was discovered in two HOSCC cells, namely WHCO1 and WHCO3. After an extensive search of the available literature, mTORβ expression is currently only confirmed in HEK-293 cells and, to our knowledge; this is the only report of mTORβ in HOSCC, as well as MCF-7 cells. The WHCO1 and WHCO3 cell lines were the only HOSCC's to exhibit the lowest mTOR protein expression, as well as moderate mTORC1 signalling. Since mTORβ is expressed in these cell lines only, mTORβ may compensate for reduced mTOR protein expression and function to maintain elevated mTORC1 signalling. Panasyuk *et al.* (2009) do report that mTORβ is capable of interacting with both Raptor (of mTORC1) and Rictor (of mTORC2) *in vitro*, and so may readily participate in established mTOR pathway functions, such as phosphorylating p70S6K, 4E-BP1 and PKB. Therefore, HOSCC cells expressing mTORβ will likely gain an advantage to mTORC1-dependant signalling events.

mTORβ is not expressed in the SNO cell line, however, which possesses a high mTOR protein expression, but has a low instance of mTORC1 signalling. This discrepancy between WHCO1, WHCO3 and SNO cell lines may indicate the presence of functionally crippling mutations affecting the *mTOR* gene within the SNO cell line, or hint at the presence of other common alterations affecting upstream or downstream mTOR pathway components (reviewed by Pópulo *et al.*, 2012). Therefore, the expression of mTORβ (depicted in *Figure 2.6* in HOSCC cells may be a significant discovery as its presence may indicate a further corruption affecting the mTOR signalling pathway in HOSCC.

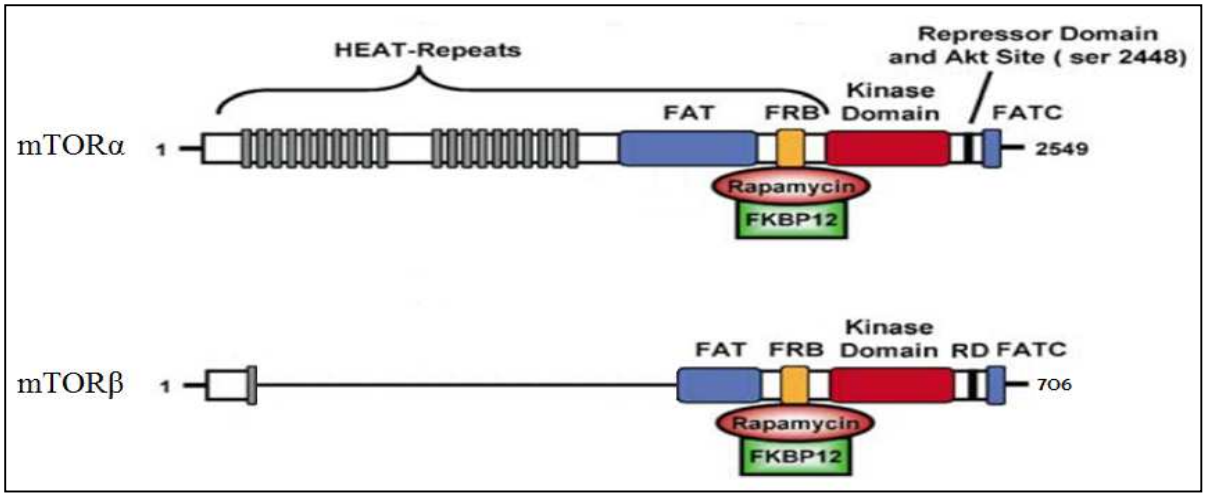

Figure 2.6: Schematic representation of the 80 kDa mTORβ splicing isoform compared to the well characterised 220 kDa mTOR protein kinase. mTORβ is composed of 706 amino-acids, in antithesis to the larger 220 kDa mTOR protein kinase, which is composed of 2 549 amino-acids. mTORβ retains an intact FRB, RD and FATC domains with a notable decrease in amino-acids comprising HEAT-repeat and FAT domains. (Adapted from Fingar and Blenis 2004, and Panasyuk *et al.*, 2009).

In conclusion, monitoring major mTOR pathway intermediates is an effective means of following the mTOR signalling pathway in HOSCC cells. By combining mTOR, p-RPS6$^{(Ser\ 235/236)}$, mATG-13, ILK and cleaved caspase-3 into as a set of protein markers, one establishes an information-rich reporter system conveying specific information about the mTOR pathway, the influence of mTORC1 on autophagy induction, as well as the potential for adhesion-based signal transduction. Through the use of these key pathway intermediates, we have established that the mTOR protein is ectopically expressed, that there is enhanced mTORC1 signalling and that an elevated rate of basal autophagy induction are common features of HOSCC cells. Importantly, by establishing marker set protein expression levels under standard tissue culture conditions, these relative protein concentrations can be used as a base line for further experimentation. This effectively allows for the comparison of protein expression levels under different tissue culture conditions, which forms the basis for the next chapter of this investigation.

CHAPTER 3

3. INVESTIGATION OF THE mTOR SIGNALLING NETWORK IN HOSCC CELLS

3.1. Introduction

A survey of the current literature shows that extracellular-originating signals may be either agonistic or antagonistic towards the mTOR signalling pathway (Sarbassov *et al.*, 2005b; Corradetti and Guan, 2006; Sabatini, 2006; Shor *et al.*, 2009; Caron *et al.*, 2010). Soluble mitogens, such as growth factors and amino-acids, activate mTORC1 under conditions of high abundance (Sarbassov *et al.*, 2005b; Corradetti and Guan, 2006; Sabatini, 2006). However, hypoxia, hyper-osmotic pressure, energy depletion, viral infection, as well as reactive oxygen species (ROS) and DNA damaging agents, may cause cellular stress inhibiting the activation of mTORC1 (Corradetti and Guan, 2006; Shor *et al.*, 2009; Caron *et al.*, 2010). While the influence of each is clearly important for the specific regulation of mTOR within the broader context of mammalian systems (see *Table 3.1* summarising the effects of major agonists and antagonists on mTORC1 activation), this set of analyses focuses mainly on those factors influencing the ability of mTORC1 to regulate autophagy induction in HOSCC cells.

It is well established that mitogenic stimuli derived from growth factors and amino-acids influence homeostasis by augmenting cell growth and proliferation, as well as by triggering autophagy as a cell survival response when absent (Levine and Klionsky, 2004; Zustiak *et al.*, 2008; Burman and Ktistakis, 2010; Wang and Levine, 2010). Since mitogenic signalling may directly affect the intracellular signalling pathways regulating growth and proliferation processes, such as the PI3K/PKB, MAPK signalling cascade and mTOR signalling pathway (Seger and Krebs, 1995; Lemmon and Schlessinger, 2010), the contribution of these stimuli becomes a major focus of this investigation. While hypoxia, hyper-osmotic stress, ROS and energy depletion may also effect the activation of mTORC1, our understanding of mTOR/mTORC1 signalling dynamics leads us to believe that these influences are context-dependant, and so would be standardized under standard tissue culture conditions.

Soluble mitogens therefore elicit biochemical signals that affect mTORC1 signalling through two main modes of regulation, forming what is generally accepted as canonical and non-canonical mTOR regulation (Memmott and Dennis, 2009). Canonical mTOR regulation primarily involves input from the PI3K/PKB pathway and requires a PKB-dependant mechanism for mTORC1 activation. Input from the PI3K/PKB signalling pathway (shown in red) directly causes mTORC1 activation as depicted in *Figure 3.1*. Non-canonical mTOR regulation circumvents biochemical signals transmitted through the PI3K/PKB pathway, and so rather utilizes PKB-independent mechanisms (depicted in blue) to affect mTORC1 (Memmott and Dennis, 2009).

3.1.1. The canonical mTOR pathway utilizes a PKB-dependent mechanism

In response to mitogenic stimuli elicited by RTK's, intracellular propagation of biochemical signals ultimately influences mTOR signalling through PI3K/PKB signalling pathway (see *Figure 3.1, Box A*). PI3K is a lipid kinase activated by the binding of growth factors (such as EGF) to RTK's (such as EGR – which is over-expressed in HOSCC cells) (Osaki *et al.*, 2004; Driver and Veale, 2006), which phosphorylates phosphoinositides and activates PKB. This process is itself regulated by the tumour suppressor PTEN (Harrington *et al.*, 2005). PKB is sequentially phosphorylated on of Thr 308 (by PDK1) and Ser 473 (by either ILK or mTORC2) resulting in its complete activation (Walker *et al.*, 1998; Harrington *et al.*, 2005). Since mTORC2 may also phosphorylate PKB$^{(Ser\ 473)}$, demonstrated both *in vitro* and *in vivo* (Sarbassov *et al.*, 2005b), mTOR may regulate itself at this level in the form of a positive feedback loop.

When active, PKB physically associates with, and thereby activates, numerous substrates; however the phosphorylation of TSC2 and PRAS40 are the most vital for mTORC1 signalling in this canonical pathway (Inoki *et al.*, 2002; Kovacina *et al.*, 2003). TSC2 forms a heterodimeric complex with TSC1 that actively inhibits mTORC1. However, when phosphorylated by PKB on Ser 939 and Thr 1462, the GAP (GTPase-activating protein) activity of TSC1/TSC2 is inhibited – leading to the activation of the Rheb-GTPase (Manning *et al.*, 2002). Consequently, Rheb may directly activate mTORC1 leading to downstream signalling through two main effector kinases: namely p70S6K and 4E-BP1. When activated, p70S6K may directly phosphorylate RPS6 at Ser 235/236, whereas phosphorylation of 4E-BP1 leads to its functional inactivation, thus diminishing its inhibitory affect on eIF4E (Bai

and Jiang, 2010). Moreover, p70S6K may target mTOR itself creating another positive feedback loop (Bai and Jiang, 2010).

Clearly, a lack of PI3K and PKB activation, as well as decreased inhibition of TSC1/TSC2 and PRAS40 leads to a decrease in signalling through mTORC1, events necessary for the induction of autophagy. However, these events are mimicked during non-canonical mTOR regulation, where the availability of nutrients, growth factors and chemical inhibition of mTOR may induce an autophagic response.

3.1.2. The non-canonical mTOR pathway functions independently of PKB

3.1.2.1. Availability of essential nutrients and amino-acids

The mTOR pathway is responsive to the availability of essential nutrients, such as amino-acids found in standard tissue culture serum (like that of foetal calf origin); in particular to levels of the branched chain amino-acids leucine and isoleucine (see *Figure 3.1, Box B*). An increase in cellular concentrations of leucine and isoleucine was shown to induce phosphorylation of p70S6K and 4E-BP1 (Findlay *et al.*, 2007). The molecular mechanisms responsible are thought to include MAP4K3 (demonstrated in serum deprived HeLa cells), however the class III PI3K (hVps34) may also be involved as hVps34 activates mTOR by a mechanism dependent on PI(3,4,5)P_3 generation, but independent of TSC2 or Rheb (Byfield *et al.*, 2005; Nobukuni *et al.*, 2005).

Despite strong support for these mechanisms accounting for mTOR activation, the recent discovery of Rag-GTPases as binding partners of Raptor have become a popular explanation for amino-acid-induced mTOR-stimulation (Sancak *et al.*, 2008). Sekiguchi *et al.* (2001) used cells transfected with constitutively active and inactive Rag mutants, and identified four Rag proteins (Rag A-D), which function as heterodimers to promote the co-localization of Rheb with mTORC1. This demonstrated that Rag proteins are both necessary and sufficient for amino-acid activation of mTOR. Therefore, these four Rag proteins (Rag A-D) may provide the molecular connection responsible for transducing amino-acid-based stimuli to the mTOR signalling machinery.

3.1.2.2. Growth factors and other mitogens

The mTOR signalling pathway may also be activated by the mitogen-activated protein kinase (MAPK) signal transduction cascade (see *Figure 3.1, Box C*). MAPK signalling is stimulated by known agonists present in tissue culture serum; such as growth factors, hormones and chemokines, which bind to cognate RTK's and G-protein coupled receptors (GPCR's) or directly activate protein kinase C (PKC) (McKay *et al.*, 2007; Rozengurt, 2007). MAPK pathways consist of an initial GTPase-regulated kinase (a MAPKKK – such as RAS-GTPase) that activates a kinase intermediate (a MAPKK – such as RAF, MEKK) through a phosphorylation event, which in turn leads activation of downstream effector kinases (a MAPK – such as ERK and p90RSK) (McKay *et al.*, 2007; Rozengurt, 2007). ERK and p90RSK are noteworthy as they participate in extensive pathway integration with the mTOR signalling network. At the upstream level, both ERK and p90RSK influence the TSC1/TSC2 complex allowing for increased signalling through mTORC1.

ERK and p90RSK may induce phosphorylation of Raptor (a defining protein subunit of mTORC1) promoting mTORC1 phosphorylation of p70S6K and 4E-BP1 (Foster *et al.*, 2010; Carreire *et al.*, 2011). Moreover, p90RSK may phosphorylate RPS6$^{(Ser\ 235/236)}$ (Roux *et al.*, 2007). This particular function of p90RSK becomes an issue of concern as p-RPS6$^{(Ser\ 235/236)}$ is used in this study as a marker for active mTORC1 signalling.

3.1.3. Additional aspects of non-canonical mTOR regulation: specific inhibition with rapamycin

Aberrant activation of mTOR signalling contributes towards much pathology, including tumourigenesis (Foster and Toschi, 2009). In light of this, mTOR has become an attractive therapeutic target with many clinical trials experiencing some success with modern analogues of its natural inhibitor, the macrolide ester rapamycin. Rapamycin, first isolated from the bacterium *Streptomyces hygroscopicus*, is a potent antifungal and immunosuppressive agent (Vézina *et al.*, 1975). When rapamycin binds the intracellular receptor, FKBP12, rapamycin may inhibit the kinase activity of mTOR through interaction with the mTOR FRB domain (Brown *et al.*, 1994). Rapamycin treatment decreases mTORC1 activity in a dose-dependent manner (Foster and Toschi, 2009) and therefore constitutes an additional level of complexity regulating mTOR signalling (see *Figure 3.1, Box D*). Hence, it would be irresponsible to

ignore this aspect of mTOR regulation as this may afford the opportunity to explore the implications of mTOR-specific inhibition as a therapeutic tool for the treatment of SCC affecting the human oesophagus.

Therefore, with the aim of investigating the mTOR signalling network in HOSCC cells, we examined the unique contribution of soluble extracellular-originating stimuli that effectively support regulated cell growth and proliferation, under standard tissue culture conditions. This provides an opportunity to dissect the impact of canonical- and non-canonical modes of mTOR regulation in HOSCC cells known to over-express key biochemical receptors, such as EGFR. It also allows us to determine how specific modes of mTOR regulation impact mTORC1-dependant autophagy induction. Thus, the ability of HOSCC cells to modulate the signalling machinery inducing autophagy was examined through: i) negating canonical mTOR pathway regulation by specific inhibition of PI3K; ii) modulation of mTORC1 signalling by withdrawal of essential growth factors, nutrients and amino-acids found in standard tissue culture serum; iii) specific inhibition of mTOR with rapamycin; and iv) the potential for signal integration between mTOR and MAPK pathways by specific inhibition of p90RSK.

Table 3.1: Major agonists and antagonistic factors known to influence the mTOR signalling network in mammalian systems.

Agonist/ Antagonist	Affect on mTORC1 Activation	Proteins Involved	Molecular Mechanism	Major References
Growth Stimulators **EGF, Insulin**	↑	PI3K, PKB, ERK, RSK	Reduces TSC1/TSC2 inhibition by phosphorylation of PKB, ERK and RSK	Potter *et al.* (2002); Roux *et al.* (2004)
Amino-acid Depletion **Leucine, Isoleucine**	↓	Rheb, Raptor, hVps34, hVPS15	Many competing hypotheses	Hara *et al.* (1998); Gao *et al.* (2002)
Hyperosmotic Stress **Sorbitol, NACl**	↓	Not completely elucidated	An unknown osmotic stress-induced phosphatase disrupts the mitochondrial protein gradient	Parrott and Templeton (1999); Desai *et al.* (2002)
ROS **Peroxide, Thiol oxidants**	Unclear: ↑ and ↓	Raptor, mTORC1	May involve disulfide reduction of mTOR	Bae *et al*. (1999); Sarbassov and Sabatini (2005a)
Hypoxia **Decreased oxygen supply**	↓	REDD1, HIF-1	HIF-1-induced REDD1 expression enhances TSC1/TSC2 inhibition of mTOR	Hudson *et al.* (2002); Arsham *et al.* (2003)
Energy Depletion **Low ATP:ADP ratio**	↓	LKB1, AMPK	Phosphorylation of AMPK increases TSC1/TSC2 activity	Inoki *et al.* (2003b); Corradetti *et al.* (2004)
Viral Infection **Adenovirus, HCMV**	Unclear: ↑ and ↓	Adenovirus; E4-ORF1, HCMV: EGFR	Several virus-dependant mechanisms proposed	Kudchodkar *et al.* (2004); O'Shea *et al.* (2005)
DNA damaging Agents **Etoposide, Methyl methane-sulfonate**	↓	p53, REDD1	Upregulation of p53 through several proposed mechanisms	Tee and Proud (2000); Beuvink *et al.* (2005)

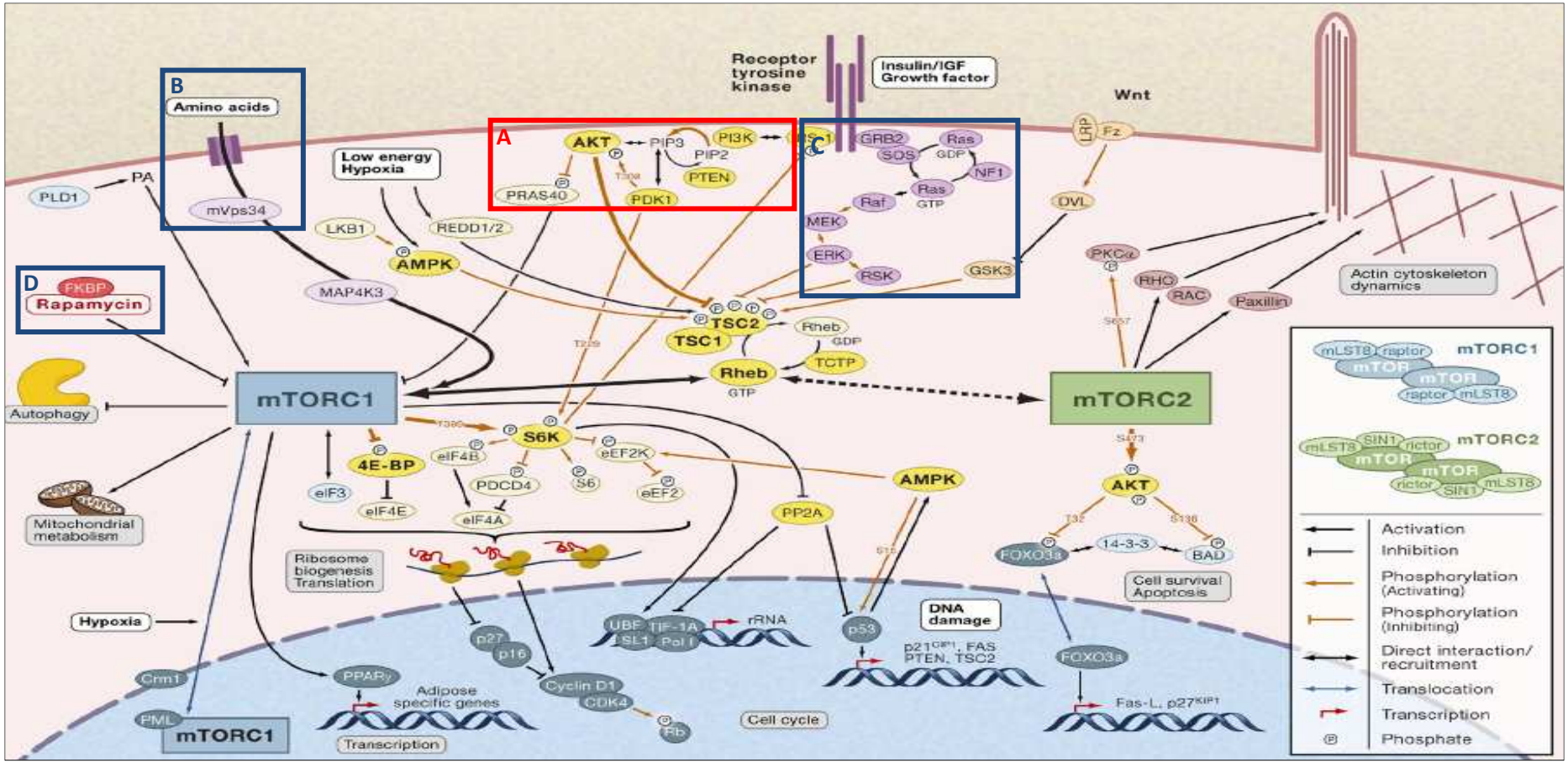

Figure 3.1: A simplified visual schematic of the mTOR signalling network. Important signal transduction pathways that influence signalling through mTORC1, as well as mTORC2, are depicted. Canonical upstream regulators of mTORC1, such as PI3K/PKB (Box A), are influenced by soluble mitogens like insulin and growth factors. In addition, non-canonical upstream regulators may influence mTORC1 activity; such as essential nutrients and amino-acids (Box B), MAPK-derived stimuli (Box C), rapamycin (Box D), as well as hypoxia, Wnt signals and energy status, either directly through physical interactions with mTOR/mTORC1 or indirectly through critical upstream nodes (Adapted from Soulard and Hall, 2007).

3.2. Materials and Methodology

3.2.1. Tissue Culture of WHCO, MCF-7 and HEK-293 Cell Lines

All cell lines were cultured as described previously in Chapter 2, Section 2.2.1.

3.2.2. Sub-culture of WHCO, MCF-7 and HEK-293 Cell Lines

As previously described (see Chapter 2, Section 2.2.2).

3.2.3. Serum-free Tissue Culture

Cell cultures were exposed to an environmental stress simulating starvation conditions so as to bring about a change in cell behaviour, and therefore a particular survival response. Since the removal of serum is a commonly used method used to achieve this in the literature (Avruch *et al.*, 2009; Bai and Jiang, 2010), serum withdrawal was employed here. Consequently, cell cultures were allowed to proliferate under standard tissue culture conditions until 10 cm dishes reached a confluence of approximately 80 %. The medium was then aspirated and cell monolayer washed twice with PBS (37 °C) (Appendix A, 1.1.1). Subsequently, 10 ml fresh tissue culture medium lacking 10 % FCS was added. Tissue cultures were then incubated in a humid, 37 °C incubator with an atmosphere of 5 % CO_2 in air for 24 hours.

3.2.4. Antibodies

As previously described (see Chapter 2, Section 2.2.3).

3.2.5. Pathway Inhibition Studies

3.2.5.1. Specific inhibition of PI3K with LY294002

Vlahos *et al.* (1994) showed that LY294002, or 2-(4-morpholinyl)-8-phenyl-4H-1-benzopyran-4-one, completely and specifically abolished Bovine brain phosphatidylinositol 3-kinase activity (IC_{50} = 0.43 μg/ml; 1.40 μM). However, previous studies in the Cell biology Research Laboratory, University of the Witwatersrand, Johannesburg, observed that 20 μM LY294002 was the appropriate concentration required to induce PI3K-specific inhibition in HOSCC cells (Shaw Ph.D. Thesis, 2011).

Therefore, cell cultures were allowed to proliferate until 6 cm dishes reached a confluence of approximately 80 %. The medium was then aspirated and cell monolayer washed twice with PBS. Subsequently, 3 ml fresh tissue culture medium with 10 % FCS was added, containing a final concentration of 20 μM LY294002 (Sigma-Aldrich®, USA) (Appendix A, 1.8.1). HOSCC cells treated with 20 μM LY294002 were designated 'L+', while an untreated control (designated 'L-') was simultaneously prepared. Tissue cultures were subsequently incubated in a humid, 37 °C incubator with an atmosphere of 5 % CO_2 in air for 1 hour. Please note that all procedures for one set of experiments were performed using the same batch of FCS.

3.2.5.2. Specific inhibition of mTOR with rapamycin

Since very few studies have specifically looked at the affect of rapamycin treatment on the mTOR/mTORC1 signalling pathway in moderately differentiated HOSCC, the appropriate tissue culture conditions were chosen after considering the study performed by Hou *et al.* (2007). Hou *et al.* (2007) investigated the effects of rapamycin and siRNA against mTOR in poorly- (EC9706) and well-differentiated (Eca 109) ESCC cells. Here, changes in both mTOR and p70S6K mRNA and protein expression levels were detected in response to 20, 50 and 100 nM concentrations of rapamycin for 6 and 24 hours, as these conditions were found to induce mTOR-specific changes to cell proliferation, survival and apoptosis in squamous cell carcinomas, specifically.

Therefore, since a similar response in South African-derived HOSCC was expected, cell cultures were allowed to proliferate until 6 cm dishes (Nunc) reached a confluence of approximately 80 %. The medium was then aspirated and cell monolayer washed twice with PBS (37 °C). Subsequently, 3 ml fresh tissue culture medium with 10 % FCS was added, containing a final concentration of 0, 20, 50 and 100 nM rapamycin (Sigma-Aldrich®, USA) (Appendix A, 1.9.1). Tissue cultures were incubated in a humid, 37 °C incubator with an atmosphere of 5 % CO_2 in air for 6 or 24 hours. Please note that all procedures for one set of experiments were performed using the same batch of FCS.

3.2.5.3. Specific inhibition of p90RSK with BI-D1870

Cell cultures were allowed to proliferate until 6 cm dishes reached a confluence of approximately 80 %. The medium was then aspirated and cell monolayer washed twice with PBS (37 °C). Subsequently, 3 ml fresh tissue culture medium with 10 % FCS was added,

containing a final concentration of 10 μM as described by Sapkota *et al*. (2007) (Appendix A, 1.10.1). BI-D1870 was obtained from the Division of Signal Transduction Therapy, University of Dundee. Simultaneously, controls for each cell line containing 0.1 % DMSO were prepared. Tissue cultures were then incubated in a humid, 37 °C incubator with an atmosphere of 5 % CO_2 in air for 30 min. Please note that all procedures for one set of experiments were performed using the same batch of FCS.

3.2.6. Triton X-100-based Protein Extraction

As previously described (see Chapter 2, Section 2.2.5).

3.2.7. Protein Estimation

As previously described (see Chapter 2, Section 2.2.6).

3.2.8. SDS-PAGE (Sodium Dodecyl Sulphate-Polyacrylamide Gel Electrophoresis)

As previously described (see Chapter 2, Section 2.2.7).

3.2.9. Western Immunoblot Analysis

As previously described (see Chapter 2, Section 2.2.8).

3.2.10. Image Capturing

As previously described (see Chapter 2, Section 2.2.9).

3.2.11. Laser Densitometry and Analysis of Relative Protein Expression

Semi-quantitative densitometric analysis was used to determine protein expression across the WHCO series, as well as MCF-7 and HEK-293 cell lines, as previously described in Chapter 2, Section 2.2.10. Additionally, both raw and worked densitometric data is available in Appendix C, *Tables C6-C13*.

3.2.12. Statistical Analysis

Results are expressed as the mean ± S.E. Statistical significance was determined by Student's *t*-test for comparative analysis (see Appendix D, *Table D3*) using Sigma Plot®, Version 12.0 (SPSS Science, Chicago, Illinois USA), where $p < 0.05$ indicates statistical significance. All experiments were repeated at least three times, unless otherwise indicated.

3.3. Results

3.3.1. Specific inhibition of PI3K with LY294002 increased mTOR and ILK protein expression, but decreased p-RPS6$^{(Ser\ 235/236)}$ and mATG-13 in HOSCC cells

Specific inhibition of PI3K with LY294002 did not visibly modulate the concentration of polypeptide bands indicative of mTOR (220 kDa), ILK (59 kDa) and cleaved caspase-3 (17 – 27 kDa) (*Figure 3.2, A and B*). However, clearly visible changes in the concentration of polypeptides indicative of p-RPS6$^{(Ser\ 235/236)}$ (36 kDa) and mATG-13 (72 kDa) were detected. In addition, multiple bands were observed in proximity to mATG-13 (*Figure 3.2, A*), while cleaved caspase-3 (17 – 27 kDa) was only visible in the WHCO6 apoptotic cell (A/C) control (*Figure 4.5, B*).

Semi-quantitative densitometric analysis of single polypeptide bands revealed a change in relative protein expression levels across all WHCO cell lines in response to PI3K-specific inhibition with LY294002 (*Figure 3.3*). Levels of marker set protein expression were expressed as a percentage of the WHCO6 cell line (without LY294002 treatment; L-), since WHCO6 cells consistently expressed high levels of all major pathway intermediates detected under standard tissue culture conditions (established earlier in Chapter 2, Section 2.4). For this reason, the WHCO6 cell line was also used as a loading control enabling the comparison of protein expression between individual western blots, and is used as such throughout the rest of this investigation.

By organising all signal transduction pathway intermediates into a table summarising changes in the levels of protein expression (such as that seen in *Table 3.2*), we observed that specific trends in protein expression emerged between the WHCO series of cell lines. In general, mTOR protein abundance was increased upon inhibition of PI3K; where HOSCC cells became high mTOR protein expressers. Only the WHCO6 was the exception to this trend. Similarly, WHCO1, WHCO3, WHCO5 and MCF-7 cells tended to increase ILK protein expression (with the exception of the WHCO6 and SNO cell lines); consequently maintaining elevated ILK in HOSCC cells.

In response to specific inhibition of PI3K, HOSCC cells became low p-RPS6$^{(Ser\ 235/236)}$ protein expressers; where WHCO1, WHCO5, WHCO6, SNO and MCF-7 cells commonly decreased p-RPS6$^{(Ser\ 235/236)}$ protein expression. However, this excluded the WHCO3 cell line, as p-RPS6$^{(Ser\ 235/236)}$ protein expression increased. Following this trend, mATG-13 protein expression remained moderate-to-high, despite HOSCC cells commonly decreasing cellular concentrations of dephosphorylated mATG-13. Only the WHCO5 cell line exhibited an increase for mATG-13 protein expression. Moreover, specific inhibition of PI3K with LY294002 was insufficient to induce an increase in cleaved caspase-3 protein expression in HOSCC cells.

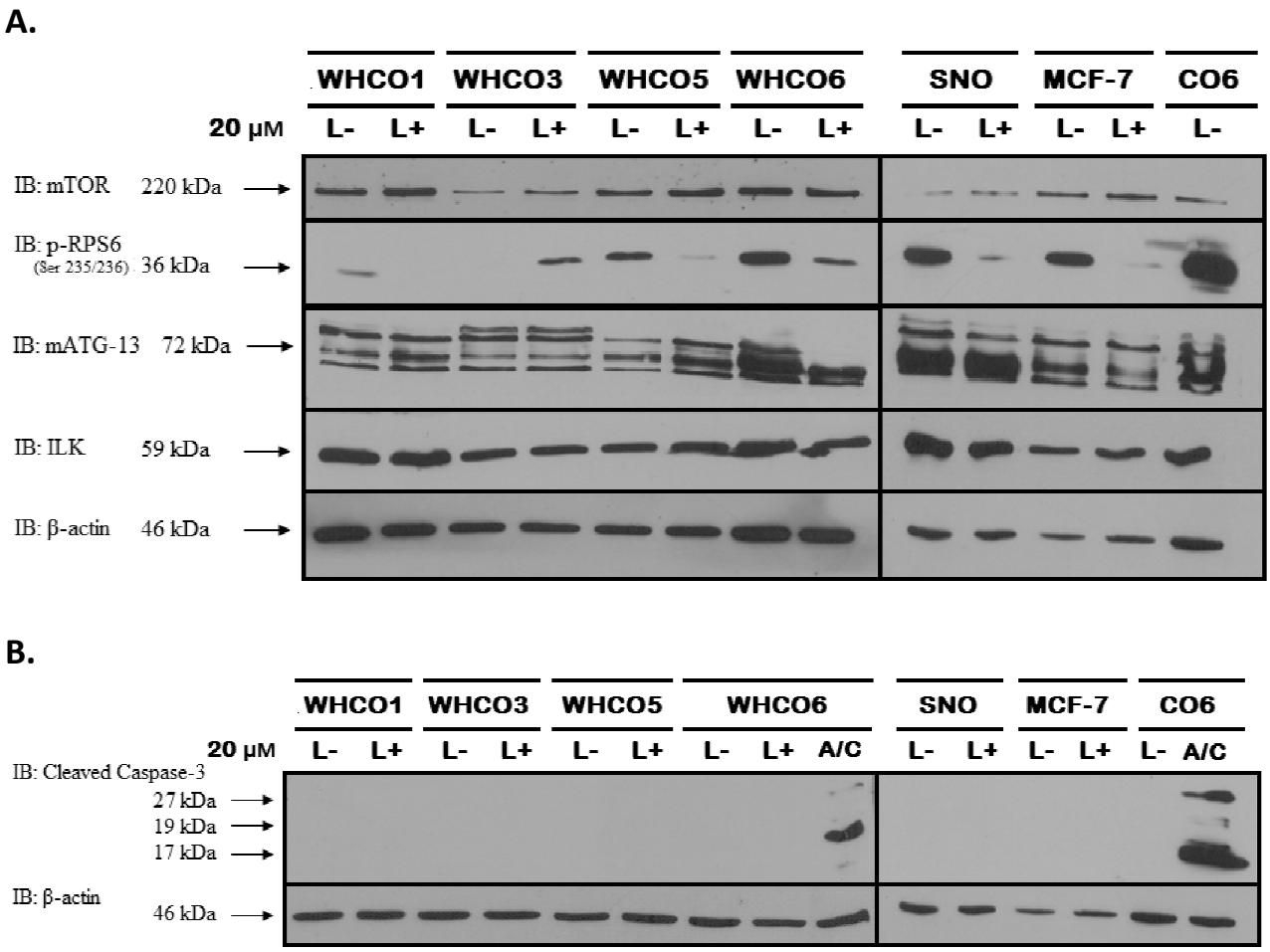

Figure 3.2: Immunodetection of significant signal transduction intermediates in HOSCC cells after specific inhibition of PI3K with LY294002. A) Visible changes in polypeptide abundance were detected for mTOR (220 kDa), p-RPS6$^{(Ser\ 235/236)}$ (36 kDa), but not for ILK (59 kDa) and mATG-13 (72 kDa), in HOSCC cells. **B)** Specific inhibition of PI3K was insufficient to induce cleavage of pro-caspase-3, as cleaved caspase-3 (17 - 27) was only detected in apoptotic cell (A/C control). In both A) and B), β-actin was used to demonstrate equal protein loading of HOSCC cell lysates. (L+/L- = With or without 20 µM LY294002; A/C = Apoptotic Cell control; CO6 = WHCO6).

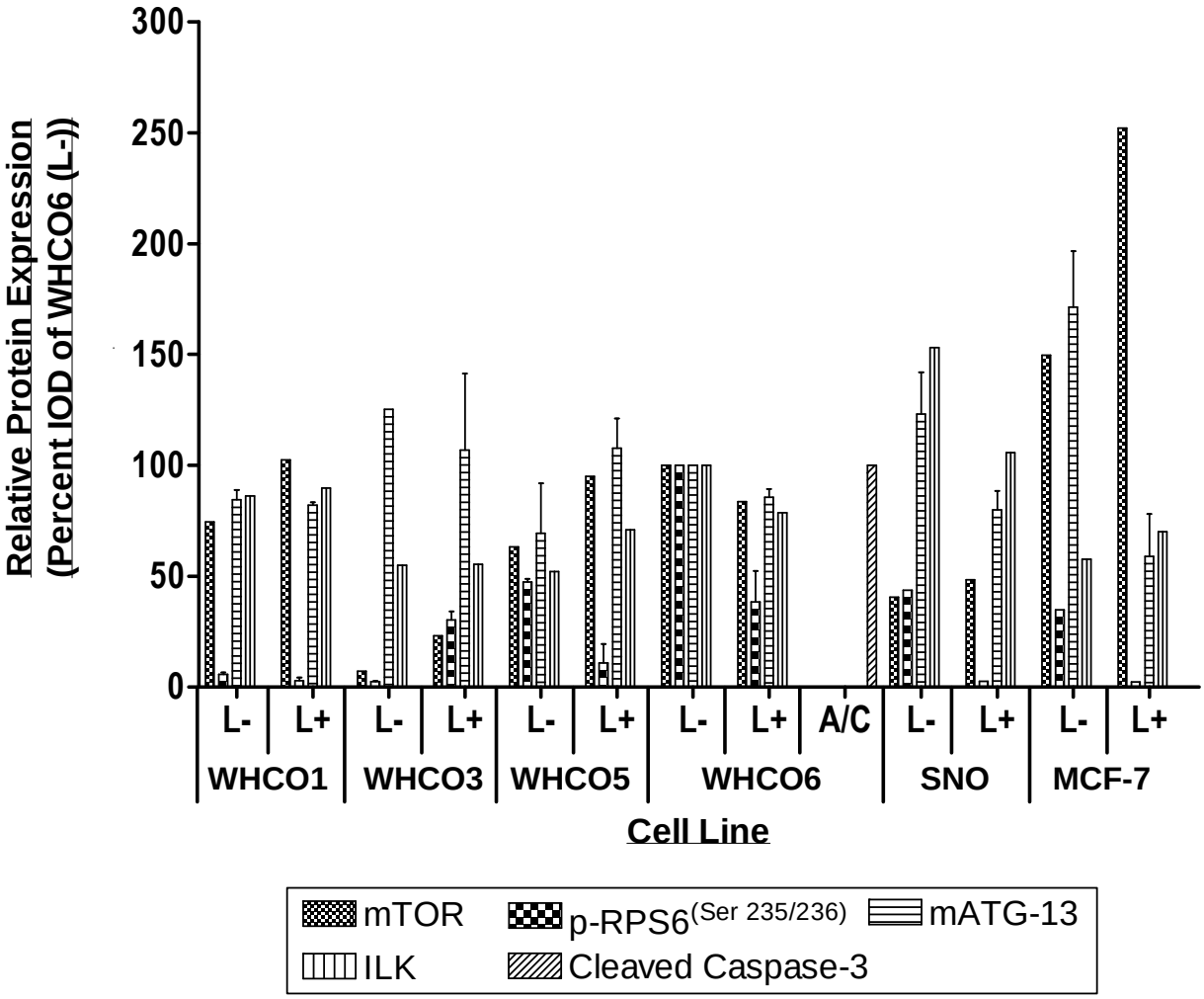

Figure 3.3: Specific inhibition of PI3K alters the expression of key mTOR pathway intermediates in HOSCC cells. Semi-quantitative densitometric analysis of protein expression was determined relative to the WHCO6 (L^-) cell line. As a common trend, HOSCC cells increased mTOR and ILK protein abundance, but decreased p-RPS6$^{(Ser\ 235/236)}$ and mATG-13 expression. Cleaved caspase-3 remained undetectable under these tissue culture conditions, and was only detectable in apoptotic control cells. Since not all western blots were repeated more than once, the significance of these data could not be calculated. (L- = Without PI3K-specific inhibition with LY294002; L+ = Including PI3K-specific inhibition with LY294002; A/C = Apoptotic Cell control).

Table 3.2: Summary of the protein expression levels obtained for significant mTOR signal transduction intermediates after specific inhibition of PI3K with LY294002.

Protein	Cell Line																	
	WHCO 1			WHCO 3			WHCO 5			WHCO 6			SNO			MCF-7		
	↑/↓	H/M/L	% Δ	↑/↓	H/M/L	% Δ	↑/↓	H/M/L	% Δ	↑/↓	H/M/L	% Δ	↑/↓	H/M/L	% Δ	↑/↓	H/M/L	% Δ
mTOR	↑	High	36.0	↑	Low	228.6	↑	High	50.8	↓	High	-16.0	↑	Med	17.1	↑	High	68.0
p-RPS6 (Ser 235/236)	↓	Low	-50.0	↑	Low	140.0	↓	Low	-76.6	↓	Low	-62.0	↓	Low	-93.2	↓	Low	-94.3
mATG-13	↓	High	-2.4	↓	High	-14.40	↑	High	56.5	↓	High	-14.0	↓	High	-35.0	↓	Med	-65.5
ILK	↑	High	4.7	↑	Med	0.010	↑	Med	36.5	↓	High	-21.0	↓	High	-30.7	↑	Med	20.7
Cleaved Caspase-3	/	Low	N.A.	/	Low	N.A.	/	Low	N.A.	/	Low	N.A.	/	Low	N.A.	/	Low	N.A.

Key: Low = 0 – 45 %; Medium (Med) = 46 – 75 %; High = 76 – 100 % (and above). Protein expression levels are based on the Hager *et al.*, (2011) classification system for analyses of mTOR and p-RPS6 proteins (see Materials and Methodology, Section 3.2.11). Change in relative marker set protein expression is expressed as percent change (% Δ), designated by either positive (↑) or negative (↓) arrows. For the calculation of percent change, see Appendix B, Equation B1. The forward slash (/) symbol indicates that no change has occurred.

3.3.2. Serum withdrawal modulates the mTOR/mTORC1 pathway in HOSCC cells

Removal of the growth stimulatory effects of serum visibly altered the protein expression of key mTOR pathway intermediates in HOSCC cells. Single polypeptide bands corresponding to mTOR (220 kDa), p-RPS6$^{(Ser\ 235/236)}$ (36 kDa), mATG-13 (72 kDa) and ILK (59 kDa) were detected, however the concentrations of mTOR and p-RPS6$^{(Ser\ 235/236)}$ was visibly diminished (*Figure 3.4, A*). Clear changes in the concentrations of mATG-13 and ILK polypeptide bands were not apparent. In addition, single polypeptide bands corresponding to cleaved caspase-3 (17 – 27 kDa) were not detected in HOSCC cells under serum-free conditions, but were only present in WHCO6 apoptotic control (A/C) cells (*Figure 3.4, B*). β-actin (46 kDa) was also detected by western blot, where its uniform expression represented equal protein loading between the WHCO series of cell lines.

Semi-quantitative densitometric analysis of single polypeptide bands revealed a change in relative protein expression levels across the WHCO series of cell lines in response to serum withdrawal after 24 hours (*Figure 3.5*). Levels of marker set protein expression were expressed as a percentage of the WHCO6 cell line (under standard tissue culture conditions; serum +), where protein expression between WHCO cell lines was determined to be low, moderate or high (see Materials and Methodology, Section 3.2.11 for an explanation of the Hager *et al.* (2011) classification system for protein expression). After organizing major signalling intermediates into a table summarising levels of protein expression, we noticed that specific trends emerged, both within the level of protein expression and between the WHCO series of cell lines (*Table 3.3*).

In general, serum withdrawal induced HOSCC cells to decrease mTOR protein expression. A decrease in mTOR expression was observed in WHCO3, WHCO5, WHCO6 and MCF-7 cells, which became moderate or low mTOR expressers. Notably, cells of the WHCO3 cell line significantly decreased mTOR protein expression (*see Appendix D, Table D3* for a complete statistical analysis). In antithesis, cells of WHCO1 and SNO cell lines increased mTOR protein expression, where the increase in SNO cells was considered to be a significant change (a report of this statistical analysis is also available in *Appendix D, Table D3*).

All HOSCC cells experienced a decrease in RPS6$^{(Ser\ 235/236)}$ phosphorylation (clearly observed in *Figure 3.5* and *Table 3.3*), where p-RPS6$^{(Ser\ 235/236)}$ expression changed to either moderate or low. Serum withdrawal significantly decreased p-RPS6$^{(Ser\ 235/236)}$ expression in WHCO3, WHCO6 and SNO cells (see *Appendix D, Table D3* for a complete statistical analysis). As a result of this decrease for RPS6$^{(Ser\ 235/236)}$ phosphorylation in all HOSCC cells, mATG-13 protein expression was generally increased (*Figure 3.5* and *Table 3.3*). There was an increase in mATG-13 abundance in WHCO1, WHCO6 and SNO cell lines; however not in cells of the WHCO3 or WHCO5 lines. The change exhibited by mATG-13 in the WHCO3 cell line was considered to be a significant decrease (a report of this statistical analysis is available in *Appendix D, Table D3*).

It was also apparent that HOSCC cells generally decreased ILK protein expression in response to serum withdrawal (seen in *Figure 3.5* and *Table 3.3*). A significant decrease was observed in WHCO3 and WHCO6 cell lines (*see Appendix D, Table D3* for all statistical analyses), however despite this trend, ILK protein expression remained high in HOSCC cells. Only SNO cells increased ILK protein abundance. Furthermore, cleaved caspase-3 remained undetectable in the WHCO series of cell lines in response to serum withdrawal. Therefore, HOSCC cells were classified as low cleaved caspase-3 expressers under serum-free tissue culture conditions.

Besides for these trends in marker set protein expression, we noticed common behavioural responses regarding the mTOR pathway between WHCO cell lines. Cell lines were observed to behave in a similar manner in response to serum withdrawal, although there were some outliers. The first type of behavioural response was shown by the WHCO3 and WHCO5 cell lines because they decreased the expression of all proteins monitored in the marker set. The second type of behavioural response was displayed by the WHCO1, WHCO6 and SNO cell lines as they followed the same trends in p-RPS6$^{(Ser\ 235/236)}$ and mATG-13 expression, but only differed by one protein trend (either mTOR or ILK expression) in response to serum withdrawal. Consequently, HOSCC cells conformed to different types of protein expression trends, as well as displayed different behavioural responses, when growth stimulatory signals from serum were removed.

A.

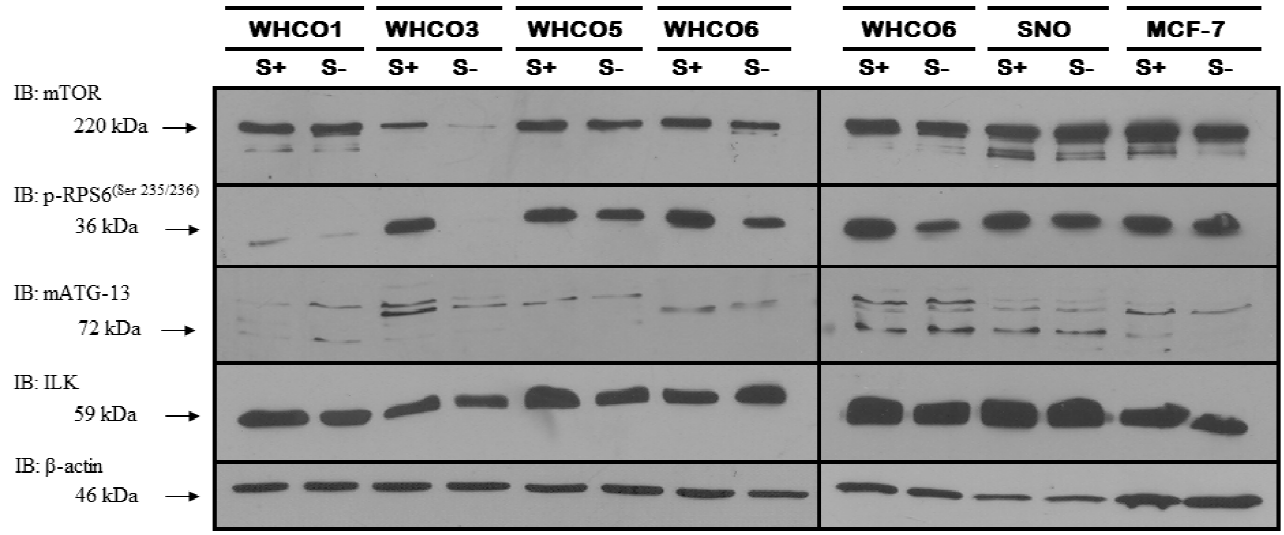

B.

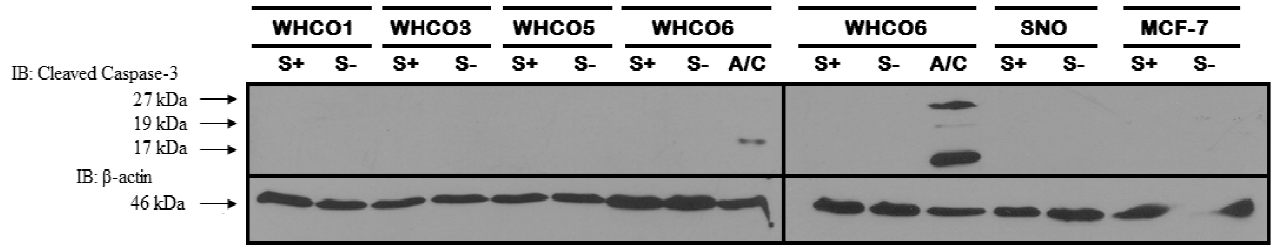

Figure 3.4: Immunodetection of critical signal transduction intermediates in HOSCC cells in response to the withdrawal of serum. A) Single polypeptide bands signifying marker set proteins were detected after serum-free tissue culture for 24 hours. mTOR, p-RPS6$^{(Ser\ 235/236)}$, mATG-13 and ILK were detected in HOSCC cells, as well as the MCF-7 cell line, at 220, 36, 72 and 59 kDa, respectively. **B)** The cleavage fragments indicative of activated caspase-3 were only detected in the apoptotic cell (A/C) control at 17, 19 and 28 kDa. In both A) and B), β-actin was used to demonstrate equal protein loading of HOSCC cell lysates. (S+ = Standard tissue culture conditions; S- = serum-free tissue culture conditions for 24 hours; A/C = Apoptotic Cell control).

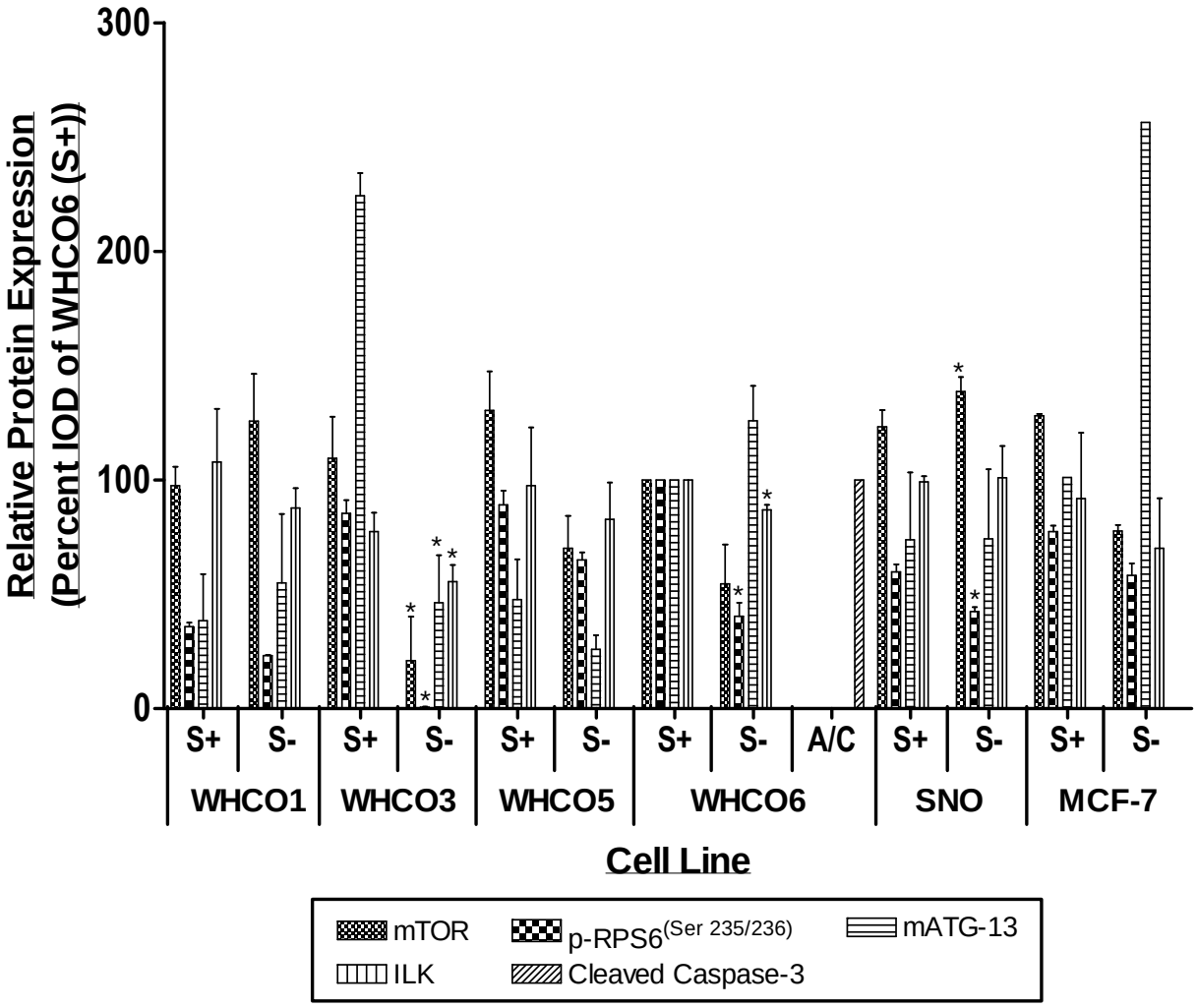

Figure 3.5: Serum withdrawal modulates the protein expression of key signal transduction intermediates of the mTOR pathway in HOSCC cells. Semi-quantitative densitometric analysis of protein expression for each signalling intermediate contained within the marker set is expressed as a percentage of the WHCO6 cell line. A visible change in protein expression can be seen for marker set proteins when each is detected under serum-free tissue culture conditions after 24 hours. As a general trend, HOSCC cells decreased mTOR, p-RPS6$^{(Ser\ 235/236)}$ and ILK protein expression, but increased mATG-13 protein expression. The cleavage fragments indicating activated caspase-3 were not detected under these conditions, indicating that serum withdrawal for this time period is insufficient to induce an apoptotic response. Since all western blots were repeated more than once, the significance of these data could be determined. Significant difference is therefore indicated graphically through the use of the star (*) symbol. (S+ = Standard tissue culture conditions; S- = serum-free tissue culture conditions for 24 hours; A/C = Apoptotic Cell control).

Table 3.3: Summary of the protein expression levels for key mTOR signal transduction intermediates in HOSCC cells after serum withdrawal for 24 hours.

Protein	Cell Line																	
	WHCO1			WHCO3			WHCO 5			WHCO6			SNO			MCF-7		
	↑/↓	H/M/L	% Δ	↑/↓	H/M/L	% Δ	↑/↓	H/M/L	% Δ	↑/↓	H/M/L	% Δ	↑/↓	H/M/L	% Δ	↑/↓	H/M/L	% Δ
mTOR	↑	High	28.6	* ↓	* Low	* -80.9	↓	Med	-46.2	↓	Med	-45.0	* ↑	* High	* 13.0	↓	High	-39.1
p-RPS6 (Ser 235/236)	↓	Low	-36.1	* ↓	* Low	* -98.8	↓	Med	-27.0	* ↓	* Low	* -60.0	* ↓	* Low	* -30.0	↓	Med	-25.6
mATG-13	↑	Med	44.7	* ↓	* Low	* -79.5	↓	Low	-45.8	↑	High	26.0	↑	Med	0.00	↑	High	153.5
ILK	↓	High	-18.5	* ↓	* Med	* -27.3	↓	High	-15.3	* ↓	* High	* -13.0	↑	High	2.02	↓	Med	-23.9
Cleaved Caspase-3	/	Low	N.A.	/	Low	N.A.	/	Low	N.A.	/	Low	N.A.	/	Low	N.A.	/	Low	N.A.

Key: Low = 0 – 45 %; Medium (Med) = 46 – 75 %; High = 76 – 100 % (and above). Protein expression levels are based on the Hager *et al.*, (2011) classification system for analyses of mTOR and p-RPS6 proteins (see Materials and Methodology, Section 3.2.11). Change in relative marker set protein expression is expressed as percent change (% Δ), designated by either positive (↑) or negative (↓) arrows. For the calculation of percent change, see Appendix B, Equation B1. The use of a star (*) symbol, as well as red text, represents a statistically significant difference when compared to WHCO6 cell line, determined using a Student's t-test; where $p < 0.05$ (see Appendix D, *Table D3 for a statistical report*). The forward slash (/) symbol indicates that no change has occurred.

3.3.3. Rapamycin treatment differentially modulates mTOR, mATG-13 and ILK expression, but abolishes RPS6$^{(Ser\ 235/236)}$ phosphorylation in HOSCC cells

Since the PI3K/PKB pathway is the most commonly accepted route for biochemical signals affecting the mTOR pathway (Hay, 2005; Bhasker and Hay, 2007; Bai and Jiang, 2010), we believed it was first necessary to assess the influence of soluble mitogenic signals transmitted from PI3K to mTOR/mTORC1. Only after these mechanisms of canonical mTOR regulation were established in HOSCC cells did we think it appropriate to examine the effects of relevant non-canonical modes of mTOR regulation, such as nutrient deprivation and rapamycin treatment. For these reasons we now continue with the second part of this analysis - specific inhibition of the mTOR signalling pathway with rapamycin.

After exposing HOSCC cells to rapamycin, we monitored the same set of key protein markers by western blotting (*Figure 3.6*). However, only cells of the WHCO6 (*Figure 3.6, A*) and SNO lines (*Figure 3.6, B*) were selected for rapamycin treatment. This was because the WHCO6 cell line is currently used as an important internal control (the reader is reminded that the WHCO6 cell line is standard carried through separate experiments providing a means to compare protein expression between different western blots). Additionally, WHCO6 and SNO cell lines conform to unique behavioural and protein expression trends (see Section 3.3.1) and so characterise the diversity present within the HOSCC model system. Since these cell lines are an appropriate representation of the WHCO series, we monitored the marker set in response to rapamycin within these HOSCC cells, only.

Exposure to rapamycin, for either 6 or 24 hours, noticeably altered polypeptides corresponding to mTOR (220 kDa), p-RPS6$^{(Ser\ 235/236)}$ and mATG-13 (72 kDa), but not ILK (59 kDa) (*Figure 3.6, A - C*). The uniformity of β-actin polypeptide bands (46 kDa) suggest that an equal amount of protein was loaded for all HOSCC cell lysates. Furthermore, since the concentration of β-actin did not change, this seems to indicate that rapamycin does not affect β-actin gene expression in HOSCC cells.

Semi-quantitative densitometric analysis confirmed that rapamycin altered marker set protein expression levels within HOSCC cells, at both 6 and 24 hours (*Figure 3.7, A - D*). Changes in protein expression were expressed as percentage of the WHCO6 cell line not treated with rapamycin (0 nM). These data show that specific inhibition of mTOR resulted in the

differential modulation of mTOR protein expression in HOSCC cells (*Figure 3.7*, *A*). As the concentration of rapamycin increased, so too did the level of mTOR protein expression in WHCO6 and MCF-7 cell lines. This trend was not observed in the SNO cell line, however. We could not identify any definitive protein expression trend for mTOR in the SNO cell line as the expression of mTOR varied greatly in response to rapamycin treatment. Despite this, mTOR protein expression was generally higher in HOSCC cells treated for 6 hours than HOSCC cells treated for 24 hours, but generally lower after treatment in comparison to HOSCC cells not exposed to rapamycin.

Semi-quantitative densitometric analysis also showed that rapamycin treatment decreased p-RPS6$^{(Ser\ 235/236)}$ protein expression in all HOSCC cells (*Figure 3.7*, *B*). These changes occurred in a dose-dependent manner for each cell line, producing an identical decreasing trend in RPS6$^{(Ser\ 235/236)}$ phosphorylation at both 6 and 24 hours. Normally, a steep rise in mATG-13 concentration would accompany decreasing RPS6$^{(Ser\ 235/236)}$ phosphorylation (Loewith *et al.*, 2002). However, with an increase in rapamycin concentration, the protein expression of mATG-13 protein expression generally decreased in HOSCC cells, somewhat resembling a dose-dependent decrease for mATG-13 expression in WHCO6 and SNO cell lines (*Figure 3.7 C*). A steep change in mATG-13 protein expression was observed at 24 hours for WHCO6 cells, whereas this trend occurred at both 6 and 24 hours for the SNO cell line.

Furthermore, inhibition of mTOR with rapamycin did not modulate ILK protein expression (*Figure 3.7*, *D*). As the concentration of rapamycin increased, ILK protein expression remained relatively constant in both WHCO6 and SNO cell lines, as well as MCF-7 cells. A noticeable change was only observed in cells of WHCO6 cell line at 6 hours post treatment, where ILK seemed to experience a dose-dependent decrease in protein expression. However, since not all western blots were performed more than once, an accurate statistical analysis could not be performed. Consequently, this affected our reporting of significant alterations in marker set protein expression. However, we did succeed in showing that specific inhibition of mTOR modulates key mTOR pathway intermediates, especially abolishing RPS6$^{(Ser\ 235/236)}$ phosphorylation in HOSCC cells (shown in *Table 3.4*).

A.

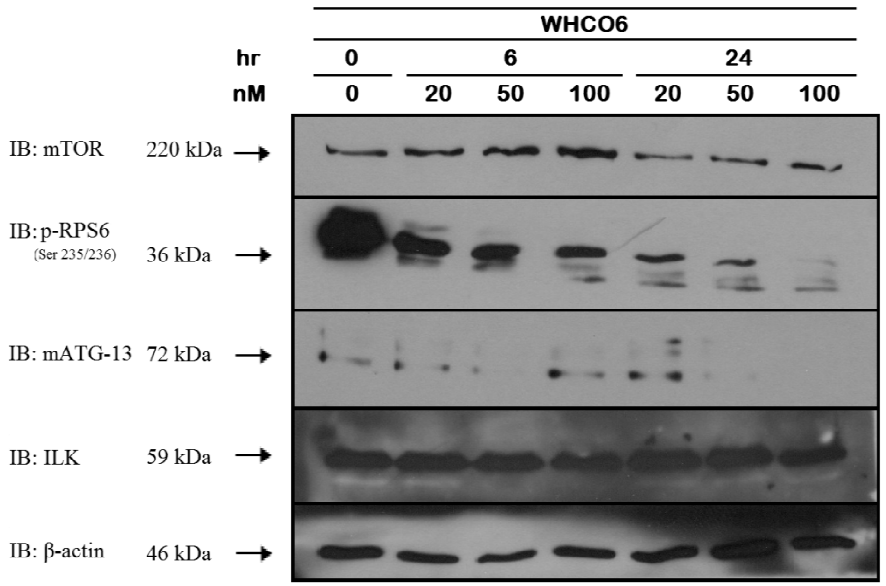

B.

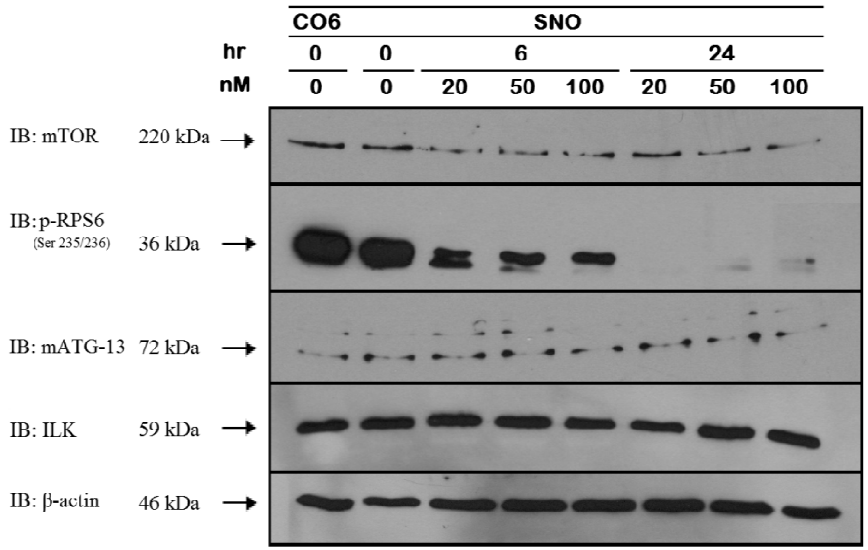

C.

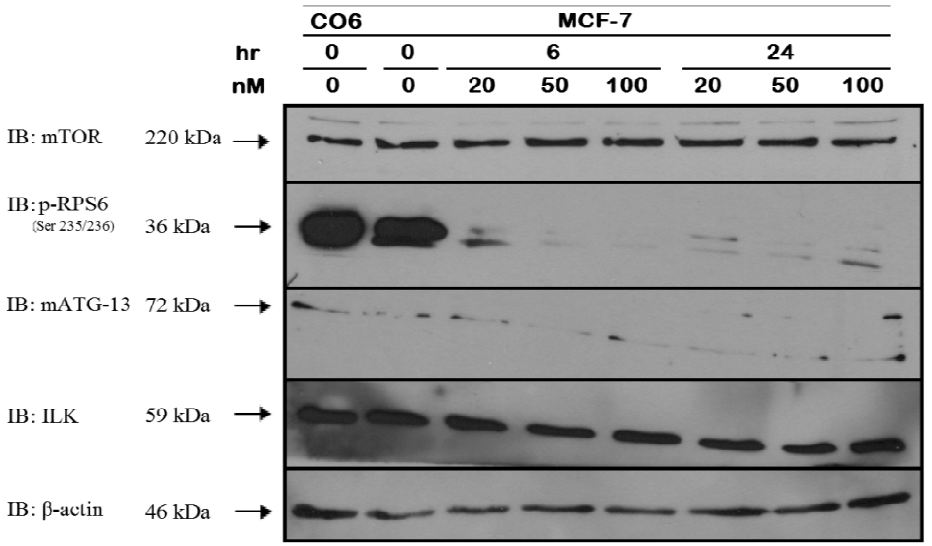

Figure 3.6: Immunodetection of important signal transduction intermediates in HOSCC cells after exposure to rapamycin. Increasing concentrations of rapamycin induced visible changes in polypeptides corresponding to mTOR (220 kDa), p-RPS6$^{(Ser\ 235/236)}$ (36 kDa), mATG-13 (72 kDa), but not ILK (59 kDa). This was observed in WHCO6 **(A)**, SNO **(B)** and MCF-7 **(C)** lines, where β-actin (46 kDa) demonstrated equal protein loading of HOSCC cell lysates. HOSCC cells are clearly susceptible to rapamycin treatment as exposure modulated mTOR and p-RPS6$^{(Ser\ 235/236)}$ protein concentrations, even at concentrations as low as 20 nM. However, an increase in mATG-13 polypeptides did not accompany this decrease in mTORC1 signalling and ILK expression appeared to be unaffected by rapamycin treatment. (hr = time, in hours, cells were treated with rapamycin; nM = nanomolar concentration of rapamycin used; CO6 = WHCO6).

A.

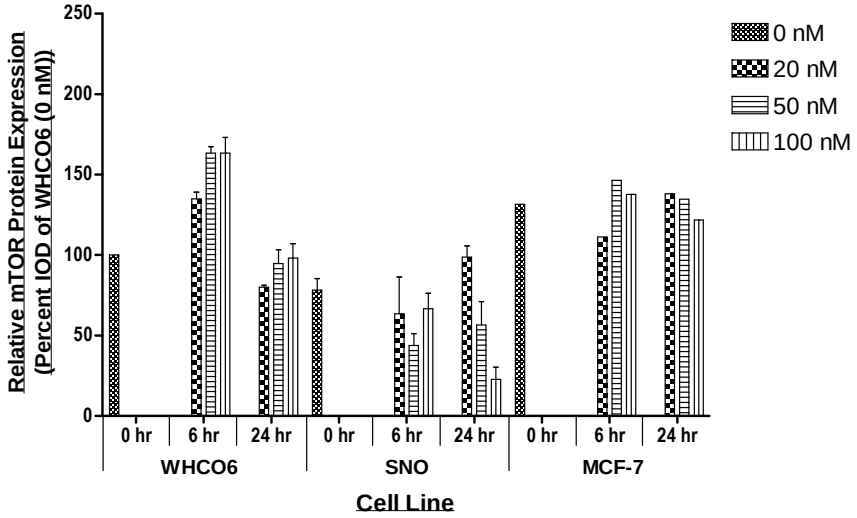

B.

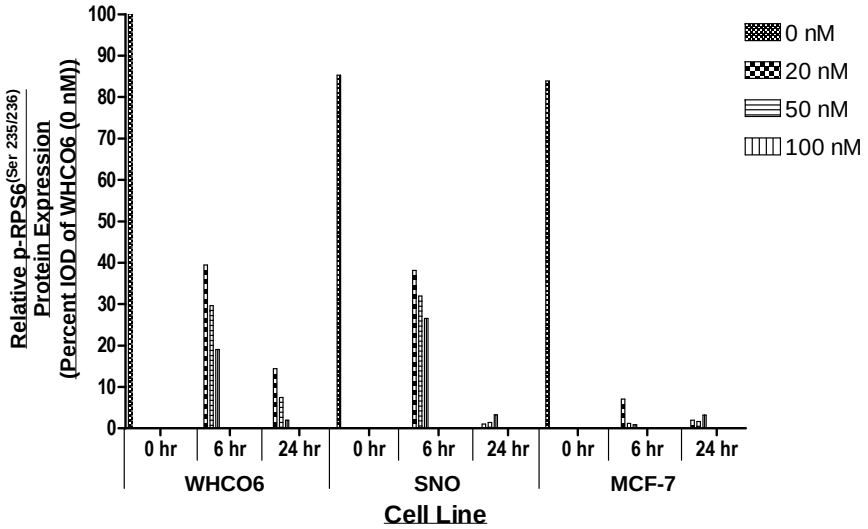

C.

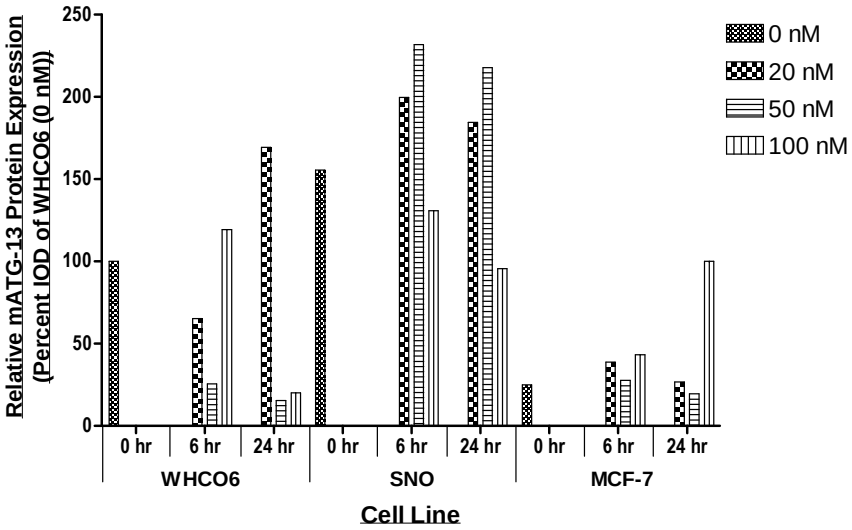

D.

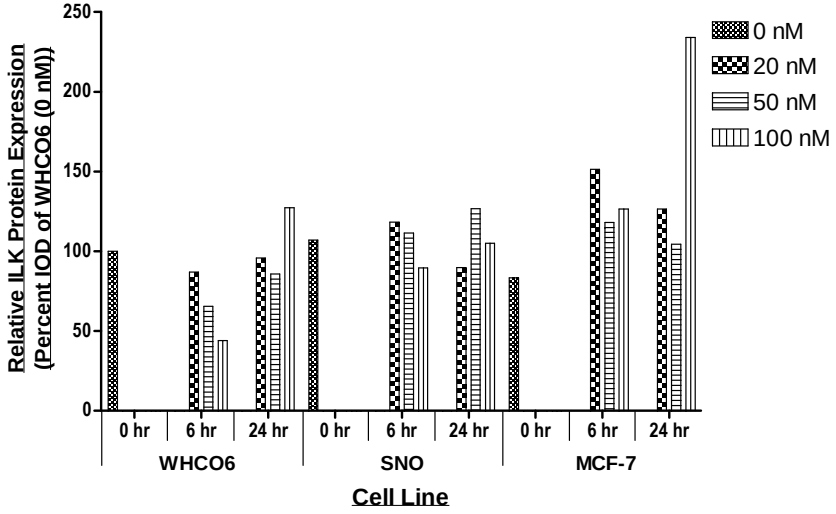

See next page for legend.

Figure 3.7: Effects of rapamycin on the protein expression of key signal transduction pathway intermediates. A) mTOR protein expression increased in a dose-dependent manner in cells of the WHCO6 line, however this trend was not evident in SNO or MCF-7 cells. **B)** RPS6$^{(Ser\ 236/236)}$ phosphorylation was also completely abolished in all HOSCC cells, occurring in a dose-dependent manner. **C)** A trend increase in mATG-13 protein expression was observed only in the SNO cell line, while there was no clear pattern for mATG-13 expression in the WHCO6 cell line 6 or 24 hours post rapamycin treatment. **D)** ILK protein expression was generally unaffected after rapamycin treatment and remained high in cells of the SNO line. However, a dose-dependent decrease for ILK expression was observed 6 hours post treatment in WHCO6 cells. Since not all western blots were repeated more than once, the significance of these data could not be determined. (hr = indicates the amount of hours cells were treated with rapamycin; nM = the specific nanomolar concentration of rapamycin used).

Table 3.4: Summary of protein expression levels obtained after specific inhibition of mTOR with rapamycin.

Protein	Rapamycin Treatment Conditions		Cell Line								
			WHCO6			SNO			MCF-7		
	Time (hr)	Concentration (nM)	↑/↓	H/M/L	% Δ	↑/↓	H/M/L	% Δ	↑/↓	H/M/L	% Δ
mTOR	6	20	↑	High	35.00	↓	Med	-19.23	↓	High	-15.91
		50	↑	High	63.00	↓	Low	-43.59	↑	High	10.61
		100	↑	High	98.00	↓	Med	-14.10	↑	High	4.55
	24	20	↓	High	-20.00	↑	High	26.92	↑	High	4.55
		50	↓	High	-5.00	↓	Med	-26.92	↑	High	2.27
		100	↓	High	-2.00	↓	Low	-70.51	↓	High	-7.58
p-RPS6 (Ser 235/236)	6	20	↓	Low	-61.00	↓	Low	-55.29	↓	Low	-91.67
		50	↓	Low	-70.00	↓	Low	-62.35	↓	Low	-98.81
		100	↓	Low	-81.00	↓	Low	-68.24	↓	Low	-98.81
	24	20	↓	Low	-86.00	↓	Low	-98.82	↓	Low	-97.62
		50	↓	Low	-93.00	↓	Low	-98.82	↓	Low	-97.62
		100	↓	Low	-98.00	↓	Low	-96.47	↓	Low	-96.43

Table 3.4 continued												
Protein	**Rapamycin Treatment Conditions**		**Cell Line**									
			WHCO6			**SNO**			**MCF-7**			
	Time (hr)	**Concentration (nM)**	**↑/↓**	**H/M/L**	**% Δ**	**↑/↓**	**H/M/L**	**% Δ**	**↑/↓**	**H/M/L**	**% Δ**
mATG-13	**6**	**20**	↓	Med	-35.00	↑	High	29.03	↑	Low	56.00
		50	↓	Low	-74.00	↑	High	49.68	↑	Low	12.00
		100	↑	High	19.00	↓	High	-15.48	↑	Low	72.00
	24	**20**	↑	High	69.00	↑	High	18.71	↑	Low	8.00
		50	↓	Low	-84.00	↑	High	40.65	↓	Low	-24.00
		100	↓	Low	-80.00	↓	High	-38.06	↑	High	300.00
ILK	**6**	**20**	↓	High	-13.00	↑	High	10.28	↑	High	81.93
		50	↓	Med	-34.00	↑	High	3.74	↑	High	42.17
		100	↓	Low	-56.00	↓	High	-15.89	↑	High	53.01
	24	**20**	↓	High	-4.00	↓	High	-15.89	↑	High	51.81
		50	↓	High	-14.00	↑	High	18.69	↑	High	25.30
		100	↑	High	27.00	↓	High	-1.87	↑	High	181.93

Key: Low = 0 – 45 %; Medium (Med) = 46 – 75 %; High = 76 – 100 % (and above). Protein expression levels are based on the Hager *et al.*, (2011) classification system for analyses of mTOR and p-RPS6 proteins (see Materials and Methodology, Section 3.2.11). Change in relative marker set protein expression is expressed as percent change (% Δ), designated by either positive (↑) or negative (↓) arrows. For the calculation of percent change, see Appendix B, Equation B1. The use of a forward slash (/) symbol indicates that no change has occurred.

3.3.4. RPS6$^{(Ser\ 235/236)}$ is phosphorylated by mTORC1 in the absence of MAPK/p90RSK signals in HOSCC cells

Although recent reports suggest that BI-D1870 is an effective and specific inhibitor of p90RSK signalling (Kang *et al.*, 2007; Chen and MacKintosh, 2009; Xian *et al.*, 2009), we needed to establish that BI-D1870 could produce an observable decrease in RPS6$^{(Ser\ 235/236)}$ phosphorylation. Therefore, we specifically inhibited p90RSK in HEK-293 cells with BI-D1870 according to the manufacturer's instructions (see Materials and Methodology, Section 3.2.5.3). Through western blotting we observed that only the abundance of p-RPS6$^{(Ser\ 235/236)}$ (36 kDa) polypeptides, and not mTOR (220 kDa), were affected (*Figure 3.8, A*). β-actin (46 kDa) was also detected, where its expression was found to be uniform, thus representing equal protein loading of the HEK-293 cell lysates.

Once we established that this concentration of BI-D1870 could effectively reduce p-RPS6$^{(Ser\ 235/236)}$ protein expression in commonly used substrate-dependent cells of mammalian origin, we used BI-D1870 to inhibit p90RSK signalling in the WHCO series of cell lines. Here, the WHCO5, WHO6, and SNO cell lines were used as representatives of HOSCC. Immunodetection of mTOR (200 kDa) and p-RPS6$^{(Ser\ 235/236)}$ (36 kDa) polypeptides revealed that inhibition of p90RSK with the same concentration of BI-D1870 produced no clear change in mTOR or p-RPS6$^{(Ser\ 235/236)}$ protein abundance (*Figure 3.8*, *B*). This lack of change was corroborated by the detection of identical β-actin polypeptide bands (46 kDa), which indicate consistency during protein loading of HOSCC cell lysates.

Semi-quantitative densitometric analysis of mTOR and p-RPS6$^{(Ser\ 235/236)}$ polypeptide revealed that only RPS6$^{(Ser\ 235/236)}$ phosphorylation, and not mTOR protein expression levels, were decreased in HEK-293 cells following specific inhibition of p90RSK with BI-1870 (*Figure 3.9*). However, similar modulation of mTOR and p-RPS6$^{(Ser\ 235/236)}$ protein expression levels was not observed in HOSCC cells. mTOR and p-RPS6$^{(Ser\ 235/236)}$ protein expression did not decrease appreciably in HOSCC cells. In fact, besides these minimal changes, p-RPS6$^{(Ser\ 235/236)}$ protein expression increased in the SNO cell line. Furthermore, no noteworthy changes to mTOR or p-RPS6$^{(Ser\ 235/236)}$ protein expression were observed in the MCF-7 cell line. Consequently, when p90RSK signalling was inhibited with BI-D1870, HOSCC cells were observed to generally decrease both mTOR and p-RPS6$^{(Ser\ 235/236)}$ protein expression (see *Table 3.5* for a summary of these trends).

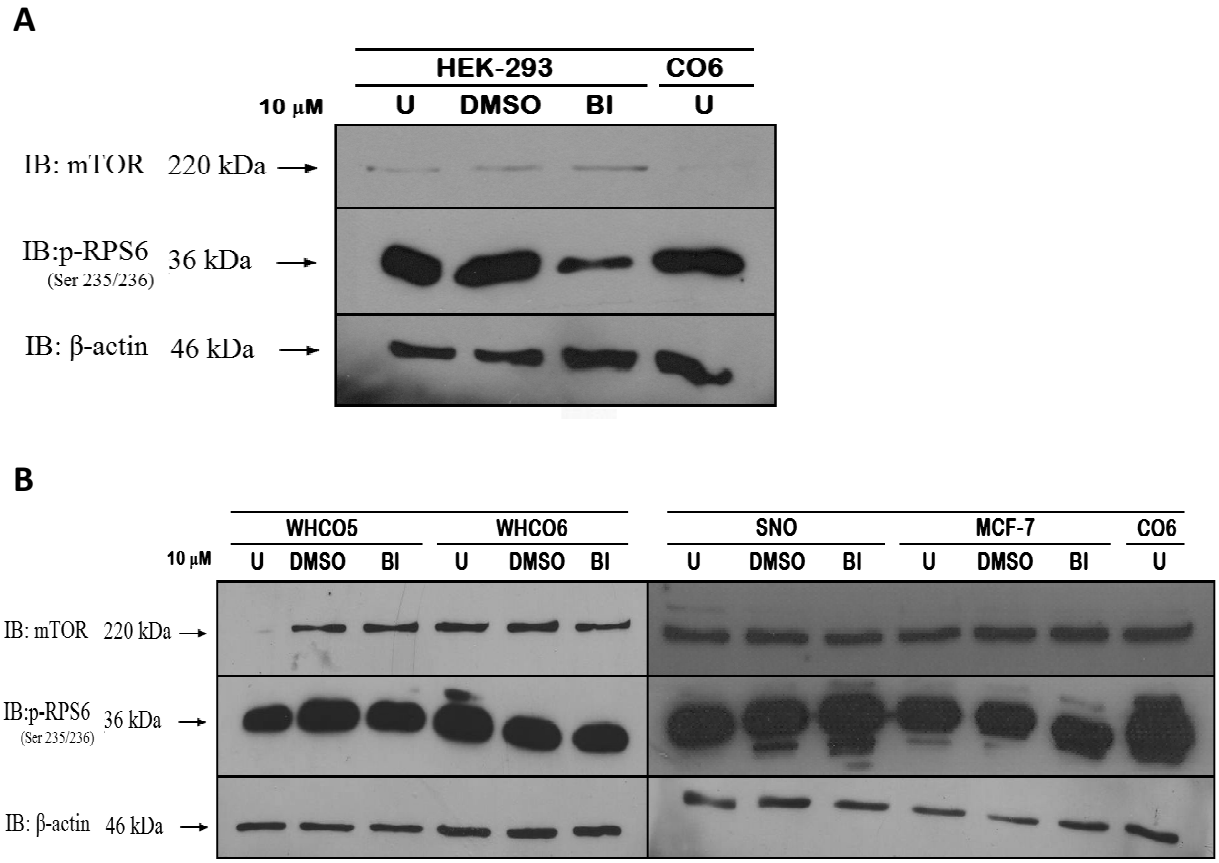

Figure 3.8: Immunodetection of critical signal transduction intermediates after inhibition of p90RSK with BI-D1870. A) Specific inhibition of p90RSK with BI-D1870 visibly reduced the concentration of p-RPS6$^{(Ser\ 235/236)}$ (36 kDa) polypeptide band in the HEK-293 cell line. However, no clear change in mTOR (220 kDa) was observed. **B)** Similarly, specific inhibition of p90RSK with BI-D1870 did not visibly reduce the concentration of mTOR (220 kDa) or p-RPS6$^{(Ser\ 235/236)}$ (36 kDa) polypeptides in HOSCC cells. By including the detection of β-actin (46 kDa), we demonstrate that equal amounts of protein were loaded for all HOSCC cell lysates. (U = Untreated cells; DMSO = cells treated with 0.1 % dimethyl sulphoxide; BI = cells treated with the p90RSK-sepcific inhibitor BI-D1870; CO6 = WHCO6).

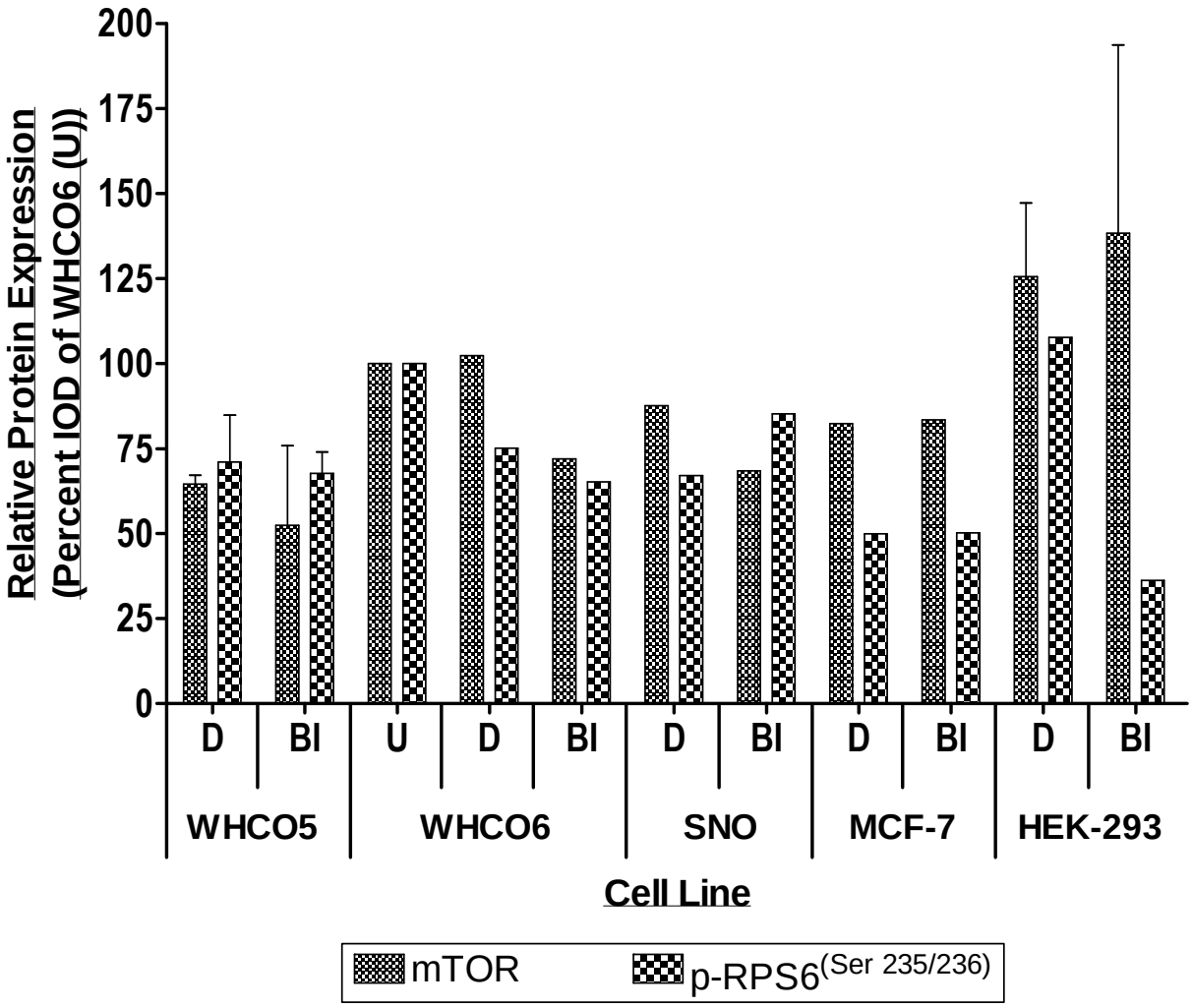

Figure 3.9: Relative protein expression levels for mTOR and p-RPS6$^{(Ser\ 235/236)}$ after specific inhibition of p90RSK with BI-D1870. Semi-quantitative densitometric analysis revealed that HOSCC cells decrease mTOR protein expression minimally after inhibiting p90RSK signalling with BI-D1870, in comparison to an empty vector containing only 0.1 % DMSO. p-RPS6$^{(Ser\ 235/236)}$ protein expression was simiarly affected in HOSCC cells, however an increase in RPS6$^{(Ser\ 235/236)}$ was apparent in the SNO cell line. Since treatment with BI-D1870 clearly decreased p-RPS6$^{(Ser\ 235/236)}$ protein expression in the HEK-293 cell line, these data show that the action of BI-D1870 could be reproduced as reported in the literature. Since not all western blots were repeated more than once, the significance of these changes in protein expression was not determined. (U = Untreated cells; DMSO = cells treated with 0.1 % dimethyl sulphoxide; BI = cells treated with the p90RSK-sepcific inhibitor BI-D1870).

Table 3.5: Summary of mTOR and p-RPS6$^{(Ser\ 236/236)}$ protein expression levels obtained after specific inhibition of p90RSK with BI-D1870.

Protein	Cell Line														
	WHCO 5			WHCO6			SNO			MCF-7			HEK-293		
	↑/↓	H/M/L	% Δ	↑/↓	H/M/L	% Δ	↑/↓	H/M/L	% Δ	↑/↓	H/M/L	% Δ	↑/↓	H/M/L	% Δ
mTOR	↓	Med	-20.00	↓	Med	-29.41	↓	Med	-22.73	↑	High	1.22	↑	High	9.52
p-RPS6$^{(Ser\ 235/236)}$	↓	Med	-5.63	↓	Med	-13.33	↑	High	26.87	↑	Med	2.04	↓	Low	-66.67

Key: Low = 0 – 45 %; Medium (Med) = 46 – 75 %; High = 76 – 100 % (and above). Protein expression levels are based on the Hager *et al.*, (2011) classification system for analyses of mTOR and p-RPS6 proteins (see Materials and Methodology, Section 3.2.11). Change in relative marker set protein expression is expressed as percent change (% Δ), designated by either positive (↑) or negative (↓) arrows. For the calculation of percent change, see Appendix B, Equation B1.

3.4. Discussion

3.4.1. The PI3K/PKB signalling pathway is an upstream regulator of the mTOR signalling pathway in HOSCC cells

Having demonstrated that key signal transduction intermediates may function as a set of protein markers providing specific mTOR pathway information (see Chapter 2); we monitored these same protein intermediates during our investigation of mechanisms influencing canonical and non-canonical mTOR signalling in HOSCC cells. Although numerous factors are known to affect signalling through the mTOR pathway, we believed biochemical signals elicited by soluble stimuli to be the most relevant, as these types of signals are reported to have the greatest effect during mTORC1-dependant autophagy induction (Yan and Lamb, 2012). Therefore, by denying HOSCC cells the appropriate means to regulate mTOR and mTORC1, we are able to determine how HOSCC cells affect cell survival by altering the mTOR signalling pathway. In this way, it becomes possible to delineate the circumstances, as well as the signalling sequences, regulating mTORC1-dependant autophagy induction in HOSCC cells.

The first form of mTOR regulation we examined was signal transduction through the PI3K/PKB signalling pathway, since this pathway is widely accepted as the canonical regulator of mTOR signalling. Indeed, previous studies probing the relationship between PI3K and mTOR show that PI3K and PKB are situated upstream of mTOR (Hay, 2005; Bhaskar and Hay, 2007), and actively regulates signal transmission through mTORC1 (Hay, 2005; Bai and Jiang, 2010). Thus, we believed it was necessary to confirm this signalling paradigm in HOSCC cells. Since inhibition of PI3K commonly decreases PKB activation, and consequently mTORC1 signalling (Martelli *et al.*, 2010), we perturbed the activity of PI3K with a commonly used inhibiter, commercially known as LY294002 (Blommaart *et al.*, 1997).

Inhibition of PI3K with LY294002 specifically affects signalling through the PI3K/PKB pathway in HOSCC cells. PI3K-specific inhibition was shown to decrease $PKB^{(Ser\ 473)}$ phosphorylation (see *Appendix B, Table B2*), thus directly affecting the activation of downstream signal transduction pathways reliant on PKB-dependant signals (Shaw Ph.D.

Thesis, 2011). Since inhibition of PI3K reduced mTOR and mTORC1 signalling, this confirmed a direct relationship between the PI3K/PKB signalling pathway and the mTOR signalling pathway in HOSCC cells. Having shown that specific inhibition of PI3K with LY294002 effectively inhibits mTORC1 signalling, we expected that reduced mTORC1-dependant regulation of the ~ 3 MDa autophagy induction complex would follow. Consequently, we believed that HOSCC cells would possess an elevated potential for autophagy. However, the potential for autophagy induction (conveyed through dephosphorylated mATG-13 in the protein marker set) seemed to abate when we obstructed PI3K signalling. Therefore, this may indicate that mTOR-dependent autophagy induction may not be critically influenced by the PI3K/PKB signalling pathway in HOSCC cells.

mATG-13 has only recently become an important autophagy marker because its dephosphorylation directly precedes the initiation of autophagy induction (Hara *et al.*, 2008; Chan *et al.*, 2009; Hosokawa *et al.*, 2009; Jung *et al.*, 2009). However, the phosphorylation status of mATG-13 may be difficult to decipher by immunoblot (Hara *et al.*, 2008; Hosokawa *et al.*, 2009; Jung *et al.*, 2009), since multiple mATG-13 bands are common (Chan *et al.*, 2009), a phenomenon we also observed. The main reason given for this occurrence is the different states of mATG-13 phosphorylation which exist, both *in vitro* and *in vivo*¸ resulting from subsequent interactions with ULK – which may also phosphorylate mATG-13 (Hara *et al.*, 2008; Hosokawa *et al.*, 2009; Jung *et al.*, 2009). Nevertheless, we believe that these polypeptide bands do represent different states of mATG-13 phosphorylation, and may be a consequence of negating PI3K-dependant survival signals through the application of LY294002. Therefore, depletion of PI3K/PKB survival signalling may modulate the behaviour of other autophagy-regulatory elements, such as Bim and Beclin-1 (Luo *et al.*, 2012). Since there is a lack of comparable data within the current literature, showing this influence on autophagy induction by way of mATG-13 expression, we believe these findings to be unique, but in need of further corroboration.

Inhibition of PI3K signalling was also insufficient to induce an apoptotic response in HOSCC cells. Moreover, since negating these types of survival signals did not affect integrin-triggered focal adhesion protein kinases, such as ILK, it may be concluded that ILK protein expression is not transcriptionally regulated by PI3K signalling. Rather, ILK is situated upstream of the PI3K/PKB pathway in HOSCC cells.

3.4.2. Excluding essential nutrients alters mTORC1 signalling to autophagy induction in HOSCC cells

The removal of growth stimulants (such as essential amino-acids, growth factors and other soluble mitogens) ultimately affects the activation of those signal transduction cascades regulated by RTK's and MAPK's (Tsujimoto and Shimizu, 2005; Avruch *et al.*, 2009; Takahara *et al.*, 2006; Mason and Rathmell, 2010). Therefore, by excluding serum from standard tissue culture conditions, we negate these survival signals and isolate non-canonical mechanisms regulating mTOR signalling. In the absence of serum, HOSCC cells were forced to alter the concentration of mTOR and signalling through mTORC1. This means that even though HOSCC cells possess an aberrantly activated mTOR pathway under standard tissue culture conditions (established in Chapter 2), the upstream regulators of mTOR signalling in HOSCC maintain susceptibility to typical agonists found in serum, which impinge on mTORC1 activity during conditions of nutrient deprivation.

We believed that HOSCC cells would undergo autophagic processing as a result of reduced signalling through mTORC1, because autophagy is reportedly triggered through the removal of essential nutrients and soluble mitogens (Fingar *et al.*, 2002: Fingar and Blenis, 2004; Fingar *et al.*, 2004). By inhibiting mTORC1 signalling through the exclusion of serum, we confirmed that autophagy was induced in HOSCC cells through a similar nutrient-dependant mechanism. HOSCC cells maintained a moderate to high potential for autophagic processing (as shown by increasing concentrations of dephosphorylated mATG-13). An increase in the potential for autophagy under these tissue culture conditions indicates that signals initiating autophagy induction remain under control of the mTOR/mTORC1 pathway in HOSCC cells.

Autophagy induction is a very rapid response (approximately 8 minutes), occurring very soon after excluding these types of mTOR pathway agonists (Kabeya *et al.*, 2000). Fully mature autophagolysosomes are readily observed after 15 – 30 minutes (Kabeya *et al.*, 2000). The rapid onset of autophagy in response to a lack of soluble extracellular-originating signals suggests that autophagy serves an important survival role ensuring cell longevity in response to nutrient limiting conditions, until pro-survival signals are re-attained. Since those initial signalling events signalling apoptosis did not occur (evident from a lack of detectable cleaved caspase-3), this suggests that the induction of autophagy precedes the initiation of pro-death signals.

3.4.3. Rapamycin inhibits mTORC1 signalling in HOSCC cells

We have established that a biochemical signal must first stimulate PI3K signalling before reaching the mTOR signalling pathway. This indicates that the most commonly accepted mechanism of mTORC1 regulation is canonical regulation through the PI3K/PKB signalling pathway in HOSCC cells. Additionally, we have established that the mTOR pathway is susceptible to nutrient deprivation triggering an autophagic response in HOSCC cells, suggesting that mTOR maintains the ability to sense cellular abundance of essential nutrients and amino-acids. Therefore, in the general scheme of intracellular cellular signalling, these conclusions represent key findings contributing to our understanding of the mTOR signalling network in HOSCC. Since we have now gained both a positional and functional context for the mTOR signalling pathway in HOSCC cells, it was appropriate that these discoveries precede an investigation into the susceptibility of the mTOR pathway to rapamycin inhibition.

The susceptibility of the mTOR pathway to rapamycin in HOSCC was investigated, assuming that rapamycin could bind to mTOR and suppress its kinase activity in a similar manner as described by Foster and Toschi (2009). Here, rapamycin sterically hinders the ATP binding pocket, disallowing ATP to associate with mTOR. In support of this assumption, a detailed survey of the literature revealed no missense mutations affecting rapamycin binding in HOSCC (Hou *et al.*, 2007; Karbowiniczek *et al.*, 2008; Molinolo *et al.*, 2007; Chantaravisoot and Tamanoi, 2010; Hirashima, *et al.*, 2012).

In response to different nanomolar concentrations of rapamycin (where HOSCC cells exposed to rapamycin for either 6 or 24 hours), a trend increase in mTOR protein expression was observed in HOSCC cells of South African origin. In contrast, this trend was not observed in a study by Hou *et al.* (2007), where the authors investigated the effects of rapamycin and siRNA against mTOR in poorly- (EC9706) and well-differentiated (Eca 109) HOSCC cells of Chinese origin (otherwise known as ESCC cells). Here, both mTOR and p70S6K mRNA and protein expression levels decreased in response to 20 nM and 50 nM rapamycin. This apparent disparity between squamous cell carcinomas of South African and Chinese origin may signify a particularly insightful difference into HOSCC aetiology. Despite this difference in mTOR abundance, the signalling potential of mTORC1 was completely diminished in HOSCC cells of the WHCO series, as well as MCF-7 breast

carcinoma cells. This trend was also reported in ESCC cells according to Hou *et al.* (2007). Therefore, HOSCC cells exhibited a dose-dependent decrease in mTORC1 signalling, observed in part through mTOR inhibition, as well as a rapamycin-induced decrease in p70S6K protein expression – also observed by Hou *et al.* (2007).

Decreasing mTORC1 signalling should produce an increase in dephosphorylated mATG-13, signifying autophagy induction. This trend increase was not always observed in HOSCC, where mATG-13 protein expression steadily decreased in response to 20 and 50 nM rapamycin (6 hours post treatment) and 50 and 100 nM rapamycin (24 hours post treatment). This was an unexpected result since signalling through mTORC1 is reported to be the main regulator triggering autophagy (Tsuchihara *et al.*, 2009). An evaluation of current literature revealed that while mTOR is considered the principal regulator of autophagy, other cellular mechanisms may also play a role in autophagy induction. For example the tumour suppresser p53, as well as Beclin1, Bif1 and UVRAG pathway elements may also regulate autophagy induction, and importantly, are unaffected by rapamycin treatment (Brech *et al.*, 2009; Chen and Debnath, 2010). Therefore, these other autophagy regulating mechanisms may compensate for the loss in mTORC1 signalling as a result of rapamycin treatment.

The protein abundance of ILK is not especially affected by rapamycin treatment; however rapamycin may affect the recruitment of ILK to focal adhesions (Foster and Toschi, 2009). However, the impact of this influence of rapamycin in HOSCC cells would perhaps form the basis of another investigation, and would rather be of outstanding interest to studies focussing on adhesion-based signal transduction if an association between ILK and mTOR (or other mTOR pathway components) was determined.

3.4.4. The mTOR/mTORC1 signalling pathway leads to RPS6$^{(Ser\ 235/236)}$ phosphorylation in HOSCC cells

Upon forming a multi-protein complex with Raptor, mLST8 and PRAS40, mTOR forms a functional, rapamycin-sensitive signalling complex known as mTORC1 (Abraham, 2002; Zhou and Huang, 2010). mTORC1 directly phosphorylates and activates p70S6K, a well characterised downstream target of mTOR, which subsequently phosphorylates and activates RPS6$^{(Ser\ 235/236)}$ (Abraham, 2002; Zhou and Huang, 2010). p-RPS6$^{(Ser\ 235/236)}$ plays a key role in cap-dependant translation initiation of 5′-Top mRNA's, and is therefore fundamental

during cell growth and proliferation processes (Gingras *et al.*, 2001; Roux *et al.*, 2007; Zhou and Huang, 2010). Hence, the phosphorylation status of RPS6$^{(Ser\ 235/236)}$ and p70S6K is regarded as a molecular marker indicating active signalling through mTORC1 (Dazert and Hall, 2011). For these reasons, p-RPS6$^{(Ser\ 235/236)}$ was selected as a relevant signalling intermediate. However, phosphorylation of RPS6$^{(Ser\ 235/236)}$ may also occur through another cellular pathway component, namely p90RSK; an effector kinase of the MAPK signalling cascade (Dazert and Hall, 2011; Roux *et al.*, 2007).

Both MAPK/p90RSK and mTOR/mTORC1 signalling pathways experience extensive signal integration (or pathway crosstalk) (Carrière *et al.*, 2008; Mendoza *et al.*, 2011). p90RSK may bind to and activate Raptor of mTORC1, as well as negate the inhibitory action of the TSC1/TSC2 complex, a critical upstream regulatory node of the mTOR signalling pathway, (Carrière *et al.*, 2008; Mendoza *et al.*, 2011). In light of the above, we ascertained the unique contribution of MAPK/p90RSK- and mTOR/mTORC1-dependent signalling on RPS6$^{(Ser\ 235/236)}$ phosphorylation in WHCO and MCF-7 cell lines. Therefore, the ability of mTORC1 to phosphorylate RPS6$^{(Ser\ 235/236)}$ in the absence of MAPK/p90RSK was assessed using a newly developed p90RSK-specific inhibitor, BI-D1870, which targets all four RSK isoforms (Sapkota *et al*., 2007). Before assessing the action BI-D1870 in HOSCC cells, we confirmed that BI-D1870 could specifically inhibit p90RSK-dependant RPS6$^{(Ser\ 235/236)}$ phosphorylation in the HEK-293 cell line. HEK-293 cells were used because Sapkota *et al*. (2007) initially demonstrated a BI-D1870-dependent reduction in p-RPS6$^{(Ser\ 235/236)}$ using this cell line.

Sapkota *et al.* (2007) also demonstrated that concentrations of 0.1 μM BI-D1870 was sufficient to inhibit p90RSK-dependent signalling *in vitro*. However, ten times this concentration was necessary to achieve the same effect *in vivo*. Therefore, after demonstrating that 10 μM BI-D1870 was sufficient to decrease p-RPS6$^{(Ser\ 235/236)}$ in HEK-293 cells, it was shown that p90RSK-specific inhibition did not appreciably change p-RPS6$^{(Ser\ 235/236)}$ in HOSCC cells. This indicates that while MAPK/p90RSK signalling is responsible for a small component of RPS6$^{(Ser\ 235/236)}$ phosphorylation, mTORC1-dependant signalling is the major upstream regulator responsible for a larger fraction of RPS6$^{(Ser\ 235/236)}$ phosphorylation. This would further corroborate our using p-RPS6$^{(Ser\ 235/236)}$ in the protein marker set to indicate mTORC1 signalling.

Since p90RSK-specific inhibition differentially also altered mTOR protein expression in HOSCC cells, these data indicate that, the MAPK/p90RSK signalling pathway may play an uncharacterised role in the regulation of mTOR transcriptional events. However, this observation may only apply to squamous cells carcinomas affecting the human oesophagus. Since not all western blots were repeated more than once, however, a better indication of this would be given through statistical analysis of RPS6$^{(Ser\ 235/236)}$ phosphorylation. Nevertheless, the design of this investigation served our purposes to show that the majority of RPS6$^{(Ser\ 235/236)}$ is phosphorylated by mTORC1 in HOSCC cells.

In conclusion, an investigation of the mTOR signalling network in HOSCC cells revealed that soluble extracellular-originating stimuli are capable of regulating the concentration of mTOR, and signalling through mTORC1 by way of canonical and non-canonical mechanisms. In the absence of PI3K-dependent signals, we established that the mTOR pathway generally reduces signalling through mTORC1, indicating a canonical form of mTOR pathway regulation, as well as that mTOR is situated downstream of the PI3K/PKB pathway in HOSCC cells. We also established that mTOR maintains the ability to sense cellular abundance of essential nutrients and amino-acids, thereby triggering an autophagic response in HOSCC cells. However, while rapamycin was shown to potently inhibit mTORC1 in HOSCC cells, the same effect on autophagy induction was not observed. This was found to be unique to HOSCC and may indicate that induction of the autophagic process is more tightly regulated by other signalling inputs, which may supersede mTORC1, in HOSCC cells in comparison to other squamous cell carcinomas. Lastly, we established that while the MAPK/p90RSK pathway contributes to RPS6$^{(Ser\ 235/236)}$ phosphorylation, signalling through mTOR/mTORC1 is the major player in HOSCC. Therefore, all of the above analyses forms the necessary foundation to investigate whether mechanical extracellular-originating stimuli (derived from adhesion-based signal transduction) influences the mTOR/mTORC1 signalling pathway in HOSCC cells.

CHAPTER 4

4. ECM MODULATION OF THE mTOR/mTORC1 SIGNALLING PATHWAY IN HOSCC CELLS

4.1. Introduction

Epithelial cells require stable connections between one another, as well as with a supporting extracellular matrix (ECM), in order to create an organized three-dimensional tissue structure (Gumbiner, 1996). Specialised components of the cell adhesion machinery facilitate these cell-cell and cell-ECM connections, ultimately allowing the assembly of different tissue types (Juliano, 2002). While cell-cell interconnectivity is mediated by cadherins and adherens junctions, forming intercalated epithelial sheets (Gumbiner, 1996), adhesion to the ECM arises through different permutations of α and β integrin heterodimers that bind specific extracellular matrix components (Gumbiner, 1996; van Der Flier and Sonenberg, 2001). Integrin-mediated cell-ECM adhesion, in particular, plays an important role during the regulation of numerous cellular processes; such as proliferation, differentiation, migration, cell survival and even tumour progression (Juliano, 2002; Brakebusch and Fässler, 2003; Brunton *et al.*, 2004). Therefore, attachment to the ECM is an essential cellular requirement in order to maintain cellular homeostasis and the integrity of epithelial tissue (Gumbiner, 1996; Juliano, 2002).

The extracellular matrix is secreted and thus formed by surrounding epithelial cells (Shwartz, 2010). The ECM is composed of several different types of glycoproteins, such as fibronectin and laminin, proteoglycans, such as heparin sulphate, and collagens that together form an integrated three-dimensional extracellular network to which cells adhere (Boudreau and Bissell, 1998). Collagen is reported to be the most abundant ECM molecule, where more than 20 different types are known to exist (Boudreau and Bissell, 1998; Rozario and DeSimone, 2010). Of these present within mammalian ECM networks, Type I collagen is the most ubiquitous and well described structural collagen, whereas Type IV collagen is mainly present within the basal lamina or basement membrane (Roskelley *et al.*, 1995; Rozario and DeSimone, 2010). Similarly, fibronectin is also an important ECM constituent; however fibronectin is present in appreciably lower quantities to collagen, but remains an important

ligand for cell adhesion and during adhesion-based signal transduction (Roskelley *et al.*, 1995; Shwartz, 2010).

When collagen and fibronectin physically interact with specific α/β integrin heterodimers, these associations stimulate adhesion-based signalling events in substrate-dependant epithelial cells (Brakebusch and Fässler, 2003). This type of integrin-mediated signalling is currently understood to be bi-directional, where cells may influence their microenvironment through a process known as inside-out signalling (Harburger and Calderwood, 2009). However, outside-in signalling may also occur (illustrated in *Figure 4.1*); whereby the microenvironment rather influences numerous cellular processes. For example substrate composition, stiffness and geometry may function as guidance cues during stem-cell differentiation and development (Engler *et al.*, 2006). Additionally, mechanical stress in muscle, bone, cartilage and blood vessels plays a critical role in the maintenance of tissue homeostasis (Jaalouk and Lammerding, 2009).

The process of ECM-originating signalling (depicted in *Figure 4.1*) shows how focal adhesions become enriched with activated integrins, such as $\alpha_1\beta_1$ and $\alpha_2\beta_1$, in response to collagen (van Der Flier and Sonnenberg, 2001). However, focal adhesions may become enriched with $\alpha_v\beta_3$ and $\alpha_5\beta_1$ integrins in response to fibronectin (van Der Flier and Sonnenberg, 2001). These cell-ECM binding events induce conformational changes within integrin extracellular and cytoplasmic domains (Harburger and Calderwood, 2009). Subsequently, structural proteins are recruited, such as Nck2, PINCH, Parvin and Paxillin, which serve as molecular platforms supporting protein-protein interactions around the cytoplasmic tails of activated integrin heterodimers (Baker and Zaman, 2010). In addition, the phosphorylation (and activation) of protein kinases involved in intracellular signalling cascades occurs, in particular ILK (Brabek *et al.*, 2004; Subauste *et al.*, 2004). Since protein recruitment and phosphorylation occurred mainly at sites of focal adhesion, focal adhesions rather than the actin cytoskeleton are considered the origin of mechanotransduction events (Goldmann, 2012).

The intracellular transmission of extracellular-originating stimuli may also have far reaching affects on context-dependent cell survival processes, such as the induction of autophagy, which is triggered when cell-ECM contacts are lost (Fung *et al.*, 2008). These findings suggest that cell-ECM interactions are essential for mechanotransduction to occur, providing a rationale for the importance of attachment during adhesion-based signalling. Furthermore, these observations demonstrate a functional linkage exists between ECM-originating signals, integrin-triggered protein kinases and specific cell survival processes. Therefore, we believe that autophagy may share a similar functional linkage with components of integrin-mediated cell adhesion, such as ILK.

It is therefore increasingly apparent that cells perceive biophysical information, such as traction forces, matrix geometry and substrate elasticity, in addition to biochemical cues (Lim *et al.*, 2010). Considering the exact molecular mechanisms controlling the induction of autophagy by ECM-originating signals are still incompletely delineated, by investigating this aspect we may uncover a role for ILK as a conduit during ECM regulation of autophagy induction. Moreover, since autophagy induction is regulated by the mTOR signalling pathway, we believe that ILK achieves this by interacting with components of the mTOR pathway. Therefore, with the aim of delineating the route of mechanotransduction from sites of cell-substrate contact to the cellular machinery initiating autophagy induction, we examined the influence of mechanically-derived extracellular-originating on the mTOR/mTORC1 signalling pathway in HOSCC cells.

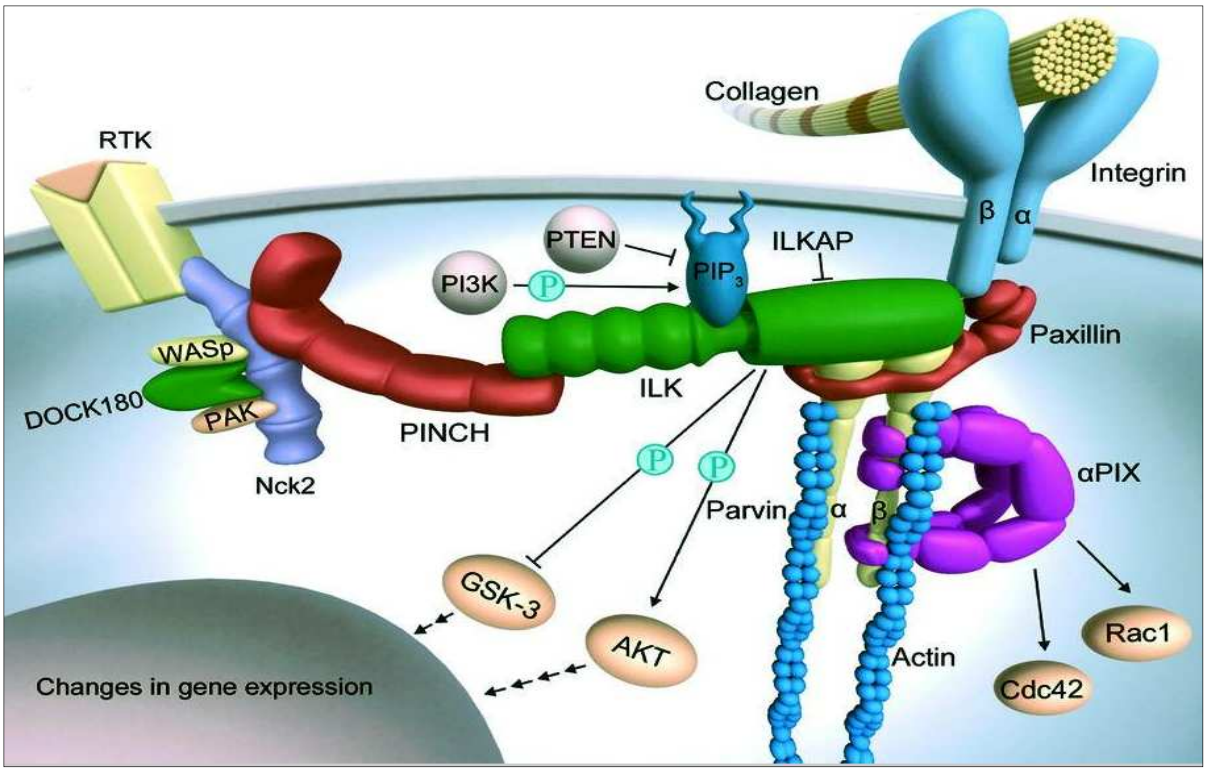

Figure 4.1: Mechanotransduction of extracellular-originating stimuli through ILK. After unmasking of integrin extracellular domains, specific pairs of α/β integrins bind components of the extracellular matrix, such as collagen and fibronectin. Cell-ECM interactions recruit focal adhesion proteins that tether integrins to the actin cytoskeleton, and signal to important pathway intermediates. ILK is the main example of an integrin-triggered focal adhesion protein kinase that in fact functions as both a molecular scaffold for multi-protein assemblies, as well as a molecular conduit for mechanotransduction. Since ILK directly phosphorylates numerous key pathway intermediates (such as Akt/PKB and GSK-3β), mechanically-derived extracellular-originating signals may be propagated intracellular to bring about a change in gene expression, consequently influencing cell behaviour and survival processes. Consequently, we believe that autophagy is a cell survival pathway affected by adhesion-based signalling. (Figure adapted from Brakebusch and Fässler, 2003).

4.2. Materials and Methodology

4.2.1. Tissue Culture of WHCO and MCF-7 Cell Lines

All cell lines were cultured as described previously in Chapter 2, Section 2.2.1.

4.2.2. Sub-culture of WHCO and MCF-7 Cell Lines

As previously described (see Chapter 2, Section 2.2.2).

4.2.3. Provision of Extracellular matrix (ECM)-originating Stimuli

4.2.3.1. Growth of WHCO and MCF-7 Cell Lines on a Fibronectin-coated Substrate

Cell cultures were supplied with mechanical stimuli in the form of sterile 6 cm standard tissue culture dishes (Nunc) pre-coated with 10 μg/ml fibronectin (Roche) (Appendix A, 1.11.1). Fibronectin was left to polymerize for 1 hour under a sterile laminar flow cabinet. Before use, the supernatant was carefully removed and washed twice with PBS. Standard tissue culture then continued as previously described. Please note that all procedures for one set of experiments were performed using the same batch of FCS.

4.2.3.2. Growth of WHCO and MCF-7 Cell Lines on a Collagen-coated Substrate

Cell cultures were supplied with mechanical stimuli in the form of sterile 6 cm standard tissue culture dishes pre-coated with 100 μg/ml collagen. Collagen was purified from rat-tail tendon, as described by Teng *et al.* (2006) (Appendix A, 1.12.1). Subsequently, collagen-coated substrates were left to polymerize for 2.5 hours under a sterile laminar flow cabinet. Before use, the supernatant was carefully removed and washed twice with PBS. Standard tissue culture then continued as previously described. Please note that all procedures for one set of experiments were performed using the same batch of FCS.

4.2.4. Antibodies

Immunochemical analysis of all key protein intermediates was performed using an indirect antibody detection system. However, in addition to the primary and HRP-conjugated secondary antibodies listed in Chapter 2 (Section 2.2.3), focal adhesion kinase (anti-FAK) was detected with rabbit polyclonal antibodies obtained from Santa Cruz Technology®, whereas the regulatory associated protein of mTOR (anti-Raptor) was detected with rabbit monoclonal antibodies obtained from Cell Signalling Technology®, USA.

4.2.5. Combinatorial Tissue Culture with an ECM-originating Stimulus and Specific Inhibition of PI3K

4.2.5.1. Growth of WHCO and MCF-7 cells on a Fibronectin-coated Substrate with the concurrent inhibition of PI3K with LY294002

Sterile 6 cm standard tissue culture dishes were pre-coated with 10 μg/ml fibronectin as described above (see Section 4.2.3.1). Subsequently, cell cultures were allowed to proliferate until 6 cm dishes reached a confluence of approximately 80 %. The medium was then aspirated and cell monolayer washed twice with PBS. Subsequently, 3 ml fresh tissue culture medium with 10 % FCS was added, containing a final concentration of 20 μM LY294002 (Appendix A, 1.8.1). Henceforth, these samples were referred to as 'FN & L+'. Tissue cultures were then incubated in a humid, 37 °C incubator with an atmosphere of 5 % CO_2 in air for 1 hour. Simultaneously, untreated (U), 10 μg/ml fibronectin (FN) and 20 μM LY294002 (L+) controls were prepared for comparative purposes. It is important to note that all procedures for one set of experiments were performed using the same batch of FCS.

4.2.6. 2 % Triton-X-100-based Protein Extraction

As previously described (see Chapter 2, Section 2.2.5).

4.2.7. Protein Estimation

As previously described (see Chapter 2, Section 2.2.6).

4.2.8. Co-Immunoprecipitation Assay

Co-Immunoprecipitation (Co-IP) is a sensitive immunoassay allowing for the determination of a physical association between proteins of interest from a complex mixture of cellular extracts (Wang and Malbon, 2011). By exploiting the specific nature of antibody-antigen interactions, this molecular method conveys information pertaining to the presence, or absence, of specific protein-protein interactions that occur under standard tissue culture conditions.

In order to ascertain if mechanically-derived extracellular-originating signals are transmitted directly to mTORC1, we investigated whether a physical association occurred between mTOR and key integrin-triggered protein kinase intermediates, such as ILK and FAK. Cells were lysed in RIPA buffer (Appendix A, 1.7.1) for approximately 3 hours at 4 °C.

Afterwards, lysates containing 400 µg of protein (determined by Protein Estimation as described in 4.2.7) were incubated with 2 µl undiluted anti-mTOR antibody (Cell Signalling Technology®, USA), overnight at 4 °C in IP buffer (pH 8.0; Appendix A, 1.7.4). This allows the anti-mTOR antibody to bind to the mTOR protein kinase by means of the Fab-region. The above was performed on WHCO and MCF-7 cell lines and included a negative control, to which no anti-mTOR antibody was added.

The following day, immune complexes were precipitated with 20 µl protein G Sepharose beads (overnight at 4 °C) allowing Protein G Sepharose beads to bind the Fc-region of the antibody, bound to mTOR. Beads were initially washed thrice with 1 ml IP buffer in order to remove any ethanol in which beads were stored. The following day, samples were centrifuged in a SORVAL® MC (12V) centrifuge (12 000 x g; 30 sec) and the supernatant removed. The pellet was then washed thrice with 700 µl IP buffer, the last wash being 0.1% IP buffer.

IP samples were prepared for SDS-PAGE by centrifugation (12 000 x g; 30 sec; 4 °C), by discarding the supernatant and adding 40 – 50 µl single Laemmli lysis buffer. Samples were then boiled for 5 min in a boiling water bath, centrifuged (12 000 x g; 10 min; 4 °C) and stored at – 20 °C. This preparation releases the protein of interest and associated protein. IP samples consisting of Protein G Sepharose beads, anti-mTOR antibodies, the 220 kDa mTOR protein kinase, as well as any proteins physically associated with mTOR, were resolved by 10 % SDS-PAGE (Section 4.2.9). Subsequently, the presence of mTOR-associated proteins, such as Raptor, as well as focal adhesion protein kinases thought to interact with mTOR, such as ILK and FAK, were detected by western immunoblotting analysis (Section 4.2.10).

4.2.9. SDS-PAGE (Sodium Dodecyl Sulphate-Polyacrylamide Gel Electrophoresis)

As previously described (see Chapter 2, Section 2.2.7).

4.2.10. Western Immunoblot Analysis

Immunodetection of key protein intermediates present within WHCO and MCF-7 cell lysates was performed as previously described (see Chapter 2, Section 2.2.8). Additionally, see Appendix B, *Table B1* for commonly used primary and secondary antibody dilutions, including incubation conditions for FAK and Raptor.

4.2.11. Image Capturing

As previously described (see Chapter 2, Section 2.2.9).

4.2.12. Laser Densitometry and Analysis of Relative Protein Expression

Semi-quantitative densitometric analysis was used to determine protein expression across WHCO and MCF-7 cell lines, performed as previously described (see Chapter 2, Section 2.2.10). Additionally, raw and worked densitometric data is available in Appendix C, *Tables C14 - C17*.

4.2.13. Statistical Analysis

Results are expressed as the mean ± S.E. Statistical significance was determined by Student's *t*-test for comparative analysis (see Appendix D, *Table D4* and *Table D5*) using Sigma Plot®, Version 12.0 (SPSS Science, Chicago, Illinois USA), where $p < 0.05$ indicates statistical significance. All experiments were repeated at least three times, unless otherwise indicated.

4.3. Results

4.3.1. ECM-originating signals modulate mTOR abundance and RPS6$^{(Ser\ 235/236)}$ phosphorylation in HOSCC cells

Appreciable changes in the concentration of both mTOR and p-RPS6$^{(Ser\ 235/236)}$ polypeptides were observed when HOSCC cells were grown on substrates coated with either fibronectin or collagen (*Figure 4.2*). Immunodetection revealed that the concentration of polypeptide bands indicative of mTOR (220 kDa) increased after the WHCO series of cell lines were grown on fibronectin. However, noticeable decreases in mTOR abundance occurred within WHCO5 and SNO cell lines. Furthermore, the concentration of polypeptide bands at 36 kDa were also absent in the WHCO5 cell line, indicating a decrease in p-RPS6$^{(Ser\ 235/236)}$. Immunodetection also revealed that HOSCC cells grown in the presence of collagen decreased the concentration of both mTOR (220 kDa) and p-RPS6$^{(Ser\ 235/236)}$ (36 kDa) polypeptides within WHCO5 and WHCO6 cells. These obvious changes in mTOR and p-RPS6$^{(Ser\ 235/236)}$ polypeptide abundance were not observed in MCF-7 cells grown in the presence of either fibronectin or collagen.

Since we were unable to detect mTOR and p-RPS6$^{(Ser\ 235/236)}$ in the WHCO5 cell line (after growth on fibronectin- or collagen-coated substrates), as well as in the WHCO6 cell line (after exposure to collagen), we repeated immunodetection for these proteins. By doubling the amount of protein for each cell lysate, we were able to detect polypeptides indicative of mTOR (220 kDa) and p-RPS6$^{(Ser\ 235/236)}$ (36 kDa) (see Appendix B, *Figure B2* for these repeated western blots).

Semi-quantitative densitometric analysis revealed that exposure to fibronectin and collagen altered mTOR (220 kDa) and p-RPS6$^{(Ser\ 235/236)}$ (36 kDa) protein expression in all HOSCC cells (*Figure 4.3*). Relative protein expression was calculated as a percentage of that determined for untreated (U) cells of the WHCO6 cell line (see Chapter 3 for a clear explanation regarding the continued use of this line). This enabled us to determine the levels of mTOR and p-RPS6$^{(Ser\ 235/236)}$ protein expression (see Materials and Methodology, Section 4.2.12 for an explanation of this analysis). Consequently, this allowed the identification of

trends in protein expression and HOSCC cell behaviour in response to substrates coated with fibronectin or collagen.

When fibronectin was provided as a substrate, HOSCC cells commonly increased mTOR and p-RPS6$^{(Ser\ 235/236)}$ protein expression (*Figure 4.3*). Summarising these data clearly identified these trends (see *Table 4.1*). WHCO1, WHCO3, WHCO6, SNO, as well as MCF-7 cells, responded by increasing mTOR protein expression, significantly in the SNO cell line (see *Appendix D, Table D4* for a complete statistical analysis). The WHCO5 cell line, however, responded by decreasing mTOR protein expression levels. Furthermore, WHCO3, WHCO6, SNO and MCF-7 cells showed an increase for p-RPS6$^{(Ser\ 235/236)}$. The WHCO1 cell line showed a decrease in p-RPS6$^{(Ser\ 235/236)}$ protein expression, however this was found to be a minimal change. Thus RPS6$^{(Ser\ 235/236)}$ phosphorylation remained high in the WHCO1 cell line.

When collagen was provided as a substrate, HOSCC cells generally increased mTOR and p-RPS6$^{(Ser\ 235/236)}$ protein expression (see *Figure 4.3* and *Table 4.1*). WHCO1, WHCO3, SNO, as well as MCF-7 cells, responded by increasing mTOR, whereas the WHCO5 and WHCO6 cell lines decreased mTOR expression to low levels. Significant changes were determined in the WHCO1 and WHCO6 cell lines (see *Appendix D, Table D4* for these statistical analyses). Additionally, WHCO3, SNO and MCF-7 cells showed an increase for p-RPS6$^{(Ser\ 235/236)}$ (*Table 4.1*). The WHCO1, WHCO5 and WHCO6 cell lines were found to decrease p-RPS6$^{(Ser\ 235/236)}$ protein expression to low levels. However, this change in p-RPS6$^{(Ser\ 235/236)}$ was minimal in the WHCO1 cell line. Thus RPS6$^{(Ser\ 235/236)}$ phosphorylation remained high in the WHCO1 cell line.

A.

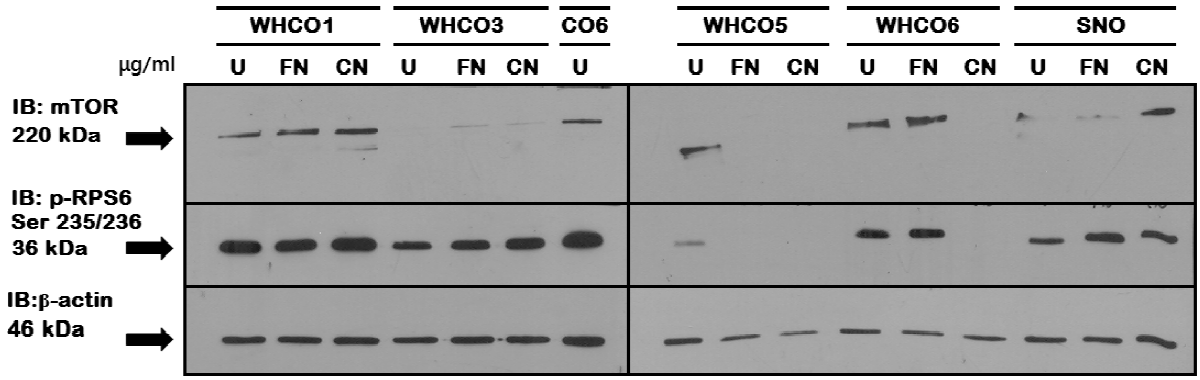

B.

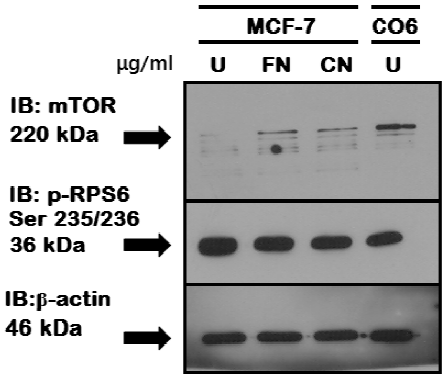

Figure 4.2: mTOR and p-RPS6$^{(Ser\ 235/236)}$ were visibly altered after HOSCC cells were grown on fibronectin or collagen. A) Clearly visible changes in polypeptide abundance, corresponding to mTOR (220 kDa) and p-RPS6$^{(Ser\ 235/236)}$ (36 kDa), were detected in WHCO5, WHCO6 and SNO cell lines in response to fibronectin and collagen. **B)** However, the same alterations were not observed in mTOR (220 kDa), but were seen in p-RPS6$^{(Ser\ 235/236)}$ (36 kDa) polypeptide bands in MCF-7cells. β-actin (46 kDa) was used to demonstrate equal protein loading of HOSCC cell lysates. Since polypeptide bands indicative of mTOR were not detected within WHCO5 (FN and CN) and WHCO6 (CN) cell lines, western immunoblots were repeated to confirm mTOR (220 kDa) and p-RPS6$^{(Ser\ 235/236)}$ (36 kDa) protein expression in response to treatment (see Appendix B, *Figure B2* for these repeated western blots showing that mTOR and p-RPS6$^{(Ser\ 235/236)}$ were indeed detected in response to tissue culture substrates coated with either fibronectin or collagen). (U = Untreated; FN = Fibronectin; CN = Collagen).

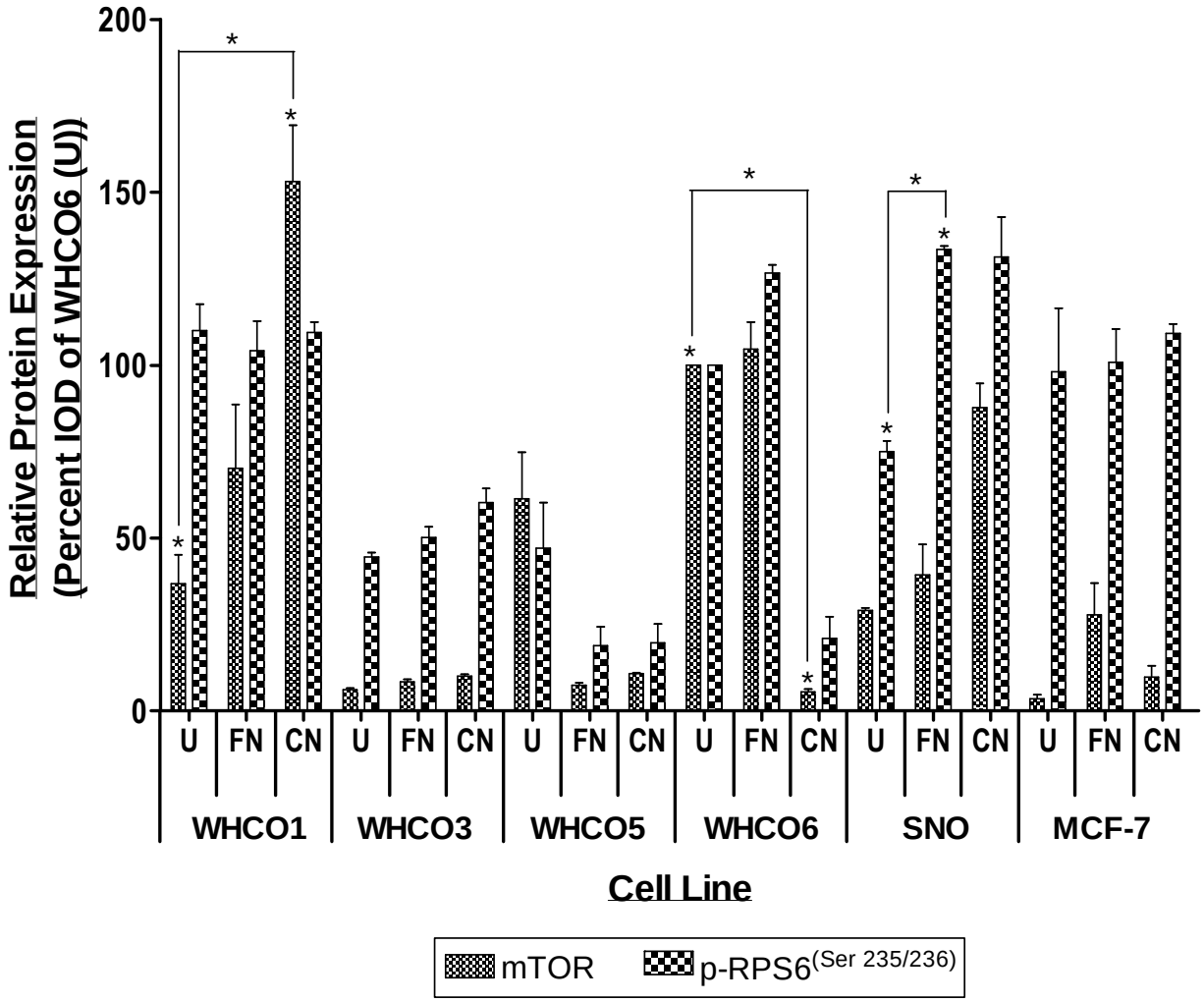

Figure 4.3: Relative mTOR and p-RPS6$^{(Ser\ 235/236)}$ protein expression changed in response to substrates coated with fibronectin or collagen. Changes in protein expression were calculated as a percentage of that determined for the untreated (U) WHCO6 cell line. Treatment with either fibronectin or collagen resulted in the modulation of mTOR and p-RPS6$^{(Ser\ 235/236)}$ protein expression in all HOSCC cells. As a general trend, fibronectin and collagen increased mTOR and p-RPS6$^{(Ser\ 235/236)}$ protein expression. In addition, Fibronectin induced a significant increase in p-RPS6$^{(Ser\ 235/236)}$ protein expression in the SNO cell line. Collagen, however, induced a significant increase in mTOR expression in WHCO1 cells, but also induced a significant decrease in mTOR expression in WHCO6 cells. Since all western blots were repeated more than once, the significance of these data could be determined. Significant difference is therefore indicated graphically through the use of joined star (*) symbols.

Table 4.1: Summary of mTOR and p-RPS6$^{(Ser\ 236/236)}$ protein expression levels after growth HOSCC cells were grown on either fibronectin or collagen.

		Cell Line															
		WHCO 1			WHCO 3			WHCO 5			WHCO 6			SNO			MCF-7		
		↑/↓	H/M/L	% Δ	↑/↓	H/M/L	% Δ	↑/↓	H/M/L	% Δ	↑/↓	H/M/L	% Δ	↑/↓	H/M/L	% Δ	↑/↓	H/M/L	% Δ
Fibronectin (FN)	mTOR	↑	Med	89.2	↑	Low	33.3	↓	Low	-88.5	↑	High	5.0	↑	Low	34.5	↑	Low	600.0
	p-RPS6 (Ser 235/236)	↓	High	313.5	↑	Med	66.6	↓	Low	-82.0	↑	High	-95.0	* ↑	* High	* 203.5	↑	Low	150.0
Collagen (CN)	mTOR	* ↑	* High	* -5.45	↑	Low	11.1	↓	Low	-59.6	* ↓	* Low	* 27.0	↑	High	78.7	↑	High	3.06
	p-RPS6 (Ser 235/236)	↓	High	0.01	↑	Med	33.3	↓	Low	-57.5	↓	Low	-79.0	↑	High	74.7	↑	High	11.2

Key: Low = 0 – 45 %; Medium (Med) = 46 – 75 %; High = 76 – 100 % (and above). Protein expression levels are based on the Hager *et al.*, (2011) classification system for analyses of mTOR and p-RPS6 proteins (see Materials and Methodology, Section 4.2.12). Change in relative marker set protein expression is expressed as percent change (% Δ), designated by either positive (↑) or negative (↓) arrows. For the calculation of percent change, see Appendix B, Equation B1. The use of a star (*) symbol, as well as red text, represents a statistically significant difference when compared to WHCO6 (U) cell line, determined using a Student's t-test; where $p < 0.05$ (see Appendix D, *Table D4 for a statistical report*).

4.3.2. Neither ILK nor FAK influence the transduction of ECM-originating signals to mTOR

Having determined that exposure to fibronectin and collagen influence the cellular abundance of mTOR and p-RSP6$^{(Ser\ 235/236)}$ in HOSCC cells, we considered the possibility that mechanotransduction to the mTOR pathway may occur through a direct protein-protein interaction with an integrin-triggered focal adhesion protein kinase intermediate, such as ILK. Moreover, since autophagy was demonstrated to occur in an FAK-independent manner (Hara *et al.*, 2008), we believed it was also necessary to confirm this in HOSCC. We therefore examined whether ILK acted as a relay for mechanotransduction linking adhesion-based signals to mTOR and mTORC1.

Co-immunoprecipitation analysis revealed that neither ILK nor FAK participated in a physical protein-protein interaction with mTOR in HOSCC cells (*Figure 4.4, A*). The inclusion of both positive and negative controls corroborated these results. Subsequently, polypeptide bands indicative of ILK (59 kDa) and FAK (125 kDa) were only detected in the positive control. The positive control constituted a WHCO6 cell lysate obtained under standard tissue culture conditions, whereas the negative control comprised a co-immunoprecipitation sample lacking anti-mTOR antibodies.

The co-immunoprecipitation analysis was repeated to detect an mTOR-Raptor interaction in HOSCC cells to ensure that the lack of detectable ILK and FAK polypeptides was not a technique-based error. Raptor is known to interact with the 220 kDa mTOR protein and is generally considered the defining protein binding partner associated with the mTORC1 complex (Kim *et al.*, 2002; Hara *et al.*, 2002; Zhou and Huang, 2010). Essentially, the ability to detect an mTOR-Raptor interaction would represent a ‘proof of principle’ control verifying that mTOR does not interact with ILK or FAK in HOSCC cells. Polypeptides indicative of the Raptor protein were detected at 150 kDa in HOSCC cells, as well as the MCF-7 cell line (*Figure 4.4, B*). Raptor was not detected in the negative control sample lacking anti-Raptor antibodies, but was clearly present at 150 kDa in the positive control comprising a WHCO6 cell lysate obtained under standard tissue culture conditions (*Table 4.2*). Therefore, a physical protein-protein interaction between mTOR and Raptor was observed in all HOSCC cells, validating the negative result between mTOR, and ILK and FAK.

A.

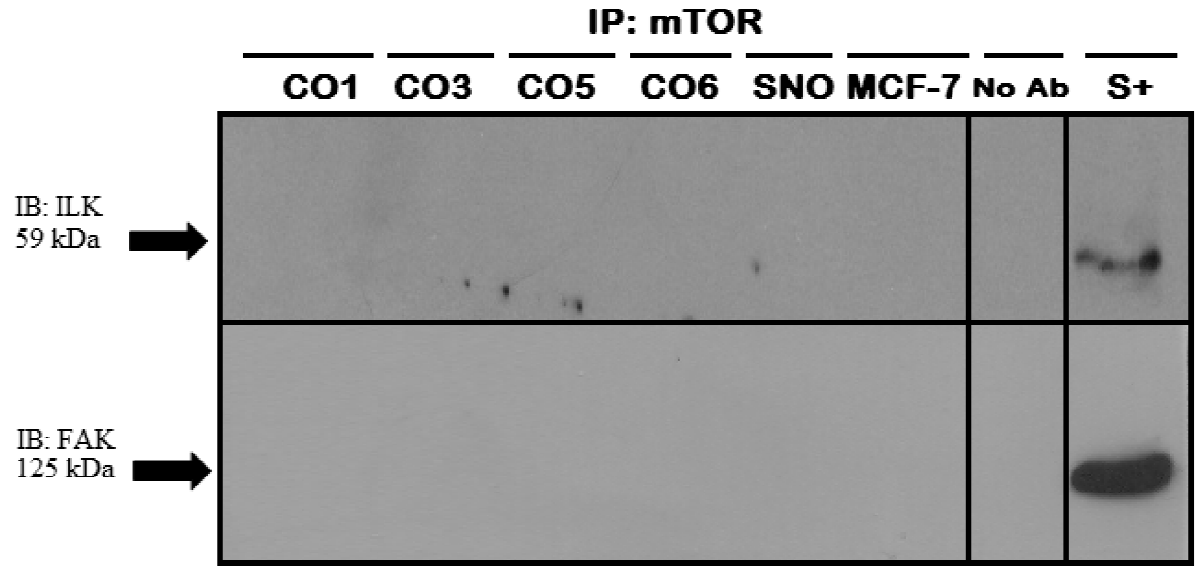

B.

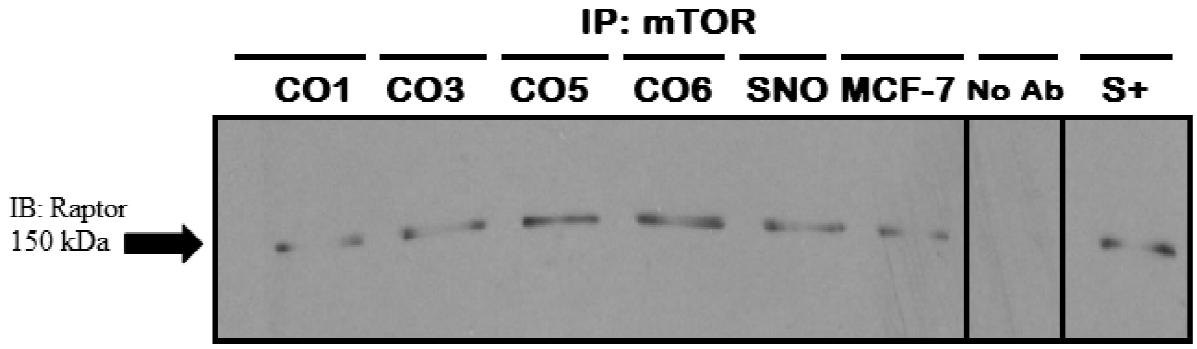

Figure 4.4: mTOR does not physically associate with common integrin-triggered protein kinase intermediates, such as ILK or FAK. A) Polypeptide bands indicative of ILK (59 kDa) and FAK (125 kDa) were not observed after co-immunoprecipitation analysis using mTOR (220 kDa) as a bait protein. **B)** The lack of a physical protein interaction between mTOR and ILK, as well as mTOR and FAK, was corroborated through the detection of a physical protein-protein interaction between mTOR and Raptor (150 kDa), providing an additional 'proof of principle' control.

Table 4.2: Protein-protein interaction profile established between mTOR and common integrin-triggered focal adhesion proteins in HOSCC cells.

Protein	Molecular Weight (kDa)	Cell Line					
		WHCO1	WHCO3	WHCO5	WHCO6	SNO	MCF-7
ILK	**59**	No	No	No	No	No	No
FAK	**125**	No	No	No	No	No	No
Raptor	**150**	Yes	Yes	Yes	Yes	Yes	Yes

4.3.3. ECM-modulation of mTOR and p-RPS6$^{(Ser\ 235/236)}$ is disrupted after specific inhibition of PI3K in HOSCC cells

Thus far we established that integrin stimulation influences the mTOR signalling pathway in HOSCC cells, and that the intracellular propagation of ECM-based signals to mTOR does not involve a direct interaction with ILK or FAK. Consequently, we believe these data point towards the involvement of a critical upstream signalling node which is both intimately involved during the regulation of mTOR/mTORC1, and affected by adhesion-based signalling. We are of the opinion that the PI3K/PKB pathway constitutes the signalling machinery responsible for relaying mechanotransduction information to mTOR for three main reasons: 1) PI3K is positioned upstream of the mTOR pathway (established in Chapter 3); 2) PI3K regulates mTORC1 signalling (also confirmed in Chapter 3); and 3) PI3K signalling is influenced by mechanical stimuli (Guinebault, 1995). Considering the above, adhesion-based signalling through PI3K may also influence the induction of cellular autophagy through its regulation of mTORC1. Therefore, we investigated adhesion-based regulation of mTOR/mTORC1 signalling in HOSCC cells by providing mechanical stimuli, while simultaneously disrupting signals propagated through the PI3K/PKB pathway.

By specifically blocking the kinase ability of PI3K with LY294002, we effectively inhibited the transduction of adhesion-based stimuli to the mTOR/mTORC1 signalling pathway in HOSCC cells. Immunodetection revealed that HOSCC cells produced clearly visible changes in mTOR and p-RPS6$^{(Ser\ 235/236)}$ polypeptide abundance, at 200 kDa and 36 kDa respectively in both the WHCO series, as well as the MCF-7 cell line (*Figure 4.5*). The WHCO5, WHCO6, SNO and MCF-7 cell lines were chosen in particular because they represent lines that modulate the mTOR pathway in a unique manner when exposed to either canonical stimuli (such as PI3K-specific inhibition with LY294002), or non-canonical stimuli (for example nutrient deprivation, inhibition of mTOR with rapamycin, as well as when mechanical signals are provided in the form of a fibronectin-coated substrate).

Semi-quantitative densitometric analysis of mTOR polypeptide bands revealed that the WHCO series of cell lines commonly increased mTOR expression in response to fibronectin (*Figure 4.6, A*). The WHCO series also increased mTOR expression after specific inhibition of PI3K with LY294002 (*Figure 4.6, A*). Only the WHCO6 cell line responded differently and rather significantly decreased mTOR expression to low levels (see *Appendix D, Table D5*

for a complete statistical analysis). Interestingly, the combination effect of fibronectin and PI3K-specific inhibition mimicked the changes seen in mTOR expression reported after inhibition of PI3K with LY294002 (*Table 4.3.*). Here, mTOR protein expression was generally increased in HOSCC cells, but decreased in the WHCO6 cell line.

Furthermore, densitometric analysis of p-RPS6$^{(Ser\ 235/236)}$ polypeptides revealed that HOSCC cells generally exhibited high RPS6$^{(Ser\ 235/236)}$ phosphorylation in response to fibronectin (*Figure 4.6, B*). However, specific inhibition of PI3K with LY294002 commonly reduced the phosphorylation of RPS6$^{(Ser\ 235/236)}$ in the WHCO series of cell lines. This modulation caused a significant change in the WHCO6 cell line (see *Appendix D, Table D5* for a complete statistical report). Combination treatment with fibronectin and PI3K-specific inhibition reproduced the trend reported for PI3K-specific inhibition with LY294002 (*Table 4.3.*). Here, p-RPS6$^{(Ser\ 235/236)}$ expression was reduced in all HOSCC cells, but was significantly altered in the WHCO6 and even MCF-7 cell lines (see *Appendix D, Table D5* for a complete statistical report). Therefore, blocking PI3K with LY294002 disrupts the mechanotransduction of fibronectin-derived adhesion-based stimuli to mTOR and mTORC1 in HOSCC cells.

A.

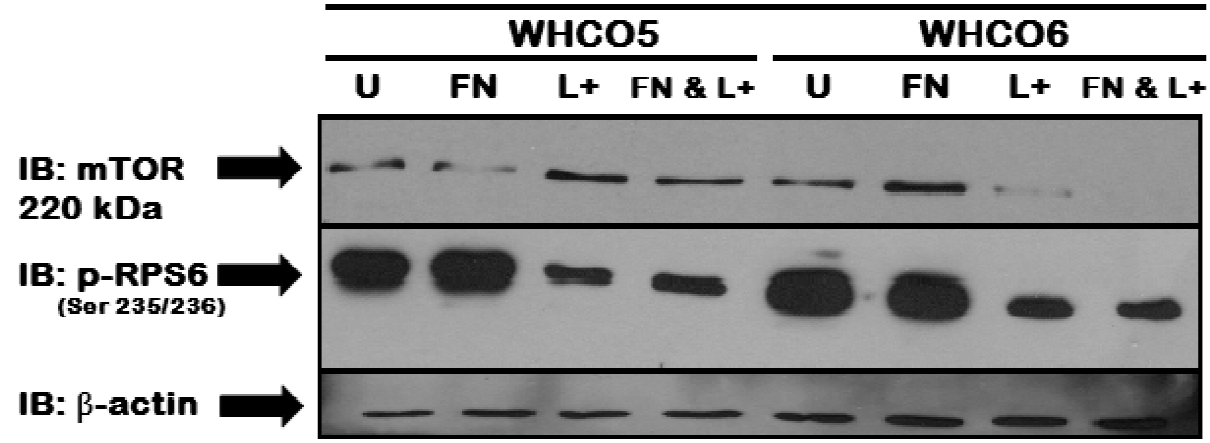

B.

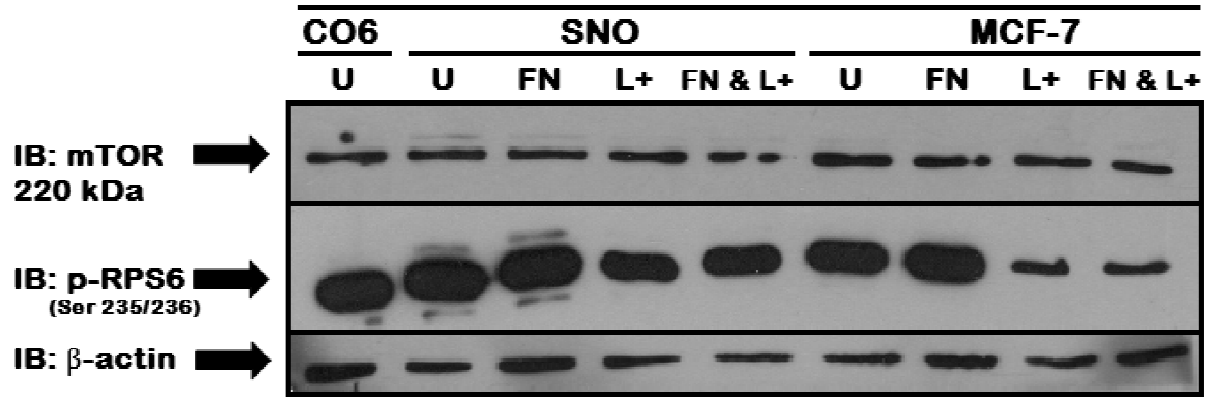

Figure 4.5: mTOR and RPS6$^{(Ser\ 235/236)}$ phosphorylation were altered after combination treatment with fibronectin and specific inhibition of PI3K. Western blotting confirmed visible changes in polypeptide abundance for mTOR (220 kDa) and p-RPS6$^{(Ser\ 235/236)}$ (36 kDa). WHCO5, WHCO6 and SNO cell lines were chosen to represent the diverse behavioural and protein expression trends present within the HOSCC model system. β-actin demonstrated equal protein loading of HOSCC and MCF-7 cell lysates. (U = Untreated HOSCC cells; FN = Substrate coated with Fibronectin; L+ = specific inhibition of PI3K with LY294002).

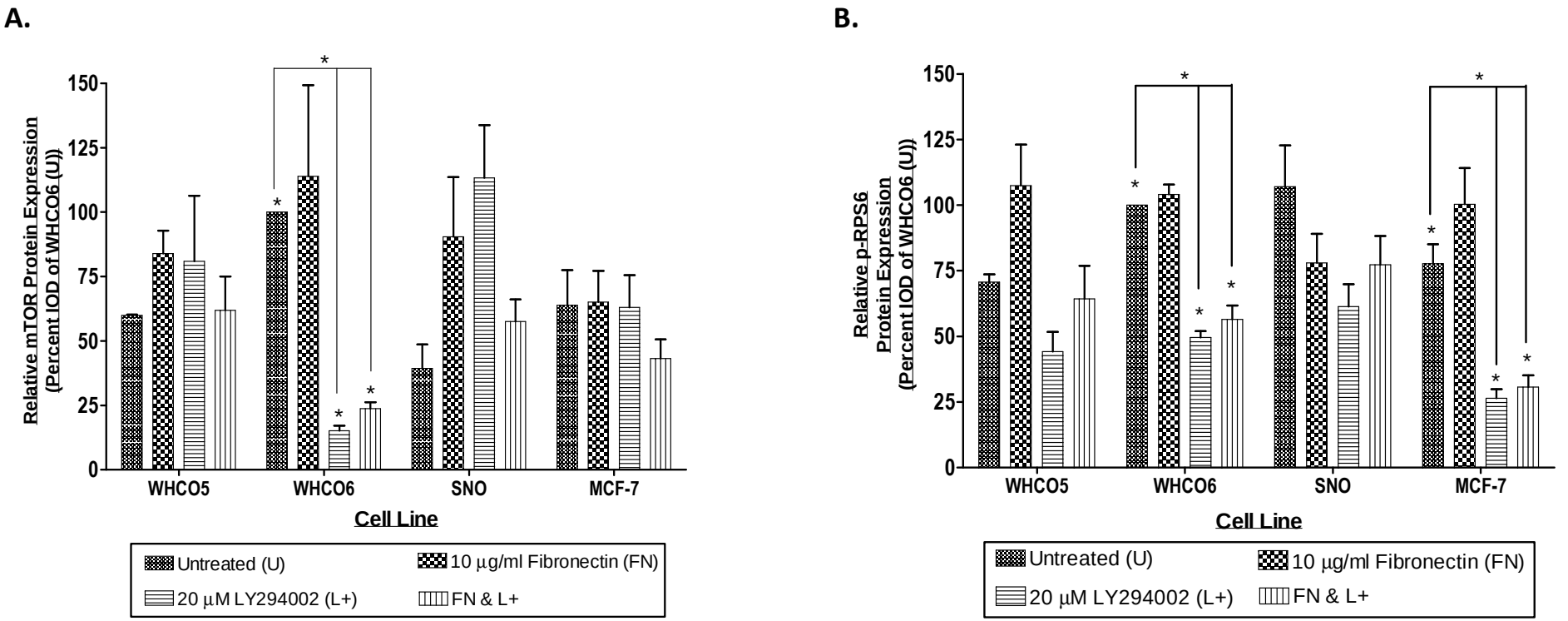

Figure 4.6: Relative percentage of mTOR and p-RPS6$^{(Ser\ 235/236)}$ protein expression after HOSCC cells were treated with a combination of fibronectin and specific inhibition of PI3K with LY294002. Semi-quantitative densitometric analysis of mTOR and p-RSP6(Ser 235/236) protein expression was determined relative to the untreated (U) WHCO6 cell line. **A)** HOSCC cells generally increased mTOR protein expression in response to fibronectin and after specific inhibition of PI3K. This trend was also observed in response to combined treatments. **B)** HOSCC cells generally increased RPS6$^{(Ser\ 235/236)}$ phosphorylation in response to fibronectin treatment. However, in response to PI3K-specific inhibition, HOSCC cells decreased p-RPS6$^{(Ser\ 235/236)}$ protein expression as a common trend. Similarly, this effect was observed in response to the combined treatment with fibronectin and PI3K-specific inhibition; where HOSCC cells decreased RPS6$^{(Ser\ 235/236)}$ phosphorylation. Since all western blots were repeated more than once, the significance of these data could be determined. Significant difference is therefore indicated graphically through the use of lines connecting star (*) symbols. ((U = Untreated HOSCC cells; FN = Substrate coated with Fibronectin; L+ = specific inhibition of PI3K with LY294002).

Table 4.3: Summary of mTOR p-RPS6$^{(Ser\ 235/236)}$ protein expression levels after combination treatment with fibronectin and specific inhibition of PI3K with LY294002.

Protein	Treatment	Cell Line											
		WHCO5			WHCO6			SNO			MCF-7		
		↑/↓	H/M/L	% Δ	↑/↓	H/M/L	% Δ	↑/↓	H/M/L	% Δ	↑/↓	H/M/L	% Δ
mTOR	Fibronectin (FN)	↑	High	40.00	↑	High	14.00	↑	High	130.77	↑	Med	1.56
	LY294002 (L+)	↑	High	35.00	* ↓	* Low	* -85.00	↑	High	189.74	↓	Med	-1.56
	FN & L+	↑	Med	35.00	* ↓	* Low	* -85.00	↑	Med	189.74	↓	Low	-1.56
p-RPS6 (Ser 235/236)	Fibronectin (FN)	↑	High	50.70	↑	High	4.00	↓	High	-27.10	↑	High	28.21
	LY294002 (L+)	↓	Low	-38.03	* ↓	* Med	* -50.00	↓	Med	-42.99	* ↓	* Low	* -66.67
	FN & L+	↓	Med	-9.86	* ↓	* Med	* -44.00	↓	High	-28.04	* ↓	* Low	* -60.26

Key: Low = 0 – 45 %; Medium (Med) = 46 – 75 %; High = 76 – 100 % (and above). Protein expression levels are based on the Hager *et al.*, (2011) classification system for analyses of mTOR and p-RPS6 proteins (see Materials and Methodology, Section 4.2.12). Change in relative marker set protein expression is expressed as percent change (% Δ), designated by either positive (↑) or negative (↓) arrows. For the calculation of percent change, see Appendix B, Equation B1. The use of a star (*) symbol, as well as red text, represents a statistically significant difference when compared to the WHCO6 (U) cell line, determined using a Student's t-test; where $p < 0.05$ (see Appendix D, *Table D5 for a statistical report*).

4.4. Discussion

4.4.1. Mechanical stimuli influence the mTOR/mTORC1 signalling pathway in HOSCC cells

Observations of cell spreading on fibronectin-coated substrates demonstrate that mechanical signalling induces the phosphorylation and activation of integrin-triggered focal adhesion protein kinases, such as FAK (Wu and Dedhar, 2001; Hanks *et al.*, 2003). This presumably allows for the induction of matrix-derived survival signalling through FAK/c-Jun interactions (Almeida *et al.*, 2000), as well as Rac and Rho signalling events (Huveneers and Danen, 2009). Fibronectin treatment also stimulates cap-dependant translation initiation, an mTOR-dependant process (Gorrini *et al.*, 2005). Therefore, fibronectin-induced FAK phosphorylation provides a regulatory link between mechanical stimuli originating from the ECM and mTOR/mTORC1 activation, as activated FAK causes TSC2 inactivation (Gan *et al.*, 2006), which is a negative regulator of p-p70S6K. This allows FAK to activate mTOR/mTORC1 signalling on this level. The possibility of this form of mTOR regulation was observed in HOSCC cells as fibronectin commonly increased both mTOR abundance and RPS6$^{(\text{Ser } 235/236)}$ phosphorylation. Since mTORC1 may be activated by ECM-originating stimuli through focal adhesion protein kinases, like FAK, this provided a rationale to further examine the molecular mechanisms achieving this.

When oesophageal cells attached to collagen, signalling through mTOR/mTORC1 increased. Consequently, exposure of HOSCC to this type of ECM component may affect the mTOR signalling machinery in a manner akin to fibronectin-induced mechanotransduction. Collagen positively regulates PKB phosphorylation through the action of ILK, allowing for the survival of substrate-dependant cells like fibroblast (Nho *et al.*, 2005). In addition, both ILK and PKB may phosphorylate and inhibit GSK-3β, which normally regulates TSC1/TSC2, leading to increased mTORC1 signalling (Mak *et al.*, 2005; Volker *et al.*, 2007). Increased collagen-dependant signalling in this manner implicates signalling through ILK, which is suggested as an instigator of epithelial morphogenesis (Schöck and Perrimon, 2002), as architectural changes in fibrillar collagen, and subsequently ILK activation, may contribute towards cancer progression (Egeblad *et al.*, 2010). Therefore, this form of ILK-dependent

mTOR regulation may contribute to tumourigenesis in HOSCC, given that HOSCC cells commonly over-express ILK (Driver and Veale, 2006).

Mechanically-derived extracellular-originating stimuli clearly impinge on the mTOR pathway. Mechanotransduction subsequently influences both cellular concentrations of mTOR, as well as signalling through mTORC1, which may explain seminal observation by Fung e*t al.* (2008) regarding autophagy induction in substrate-dependant cells. Fung and colleagues (2008) observed that the induction of autophagy followed cell detachment from the ECM. Therefore, since it is apparent that ECM-dependant mechanotransduction enhances mTORC1 signalling, and considering the mTOR pathway is responsible for autophagy inhibition, the lack of adhesion-based signalling to the mTOR pathway (arising when cells become detached from a substrate) may account for decreased signalling through mTORC1. Consequently, decreased signalling through mTORC1 would allow for increased cellular concentrations of dephosphorylated mATG-13. Therefore, increased mATG-13 would enhance pro-autophagy signalling and the potential for autophagy induction.

4.4.2. ILK, an integrin-triggered focal adhesion protein kinase, does not physically associate with mTOR

The realisation that mechanically-derived stimuli directly impinge upon the mTOR/mTORC1 pathway calls into question the exact route of signal transmission from sites of cell-ECM contact to the mTOR signalling machinery. The intracellular propagation of adhesion-based signals is known to involve the activation of integrin-triggered protein kinases, such as ILK and FAK (Wu and Dedhar, 2001; Hanks *et al.*, 2003), which cluster around sites of focal contact. When activated, these protein kinases assist in focal adhesion biogenesis, as well as mechanotransduction events influencing gene expression and ultimately cell behaviour (Brakebusch and Fässler, 2003; Legate *et al.*, 2006; Hannigan *et al.*, 2011). Therefore, the involvement of an integrin-triggered focal adhesion protein kinase may provide the molecular connection required between the integrin adhesion system and mTOR. Consequently, we hypothesised a direct protein-protein interaction between mTOR and ILK, since autophagy induction was found to be FAK-independent (Hara *et al.*, 2008). However, we also included FAK considering the integral involvement of FAK during anoikis resistance in HOSCC cells (Fanucchi and Veale, 2011).

Proteins require a means of physical interaction facilitating the transmission of biochemical information (Ubbink, 2009). Intracellular signals are therefore conveyed by creating a short lived (nanosecond) encounter complex, formed by interacting protein species (Ubbink, 2009). By exploiting protein-protein complex formation, one may detect the protein components of the so-called 'signalsomes' through molecular techniques, such as fluorescently-tagged fusion proteins, as well as co-immunoprecipitation analysis (Wang and Malbon, 2011).

Co-immunoprecipitation revealed that mTOR does not form a signalsome complex with either ILK or FAK. This means that neither ILK nor FAK functions as direct conduit for mechanotransduction to the mTOR/mTORC1 pathway. Therefore, autophagy regulation presumably involves an indirect mechanism using one of these focal adhesion protein kinases. The lack of involvement of FAK was expected; since a recent study observed that abnormalities were not encountered by $FAK^{-/-}$ knockout mouse embryonic fibroblasts (MEF's) to induce autophagy (Hara *et al.*, 2008). This suggests that FAK does not play a critical role in autophagy through mTOR regulation. Consequently, it follows that ILK is the focal adhesion protein kinases involved, however clearly not through a direct protein-protein interaction with mTOR.

We initially hypothesised that the transmission of ECM-originating signals occurs by means of a direct ILK/mTOR protein interaction. An association between ILK and the main protein component of mTORC2; Rictor (McDonald *et al.*, 2008), was thought to allude to this possibility. However, exclusion of an ILK-mTOR protein complex rather suggests potential for an indirect functional relationship between ILK and mTORC1. This was determined to be a valid observation, and not a product of the methodology, because a true mTOR-Raptor interaction was detected. This means that the intracellular propagation of adhesion-based stimuli may only occur through a common signalling pathway downstream of ILK, but upstream of mTOR. Since canonical regulation of mTOR through PI3K suits these criteria (determined previously in Chapter 3), the involvement of the PI3K/PKB pathway was thought to provide this indirect, molecular connection between ILK and mTOR/mTORC1.

4.4.3. ECM-modulation of mTOR/mTORC1 signalling occurs in an integrin-triggered, but PI3K-dependent manner

While there is considerable information available pertaining to the regulation of mTOR signalling in response to soluble stimuli (Soulard and Hall, 2007; Memmot and Dennis, 2009), comparatively less is known concerning the contribution of ECM-originating signals. Therefore, to understand how attachment to an extracellular matrix may influence the mTOR signalling pathway in HOSCC, we provided ECM components normally encountered by oesophageal cells, while simultaneously negating signal transduction through channels used by soluble mitogenic stimuli. In this way, we provide evidence for a PI3K-dependant mechanism during the ECM modulation of mTOR/mTORC1. To our knowledge, this is also the first report of such regulation of mTOR in SCC of the human oesophagus.

One of the few studies demonstrating ECM modulation of the mTOR/mTORC1 signalling pathway found that fibronectin influences cap-dependant translation initiation by activating mainly β1 integrins (Gorrini *et al.*, 2005). Importantly, this process was highly sensitive to the inhibition of PI3K, suggesting this pathway may play a role during adhesion-based signal transduction. Furthermore, only one other analysis investigated the importance of common ECM components, like fibronectin, on the mTOR pathway in non–small cell lung carcinoma (NSCLC) cells (Han *et al.*, 2006). During this investigation, the authors demonstrated that attachment to fibronectin increased p-PKB, p-p70S6K and p-4EBP-1 protein expression in NSCLC. Moreover, growth on fibronectin reduced PTEN and p-AMPKα activity, which are both negative regulators of mTOR/mTORC1 signalling. Therefore, these data strongly suggests that fibronectin activates the PI3K/PKB/mTOR/mTORC1 pathway, at least in NSCLC cells. However, one aspect of adhesion-based signalling these findings do not adequately explore is the molecular mechanisms achieving this type of pathway activation. This is because the sequence of activated pathway intermediates, from a cell signalling point of view, is not clearly delineated.

In comparison to the above, we showed that the mTOR pathway in HOSCC cells is also activated in response to fibronectin. By using fibronectin in combination with specific PI3K inhibition, we demonstrated that fibronectin stimulates mTORC1 through a mechanism dependent on the activation of PI3K. Here, when PI3K was blocked, mechanical stimuli elicited by fibronectin were diminished. Consequently, we believe this would also directly

impinge on the ability of mTORC1 to regulate autophagy induction, resulting in an increased autophagy potential in HOSCC cells when mechanical signals are not transduced through the PI3K/PKB pathway.

Based on our understanding of ECM modulation of mTOR/mTORC1 signalling in HOSCC cells, we believe these findings indicate that cellular attachment to the ECM enhances the ability of mTOR to regulate autophagy. Indeed the ECM is capable of directing intricate cellular process, such as gene expression, epithelial morphogenesis, as well as cell survival (Ramirez and Rifkin, 2003; Berrier and Yamada, 2007; Rozario and DeSimone, 2010). However when HOSCC cells lose cell-ECM attachment, this diminishes signal transduction to mTORC1, subsequently affecting mTOR-dependent autophagy regulation, thus increasing autophagic processing. In highly tumourigenic epithelial phenotypes with an increased propensity for metastasis, like HOSCC (Lam, 2000; Lehrbach *et al.*, 2003; Lin *et al.*, 2009), the induction of autophagy in this manner may constitute a cell survival strategy augmenting dissemination to distant sites.

In conclusion, it is evident that extracellular matrix-originating stimuli are capable of influencing the mTOR signalling pathway in HOSCC. By exposing HOSCC cells to major ECM components naturally encountered by oesophageal epithelial cells (such as fibronectin and collagen), we demonstrate that biophysical stimuli modulate cellular concentrations of mTOR and enhance signalling through mTORC1. We also establish that the intracellular propagation of ECM-based signals to mTOR does not involve a direct interaction with ILK or FAK. Rather, adhesion-based stimuli influences the mTOR/mTORC1 signalling pathway in an integrin-triggered, but PI3K-dependant manner – since specifically blocking PI3K perturbed transmission of adhesion-based stimuli to the mTOR/mTORC1 signalling pathway. Moreover, since signalling through mTORC1 increased in the presence of adhesion-based stimuli, but was diminished when PI3K/PKB signalling is blocked, we believe that mTORC1-dependent autophagy induction is affected by the state of cellular attachment. Importantly, these findings indicate that the potential for autophagy induction increases as cell-ECM interactions dissipate. Therefore, these data strongly suggest mTOR is a target for adhesion-based signal transduction, which influences cell survival through mTORC1.

CHAPTER 5

5. GENERAL DISCUSSION AND CONCLUSION

5.1. The mTOR/mTORC1 signalling pathway is activated in moderately differentiated HOSCC cells

The mammalian target of rapamycin (mTOR) is a 220 kDa Ser/Thr protein kinase comprising the main signal transduction intermediate of the mTOR signalling pathway (Schmelzle and Hall, 2000; Caron *et al.*, 2010; Foster and Fingar, 2010; Dobashi *et al.*, 2011). mTOR functions as a master regulator of intracellular signals and so combines nutrient, energy and mechanical stimuli to maintain homeostasis in epithelial tissue (Schmelzle and Hall, 2000; Foster and Fingar, 2010; Dobashi *et al.*, 2011). Aberrant signalling through the mTOR pathway is associated with numerous human pathologies; such as melanoma, Tuberous Sclerosis complex, Cowden's disease, Proteus syndrome and Peutz-Jeghers syndrome (reviewed by Vivanco and Sawyers, 2002; Guerten and Sabatini, 2005; Inoki *et al.*, 2005). In addition, inappropriate signalling through the mTOR pathway is reported to be transforming within solid epithelial tumours affecting the prostate (Li *et al.*, 1997; Dreher *et al.*, 2004), breast (Li *et al.*, 1997; Vivanco and Sawyers, 2002) and lungs (Vivanco and Sawyers, 2002; Barnes and Kumar, 2003). Therefore, any alteration to the normal operating procedure of the mTOR signalling pathway may result in aberrant mTOR function, and consequently mTOR-based disease progression.

Despite a history of mTOR-specific analyses of solid epithelial tumours, very few studies have focussed on characterising the mTOR pathway as a molecular mechanism promoting progression of human oesophageal squamous cell carcinoma (HOSCC). HOSCC is a highly metastatic epithelial cancer with great tumourigenic potential (Tew *et al,* 2005; Bird-Lieberman and Fitzgerald, 2009), currently rated the eighth most common cancer in the world, and is responsible for approximately one sixth of all cancer related deaths worldwide (Scully and Bagan, 2009; Melhado *et al.*, 2010). HOSCC presents symptomatically late, with a poor prognosis, and so any measurable molecular irregularities would be useful to improve diagnosis. Currently, elevated mTOR protein abundance, as well as increased expression of mTOR downstream targets (such as p-p70S6K, 4E-BP1 and p-RSP6$^{(Ser\ 235/236)}$) are used with

increasing frequency as biomarkers indicating transformation (Lin *et al.*, 2009; Hager *et al.*, 2011; Pal and Figlin, 2011). This suggests that modifications to the mTOR/mTORC1 signalling pathway may serve as a central instigator for tumourigenesis. Therefore, significant changes to mTOR and mTORC1 are noteworthy and may improve diagnosis of HOSCC at even earlier stages.

In this study, moderately differentiated HOSCC cells were used as a cellular model in which to investigate major signal transduction intermediates associated with the mTOR pathway. We determined that these intermediates conveyed pathway-specific information, such as signalling through mTORC1, regulation of autophagy induction and mechanotransduction through integrin-adhesion systems. Additionally, controlled tissue culture conditions permitted the manipulation of appropriate growth-stimulatory signals. These parameters allowed essential growth and proliferation to occur, as well as the establishment of important baseline data to which further manipulations could be compared.

Inherently, the MCF-7 cell line served as a useful comparison to analyse the mTOR/mTORC1 signalling pathway in HOSCC. The main reasons for this included: a) MCF-7 cells over-express the mTOR protein kinase (Hagner *et al.*, 2009); b) MCF-7 cells display elevated signalling through mTORC1 (Hagner *et al.*, 2009), thought to be a consequence of a constitutively active PI3K/PKB signalling pathway (deGraffenried *et al.*, 2004). Activating mutations affecting the p110 subunit of PI3K (Bachman *et al.*, 2004) directly affect mTOR signalling as the PI3K/PKB pathway is an upstream regulator of mTOR (Sekulic *et al.*, 2000); c) The *S6K1* gene is amplified in MCF-7 cells (Bärlund *et al.*, 2000a; Bärlund *et al.*, 2000b).

Similar to MCF-7 cells, we determined that the majority of HOSCC cells expressed elevated cellular concentrations of mTOR, as well as enhanced signalling through mTORC1 – observed through high instances of $RPS6^{(Ser\ 235/236)}$ phosphorylation. Surprisingly, we also discovered that HOSCC cells exhibited an elevated autophagy induction potential; a characteristic of transformation providing a distinct survival advantage to solid epithelial tumours (Chen and Debnath, 2010). Elevated autophagy reportedly supports cellular fitness and survival of established tumour cells, such as iBMK and HeLa cells, in response to stress (Degenhardt *et al.*, 2006). Moreover, we also discovered that ILK was expressed ectopically in both HOSCC and MCF-7 cells, suggesting an increased transduction potential for

adhesion-based stimuli. Ultimately, we do find that HOSCC cells exhibit similar trends to transformed MCF-7 cells; such as an activated mTOR signalling pathway, where increased mTOR abundance and mTORC1 signalling are commonplace. It must be noted that we do not mean to suggest that the molecular mechanisms which underpin aberrant mTOR/mTORC1 signalling are the same for HOSCC and MCF-7 cells. We only highlight the fact that the mTOR pathway manifest in HOSCC cells is analogous to a cellular system known to possess a corrupt mTOR signalling pathway, such as MCF-7. Therefore, aberrations such as these may contribute towards corruption of mTOR-dependant cellular processes, such as proliferation and autophagy, resulting in tumourigenesis and inappropriate survival signalling in HOSCC cells.

5.2. Expression of the 80 kDa mTORβ splicing isoform is variable in HOSCC cells

We established an association between cellular concentrations of mTOR and the degree of $RPS6^{(Ser\ 235/236)}$ phosphorylation in HOSCC, where a high occurrence of mTOR generally indicated a high degree of $RPS6^{(Ser\ 235/236)}$ phosphorylation. This type of association was clear in the MCF-7 cell line, and has also been reported in patients with advanced renal cell carcinoma (Cho *et al.*, 2007). In fact, the link between the expression of mTOR and $p\text{-}RSP6^{(Ser\ 235/236)}$ has proved invaluable as a predictive tool for sarcomas during targeted mTOR therapy (Iwenofu *et al.*, 2008). However, in certain HOSCC cell lines (WHCO1 and WHCO3) where this relationship did not occur, we noted that high mTORC1 signalling did not necessitate high concentrations of mTOR. Interestingly, only these WHCO cell lines expressed the 80 kDa mTOR splicing isoform, termed mTORβ (Panasyuk *et al.*, 2009).

mTORβ was found to be neither a cleavage product, nor the result of protein degradation and possesses the required potential to affect signal transmission through mTORC1 (Panasyuk *et al.*, 2009). The mTORβ splice variant is capable of interacting with known upstream regulators of the 220 kDa version of mTOR, namely Raptor and Rictor (Panasyuk *et al.*, 2009). In addition, mTORβ readily phosphorylates p70S6K, 4EBP-1 and PKB *in vitro*. Panasyuk *et al.* (2009) report further that mTORβ over-expression transforms immortalized cells, is tumourigenic in nude mice models and significantly reduces the G1 phase of the cell cycle. Since mTORβ retains intact FRB, RD and FATC domains, remaining subject to all mTOR-like regulation, and assuming mTORβ possess the above qualities in HOSCC, the

expression of mTORβ in WHCO1 and WHCO3 cells may be a plausible explanation for the maintenance of elevated RPS6$^{(Ser\ 235/236)}$ phosphorylation levels in these lines only.

In the SNO cell line, where the opposite was true (i.e. high mTOR expression, but low RPS6$^{(Ser\ 235/236)}$ phosphorylation), we considered that activating mutations affecting mTOR gene expression or the mTOR kinase domain were possible explanations for this disparity, in light of no mTORβ expression. Significant differences in gene expression are reported to result from ectopic mTOR-related tumour suppressers and oncogenes in ovarian and breast cancer (Heinonen *et al.*, 2008; Laudański *et al.*, 2011). Furthermore, single amino acid changes have been identified with regard to mTOR and human cancer. Sato *et al.* (2010) recently examined the Sanger Centre Cancer Genome Database (COSMIC) for changes such as these, identifying ten functional amino acid changes relating to the *mTOR* gene in tumours affecting skin, breast, intestine and the digestive tract. Only four mutations involving the kinase domain, M2011V (mucinous carcinoma of the overy), S2215Y (adenocarcinoma affecting the large intestine), P2476L (glioma in the brain) and R2505P (kidney clear cell renal carcinoma), was examined for mutant expression and constitutive mTOR activation. Interestingly, only S2215Y and R2505P conferred constitutive activation to mTOR. Therefore, it is conceivable that WHCO1, WHCO3, WHCO5 and WHCO 6 cell lines contain mutations akin to either S2215Y and R2505P, while the SNO cell line may contain M2011V and/or P2476L – possible kinase inactivating mutations.

Frequent activation of mTOR-dependant signalling in human cancer may also arise from constitutive activation of upstream regulators, such as PKB, TSC1, TSC2 and Rheb, leading to the activation of mTOR (Yuan and Cantley, 2008). It is important to remember that PKB negates the inhibitory affect of TSC1/TSC2 which impinges on the mTOR-activating Rheb-GTPase. Therefore, one would need to investigate TSC1 and TSC2, as well as the Rheb-GTPase, for functional mutations to ascertain a proper understanding. Moreover, experimental evidence from human colorectal cancer (Nozawa *et al.*, 2007) and malignant melanoma (Karbowiniczek *et al.*, 2008) implicate a role for hyperphosphorylation of mTOR, p70S6K and RPS6. Moreover, genetic disorders resulting from the activation of TSC1/TSC2 (Inoki *et al.*, 2005), or decreased expression of negative upstream regulators, such as PRAS40 and DEPTOR, may lead to the activation of mTOR (Sancak *et al.*, 2007; Peterson *et al.*, 2009). Consequently, while single amino acid changes affecting the mTOR kinase domain may play a role, the contribution of the plethora of other upstream possibilities

activating mTOR cannot be discounted and could be explored further as component of another investigation. However, the fact that SNO does not express mTORβ reinforces the notion that one (or more) of these common functionally crippling mutations may be present within the mTOR protein kinase expressed specifically by the SNO cell line.

5.3. The PI3K/PKB signalling pathway functions as a canonical regulator of mTOR/mTORC1

The PI3K/PKB signalling pathway is now known to function as a critical, upstream regulatory system controlling essential cellular processes; such as growth, proliferation and cell survival (Cantley, 2002). Specific inhibitors of this pathway (such as Wortmannin and LY294002) are used to target phosphatidylinositol 3-kinases, ultimately showing that the lipid products generated by PI3K's are essential for PKB activation (Vlahos *et al.*, 1994; Nicholson *et al.*, 2003). As a result, PI3K-dependant PKB activation was identified as a ubiquitous intracellular signalling scheme, since the importance of PI3K/PKB signalling was also observed in KB-3-1 and KB-v1 cells (Nicholson *et al.*, 2003), as well as in HeLa, HEK-293T, A549 and BEL-7404 cell lines (human liver cancer cells) (Crabbe, 2007; Liu *et al.*, 2011). Deregulated signalling through PI3K and PKB is known to contribute towards malignant transformation in epithelial tissues (Krasilnikov, 2000). This indicates that PI3K-dependant PKB activation is a key regulatory event necessary for growth, proliferation and cell survival, and even tumourigenesis.

Inhibition of PI3K was shown to decrease PKB activation, and thus mTORC1 signalling (Martelli *et al.*, 2010). We demonstrate this also occurs in HOSCC cells, where mTORC1 signalling commonly decreased in response to specific inhibition of PI3K. These results convey specific positional information pertaining to the PI3K and mTOR pathways in HOSCC cells; where PI3K is situated upstream of mTOR/mTORC1. Furthermore, these findings indicate that the PI3K/PKB signalling pathway indeed functions as a canonical, upstream regulator of mTORC1 signalling in the WHCO series of cell lines. In addition, these results signify that PI3K signalling may critically influence mTORC1-dependent survival signalling. This was observed through an increase in autophagy induction potential, demonstrated by the increase in dephosphorylated mATG-13 protein expression in HOSCC cells.

Interestingly, this potential increase in autophagy initiation was not observed in earlier studies using thrombin-activated platelets, where specific inhibition of PI3K (also by LY294002) negated complete autophagosome formation (Blommaart *et al.*, 1997). These finding are therefore unique in this respect, and point towards the involvement of the PI3K/PKB pathway during the regulation of autophagy induction signals – perhaps through those cellular proteins that play important roles in autophagosome formation; such as ULK1/2, Bif and Beclin 1 (Brunn *et al.*, 1996; Blommaart *et al.*, 1997). Specific inhibition of PI3K and mTORC1, was in fact was found to contribute directly to autophagy induction and promote autophagosome formation (Xie and Klionsky, 2007; Jung, *et al.*, 2009). Currently, the use of tailored multi-kinase inhibitors (such as PI-103) is a novel means of targeting both PI3K and mTOR (Hayakawa *et al.*, 2007), compounding decreased signalling through both pathways. Such strategies have proved useful in a panel of aggressive glioma cell lines, both *in vitro* and *in vivo* (Fan *et al.*, 2006), and so may hold similar promise in HOSCC considering the efficacy of hindering PI3K and mTOR signalling through PI3K inhibition.

5.4. Removal of proliferative signals triggers an autophagic response in HOSCC cells

Tissue culture in the absence of serum constitutes a useful method to investigate the cellular responses reliant on these growth-promoting factors, such as the induction of autophagy, demonstrated by modulation of both mTOR and mTORC1 signalling in HOSCC upon the removal of serum (Langdon, 2004; O'Conner and O'Driscoll, 2006). During standard tissue culture conditions, serum supplies the agonistic factors necessary for the appropriate regulation of mTOR signalling through canonical and non-canonical mechanisms. Therefore, the withdrawal of serum was shown to affect normal intracellular signal transduction from pathways such as PI3K/PKB, hsVP34 and Rag GTPases (Yan *et al.*, 2010), since these signalling mechanisms transduce growth factor and amino-acid stimuli to the mTOR pathway (Avruch *et al.*, 2009; Foster and Fingar, 2010). In Chapter 3, we observed serum-dependant modulation of the mTOR signalling pathway in HOSCC cells (i.e. altered cellular concentrations of mTOR and decreased signalling thorough mTORC1), a cellular response also documented in human neuroblastoma (Edelstein *et al.*, 2011), as well as human U2OS osteosarcoma cells (Fingar *et al.*, 2004). As a consequence of nutrient depletion, decreased mTOR/mTORC1 signalling slows cell growth by arresting the G1 phase of the cell cycle

(Fingar *et al.*, 2002; Fingar and Blenis, 2004; Fingar *et al.*, 2004), supporting the role of mTOR as a sensor of nutrient availability in HOSCC.

While growth factor-dependant signalling to mTOR (supplied by serum) involves canonical regulation through PI3K/PKB, the mechanism for amino-acid-dependant regulation of mTOR by RagGTPases remained incompletely understood. However, the recent discovery that glutamine, in combination with the branched chain amino-acids leucine and isoleucine, positively regulate mTORC1 signalling through RagB- and RagC-GTPases (Durán *et al.*, 2012), constitutes a major breakthrough in understanding the mechanism of mTOR regulation by amino-acids. Durán *et al.* (2012) recently demonstrated that inhibition of glutaminolysis (the conversion of glutamine into α-ketoglutarate) prevents RagB- and RagC-GTPase activity, and as a result, signalling through mTORC1. Conversely, enhanced glutaminolysis increased signalling through mTORC1. Therefore, these and future discoveries in this regard may provide a basis to understanding the contribution of nutrients in disease; such as glutamine addiction prevalent in many cancers (Fingar and Blenis, 2004; Durán *et al.*, 2012).

5.5. The mTOR signalling pathway in HOSCC is susceptible to rapamycin

mTOR was first identified as a biologically relevant target of rapamycin by Brown *et al.* (1994) when two structural variants of rapamycin (16-keto-rapamycin and 25,26-iso-rapamycin) were used to classify targets of the FKBP-rapamycin complex. Soon after, it was discovered that treatment with rapamycin (at physiologically relevant concentrations as low as 1 nanomolar (Sabers *et al.*, 1995; Zhou and Huang, 2010) could specifically suppress the phosphorylation of common mTOR substrates (such as p70S6K and 4E-BP1) in transformed epithelial cell lines; including Human breast cancer cells MCF-7 and MCF-7R (Chen *et al.*, 2003). Investigations focussing on the specific inhibition of mTOR within these rapamycin-sensitive cells in comparison to rapamycin-resistant cell lines, such as MDA-MB-231 cells, revealed that mTOR functions as a 'master signal regulator' directing essential cellular processes; such as cell growth, cell cycle, metabolism and autophagy (Fingar and Blenis, 2004; Zhou and Huang, 2010).

In Chapter 3 we explored the impact of the mTOR/mTORC1 signalling pathway on cell proliferation (the extent of RPS6$^{(Ser\ 235/236)}$ phosphorylation) and autophagy induction (cellular

concentration of mATG-13) by inhibiting the kinase ability of mTOR. We demonstrated that while mTOR inhibition does not affect the protein expression of focal adhesion kinases (such as ILK), rapamycin potently perturbs elevated signalling through mTORC1 in HOSCC of South African origin. In fact, RPS6$^{(Ser\ 235/236)}$ phosphorylation, and thus mTORC1 signalling, may be completely abolished through exposure to low (nanomolar) concentrations of rapamycin. These findings may indicate promise for those diagnosed with HOSCC in Southern Africa, since those affected experience late detection resulting from poor diagnostic methodologies for screening high-risk populations (Kachala, 2010). Decreasing signalling through the mTOR/mTORC1pathway through exposure to rapamycin may therefore provide a form of control for this disease, other than a surgical option (Bancewicz, 1990). Moreover, aberrant mTOR signalling is implicated in the progression of other human cancers; such as breast and ovarian (Campbell *et al.*, 2004), melanoma (Madhunapantula *et al.*, 2009), and renal cell carcinomas (Kondo *et al.*, 2001). In addition, deregulated mTOR/mTORC1 pathway activities have been observed in several other human diseases; such as diabetes, Cowden's disease (Inoki *et al.*, 2005), Tuberous Sclerosis complex (TSC) (Kenerson *et al.*, 2002), Lymphangioleiomyomatosis (LAM) (Johnson and Tattersfield, 2002). Therefore, we strongly contend that these findings provide support for rapamycin and its derivatives as viable therapeutic agents to curb aberrant mTOR-dependant signalling events.

5.6. RPS6$^{(Ser\ 235/236)}$ is phosphorylated by mTORC1 in the absence of MAPK/p90RSK-dependent signal transduction in HOSCC

Initially, we considered the activation state of each mTOR multi-protein complex (i.e. mTORC1 or mTORC2) as a possibly more informative means to monitor the signalling potential of mTOR. This was a viable option since each mTOR complex displays mTOR-specific phosphorylation patterns. Copp *et al.* (2009) established that mTORC1 is predominantly phosphorylated at S2448, by both PKB and p70S6K, whereas mTORC2 is predominantly phosphorylated at S2481. Commercial phospho-mTOR antibodies for these sites are also available, allowing for immunodetection of each active complex. However, this line of reasoning was abandoned after considering the propensity for carcinomas to hyperphosphorylate mTOR at these sites (Karbowiniczek *et al.*, 2008; Sato *et al.*, 2010). In addition, since the mutational status of mTOR is currently unknown in these HOSCC cell lines, detecting phosphorylated mTOR may convey incorrect information concerning the

activation of mTORC1 – the complex responsible for RSP6$^{(Ser\ 235/236)}$ and mATG-13 phosphorylation.

Since the anti-mATG-13 antibody was used to detect dephosphorylated mATG-13, specifically (Chan *et al.*, 2009), we used the extent of RPS6$^{(Ser\ 235/236)}$ phosphorylation as downstream marker for active mTORC1 signalling. However, p90RSK (an effector kinase of the MAPK signalling cascade) may also phosphorylate RPS6$^{(Ser\ 235/236)}$ (Nguyen, 2008). Therefore, we assessed the ability of mTORC1 in HOSCC cells to phosphorylate RPS6$^{(Ser\ 235/236)}$ in the absence of MAPK/p90RSK signals by using a newly developed p90RSK-specific inhibitor, BI-D1870, designed to target all four RSK isoforms (Sapkota *et al*., 2007). As specific p90RSK inhibition with BI-D1870 decreases p-PKB$^{(Thr\ 308)}$, but not the degree of PKB$^{(Ser\ 473)}$ phosphorylation – a downstream target of mTORC2 (Chen and MacKintosh, 2009), we expected that mTORC1 activity would be similarly unaffected by BI-D1870. Indeed we demonstrated, for the first time, that inhibition of p90RSK decreased the phosphorylation of RPS6$^{(Ser\ 235/236)}$ in HOSCC cells between 5.0 and 13.0 % only, where appreciable levels of p-RPS6$^{(Ser\ 235/236)}$ remained. This indicates that mTOR/mTORC1-based signals are responsible for RPS6$^{(Ser\ 235/236)}$ phosphorylation in the absence of active p90RSK in the WHCO cell lines investigated here.

In contrast to other small molecule inhibitors of p90RSK (such as FMK and SL0101), BI-D1870 has shown remarkable affinity for all four RSK splice variants, especially in HEK-293 cells, while not significantly affecting the important cellular kinases; such as GSK-3β, PKB, mTOR, AGC-like kinases and PDK1 (Sapkota *et al*., 2007; Nguyen, 2008). For these reasons, BI-D1870 (an amino-terminal kinase domain - or NTKD - ATP-binding dihydropteridinone) was a superior choice over the NTKD ATP-binding inhibiter kaemperfol-glycoside SL0101, as well as the pyrolopyrumidine FMK (which binds irreversibly to the CTKD ATP-binding region of RSK2) (Nguyen, 2008). However, since BI-D1870 is both a novel and expensive inhibitor, the use of BI-D1870 is poorly reported in the literature. Other than Sapkota *et al*. (2007), the publications of Kang *et al.* (2007), Chen and MacKintosh (2009) and Xian *et al.* (2009) are the only examples in the primary literature to specifically inhibit p90RSK with BI-D1870. Therefore, these findings are unique in that, to our knowledge, the inhibition of MAPK/p90RSK signalling has never been attempted in SCC of the oesophagus. Furthermore, this is the first study comparing differential RSP6$^{(Ser\ 235/236)}$

phosphorylation by mTORC1 and p90RSK to gain an understanding of those initial signalling events indicating proliferative cellular events.

Considering the influence of the MAPK pathway in mTORC1 signalling (seen through some HOSCC cells increasing p-RPS6$^{(Ser\ 235/236)}$, as well as p90RSK-sepcific inhibition modulating the concentration of cellular mTOR), it would be interesting to determine the concentration of BI-D1870 necessary for p90RSK-specific inhibition in order to critically decrease p-RPS6$^{(Ser\ 235/236)}$. In addition, it would also be interesting to investigate the combined effect of rapamycin and BI-D1870 on both mTOR and mTORC1 signalling in HOSCC, as these data may have therapeutic implications for curbing hyperactive p-p38 induced MAPK/p90RSK signalling, recently shown to play a key role in malignant transformation in ESCC's (Zheng *et al.*, 2012). Therefore, through the use of this p90RSK inhibitor, we determined that an activated mTOR signalling pathway leads to RPS6$^{(Ser\ 235/236)}$ phosphorylation in HOSCC cells, of which an essential requirement for this is signalling through mTORC1.

5.7. ECM-modulation of the mTOR signalling pathway utilizes PI3K to regulate autophagy induction in HOSCC

Cells require stable cell-cell and cell-ECM connections to create an organized tissue structure (Gumbiner, 1996). Components of the cell adhesion machinery facilitate these types of connections and allow individual cells to assemble into diverse and distinctive three-dimensional structures (Juliano, 2002). While, cadherins and adherens junctions facilitate cell-cell interconnectivity, allowing formation of intercalated, epithelial sheets (Gumbiner, 1996), adhesion to a supporting substrate is facilitated by different permutations of α and β integrin heterodimers (Gumbiner, 1996; van Der Flier and Sonnenberg, 2001). Consequently, integrin-mediated cell-ECM adhesion is implicated in the regulation of cell survival, migration, proliferation, differentiation and even tumour progression (Juliano, 2002; Brakebusch and Fässler, 2003; Brunton *et al.*, 2004). Thus, ECM-attachment to a collagen- or fibronectin-rich interstitial matrix (ECM) is an essential requirement for tissue integrity and homeostasis in epithelial cells (Gumbiner, 1996).

This importance of cell-ECM attachment during cell survival is demonstrated through adhesion-based signals (originating from cell-ECM interactions) supporting tumour progression by promoting anoikis resistance (Fanucchi and Veale, 2011) and autophagy

induction (Fung *et al.*, 2008; Lock and Debnath, 2008; Chen and Debnath, 2010). Previous studies involving skeletal muscle cells often suggested a form of mTOR regulation via mechanotransduction-based events. Here, the ECM was shown to play a role in cell growth signals propagated through the mTOR signalling pathway, which occurred in a PI3K-dependent manner (Baar and Esser, 1999; Hornberger, 2011). Three main observations lead to this conclusion. Firstly, mechanical stimulation induces signalling through the integrin-triggered focal adhesion protein kinase, ILK (Legate *et al.*, 2006; Hannigan *et al.*, 2011). Secondly, mechanical stimulation in this manner also leads to the activation of both PI3K and PKB (Bolster *et al.*, 2003; Hornberger *et al.*, 2003). Thirdly, constitutive signalling through PI3K/PKB promotes skeletal muscle growth in a rapamycin-sensitive manner (Bodine *et al.*, 2001; Varma and Khandelwal, 2007). Thus, mechanically-derived stimuli could, in theory, activate mTORC1 through the PI3K/PKB signalling machinery.

In confirmation of the above, the data presented in Chapter 4 provide evidence for the activation mTORC1 signalling in HOSCC cells in response to mechanically-derived extracellular-originating stimuli. Although p-PKB$^{(Ser\ 473)}$ were not measured here, it was observed that mechanical signals commonly increase both mTOR and p-RPS6$^{(Ser\ 235/236)}$ protein expression levels in HOSCC cells – indicating a novel, non-canonical mode of mTOR/mTORC1 regulation through adhesion to the physical environment. With regard to the route of signal transmission, the lack of a detectable protein-protein interaction between mTOR and both ILK and FAK in the WHCO series of cell lines highlights an indirect mechanism of signal transduction from mechanical stimulus to mTORC1. Thus, we strongly believe that since specific inhibition of the kinase ability of PI3K perturbs this mechanotransduction effect on mTORC1, these results demonstrate unequivocally that intracellular signal transduction of adhesion-based signals 1) modulate mTOR/mTORC1 signalling, and 2) occurs in a PI3K-mediated manner in HOSCC cells.

Combined, these observations provide a solid rationale to support our hypothesis that mechanical stimuli activate mTORC1 signalling through a mechanism involving the activation of ILK, thereby regulating autophagy induction and consequently supporting HOSCC cell survival. To provide further support for our contention, we illustrate these findings in *Figure 5.1* and highlight the response of a substrate-dependant epithelial cellular system to this form of adhesion-based signal transduction. Under standard tissue culture condition, HOSCC's maintain an enhanced rate of flux through the mTOR signalling

pathway (denoted by the elevated blue squares during State 1 “Homeostasis” in *Figure 5.1, A versus B*). Here, we demonstrated that soluble stimuli; such as growth factor, amino-acids and rapamycin treatment, impinge on this flux, therefore affecting homeostasis of HOSCC cells. Interestingly, autophagy seems to play an important survival role in HOSCC as we observed elevated expression of markers for autophagy induction potential (i.e. dephospho-mATG-13) under these conditions. Therefore, HOSCC cells tend to maintain an elevated basal rate of autophagy (represented as elevated red triangles). Conversely, pro-death signals mediated through apoptotic regulators, such as cleaved caspase-3, are completely down-regulated (indicated by purple circles touching the X-axis).

Crucially, we demonstrated that mTOR/mTORC1 signalling may be increased by growth in the presence of fibronectin- or collagen-coated substrates (signified by the increase in blue squares over and above elevated signalling levels). This cell-substrate dependant increase in mTORC1 signalling may provide a rationale for the increase in autophagy observed when cell-substrate connections are abolished (denoted by State 2 “Transition” in *Figure 5.1, B*). Since we showed that a direct mTOR-ILK protein interaction does not account for this signal transduction, cell-substrate connections may signal to mTOR/mTORC1 through an integrin-triggered medium, but one utilizing PI3K-mediated machinery to inhibit autophagy induction. Consequently, when these integrin-activating stimuli are lost, positive regulation of cellular concentrations of mTOR and mTORC1 signalling is diminished, allowing for the initiation of autophagy induction – as previously reported by Fung *et al.* (2008). Interestingly, we discovered that these autophagy induction signals precede pro-death signals in HOSCC cells (See Chapter 2 and Chapter 3 where autophagy induction increased while cleaved caspase-3 was not detected under autophagy-promoting conditions; such as nutrient withdrawal for 24 hours and PI3K-specific inhibition with LY294002). Together, this provides a rationale for autophagy to promote cell survival before cell death signals are properly initiated.

In transformed epithelial phenotypes, exemplified by HOSCC, where anoikic-based pro-death signals are delayed (Fanucchi and Veale, 2009; Fanucchi and Veale, 2011), this mechanism of autophagy induction may be exploited to enhance survival during dissemination before cell-ECM connections can be re-established. We illustrate this as apoptotic ‘pro-death’ signals (purple circles) do not out-compete autophagic pro-survival signals (red triangles) during State 3 “Pro-death Signals” in *Figure 5.1, B.* Supporting this contention is the tendency for HOSCC to display anoikis resistance, as shown by Fanucchi

and Veale, (2011). Therefore, the adhesion-based autophagy induction occurs through substrate-dependant regulation of the mTOR/mTORC1 signalling pathway, which is facilitated by the integrin-triggered focal adhesion protein kinase, ILK, positively regulating PI3K/PKB signalling and therefore mTOR/mTORC1 pathway.

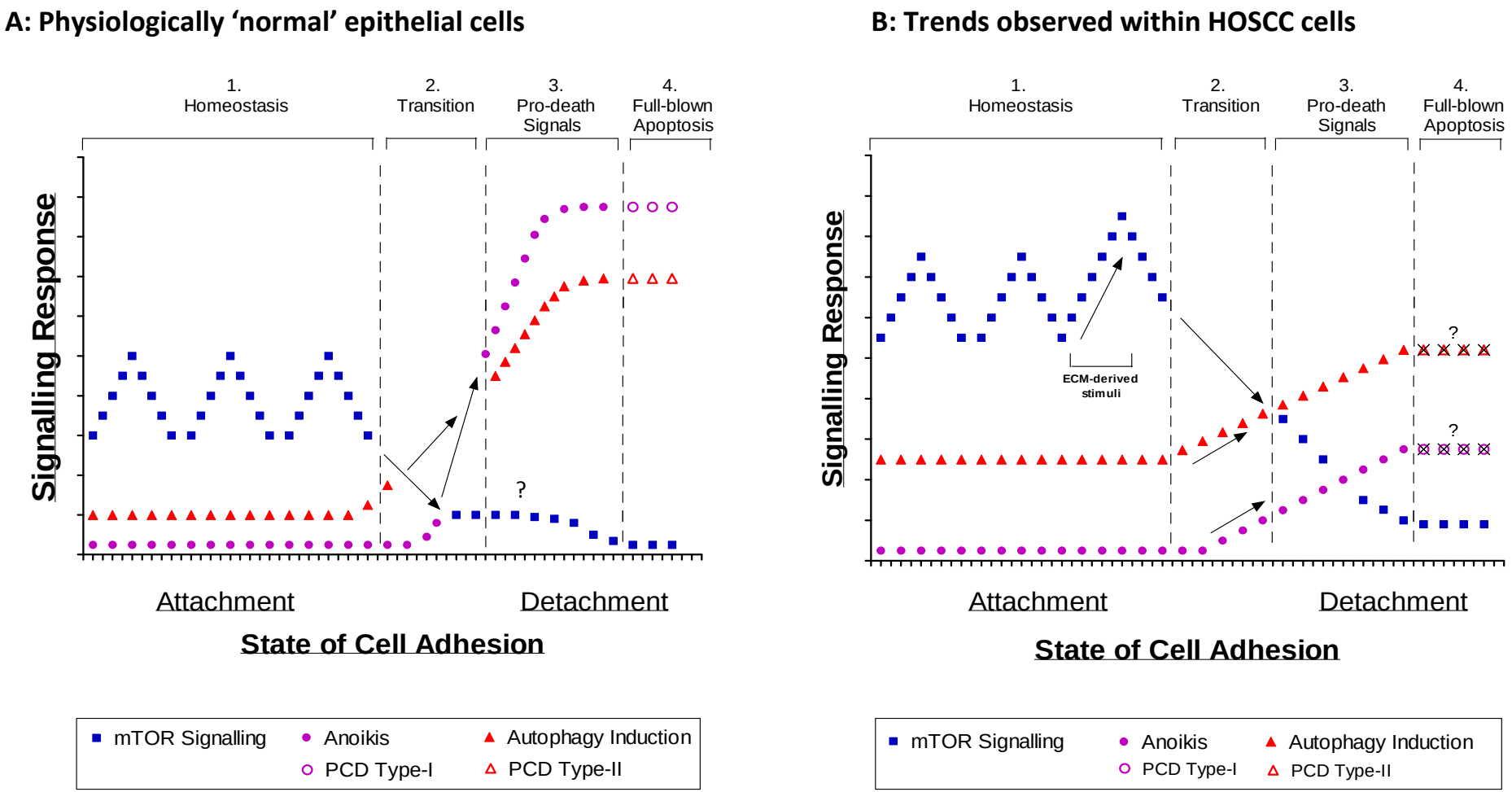

Figure 5.1: Cellular response to changes in the state of cell-ECM adhesion. Comparison of the influence of essential signalling machinery on cell behaviour between a physiologically normal epithelial cell systems and the transformed HOSCC phenotype. The signalling response for mTOR/mTORC1 (blue squares), autophagy induction (red triangles) and apoptosis (purple circles) are described as a function of the state of cell adhesion, which transitions from cell-ECM attachment to cell-ECM detachment.

5.8. Conclusion

Aberrant integrin-mediated adhesion and enhanced survival signalling are hallmarks of transformation associated with metastasis (Hanahan and Weinberg, 2011). These events oppose anoikic death programmes and induce autophagy; an evolutionary conserved cell survival mechanism, inappropriately (Fung *et al.*, 2008; Lock and Debnath, 2008). Since detachment-induced autophagy indicates a form of adhesion-based regulation, ECM-originating signals may be transmitted to the cellular machinery controlling autophagy induction – a form of regulation which is subsequently lost when epithelial cells become detached from a substrate. This type of control implicates crosstalk between an integrin-triggered focal adhesion protein kinases (such as ILK) the mTOR signalling pathway, which is a critical regulator of autophagy induction (Foster and Fingar, 2010; Dobashi *et al.*, 2011). Consequently, molecular analysis of the most significant cell adhesion, mTOR and autophagy signal transduction pathway intermediates constitutes an information-rich reporter system, enabling the examination of such crosstalk.

Pivotal to this investigation was the use of a series of highly tumourigenic epithelial cell lines, with a propensity for metastasis, inappropriate survival signalling and anoikis evasion potential; human oesophageal squamous cell carcinoma (HOSCC) (Miller and Veale, 2001; Driver and Veale, 2006; Fanucchi and Veale, 2011). Up until now, very few studies have focussed on characterising the mTOR pathway as a molecular mechanism promoting progression of HOSCC. Only the work by Hou *et al.* (2007) and Hirashima *et al.* (2012) demonstrate that poorly- and well-differentiated ESCC cells of Chinese origin display ectopic mTOR expression and aberrant mTORC1 signalling, which is associated with the progression of solid epithelial tumours. In this study, we reveal that HOSCC cells parallel ESCC cells in this regard, providing a reasonable basis to suggest that aberrant mTOR/mTORC1 signalling plays a similar role in HOSCC of South African origin.

Most importantly however, these data highlight that mTORC1-dependent autophagy induction is affected by the state of cellular attachment, which is advantageous for disseminating cells capable of evading anoikic cell death. Moreover, this type of regulation is not by way of a direct interaction with an integrin-triggered protein kinase, such as ILK, as first thought. Rather, ECM-modulation of mTOR acts through the PI3K signalling pathway. Therefore, these findings support our contention that the mTOR protein kinase is a target for adhesion-based signal transduction, which influences cell survival through mTORC1.

REFERENCES

Abraham, R. (2002) Identification of TOR signaling complexes: more TORC for the cell growth engine. *Cell*, **111**: 9-12.

Abraham, R. (2004) PI 3-indase related kinases: 'big' players in stress-induced signalling pathways. *DNA Repair*, **3**: 883 – 887.

Almeida, E., Ilic′, D., Han, Q., Hauck, C., Jin, F., Kawakatsu, H., Schlaepfer, D. and Damsky, C. (2000) Matrix survival signaling: from fibronectin via focal adhesion kinase to c-Jun NH2-terminal kinase. *J Cell Biol*, **149**: 741-754.

Aplin, A., Howe, A., Alahari, S. and Juliano, R. (1998) Signal transduction and signal modulation by cell adhesion receptors: the role of integrins, cadherins, immunoglobulin-cell adhesion molecules and selectins. *The American Soc Pharmacol Exp Therapeut*, **50**: 197-263.

Arcaro, A. and Guerreiro, A. (2007) The phosphoinositide 3-kinase pathway in human cancer: Genetic alterations and therapeutic implications. *Curr Genomics*, **8**: 271-306.

Arsham, A., Howell, J., Simon, M. (2003) A novel hypoxia-inducible factor-independent hypoxic response regulating mammalian target of rapamycin and its targets. *J Biol Chem*, **278**: 29 655-29 660.

Asthagiri, A. and Lauffenbburger, D. (2000) Bioengineering models of cell signalling. *Annu Rev Biomed Eng*, **2**: 31-53.

Attwell, S., Mills, J., Troussard, A., Wu, C. and Dedhar, S. (2003*)*. Integration of Cell Attachment, Cytoskeletal Localization, and Signaling by Integrin-linked Kinase (ILK), CH-ILKBP, and the Tumor Suppressor PTEN. *Mol Biol Cell*, **14**: 4 813-4 825.

Attwell, S., Roskelley, C. and Dedhar, S. (2000*)* The integrin-linked kinase (ILK) suppresses anoikis. *Oncogene*, **19**: 3 811-3 815.

Avruch, J., Long, X., Oritz-Vega, S., Rapley, J., Papageorgiou, A. and Dai, N. (2009) Amino acid regulation of TOR complex 1. *Am J Physiol Endocrinol Metab*, **296**: 592-602.

Baar, K., and Esser, K. (1999) Phosphorylation of $p70^{S6k}$ correlates with increased skeletal muscle mass following resistance exercise. *Am J Physiol*, **45**: C120–C127.

Bachman, K., Argani, P., Samuels, Y., Silliman, N., Ptak, J., Szabo, S., Konishi, H., Karakas, B., Blair, B., Lin, C., Peters, B., Velculescu, V. and Park, B. (2004) The PI3KCA gene is mutated with high frequency in human breast cancers. *Cell Biol Ther*, **3**: 772-775.

Bae, G., Seo, D., Kwon, H., Lee, H., Hong, S., Lee, Z., HA, K., Lee, H. and Han, J. (1999). Hydrogen peroxide activates p70(S6k) signaling pathway. *J Biol Chem*, **274**: 32 596-32 602.

Bai, X. and Jiang, Y. (2010) Key factors in mTOR regulation. *Cell Mol Life Sci*, **67**: 239-253.

Baker, E. and Zaman, M. (2010) The biomechanical integrin. *J Biomech*, **43**: 38-44.

Bancewicz, J. (1990) Cancer of the oesophagus: Find a good surgeon. *Brit Med J*, **300**: 3.

Barnes, C. and Kumar, R. (2003) Epidermal growth factor receptor family tyrosine kinases as signal integrators and therapeutic targets. *Cancer Metastasis Rev*, **22**: 301-307.

Behrens, J., Mareel, M., van Roy, F. and Birchmeier, W. (1989) Dissecting Tumor Cell Invasion: Epithelial Cells Acquire Invasive Properties after the Loss of Uvomorulin-mediated Cell-Cell Adhesion. *J Cell Biol*, **108**: 2 435-2 447.

Berrier, A. and Yamada, K. (2007) Cell-matrix adhesion. *J Cell Physiol*, **213**: 565-573.

Bertram, J. (2001) The Molecular Biology of Cancer. *Mol Asp Med*, **21**: 167-223.

Beuvink, I., Boulay, A., Fumagalli, S., Zilbermann, F., Ruetz, S., O'Reilly, T., Natt, F., Hall, J., Lane, H. and Thomas, G. (2005) The mTOR inhibitor RAD001 sensitizes tumor cells to DNA-damaged induced apoptosis inhibition of p21 translation. *Cell*, **120**: 747-759.

Bey, E., Alexander, J., Whitcutt, J.N., Hunt, J.A. and Gear, J.H.S. (1976). Carcinoma of the oesophagus in Africans: establishment of a continuously growing cell line from a tumour specimen. *In Vitro*, **12**: 107-114.

Bhaskar, P. and Hay, N. (2007) The two TORCs and Akt. *Dev Cell*, **12**: 487-502.

Bird-Lieberman, E.L. and Fitzgerald, R.C. (2009) Early diagnosis of oesophageal cancer. *Br J Cancer*, **101**: 1-6.

Blommaart, E., Luiken, J., Blommaart, P., van Woerkom, G. and Meijer, A. (1995). Phosphorylation of ribosomal protein S6 is inhibitory for autophagy in isolated rat hepatocytes. *J Biol Chem*, **270**: 2 320-2 326.

Blommaart,E., Krause, U., Schellins, J., Vreeling-Sindelarova, H. and Meijer, A. (1997) The phosphatidylinositol 3-kinase inhibitors wortmannin and LY294002 inhibit autophagy in isolated rate hepatocytes. *Eur J Biochem*, **243**: 240-246.

Bodine, S., Stitt, T., Gonzalez, M., Kline, W., Stover, G. and Bauerlein, R. (2001) Akt/mTOR pathway is a crucial regulator of skeletal muscle hypertrophy and can prevent muscle atrophy in vivo. *Nat Cell Biol*, **3**: 1 014-1 019.

Bolster, D., Kubica, N., Crozier, S., Williamson, D., Farrell, P. and Kimball, S. (2003) Immediate response of mammalian target of rapamycin (mTOR)-mediated signalling following acute resistance exercise in rat skeletal muscle. *J Physiol*, **553**: 213-220.

Boudreau, N. and Bissell, M. (1998) Extracellular matrix signaling: integration of form and function in normal and malignant cells. *Curr Opin Cell Biol*, **10**: 640-646.

Brabek, J., Constancio, S., Shin, N., Pozzi, A., Weaver, A. and Hanks, S. (2004) CAS promotes invasiveness of Src-tranformed cells. *Oncogene*, **23**: 7 406-7 415.

Brakebusch, C. and Fässler, R. (2003) The integrin-actin connection, an eternal love affair. *EMBO J*, **22**: 2 324-2 333.

Bramhall, S., Novack, N., Wu., M., and Loewenberg, J.R. (1969) A Simple Colorimetric Method for the Determination of Protein. *Analyt Biochem*, **31**: 146-148.

Brech, A., Ahlquista, T., Lothea, R. and Stenmarka, H. (2009) Autophagy in tumour suppression and promotion. *Mol Oncol*, **3**: 366-375.

Brown, E., Alberts, M., Shin, T., Ichikawa, K., Keith, C., Lane, W. and Schreiber, S. (1994) A mammalian protein targeted by G1-arresting rapamycin-receptor complex. *Nature*, **369**: 756-758.

Brown, E., Beal, P., Keith, C., Chen, J., Shin, T. and Schreiber, S. (1995) Control of p70 S6 kinase by kinase activity of FRAP *in vivo*. *Nature*, **377**: 441-446.

Brunn, G., Williams, J., Sabers, C., Wiederrecht, G., Lawrence, J., Abraham, R. (1996) Direct inhibition of the signaling functions of the mammalian target of rapamycin by the phosphoinositide 3-kinase inhibitors, wortmannin and LY294002. *EMBO J*, **15**: 5 256-5 267.

Brunton, V., MacPherson, I. and Frame, M. (2004) Cell adhesion receptors, tyrosine kinases and actin modulators: a complex three-way circuitry. *Biochim Biophys Acta*, **1 692**: 121-144.

Burman, C. and Ktistakis, N. (2010) Regulation of autophagy by phosphatidylinositol 3-phosphate. *FEBS Lett*, **584**: 1 302-1 312.

Burnette, W. (1981) "Western Blotting": Electrophoretic Transfer of Proteins from Sodium Dodecyl Sulfate – Polyacrylamide Gels to Unmodified Nitrocellulose and Radiographic Detection with Antibody and Radioiodinated Protein A. *Analyt Biochem*, **112**: 195-203.

Bursch, W., Ellinger, A., Kienzl, H., Torok, L., Pandey, S., Sikorska, M., Walker, R. and Herman, R. (1996). Active cell death induced by the anti-estrogens tamoxifen and ICI 164 384 in human mammary carcinoma cells (MCF-7) in culture: The role of autophagy. *Carcinogenesis*, **17**: 1 595-1 607.

Byfield, M., Murray, J. and Backer, J. (2005) hVps34 is a nutrient-regulated lipid kinase required for activation of p70 S6 kinase. *J Biol Chem*, **280**: 33 076-33 082.

Bärlund, M., Forozan, F., Kononen, J., Bubendorf, L., Chen, Y., Bittner, M., Torhorst, J., Haas, P., Bucher, C., Sauter, G., Kallioniemi, O. and Kallioniemi, A. (2000a) Detecting activation of ribosomal protein S6 kinase by complimentary DNA and tissue microarray analysis. *J Natl Cancer I*, **92**: 1 252-1 259.

Bärlund, M., Monni, O., Kononen, J., Cornelison, R., Torhorst, J., Sauter, G., Kallioniemi, O. and Kallioniemi, A. (2000b) Multiple genes at 17q23 undergo amplification and overexpression in breast cancer. *Cancer Res*, **92**: 1 252-1 259.

Campbell, I., Russell, S., Choong, D., Montgomery, K., Ciavarella, M., Hooi, C., Cristiano, B., Pearson, R. and Phillips, W. (2004) Mutation of the PIK3CA gene in ovarian and breast cancer. *Cancer Res*, **64**: 7 678-7 681.

Cantley, L. (2002) The phosphatidylinositol 3-kinase pathway. *Science*, **296**: 1 655-1 657.

Caron, E., Ghosh, S., Matsuoka, Y., Ashton-Beaucage, D., Therrien M., Lemiuex, S., Perreault, C., Roux, P. and Kitano, H. (2010) A comprehensive map of the mTOR signalling network. *Mol Sys Biol*, **6**: 1-14.

Carrière, A., Romeo, Y., Acosta-Jaquez, H., Moreau, J., Bonneil, E., Thibault, P., Fingar, D. and Roux, P. (2008) ERK1/2 phosphorylate Raptor to promote Ras-dependent activation of mTOR complex 1 (mTORC1). *J Biol Chem*, **286**: 567-577.

Cecconi, F. and Levine, B. (2008) The Role of Autophagy in Mammalian Development: Cell Makeover Rather than Cell Death. *Dev Cell*, **15**: 344-357.

Chan, E., Longatti, A., McKnight, N. and Tooze, S. (2009) Kinase-Inactivated ULK Proteins Inhibit Autophagy via Their Conserved C-Terminal Domains Using an Atg13-Independant Mechanism. *Mol Cell Biol*, **29**: 157-171.

Chantaravisoot, N. and Tamanoi, F. (2010) TOR signaling and human cancer. *The Enzymes*, **28**: 301-314.

Chen, N. and Karantza-Wadsworth, V. (2009) Role and regulation of autophagy in cancer. *Biochim Biophys Acta*, **1 793**: 1 516-1 523.

Chen, N. and Debnath, J. (2010) Autophagy and tumourigenesis. *FEBS Lett*, **584**: 1 427-1 435.

Chen, S. and MacKintosh, C. (2009) Differential regulation of NHE1 phosphorylation and glucose uptake by inhibitors of the ERK pathway and p90RSK in 3T3-L1 adipocytes. *Cell Sig*, **21**: 1 984-1 993.

Chen, Y., Zheng, Y. and Foster, D. (2003) Phospholipase D confers rapamycin resistance in human breast cancer cells. *Oncogene*, **22**: 3 937-3 942.

Cho, D., Signoretti, S., Dabora, S., Regan, M., Seeley, A., Mariotti, M., Youmans, A., Polivy, A., Mandato, L., McDermott, D., Stanbridge, E. and Atkins, M. (2007) Potential histologic and molecular predictors of response to temsirolimus in patients with advanced renal cell carcinoma. *Clin Genitourin Cancer*, **5**: 379-385.

Chowdhury, I., Tharakan, B. and Bhat, G. (2008) Caspases – an update. *Comp Biochem Physiol, Part B*, **151**: 10-27.

Chung, D., Lee, J., Kook, M., Kim, J., Kim, S., Choi, E., Park, S. and Song, H. G. (1998). ILK (beta1-integrin-linked protein kinase): A Novel Immunohistochemical Marker for Ewing's Sarcoma and Primitive Neuroectodermal Tumour. Virchows Archiv, **433**: 113 -117.

Clarke, E. and Brugge, J. (1995) Integrins and Signal Transduction Pathways: The Road Taken. *Science*, **268**: 233-239.

Copp, J., Manning, G. and Hunter, T. (2009) TORC-specific phosphorylation of mammalian target of rapamycin (mTOR): phospho-Ser^{2481} is a marker for intact mTOR signaling complex 2. *Cancer Res*, **69**: 1 821-1 827.

Corradetti, M. and Guan, K-L. (2006) Upstream of the mammalian target of rapamycin: do all roads pass through mTOR? *Oncogene*, **25**: 6 347-6 360.

Corradetti, M., Inoki, K., Bardeesy. N., DePinho, R. and Guan, K-L. (2004) Regulation of the TSC pathway by LKB1: evidence of a molecular link between tuberous sclerosis complex and Peutz-Jeghers syndrome. *Genes Dev*, **18**: 1 533-1 538.

Cox, B, Natarajan, M., Stettner, M. and Gladson, C. (2006) New concepts regarding focal adhesion kinase promotion of cell migration and proliferation. *J Cell Biochem*, **99**: 36-52.

Crabbe, T., Welham, M. and Ward, S. (2007) The PI3K inhibitor arsenal: choose your weapon! *TRENDS Biochem Sci*, **32**: 450-456.

Dazert, E. and Hall, M. (2011) mTOR signaling in disease. *Curr Opin Cell Biol*, **23**: 744-755.

Degenhardt, K., Mathew, R., Beaudoin, B., Bray, K., Anderson, D., Chen, G., Mukherjee, C., Shi, Y., Gelinas, C., Fan, Y., Nelson, D., Jin, S. and White, E. (2006) Autophagy promotes tumour cell survival and restricts necrosis, inflammation,a nd tumourigenesis. *Cancer Cell*, **10**: 51-64.

deGraffenried, L., Friedrichs, W., Russell, D., Donzis, E., Middleton, A., Silva, J., Roth, R. and Hidalgo, M. (2004) Inhibition of mTOR activity restores tamoxifen response in breast cancer cells with aberrant Akt activity. *Clin Cancer Res*, **10**: 8 059-8 067.

Desai, B., Myers, B. and Schreiber, S. (2002) FKBP-12-rapamycin-associated protein associates with mitochondria and senses osmotic stress via mitochondrial dysfunction. *Proc Natl Acad Sci USA*, **99**: 4 319-4 324.

Dobashi, Y., Watanabe, Y., Miwa, C., Suzuki, S. and Koyama, S. (2011) Mammalian target of rapamycin: a central node of complex signaling cascades. *Int J Clin Exp Pathol*, **4**: 476-495.

Doukas, J., Doukas, J., Wrasidlo, W., Noronha, G., Dneprovskaia, E., Fine, R., Weis, S., Hood, J., Demaria, A., Soll, R. and Cheresh, D. (2006) Phosphoinositide 3-kinase gamma/delta inhibition limits infarct size after myocardial ischemia/reperfusion injury. *Proc Natl Acad Sci USA*, **103**: 19 866-19 871.

Dreher, T., Zentgraf, H., Abel, U., Kappeler, A., Michel, M., Bleyl, U. and Grobholz, R. (2004) Reduction of PTEN and p27kip1 expression correlates with tumor grade in prostate cancer. Analysis in radical prostatectomy specimens and needle biopsies. *Virchows Arch*, **444**: 509-517.

Driver, G. (2007) Integrin-linked Kinase (ILK) Expression in Moderately Differentiated Human Oesophageal Squamous Carcinoma Cell Lines – Growth Factor Modulation, Activity and Link to Adhesion. A thesis submitted to the Faculty of Science, University of the Witwatersrand, Johannesburg, in fulfilment of the requirements for the degree of Ph.D.

Driver, G. and Veale, R. (2006) Modulation of integrin-linked kinase (ILK) expression in human oesophageal squamous cell lines by the EGF TGFbeat1 growth factors. *Canc Cell Int*, **6**: 1-12.

Durán, R., Oppliger, W., Robitaille, A., Heiserich, L., Skendaj, R., Gottlieb, E. and Hall, M. (2012) Glutaminolysis Activates Rag-mTORC1 Signaling. *Mol Cell*, **47**: 349-358.

Duronio, V. (2008) The life of a cell: apoptosis regulation by the PI3K/PKB pathway. *Biochem J*, **415**: 333-344.

Edelstein, J., Hao, T., Cao, Q., Morales, L. and Rockwell, P. (2011) Crosstalk between VEGFR2 and muscarinic receptors regulates the mTOR pathway in serum starved SK-N-SH human neuroblastoma cells. *Cell Sig*, **23**: 239-248.

Edinger, A. and Thompson, C. (2004) Death by design: apoptosis, necrosis and autophagy. *Curr Opin Cell Biol*, **16**: 663-669.

Egeblad, M., Rasch, M. and Weaver, V. (2010) Dynamic interplay between the collagen scaffold and tumor evolution. *Curr Opin Cell Biol*, **22**: 697-706.

Eisenberg-Lerner, A., Bialik, S., Simon, H-U and Kimchi, A. (2009) Life and death partners: apoptosis, autophagy and the cross-talk between them. *Cell Death Differ*, **16**: 966-975.

Engler, A., Sen, S., Sweeney, H. and Discher, D. (2006) Matrix elasticity directs stem cell lineage specification. *Cell*, **126**: 677-689.

Erol, A. (2011) Deciphering the intricate regulatory mechanisms for the cellular choice between cell repair, apoptosis or senescence in response to damaging signals. *Cell Sig*, **23**: 1 076-1 081.

Fan, Q., Cheng, C., Nicolaides, T., Hackett, C., Knight, Z., Shokat, K. and Weiss, W. (2006) A dual PI3K/mTOR inhibitor reveals emergent efficacy in glioma. *Cancer Cell*, **9**: 341-349.

Fanucchi, S. and Veale, R. (2009) Role of p53/FAK association and p53Ser46 phosphorylation in staurosporine-mediated apoptosis: wild-type versus mutant p53-R175H, *Febs Lett*, **583**: 3 357-3 562.

Fanucchi, S. and Veale, R. (2011) Delayed caspase-8 activation and enhanced integrin β1-activated FAK underpins anoikis in oesophageal squamous carcinoma cells harbouring mutant p53-R175H. *Cell Biol Int*, **35**: 819-826.

Findlay, G., Yan, L., Procter, J., Mieulet, V. and Lamb, R. (2007) A MAP4 kinase related to Ste20 is a nutrient-sensitive regulator of mTOR signalling. *Biochem J*, **403**: 13-20.

Fingar, D. and Blenis, J. (2004) Target of Rapamycin (TOR): an integrator of nutrient and growth factor signals and coordinator of cell growth and cell cycle progression. *Oncogene*, **23**: 3 151-3 171.

Fingar, D., Richardson, C., Tee, A., Cheatham, L., Tsou, C. and Blenis, J. (2004b) mTOR controls cell cycle progression through its cell growth effectors S6K1 and 4E-BP1/eukaryotic translation initiation factor 4E. *Mol Cell Biol*, **24**: 200-216.

Fingar, D., Salama. S., Tsou, C., Harlow, E. and Blenis, J. (2002) Mammalian cell size is controlled by mTOR and its downstream targets S6K1 and 4EBP1/eIF4E. *Genes Dev*, **16**: 1 472-1 487.

Foster, D. and Toschi, A. (2009) Targeting mTOR with rapamycin: one dose does not fit all. *Cell Cycle*, **8**: 1 026-1 029.

Foster, F., Traer, C., Abraham, S. and Fry, M. (2003) The phosphoinositide (PI) 3-kinase family. *J Cell Sci*, **116**: 3 037-3 040.

Foster, K. and Fingar, D. (2010) Mammalian target of rapamycin (mTOR): conducting the cell signaling symphony. *J Biol Chem*, **285**: 14 071-14 077.

Foster, K., Acosta-Jaquez, H., Romeo, Y., Ekim, B., Soliman, G., Carriere, A., Roux, P., Ballif, B. and Fingar, D. (2010) Regulation of mTOR complex 1 (mTORC1) by raptor Ser863 and multisite phosphorylation. *J Biol Chem*, **285**: 80-94.

Frisch, S. and Francis, H. (1994) Disruption of epithelial cell-matrix interactions induces apoptosis. *J Cell Biol*, **124**: 619-626.

Fung, C., Lock, R., Gao, S., Salas, E. and Debnath, J. (2008) Induction of Autophagy during Extracellular Matrix Detachment Promotes Cell Survival. *Mol Biol Cell*, **19**: 797-806.

Gabbert, H. (1985) Mechanism of Tumor Invasion: Evidence from in-vivo Observations. *Cancer Metastasis Rev*, **4**: 293-309.

Gabbert, H., Wagner, R., Moll, R. and Gerharz, C. (1985) Tumour Dedifferentiation: An Important Step in Tumour Invasion. *Clin Exp Metastasis*, **3**: 257-279.

Gan, B., Yoo, Y. and Guan, J-L. (2006) Association of focal adhesion kinase with tuberous sclerosis complex 2 in the regulation of s6 kinase activation and cell growth. *J Biol Chem*, **281**: 37 321-37 329.

Gao, M., Sotomayer, M., Villa, E., Lee, E. and Schulten, K. (2006) Molecular mechanisms of cellular mechanics. *Phys Chem*, **8**: 3 692-3 706.

Gao, X., Zhang, Y., Arrazola, P., Hino, O., Kobayashi, T., Yeung, R., Ru, B. and Pan, D. (2002). Tsc tumour suppressor proteins antagonize amino-acid-TOR signalling. *Nat Cell Biol*, **4**: 699-704.

Giancotti, F.G., and Ruoslahti, E. (1990) Elevated Levels of the α5β1 Fibronectin Receptor Suppress the Transformed Phenotype of Chinese Hamster Ovary Cells. *Cell*, **60**: 849-859.

Gingras, A-C., Raught, B. and Sonenberg, N. (2001) Regulation of translation initiation by FRAP/mTOR. *Genes Dev*, **15**: 807-826.

Goldmann, W. (2012) Mechanotransduction and focal adhesions. *Cell Biol Int*, **36**: 649-652.

Gorrini, C., Loreni, F., Gandin, V., Sala, L., Sonenberg, N., Marchisio, P. and Biffo, S. (2005) Fibronectin controls cap-dependant translationthrough β1 integrin and eukaryotic initiation factors 4 and 2 coordinated pathways. *PNAS*, **102**: 9 200-9 205.

Graham, F., Smiley, J., Russel, W. And Nairn, R. (1977) Characterization of a human cell line transformed by DNA from human adenovirus type 5. *J Gen Virol*, **36**: 59-72.

Grashoff, C., Thieveessen, I., Lorenz, K., Ussar, S. and Fässler, R. (2004) Integrin-linked kinase: integrin's mysterious partner. *Curr Opin Cell Biol*, **16**: 565-571.

Gray, R., Cheung, K. and Ewald, A. (2010) Cellular mechanisms regulating epithelial morphogenesis and cancer invasion. *Curr Opin Cell Biol*, **22**: 640-650.

Groves, J. and Kuriyan, J. (2010) Molecular mechanisms in signal transduction at the membrane. *Nat Struct Mol Biol*, **17**: 659-665.

Guertin, D. and Sabatini, D. (2005) An expanding role for mTOR in cancer. *TRENDS Mol Med*, **11**: 353-361.

Guinebault, C., Payrastre, B., Racaud-Sultan, C., Mazarguil, H., Breton, M., Mauco, G., Plantavid, M. and Chap, H. (1995) Integrin-dependant translocation of phosphoinositide 3-kinase to the cytoskeleton of thrombin-activated platelets involves specific interactions of p85α with actin filaments and focal adhesion kinase. *J Cell Biol*, **129**: 831-842.

Gumbiner, B. (1996) Cell adhesion: the molecular basis of tissue architecture and morphogenesis. *Cell*, **84**: 345-357.

Hager, M., Haufe, H., Alinger, B. and Kolbtisch, C. (2011) pS6 expression in normal renal parenchyma, primary renal cell carcinomas and their metastases. *Pathol Oncol Res*, Published Online: **DOI**: 10.1007/s12253-011-9439-y.

Hagner, P., Mazan-Mamczarz, K., Dai, B., Corl, S., Zhao, X. and Gartenhaus, R. (2009) Alcohol consumption and decreased risk of non-Hodgkin lymphoma: role of mTOR dysfunction. *Blood*, **113**: 5 526-5 535.

Han, S., Ritzenthaler, J., Sitaraman, S. and Roman, J. (2006) Fibronectin increases matrix metalloproteinase 9 expression through activation of c-Fos via extracellular-regulated kinase and phosphatidylinositol 3-kinase pathways in human lung carcinoma cells. *J Biol Chem*, **281**: 29 614-29 624.

Hanahan, D. and Weinberg, R. (2011) Hallmarks of cancer: the next generation. *Cell*, **144**: 646-674.

Hanks, S., Ryzhova, L., Shin, N-Y. and Brábek, J. (2003) Focal adhesion kinase signaling activities and their implications in the control of cell survival and motility. *Front Biosci*, Published Online: **DOI**: 1;8:d982-96.

Hannigan, G., Leung-Hagesteijn, C., Fitz-Gibbon, L., Coppolino, M., Radeva, G., Filmus, J., Bell, J. and Dedhar, S. (1996) Regulation of Cell Adhesion and Anchorage-dependent Growth by a New β1-integrin-linked Protein Kinase. *Nature*, **379**: 91-96.

Hannigan, G., McDonald, P., Walsh, M. and Dedhar, S. (2011) Integrin-linked kinase: Not so 'pseudo' after all. *Oncogene*, **30**: 4 375-4 385.

Hara, K., Maruki, Y., Yoshino, K-I., Hidayat, S., Avruch, J., Long, X., Oshiro, N., Tokunaga, C. and Yonezawa, K. (2002) Raptor, a binding partner of target of rapamycin (TOR), mediates TOR action. *Cell*, **110**: 177-189.

Hara, K., Yonezawa, K., Weng, Q., Kozlowski, M., Belham, C. and Avruch, J. (1998). Amino acid sufficiency and mTOR regulate p70 S6 kinase and eIF-4E BP1 through a common effector mechanism. *J Biol Chem*, **273**: 14 484-14 494.

Hara, T., Takamura, A., Kishi, C., Lemura, S-I., Natsume, T., Guan, J-L. and Mizushima, N. (2008) FIP200, a ULK-interacting protein, is required for autophagosome formation in mammalian cells. *J Cell Biol*, **181**: 497-510.

Harburger, D. and Calderwood, D. (2009) Integrin signalling at a glance. *J Cell Sci*, **122**: 159-163.

Harrington, L., Findlay, G. and Lamb, R. (2005) Restraining PI3K: mTOR signalling goes back to the membrane. *TRENDS Biochem Sci*, **30**: 35-42.

Hay, N. (2005) The AKT-mTOR tango and its relevance to cancer. *Cancer Cell*, **8**: 179-183.

Hayakawa, M., Kawaguchi, K-I., Kaizawa, H., Koizumi, T., Ohishi, T., Yamano, M., Okada, M., Ohta, M., Tsukamoto, S-I., Raynaud, F., Parker, P., Workman, P. and Waterfield, M. (2007) Synthesis and biological evaluation of pyrido[30,20:4,5]furo[3,2-d]pyrimidine derivatives as novel PI3K p110a inhibitors. *Bioorg Med Chem Lett*, **17**: 2 438-2 442.

He, C. and Klionsky, D. (2009) Regulation mechanisms and signalling pathways of autophagy. *Annu Rev Genet*, **43**: 67-93.

Heinonen, H., Nieminen, A., Saarela, M., Kallioniemi, A., Klefström, J., Hautaniemi, S. and Monni, O. (2008) Deciphering downstream gene targets of PI3K/mTOR/p70S6K pathway in breast cancer. *BMC Genomics*, **9**: 348-360.

Hendricks, D., and Parker, M. (2002) Oesophageal Cancer in Africa. *IUBMB Life*, **53**: 263-268.

Hirashima, K., Baba, Y., Watanabe, M., Karashima, R-I ., Sato1, N., Imamura, Y., Nagai, Y., Hayashi, N., Iyama, K-I. and Baba, H. (2012) Aberrant activation of the mTOR pathway and anti-tumour effect of everolimus on oesophageal squamous cell carcinoma. *Brit J Cancer*, **106**: 876-882.

Hornberger, T. (2011) Mechanotransduction and the regulation of mTORC1 signaling in skeletal muscle. *Int J Biochem Cell Biol*, **43**: 1 267-1 276.

Hornberger, T., McLoughlin, T., Leszczynski, J., Armstrong. D., Jameson, R. and Bowen, P. (2003) Selenoprotein-deficient transgenic mice exhibit enhanced exercise-induced muscle growth. *J Nutr*, **133**: 3 091-3 097.

Hosokawa, N., Hara, T., Kaizuka, T., Kishi, C., Takamura, A., Miura, Y., Iemura, S., Natsume, T., Takehana, K., Yamada, N., Guan, J., Oshiro, N. and Mizushima, N. (2009) Nutrient-dependent mTORC1 association with the ULK1-Atg13-FIP200 complex required for autophagy. *Mol Biol Cell*, **20**: 1 981-1991.

Hou, G., Xue, L., Lu, Z., Fan, T., Tian, F. and Xue, Y. (2007) An activated mTOR/p70S6K signalling pathway in esophageal squamous cell carcinoma cell lines and inhibition of the pathway by rapamycin and siRNA against mTOR. *Cancer Lett*, **253**: 236-248.

Huang, Y., Li, J., Zhang, Y. and Wu, C. (2000) The Roles of Integrin-linked Kinase in the Regulation of Myogenic Differentiation. *J Cell Biol*, **150**: 861-871.

Hudson, C., Liu, M., Chiang, G., Otterness, D., Loomis, D., Kaper, F., Giaccia, A. and Abraham, R. (2002). Regulation of hypoxia-inducible factor 1alpha expression and function by the mammalian target of rapamycin. *Mol Cell Biol*, **22**: 7 004-7 014.

Huveneers, S. and Danen, E. (2009) Adhesion signaling - crosstalk between integrins, Src and Rho. *J Cell Sci*, **122**: 1 059-1 069.

Hynes, R. (1992) Integrins: Versatility, Modulation and Signaling in Cell Adhesion. *Cell*, **69**: 11-25.

Inoki, K., Corradetti, M. and Guan, K-L. (2005) Dysregulation of the TSC–mTOR pathway in human disease. *Nat. Genet*, **37**: 19-24.

Inoki, K., Li, Y., Zhu, T., Wu, J. and Guan, K.-L. (2002) TSC2 is phosphorylated and inhibited by Akt and suppresses mTOR signalling. *Nat Cell Biol*, **4**: 648-657.

Inoki, K., Zhu, T. and Guan, K. (2003b) TSC2 mediates cellular energy response to control cell growth and survival. *Cell*, **115**: 577-590.

Isaacson, C. (2005) The Change of the Staple Diet of Black South Africans from Sorghum to Maize (Corn) is the Cause of the Epidemic of Squamous Carcinoma of the Oesophagus. *Med Hyp*, **64**: 658-660.

Iwenofu, O., Lackman, R., Staddon, A., Goodwin, D., Haupt, H. and Brooks, J. (2008) Phospho-S6 ribosomal protein: a potential new predictive sarcoma marker for targeted mTOR therapy. *Mod Pathol*, **21**: 231-237.

Jaalouk, D. and Lammerding, J. (2009) Mechanotransduction gone awry. *Nat Rev Mol Cell Biol*, **10**: 63-73.

Jacinto, E., Loewith, R., Schmidt, A., Lin, S., Ruegg, M., Hall, A. and Hall, M. (2004) Mammalian TOR complex 2 controls the actin cytoskeleton and is rapamycin insensitive. *Nat Cell Biol*, **6**: 1 122-1 128.

Jankowski, J., Henderson, K., Viaene, A., Baert, J. and Long, L. (1995) Morphological analysis of gastro-esophageal diseases by molecular techniques. *Microsc Res Techniq*, **31**: 184-192.

Johnson, S. and Tattersfield, A. (2002) Lymphangioleiomyomatosis. *Semin Respir Crit Care Med*, **23**: 85-92.

Juliano, R. (2002) Signal transduction by cell adhesion receptors and the cytoskeleton: function of integrins, cadherins, selectins and immunoglobulin-superfamily members. *Annu Rev Pharmacol Toxicol*, **42**: 283-323.

Jung, C., Jun, C., Ro, S., Kim, Y., Otto, N., Cao, J., Kundu, M. and Kim, D. (2009) ULK-Atg-13-FIP200 complexes mediate mTOR signaling to the autophagy machinery. *Mol Biol Cell*, **20**: 1 992-2 003.

Jung, C., Ro, S., Cao, J., Otto, N. and Kim, D. (2010) mTOR regulation of autophagy. *FEBS Lett*, **584**: 1 287-1 295.

Junqueira, L. and Carneiro, J. (2007) Basic Histology: Text and Atlas, 11th Edition. McGraw-Hill Companies, Chapter 4, Epithelial Tissue: Introduction. Pg 69.

Kabeya, Y., Mizushima, N. and Ueno, T. (2000) LC3, a mammalian homologue of yeast Apg8p, is localized in autophagosome membranes after processing. *EMBO J*, **19**: 5 720-5 728.

Kachala, R. (2010) Systematic review: Epidemiology of oesophageal cancer in sub-Saharan Africa. *Malawi Med*, **22**: 65-70.

Kang, S., Dong, S., Gu, T-L., Guo, A., Cohen, M., Lonial, S., Khoury, H., Fabbro, D., Gililand, D., Bergsagel, P., Taunton, J., Polakiewicz, R. and Chen, J. (2007) FGFR3 activates RSK2 to mediate hematopoietic transformation through tyrosine phosphorylation of RSK2 and activation of the MEK/ERK pathway. *Cancer Cell*, **12**: 201-214.

Kanzawa, T., Germano, I., Komata, T., Ito, H. and Kondo, S. (2004) Role of autophagy in temozolomide-induced cytotoxicity for malignant glioma cells. *Cell Death Differ*, **11**: 448-457.

Karbowiniczek, M., Spittle, C., Morrison, T., Wu, H. and Hesnke, E. (2008) mTOR is activated in the majority of malignant carcinomas. *J Invest Dermatol*, **128**: 980-987.

Kato, H., Yoshikawa, M., Miyazaki, T., Nakajima, M., Fukai, Y., Tajima, K., Masuda, N., Tsukada, K., Fukuda,T., Nakajima, T. and Kuwano, H. (2001) Expression of p53 protein related to smoking and alcoholic beverage drinking habits in patients with esophageal cancers. *Cancer Lett*, **167**: 65-72.

Kenerson, H., Aicher, L., True, L. and Yeung, R. (2002) Activated mammalian target of rapamycin pathway in the pathogenesis of tuberous sclerosis complex renal tumors. *Cancer Res*, **62**: 5 645-5 650.

Kim, D., Sarbassov, D., Ali, S., King, J., Latek, R., Erdjument-Bromage, H., Tempst, P. and Sabatini, D. (2002) mTOR interacts with raptor to form a nutrient-sensitive complex that signals to the cell growth machinery. *Cell*, **110**: 163-175.

Kim, J-H., Dooling, L. and Asthagiri, A. (2010) Intercellular mechanotransduction during multicellular morphodynamics. *J R Soc Interface*, **7**: S341-S350.

Klionsky, D. and Ohsumi, Y. (1999) Vacuolar import of proteins and organelles from the cytoplasm. *Ann Rev Cell Dev Biol*, **15**: 1-32.

Kondo, K., Yao, M., Kobayashi, K., Ota, S., Yoshida, M., Kaneko, S., Baba, M., Sakai, N., Kishida, T., Kawakami, S., Uemura, H., Nagashima, Y., Nakatani, Y. and Hosaka, M. (2001) PTEN/MMAC1/TEP1 mutations in human primary renal-cell carcinomas and renal carcinoma cell lines. *Int J Cancer*, **91**: 219-224.

Kondo, Y., Kanzawa, T., Sawaya, R. and Kondo, S. (2005) The role of autophagy in cancer development and response to therapy. *Nat Rev Cancer*, **5**: 726-734.

Kovacina, K., Park, g., Bae, S., Guzzetta, A., Schaefer, E., Birnbaum, M. and Roth, R. (2003) Identification of a proline-rich Akt substrate as a 14-3-3 binding partner. *J Biol Chem*, **278**: 10 189-10 194.

Krasilnikov, M. (2000) Phosphatidylinositol-3 kinase dependent pathways: the role in control of cell growth, survival, and malignant transformation. *Biochemistry*, **65**: 59-67.

Kudchodkar, S., Yu, Y., Maguire, T. and Alwine, J. (2004) Human cytomegalovirus infection induces rapamycin-insensitive phosphorylation of downstream effectors of mTOR kinase. *J Virol*, **78**: 11 030–11 039.

Laemmli, U. K. (1970) Cleavage of Structural Proteins During the Assembly of the Head of Bacteriophage T4. *Nature*, **227**: 680-685.

Lam, A. (2000) Molecular biology of esophageal squamous cell carcinoma. *Crit Rev Oncol/Hematol*, **33**: 71-90.

Langdon, P. (2004) Cancer Cell Culture: Methods and Protocols. Humana Press Inc., Totowa, New Jersey. Pg 23.

Laudański, P., Kowalczuk, O., Klasa-Mazurkiewicz, D., Milczek, T., Rysak-Luberowicz, D., Garbowicz, M., Baranowski, W., Charkiewicz, R., Szamatowicz, J. and Chyczewski, L. (2011) Selective gene expression profiling of mTOR-associated tumor suppressor and oncogenes in ovarian cancer. *Folia Hitochem Cytobiol*, **49**: 317-324.

Legate, K., Montanez, E., Kudlacek, O. and Fässler, R. (2006) ILK, PINCH and parvin: the tIPP of integrin signalling. *Nat Rev Mol Cell Biol*, **7**: 20-31.

Lehrbach, D., Nita, M. and Cecconello, I. (2003) Molecular Aspects of Esophageal Squamous Cell Carcinoma. *Arq Gastroenterol*, **40**: 256-261.

Lemmon, M. and Schlessinger, J. (2010) Cell signalling by receptor tyrosine kinases. *Cell*, **141**: 1 117-1 134.

Leung-Hagesteijn, C., Mahendra, A., Naruszewicz, I. and Hannigan, G. (2001) Modulation of Integrin Signal Transduction by ILKAP, a Protein Phosphatise 2C Associating with the Integrin-linked Kinase, ILK1. *EMBO J*, **20**: 2 160-2 170.

Levine, B. and Klionsky, D. (2004) Development by self-digestion: Molecular mechanisms and biological functions of autophagy. *Dev Cell*, **6**: 463-477.

Li, F., Zhang, Y. and Wu, C. (1999) Integrin-linked Kinase is Localised to Cell-matrix Focal Adhesions but not Cell-Cell Adhesion Sites and the Focal Adhesion Localisation of Integrin-linked Kinase is Regulated by the PINCH-binding ANK Repeats. *J Cell Sci*, **112**: 4 589-4 599.

Li, J., Yen, C., Liaw, D., Podsypanina, K., Bose, S., Wang, S., Puc, J., Miliaresis, C., Rodgers, L., McCombie, R., Bigner, S., Giovanella, B., Ittmann, M., Tycko, B., Hibshoosh, H., Wigler, M. and Parsons, R. (1997) PTEN, a putative protein tyrosine phosphatase gene mutated in human brain, breast, and prostate cancer. *Science*, **275**: 1 943-1 947.

Liang, C. and Jung, J. (2009) Autophagy genes as tumor supressors. *Curr Opin Cell Biol*, **22**: 1-8.

Lim, C., Bershadsky, A. and Sheetz, M. (2010) Mechanobiology. *J R Soc Interface*, 7: S291-S293.

Lin, D-C, Du, X-L. and Wang, M-R. (2009) Protein alterations in ESCC and clinical implications: a review. *Dis Esophagus*, **22**: 9-20.

Liu, Y., Mei, C., Sun, L., Li, X., Liu, M., Wang, L., Li, Z., Yin, P., Zhao, C., Shi, Y., Qiu, S., Fan, J. and Zha, X. (2011) The PI3K-Akt pathway regulates calpain 6 expression, proliferation, and apoptosis. *Cell Signal*, **23**: 827-836.

Lock, R. and Debnath, J. (2008) Extracellular matrix regulation of autophagy. *Curr Opin Cell Biol*, **20**: 583-588.

Loewith, R., Jacinto, E., Wullschleger, S., Lorberg, A., Crespo, J., Bonenfant, D., Oppliger, W., Jenoe, P. and Hall, M. (2002) Two TOR complexes, only one of which is rapamycin sensitive, have distinct roles in cell growth control. *Mol Cell*, **10**: 457-468.

Longo, L., Platini, F., Scardino, A., Alabiso, O., Vasapollo, G., Tessitore, L. (2008) Autophagy inhibition enhances anthocyanin-induced apoptosis in hepatocellular carcinoma. *Curr Opin Cell Biol*, **7**: 2 476-2 485.

Luo, S. (2012) Bim inhibits autophagy by recruiting beclin 1 to microtubules. *Mol Cell*, **47**: 359-370.

Loyd, D. (2008) Physics Laboratory Manual, Third Edition. Printed for Thomas Higher Education by David Harris Publishers, Belmont, USA. Pg 125.

Madhunapantula, S. and Robertson, G. (2009) The PTEN-AKT3 signaling cascade as a therapeutic target in melanoma. *Pig Cell Melanoma Res*, **22**: 400-419.

Mak, B., Kenerson, H., Aicher, L., Barnes, E. and Yeung, R. (2005) Aberrant β-catenin signaling in tuberous sclerosis. *Am J Pathol*, **167**: 107-116.

Mammoto, T. and Ingber, D. (2010) Mechanical control of tissue and organ development. *Development*, **137**: 1 407-1 420.

Manning, B., Tee, A., Logsdon, M., Blenis, J. and Cantley, L. (2002) Identification of the tuberous sclerosis complex-2 tumour suppresser gene product tuberin as a target of the phosphatide 3-kianse/akt pathway. *Mol Cell*, **10**: 151-162.

Martelli, A., Evangelisti, C., Chiarini, F., Grimaldi, C., Cappellini, A., Ognibene, A. and McCubrey, J. (2010) The emerging role of the phosphatidylinositol 3-kinase/Akt/mammalian target of rapamycin signaling network in normal myelopoiesis and leukemogenesis. *Biochim Biophys Acta*, **1 803**: 991-1 002.

Mason, E. and Rathmell, J. (2010) Cell metabolism: an essential link between cell growth and apoptosis. *Biochim Biophys Acta*, Published Online, **DOI**: 10.1016/j.bbamcr2010.08011.

McDonald, P., Oloumi, A., Mills, J., Dobreva, I., Maidan, M., Gray, V., Wederell, E., Bally, M., Foster, L. and Dedhar, S. (2008). Rictor and integrin-linked kinase interact and regulate Akt phosphorylation and cancer cell survival. *Cancer Res*, **68**: 1 618-1 624.

McKay, M. and Morrison, D. (2007) Integrating signals from RTKs to ERK/MAPK. *Oncogene*, **26**: 3 113-3 121.

Meijer, A. and Codogno, P. (2004) Regulation and role of autophagy in mammalian cells. *Int J Biochem Cell Biol*, **36**: 2 445-2 462.

Melhado, R., Alderson, D. and Tucker, O. (2010) The changing face of esophageal cancer. *Cancers*, **2**: 1 379-1 404.

Memmott, R. and Dennis, P. (2009) Akt-dependent and –independent mechanisms of mTOR regulation in cancer. *Cell Signal*, **21**: 656-664.

Mendoza, M., Er, E. and Blenis, J. (2011) The RAS-ERK and PI3K-mTOR pathways: crosstalk and compensation. *Trends Biochem Sci*, **36**: 320-328.

Miller, S. and Veale, R. (2001). Environmental Modulation of αv, α2 and β1 Integrin Subunit Expression in Human Oesophageal Squamous Cell Carcinomas. *Cell Biol Int*, **25**: 61-69.

Mitra, S., Hanson, D. and Schlaepfer, D. (2005) Focal adhesion kinase: in command and control of cell motility. *Nat Rev Mol Cell Biol*, **6**: 56-68.

Molinolo, A., Hewitt, S., Amornphimoltham, P., Keelawat, S., Rangdaeng, S., Meneses, Garcia, A., Raimondi, A., Jufe, R., Itoiz, M., Gao, Y., Saranath, D., Kaleebi, G., Yoo, G., Leak, L., Myers, E., Shintani, S., Wong, D., Massey, H., Yeudall, W., Lonardo, F., Ensley, J. and Gutkind, J. (2007) Dissecting the Akt/mammalian target of rapamycin signaling network: emerging results from the head and neck cancer tissue array initiative. *Clin Cancer Res*, **13**: 4 964-4 973.

Morimoto, A., Tomlinson, M., Nakatani, K., Bolen, J., Roth, R. and Herbst, R. (2000) The MMAC Tumor Suppressor Phosphatase Inhibits Phospholipase C and Integrin Linked Kinase Activity. *Oncogene*, **19**: 200-209.

Neufeld, T. (2010) TOR-dependant control of autophagy: biting the hand that feeds. *Curr Opin Cell Biol*, **22**: 157-168.

Nguyen, T. (2008) Targeting RSK: An Overview of Small Molecule Inhibitors. *Anti-Cancer Agent Me*, **8**: 710-716.

Nho, R., Xia, H., Kahm, J., Kleidon, J., Diebold, D. and Henker, C. (2005) Role of integrin-linked kinase in regulating phosphorylation of Akt and fibroblast survival in type I collagen matrices through a β1integrinviability signaling pathway. *J Biol Chem*, **280**: 26 630-26 639.

Nicholson, K., Quinn, D., Kellett, G. and Warr, J. (2003) LY294002, an inhibitor of phosphatidylinositol 3-kinase, causes preferential induction of apoptosis in human multidrug resistant cells. *Cancer Lett*, **190**: 31-36.

Nobukuni, T, Joaquin, M., Roccio, M., Dann, S., Kim, S., Gulati, P., Byfield, M., Backer, J., Natt, F., Bos, J., Zwartkruis, F. and Thomas, G. (2005) Amino acids mediate mTOR/raptor signaling through inactivation of class 3 phosphatidylinositol 3OH-kinase. *Proc Natl Acad Sci USA*, **102**: 14 238-14 243.

Nozawa, H., Wanatabe, T. and Nagawa, H. (2007) Phosphorylation of ribosomal protein p70 S6 kinase and rapamycin sensitivity in human colorectal cancer. *Cancer Lett*, **251**: 105-113.

O'Conner, R. and O'Driscoll, L. (2006) Cell and tissue culture. In "Cell Biology: a laboratory handbook", Third Edition, Edited by Julio De Celis, Academic Press, 1: Part A. Section 1. Pg 19.

O'Shea, C., Klupsch, K., Choi, S., Bagus, B., Soria, C., Shen, J., McCormick, F. and Stokoe, D. (2005) Adenoviral proteins mimic nutrient/growth signals to activate the mTOR pathway for viral replication. *EMBO J*, **24**: 1 211-1 221.

Osaki, M., Oshimura, M. and Ito, H. (2004) PI3K-Akt pathway: Its functions and alterations in human cancer. *Apoptosis*, **9**: 667-676.

Pal, S. and Figlin, R. (2011) Future directions of mammalian target of rapamycin (mTOR) inhibitor therapy in renal cell carcinoma. *Targ Oncol*, Published Online: **DOI**:10.1007/s11523-011-0172-y.

Panasyuk, G., Nemazanyy, I., Zhyvoloup, A., Filonenko, V., Davies, D., Robson, M., Pedley., R., Waterfield, M. and Gout, I. (2009) mTORβ splicing isoform promotes cell proliferation and tumourigenesis. *J Biol Chem*, **284**: 30 807-30 814.

Pantel, K., Brakenhoff, R. and Brandt, B. (2008) Detection, clinical relevance and specific biological properties of disseminating tumour cells. *Nat Rev Cancer*, **8**: 329-340.

Parrott, L. and Templeton, D. (1999) Osmotic stress inhibits p70/85 S6 kinase through inactivation of a protein phosphatase. *J Biol Chem*, **274**: 24 73-24 736.

Persad, S. and Dedhar, S. (2003) The Role of Integrin-linked Kinase (ILK) in Cancer Progression. *Canc Metastasis Rev*, **22**: 375-384.

Persad, S., Attwell, S., Gray, V., Delcommenne, M., Troussard, A., Sanghera, J. and Dedhar, S. (2000) Inhibition of integrin-linked kinase (ILK) suppresses activation of protein kinase ByAkt and induces cell cycle arrest and apoptosis of PTEN-mutant prostate cancer cells. *PNAS*, **97**: 3 207-3 212.

Persad, S., Attwell, S., Gray, V., Mawji, N., Deng, J., Leung, D., Yan, J., Sanghera, J., Walsh, M. and Dedhar, S. (2001) Regulation of Protein Kinase B/Akt-serine-473 Phosphorylation by Integrin Linked Kinase (ILK): Critical Roles for Kinase Activity and Amino Acids Arginine-211 and Serine-343. *J Biol Chem*, **276**: 27 462-27 469.

Peterson, T., Laplante, M., Thoreen, C., Sancak, Y., Kang, S., Kuehl, W., Gray, N. and Sabatini, D. (2009) DEPTOR is an mTOR inhibitor frequently overexpressed in multiple myoloma cells and required for their survival. *Cell*, **137**: 873-886.

Pópulo, H., Lopes, J. and Soares, P. (2012) The mTOR signalling pathway in human cancer. *Int J Mol Sci*, **13**: 1 886-1 918.

Potter, C., Pedraza, L., Xu, T. (2002). Akt regulates growth by directly phosphorylating Tsc2. *Nat Cell Biol*, **4**: 658-665.

Ramirez, F. and Rifkin, D. (2003) Cell signalling events: a view from the matrix. *Matrix Biol*, **22**: 101-107.

Reya, T. and Clevers, H. (2005) Wnt Signalling in Stem Cells and Cancer. *Nature*, **434**: 843-850.

Rosales, C., Gresham, H. and Brown, E. (1992) Expression of the 50-kDa Integrin-associated Protein on Myeloid Cells and Erythrocytes. *J Immunol*, **149**: 2 759-2 764.

Roskelley, C., Srebrow, A. and Bissell, M. (1995) A hierarchy of ECM-mediated signalling regulates tissue-specific gene expression. *Curr Opin Cell Biol*, **7**: 736-747.

Rosner, M., Hanneder, M., Siegel, N., Valli, A., Fuchs, C., Hengstschlager, M. (2008) The mTOR pathway and its role in human genetic diseases. *Mut Res*, **659**: 284-292.

Roux, P., Ballif, B., Anjum, R., Gygi, S. and Blenis, J. (2004). Tumor-promoting phorbel esters and activated Ras inactivate the tuberous sclerosis tumor suppressor complex via p90 ribosomal S6 kinase. *Proc Natl Acad Sci USA*, **101**: 13 489-13 494.

Roux, P., Shahbazian, D., Vu, H., Holz, M., Cohen, M, Tauton, J., Sonenberg, N. and Blenis, J. (2007) RAS/ERK signaling promotes site-specific ribosomal protein S6 phosphorylation via RSK and stimulates Cap-dependant translation. *J Biol Chem*, **282**: 14 056-14 064.

Rozario, T. and DeSimone, D. (2010) The extracellular matrix in development and morphogenesis: A dynamic view. *Dev Biol*, **341**: 126-140.

Rozengurt, E. (2007) Mitogenic signaling pathways induced by G protein-coupled receptors. *J Cell Physiol*, **213**: 589-602.

Sabatini, D. (2006) mTOR and cancer: insights into a complex relationship. Nat Rev Cancer, 6: 729-735.

Sabers, C., Martin, M., Brunn, G., Williams, J., Dumont, F., Wiederrecht, G. and Abraham, R. (1995) Isolation of a protein target of the FKBP12-rapamycin complex in mammalian cells. *J Biol Chem*, **270**: 815-822.

Sancak, Y., Peterson, T., Shaul, Y., Lindquist, R., Thoreen, C., Bar-Peled, L. and Sabatini, D. (2008) The RagGTPases bind raptor and mediate amino acid signalling to mTORC1. *Science*, **320**: 1 496-1 501.

Sancak, Y., Thoreen, C., Peterson, T., Lindquist, R., Kang, S., Spooner, E., Carr, S. and Sabatini, D. (2007) PRAS40 Is an Insulin-Regulated Inhibitor of the mTORC1 Protein Kinase. *Mol Cell*, **25**: 903-915.

Sapkota, G., Cummings, L., Newell, F., Armstrong, C., Bain, J., Frodin, M., Grauert, M., Hoffmann, M., Schnapp, G., Steegmaier, M., Cohen, P. and Alessi, D. (2007) BI-D1870 is a specific inhibitor of the p90 RSK (ribosomal S6 kinase) isoforms in vitro and in vivo. *Biochem J*, **401**: 29-38.

Sarbassov, D. And Sabatini, D. (2005a) Redox regulation of the nutrient-sensitive Raptor-mTOR pathwaycomplex. *J Biol Chem*, **280**: 39 505-39 509.

Sarbassov, D., Guertin, D., Ali, S. and Sabatini, D. (2005b) Phosphorylation and regulation of Akt/PKB by the Rictor-mTOR complex. *Science*, **307**: 1 098-1 101.

Sato, T., Nakashima, A., Guo, L., Coffman, K. and Tamanoi, F. (2010) Single amino-acid changes that confer constitutive activation of mTOR are discovered in human cancer. *Oncogene*, **29**: 2 746-2 752.

Schmelzle, T. and Hall, M. (2000) TOR, a central controller of cell growth. *Cell*, **103**: 253-262.

Schöck, F. and Perrimon, N. (2002) Molecular mechanisms of epithelial morphogenesis. *Annu Rev Cell Dev Biol*, **18**: 463-493.

Scully, C. and Bagan, J. (2009) Oral Squamous Cell Carcinoma Overview. *Oral Oncol*, Published Online, **DOI**:10.1016/j.oraloncology.2009.01.004.

Seger, R. and Krebs, E. (1995) The MAPK signaling cascade. *FASEB J*, **9**: 726-735.

Seidensticker, M. and Behrens, J. (2000) Biochemical Interactions in the Wnt Pathway. *Biochem Biophys Acta*, **1 495**: 168-182.

Sekiguchi, T., Hirose, E., Nakashima, N., Ii, M. and Nishimoto, T. (2001) Novel G protein, Rag C and Rag D, interact with GTP-binding proteins, Rag A and Rag B. *J Biol Chem*, **276**: 7 246- 7 257.

Sekulić, A., Hudson, C., Homme, J., Yin, P., Otterness, D., Karnitz, L. and Abraham, R. (2000) A direct linkage between the phosphatidylinositol 3-kinase-Akt signaling pathway and the mammalian target of rapamycin in mitogen-stimulated and transformed cells. *Cancer Res*, **60**: 3 504-3 513.

Shaw, N. (2011) PI3K in human oesophageal squamous carcinoma cells: A critical modulator in the PKB signalling pathway. A thesis submitted to the Faculty of Science, University of the Witwatersrand, Johannesburg, in fulfilment of the requirements for the degree of Ph.D.

Shor, B., Gibbons, J., Abraham, R. and Yu, K. (2009) Targeting mTOR globally in cancer. Cell Cycle, 8: 3 831-3 837.

Shwartz, M. (2001) Integrin Signaling Revisited. *TRENDS Cell Biol*, **11**: 466-470.

Shwartz, M. (2010) Integrins and extracellular matrix in mechanotransduction. *Cold Spring Harb Perspect Biol*, Published Online: **DOI**: 2010;2:a005066.

Soulard, A. and Hall, M. (2007) Snapshot: mTOR signaling. *Cell*, 129: Published Online: **DOI**: 10.1016j.cell.2007.04.010.

Soule, H., Vazquez, J., Long, A., Albert, S. and Brennan, M. (1973) A human cell line from a pleural effusion derived from a breast carcinoma. *J Natl Inst*, **51**: 1 409-1 416.

Stoner, G. and Gupta, A. (2001) Etiology and chemoprevention of Esophageal Cell Carcinoma. *Carcinog*, **22**: 1 737-1 746.

Stoner, G., Wang, L. and Chen, T. (2007) Chemoprevention of Squamous Cell Carcinoma. *Toxicol Appl Pharmacol*, **224**: 337-349.

Sturgill, T. and Hall, M. (2009) Activating mutations in TOR are in similar structures as oncogenic mutations in PI3KCalpha. *ACS Chem Biol*, **4**: 999-1 015.

Sturgill, T. and Wu, J. (1991) Recent progress in characterization of protein kinase cascades for phosphorylation of ribosomal protein S6. *Biochim Biophys Act*, **1 092**: 350-357.

Subauste, M., Pertz, O., Adamson, E., Turner, C., Junger, S. and Hahn, K. (2004) Vinculin modulation of paxillin-FAK interactions regulates ERK to control survival and motility. *J Cell Biol*, **165**: 371-381.

Takahara, T., Hara, K., Yonezawa, K., Sorimachi, H. and Maeda, T. (2006) Nutrient-dependent multimerization of the mammalian target of rapamycin through the N-terminal HEAT repeat region. *J Biol Chem*, **281**: 28 605-28 614.

Tee, A. and Proud, C. (2000) DNA-damaging agents cause inactivation of translational regulators liked to mTOR signalling. *Oncogene*, **19**: 3 021-3 031.

Teng, K., Angelstro, J., Cunningham., M. and Greene, L. (2006) Cultured PC12 cells: a model for neuronal function, differentiation, and survival. In Cell Biology: A Laboratory Handbook, Third Edition, Volume 1, Section 4, Sub-section 21. Edited by Julio E. Celis. Elsevier Academic Press, Burlington, USA, pp 172-176.

Tew, W.P., Kelsen, D.P. and Ilson, D.H. (2005) Targeted therapies for esophageal cancer. *Oncologist*, **10**: 590-601.

Thomas, G., and Hall, M. (1997). TOR signalling and control of cell growth. *Curr Opin Cell Biol*, **9**: 782-787.

Thornberry, N. and Lazebnik, Y. (1998) Caspases: the enemies within. *Science*, **281**: 1 312-1 316.

Towbin, H., Staehelin, T., and Gordon, J. (1979) Electrophoretic Transfer of Proteins from Polyacrylamide Gels to Nitrocellulose Sheets: Procedure and Some Applications. *Proc Natl Acad Sci*, **76**: 4 350-4 354.

Tsuchihara, K., Fujii, S. and Esumia, H. (2009) Autophagy and cancer: Dynamism of the metabolism of tumor cells and tissues. *Cancer Lett*, **278**: 130-138.

Tsujimoto, Y. and Shimizu, S. (2005) Another way to die: autophagic programmed cell death. *Cell Death Differ*, **12**: 1 528-1 534.

Ubbink, M. (2009) The courtship of proteins: understanding the encounter complex. *FEBS Lett*, **583**: 1 060-1 066.

Underwood, T., Derouet, M., White, M., Noble, F., Moutasim, K., Smith, E., Drew, P., Thomas, G., Primrose, J. and Blaydes, J. (2010) A comparison of primary oesophageal squamous epithelial cells with HET-1A in organotypic culture. *Biol Cell*, **102**: 635-644.

van Der Flier, A. and Sonnenberg, A. (2001) Function and interactions of integrins. *Cell Tissue Res*, **305**: 285-298.

Varma, S. and Khandelwal, R. (2007) Effects of rapamycin on cell proliferation and phospho- rylation of mTOR and p70(S6K) in HepG2 and HepG2 cells overexpressing constitutively active Akt/PKB. *Biochim Biophys Acta*, **1 770**: 71-78.

Veale, R. and Thornley, A. (1989). Increased single class low-affinity EGF receptors expressed by human oesophageal squamous cell carcinoma cell lines. *S Afr J Sci*, **85**: 375-379.

Vézina, C., Kudelski, A. and Sehgal, S. (1975) Rapamycin (AY-22, 989), a new antifungal antibiotic, taxonomy of the producing streptomycete and isolation of the active principle. *J Antibiot*, **28**: 721-726.

Villanueva, A., Chiang, D., Tovar, V., van Laarhoven, S., Fiel, Newell, P., Peix, J., Thung, S. and Llovet, J. (2008) Pivotal Role of mTOR Signaling in Hepatocellular Carcinoma. *Gastroenterology*, **135**: 1 972-1 983.

Vivanco, I. and Sawyers, C. (2002) The phosphatidylinositol 3-kinaseAKTpathway in human cancer. *Nat Rev Cancer*, **2**: 489-501.

Vlahos, C., Matter, W., Hui, K. and Brown, R. (1994) A specific inhibitor of phosphatidylinositol 3-kinase, 2-(4-morpholinyl)-8-phenyl-4H-1-benzopyran-4-one (LY294002). *J Biol Chem*, **269**: 5 241-5 248.

Vogelstein B. and Kinzler, K. (2004) Cancer Genes and the Pathways they Control. *Nat Med*, **10**: 789-799.

Volker, M., Albert, F. and Ohm, T. (2007) Coupling of mTOR- with PI3K-signaling pathway regulates PP2A and GSK-3Beta dependant phosphorylation of TAU. *JBC*, **283**: 100-109.

Walker, A., Walker, B., Isaacson, C., Segal, I. and Pryor S. (1984). Short duration of survival among South African blacks with oesophageal cancer. *S Afr Med J*, **66**: 877-878.

Walker, K., Deak, M., Paterson, A., Hudson, K., Cohen, P. and Alessi, D. (1998) Activation of protein kinase B beta and gamma isoforms by insulin in vivo and by 3-phosphoinositide-dependent protein kinase-1 in vitro: comparison with protein kinase B alpha. *Biochem J*, **331**: 299-308.

Wang, H-Y. and Malbon, C. (2011) Probing the physical nature and composition of signalsomes. *J Mol Signal*, 6:1: Published Online: **DOI**:10.1186/1750-2187-6-1.

Wang, R. and Levine, B. (2010) Autophagy in cellular growth control. *FEBS Lett*, **584**: 1 417-1 426.

Wu, C. (2005) PINCH, N(i)ck and the ILK: network wiring at cell-matrixadhesions. *TRENDS Cell Biol*, **15**: 460-466.

Wu, C. and Dedhar, S. (2001) Integrin-linked Kinase (ILK) and Its Interactors: A New Paradigm for the Coupling of Extracellular Matrix to Actin Cytoskeleton and Signalling Complexes. *J Cell Biol*, **155**: 505-510.

Wu, C., Keightley, S., Leung-Hagesteijn, C., Radeva, G., Coppolino, M., Goicoechea, S., McDonald, J. and Dedhar, S. (1998). Integrin-linked Protein Kinase Regulates Fibronectin Matrix Assembly, E-cadherin Expression and Tumorigenicity. *J Biol Chem*, **273**: 528-536.

Xian, W., Pappas, L., Pandya, D., Selfors, L., Derkson, P., de Bruin, M., Gray, N., Jonkers, J., Rosen, J. and Brugge, J. (2009) Fibroblast growth factor receptor 1-transformed mammary epithelial cells are dependent on RSK activity for growth and survival. *Cancer Res*, **69**: 2 244-2 251.

Xie, Z. and Klionsky, D. (2007) Autophagosome formation: core machinery and adaptations. *Nat Cell Biol*, **9**: 1 102-1 109.

Yan, L. and Lamb, R. (2012) Amino acid sensing and regulation of mTORC1. *Semin Cell Dev Biol*, **23**: 621-625.

Yan, L., Mieulet, V. and Lamb, R. (2010) Nutrient regulation of mTORC1 and cell growth. *Cell Cycle*, **9**: 2 473-2 474.

Yang, Z. and Klionsky, D. (2010) Mammalian autophagy: core molecular machinery and signaling regulation. *Curr Opin Cell Biol*, **22**: 124-131.

Young, B., Lowe, J., Stevens, A. and Heath, J. (2007) Wheater's Functional Histology: A Text and Colour Atlas, 5th Edition. Part 2, Chapter 5, Epithelial Tissues, Pg 80.

Yuan, T. and Cantley, L. (2008) PI3K pathway alterations in cancer: variations on a theme. *Oncogene*, **27**: 5 497-5 510.

Zhang, H., Chen, S. and Li, Y. (2004) Epidemiological Investigation of Esophageal Carcinoma. *World J Gastroentero*, **10**: 1 834-1 835.

Zheng, S-T., Zhang, C-S., Qin, X., Gen, Y-H., Liu, T., Sheyhidin, I. and Lu, X-M. (2012) The status of phosphorylated p38 in esophageal squamous cell carcinoma. *Mol Biol Rep*, **39**: 5 315-5 321.

Zhou, H. and Huang, S. (2010) The complexes of mammalian target of rapamycin. *Curr Protein Pept Sci*, **11**: 409-424.

Zustiak, M., Pollack, J., Marten, M and Betenbaugh, M. (2008) Feast or famine: autophagy control and engineering in eukaryotic cell culture. *Curr Opin Cell Biotechnol*, **19**: 518-526.

APPENDICES

APPENDIX A

1.1. Commonly Used Solutions

1.1.1 Phosphate Buffered Saline (PBS) (1X)

136.9 mM	Sodium Chloride
2.680 mM	Potassium Chloride
10.10 mM	Disodium Hydrogen Phosphate Dodecahydrate
1.769 mM	Potassium Dihydrogen Phosphate

Adjust to a pH between 7.2 – 7.3

Make up to final volume with dH_2O

Autoclave to sterilize

Store at 4 °C

1.1.2 Tris Buffered Saline (TBS) (1X)

50.00 mM	Tris-HCl (pH 7.8)
147.0 mM	Sodium Chloride
2.000 mM	Anhydrous Calcium Chloride

Make up to final volume with dH_2O

Autoclave to sterilize.

Store at 4 °C

1.1.3 Tris Buffered Saline with Tween (TBS-T)

50.00 mM	Tris-HCl (pH 7.8)
147.0 mM	Sodium Chloride
2.000 mM	Anhydrous Calcium Chloride
0.100 %	Tween

Make up to final volume with dH_2O

Store at 4 °C

1.1.4 10 % Sodium dodecyl Sulphate (SDS)

10 %	SDS

Make up to final volume with dH_2O

Heat to assist dissolution

Adjust to pH 7.2

Store at room temperature

1.2. Tissue Culture

1.2.1. DMEM/Hams F12 Medium Solution

Mix DMEM/Hams F12 Medium Solutions in a 3:1 ratio

Filter sterilize

Store at 4 °C

1.2.1.1. Dulbecco's Modified Eagles Medium (DMEM)

1.370 %	DMEM
0.370 %	Sodium Bicarbonate
2.000 %	Penicillin (500 U/ml)/Streptomycin (0.5 %) Solution

1.2.1.2. Hams F12 Medium Solution

1.070 %	Hams F12 Medium
0.118 %	Sodium Bicarbonate
2.000 %	Penicillin (500 U/ml)/Streptomycin (0.5 %) Solution

1.2.2. Trypsin/Ethylenediaminetetra-acetic Acid (EDTA)

Mix Trypsin Solution/EDTA in a 1:1 ratio

Store at 4 °C

1.2.2.1. Trypsin Solution

0.010 %	Trypsin in PBS

1.2.2.2. Ethylenediaminetetra-acetic Acid (EDTA)

0.004 %	EDTA in PBS

1.3. Protein Extraction

1.3.1. 2 % (v/v) Triton X-100 Protein Extraction Buffer

50 mM	Tris-HCl (pH 7.2)
150 mM	NaCl
1 mM	Magnesium Chloride
0.5 mM	Ethylene Glycol Tetraacetic Acid
5 µl/ml	Phenyl-methyl-sulphonyl Fluoride (PMSF)
10 µl/ml	Trasylol
2.0 %	Triton-X-100

Make up to 10 ml with dH_2O

1.3.2. Laemmli Double Lysis Buffer (2X)

123.8 mM	Tris-HCl (pH 6.8)
4.000 %	SDS
20.00 %	Glycerol
10.00 %	β-mercaptoethanol

Make up to final volume with dH_2O

Store at 4 °C

1.3.3. Laemmli Single Lysis Buffer (1X)

50 %	Laemmli Double Lysis Buffer (2X)
50 %	dH_2O

Store at 4 °C

1.4. Protein Estimation

1.4.1. 95 % Ethanol

95 %	Ethanol

Make up to final volume with dH_2O

1.4.2. 7.5 % Trichloroacetic Acid (TCA)

7.5 %	TCA

Make up to final volume with dH_2O

1.4.3. 0.25 % Coomassie Brilliant Blue Stain

0.25 %	Coomassie Brilliant Blue Powder
50.0 %	Methanol

Dissolve, and then add:

10.0 %	Glacial Acetic Acid

Make up to final volume with dH_2O

1.4.4. Destain Solution

12 %	Glacial Acetic Acid
10 %	Methanol

Make up to final volume with dH_2O

1.4.5. Elution Solution

66 %	Methanol
33 %	dH_2O
1.0 %	Concentrated Ammonia

1.5. Sodium dodecyl Sulphate – Polyacrylamide Gel Electrophoresis (SDS-PAGE)

1.5.1. Sample Preparation

1.5.1.1. Laemmli Lysis Buffer (1X)

As previously described

1.5.2. Buffers

1.5.2.1. Running Buffer

25.00 mM	Tris-HCl (pH 8.3)
192.5 mM	Glycine
3.740 mM	SDS

Adjust solution to pH 8.3 using 5 N HCl

Make up to final volume with dH_2O

Store at 4 °C

1.5.2.2. Separating Buffer

18.12 g Tris

Adjust solution to pH 8.8 using 5 N HCl

Make up to final volume with dH_2O

1.5.2.3. Stacking Buffer

6.04 g Tris

Adjust solution to pH 6.8 using 5 N HCl

Make up to final volume with dH_2O

1.5.3. Working Solutions

1.5.3.1. Separating Gel

375 mM Tris-HCl (pH 6.8)

10 - 12 % Acrylamide

0.100 % N,N'–methylenebisacrylamide

0.200 % SDS

Make up to final volume with dH_2O

Just prior to use add:

1.000 % Ammonium Persulphate Solution (APS)

0.250 N',N',N',N'–tetramethylethylene-diamene (TEMED)

1.5.3.2. Stacking Gel

125 mM Tris-HCl (pH 6.8)

5 – 8 % Acrylamide

0.100 % N,N'–methylenebisacrylamide

0.200 % SDS

Make up to final volume with dH_2O

Just prior to use add:

1.000 % Ammonium Persulphate Solution (APS)

0.250 % N',N',N',N'–tetramethylethylene-diamene (TEMED)

1.5.3.3. SDS Overlay

400 µl of 50mg/ml SDS

Make up to 10 ml with dH_2O

1.5.3.4. Tracking Dye

0.001 %	Bromophenol Blue
50.00 %	Glycerol

Make up to final volume with dH_2O

Store at – 4 °C

1.5.3.5. 0.25 % Coomassie Brilliant Blue Stain

As previously described (see Appendix A, Section 1.4.3)

1.5.3.6. Destain Solution

10 %	Acetic Acid
10 %	Methanol

Make up to final volume with dH_2O

1.6. Western Immunoblot Analysis

1.6.1. Buffers

1.6.1.1. Transfer Buffer

25 mM	Tris-HCl (pH 8.3)
20.0 %	Methanol
1.41 %	Glycine

Make up to final volume with dH_2O

1.6.1.2. TBS–for–Blotto Blocking Buffer

50 mM	Tris-HCl (pH 7.8)
2.0 mM	Anhydrous Calcium Chloride
5.00 %	Non-fat Milk Powder
0.01 %	Anti-foam
0.05 %	TritonX-100

Make up to final volume with dH_2O

1.6.1.3. 5 % Non-fat Milk Powder Blocking Solution

5.0 %	Non-fat Milk Powder

Make up to final volume with appropriate buffer

1.6.1.4. Phosphate Buffered Saline (PBS) (1X)

As previously described (see Section 1.1.1)

1.6.1.5. Tris Buffered Saline (PBS) (1X)

As previously described (see Section 1.1.2)

1.6.1.6. Tris Buffered Saline with Tween (1X)

As previously described (see Section 1.1.3)

1.6.2. SuperSignal® West Pico Chemiluminescent Substrate Kit

Before use mix in a 1:1 ratio:

50 %	Luminol Enhancer Solution
50 %	Stable Peroxide Buffer

1.6.3. Developer

6.400 M	Methanol
0.600 M	Anhydrous Sodium Sulphate
80.0 mM	Hydroquinone (Quinol)
0.45 mM	Anhydrous Sodium Carbonate
34.0 mM	Potassium Bromide

Make up to final volume with dH_2O

Store at room temperature in the dark

1.6.4. Fixer

0.8 M	Sodium Thiosulphate
0.2 M	Sodium Metasulphite

Make up to final volume with dH_2O

Store at room temperature in the dark

1.7. Co-Immunoprecipitation Analysis

1.7.1. Radio-immunoprecipitation Assay (RIPA) Buffer

50 mM	Tris-HCl (pH 7.5)
150 mM	NaCl
0.5 %	Deoxycholate
0.5 %	Triton X-100
0.05 %	SDS
1 mM	PMSF/Aprotinin

Make up to final volume with dH_2O

Store at 4 °C

1.7.2. Phenylmethanesulphonylfluoride (PMSF) Stock Solution

34.8 mg	PMSF

Make up to 10 ml with Methanol

1.7.3. PMSF/Aprotinin Solution

0.1 mM	PMSF Stock Solution
1.00 ml	Trasylol

Make up to 100 ml with PBS (1X)

1.7.4. Immunoprecipitation (IP) Buffer

20 mM	Tris (pH 8.0)
0.50 %	Nonidet P-40 (NP-40)
0.90 %	Sodium Chloride

Make up to final volume with dH_2O

1.8. Specific Inhibition of PI3K with LY294002

1.8.1. LY294002 Working Dilution

20 μM	LY294002 in 100 % DMSO

1.8.1.1. LY294002 Stock

1 mg/ml

Make up to final volume with 100 % DMSO

1.9. Specific Inhibition of mTOR with Rapamycin

1.9.1. Rapamycin Working Dilutions

20 nM	Rapamycin in 100 % DMSO
50 nM	Rapamycin in 100 % DMSO
100 nM	Rapamycin in 100 % DMSO

1.9.1.1. Rapamycin Stock

1 mg/ml

Make up to final volume with 100 % DMSO

1.10. Specific Inhibition of p90RSK with BI-D1870

1.10.1. BI-D1870 Working Dilution

10 μM	BI-D1870 in 100 % DMSO

1.10.1.1. BI-D1870 Stock

1 mg/ml

Make up to final volume with 100 % DMSO

1.11. Growth on Fibronectin

1.11.1. Fibronectin Working Dilution

10 µg/ml Fibronectin in PBS

1.11.1.1. Fibronectin Stock

1 mg/ml

Make up to final volume with PBS

1.12. Growth on Collagen

1.12.1. Collagen Working Dilution

100 µg/ml Collagen in 0.02 N Acetic Acid

Made up to volume with dH_2O

1.12.1.1. Collagen Stock

3 µg/µl Rat Tail Collagen in 0.5 M Acetic Acid

Made up to volume with dH_2O

APPENDIX B

2.1. Sample standard curve

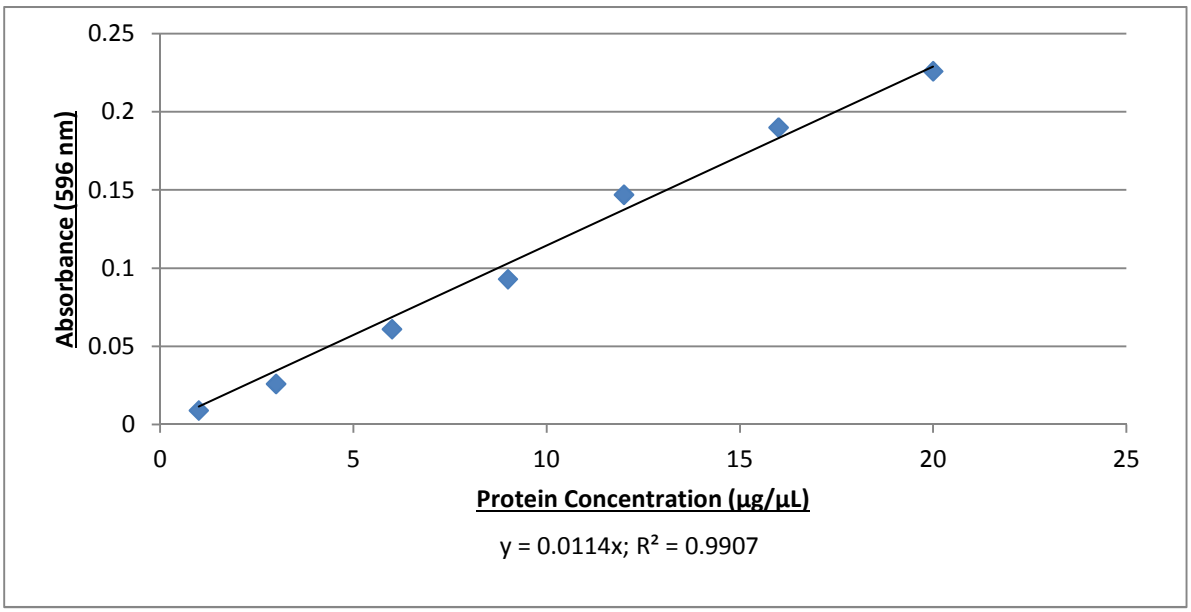

Figure B1: Sample standard curve for the estimation of protein concentration from HOSCC cells lysates. BSA standards of a known and varying concentration (1, 3, 6, 9, 12, 16 and 20 µg/µl; x-axis), together with their respective absorbance values determined at 596 nm (y-axis), were used to create the standard curve. The equation of the curve was used to calculate the amount of unknown protein in HOSCC cell lysates. R^2 is indicative of linear regression.

2.2. Calculation of percent change (% Δ) in protein expression levels after semi-quantitative densitometric analysis

Measures of relative difference may be expressed as unitless ratios. One approach to obtain percent change between two semi-quantitative measurements of % IOD is the difference between the final and initial value, divided by the initial value (Loyd, 2008). Therefore, percent change (% Δ) may be expressed as:

$$\Delta = \frac{\Delta\,\%\,\boldsymbol{IOD}}{\%\,\boldsymbol{IOD_{initial}}}$$

$$\therefore\ \%\,\Delta = \frac{\%\,\boldsymbol{IOD_{final}} - \%\,\boldsymbol{IOD_{initial}}}{\%\,\boldsymbol{IOD_{initial}}}\ \boldsymbol{x}\ \mathbf{100}\,\%$$

; where positive % Δ = increase in protein expression.

; where negative % Δ = decrease in protein expression.

2.3. Repeated western immunoblot analysis of mTOR and p-RPS6 polypeptides, in response to growth on either fibronectin or collagen.

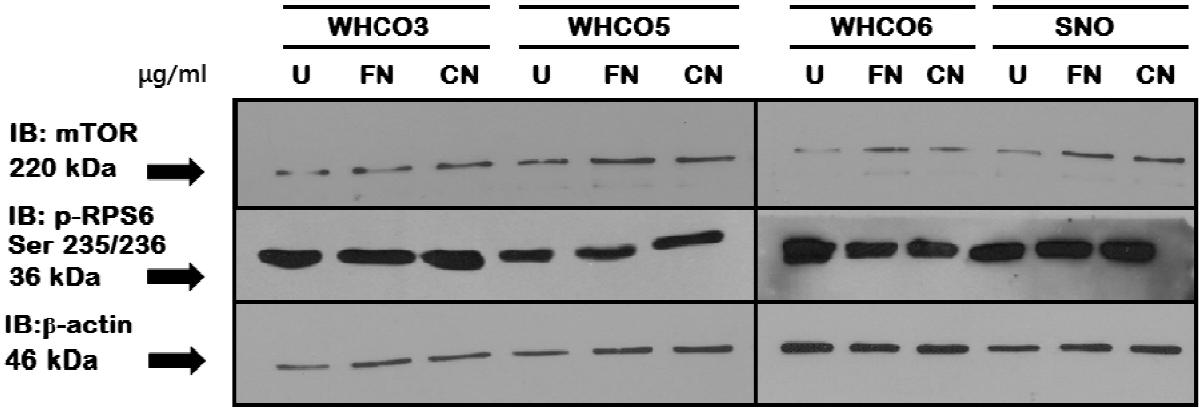

Figure B2: Repeated immunodetection of mTOR and p-RPS6$^{(Ser\ 235/236)}$ in HOSCC cells after growth on substrates coated with either fibronectin or collagen. Polypeptides indicative of mTOR (220 kDa) and p-RPS6$^{(Ser\ 235/236)}$ (36 kDa) were weakly detected in WHCO 3 cells (U, FN and CN), not detected in WHCO 5 cells (FN and CN), not detected in WHCO 6 cells (FN) and weakly in SNO cells (U and FN). Therefore, these western immunoblots were repeated. Initially, 15 µg of protein was loaded from each sample in order to detect mTOR and p-RPS6$^{(Ser\ 235/236)}$, however this value was now doubled to 30 µg of protein from each sample. Consequently, appropriate polypeptide bands indicative of mTOR (220 kDa) and p-RPS6$^{(Ser\ 235/236)}$ (36 kDa) were detected by immunoblot, relative to β-actin (46 kDa) which was used to demonstrate equal protein loading of HOSCC cell lysates.

2.4. Commonly used antibodies and incubation conditions during western immunoblot analysis

Table B1: Commonly used antibody dilutions and incubation times.

Primary Antibody	Transfer Time (hr)	Dilution (Ab:Buffer)	Incubation Time (hr)	Buffer and Temperature Conditions*	Secondary Antibody	Dilution (Ab:Buffer)	Incubation Time (hr)	Buffer and Temperature Conditions*
mTOR	3	1:1 000	2	2.5 % BSA in TBS-T:TBS (1:1) at RT	Goat anti-rabbit HRP-conjugate	1:5 000	1	TBS: TBS-T (1:1) at RT in the dark
p-RPS6 (Ser 235/236)	1.5	1:2 000	Overnight	5 % BSA in TBS-T at 4 °C	Goat anti-rabbit HRP-conjugate	1:2 000	1	5 % milk powder in TBS-T PBS at 30 °C in the dark
mATG-13	1.5	1:1 750	Overnight	1 % milk powder in TBS-T at 4 °C	Goat anti-rabbit HRP-conjugate	1:5 000	1	5 % milk powder in TBS-T at 30 °C in the dark
ILK	1.5	1:1 500	1	1 X PBS at RT	Goat anti-rabbit HRP-conjugate	1:30 000	1	1 X PBS at 30 °C in the dark
CC-3	1.5	1:500	Overnight	2.5 % milk powder in TBS-T at 4 °C	Goat anti-rabbit HRP-conjugate	1:2 000	1	5 % milk powder in TBS-T at 30 °C in the dark
β-actin	1.5	1: 1000	2	1 XPBS at RT	Goat anti-rabbit HRP-conjugate	1:35 000	1	1 X PBS at 30 °C in the dark
FAK	2	1:500	2	1 X PBS at RT	Goat anti-rabbit HRP-conjugate	1:5 000	1	1 X PBS at RT in the dark
Raptor	2.5	1:500	2	2.5 % BSA in TBS-T:TBS (1:1) at RT	Goat anti-rabbit HRP-conjugate	1:5 000	1	TBS: TBS-T (1:1) at RT in the dark

Key: The star (*) symbol indicate conditions performed at room temperature (RT).

2.5. PI3K pathway information for the WHCO series of cell lines obtained from Shaw Ph.D. Thesis (2011)

Table B2: Summary of complimentary PI3K/PKB pathway information obtained from specific inhibition of PI3K with LY294002.

Protein	Cell Line											
	WHCO1		WHCO3		WHCO 5		WHCO6		SNO		MCF-7	
	↑/↓	H/M/L	↑/↓	H/M/L	↑/↓	H/M/L	↑/↓	H/M/L	↑/↓	H/M/L	↑/↓	H/M/L
PTEN	↓	Low	↓	Low	↑	Med	↑	High	↓	Low	↓	Med
p-PKB (Ser473)	↓	Low	↓	Low	↓	Low	↓	Low	↓	Low	↓	High

Key: Low = 0 – 45 %; Medium (Med) = 46 – 75 %; High = 76 – 100 % (and above). Protein expression levels are based on the Hager *et al.*, (2011) classification system for analyses of mTOR and p-RPS6 proteins (Materials and Methodology, Laser densitometry and analysis of relative protein expression). Change in relative marker set protein expression is designated by either positive (↑) or negative (↓) arrows. These data were obtained from the Ph.D. Thesis of Shaw (2011).

Appendix C

3.1. Raw IOD and % IOD data obtained from semi-quantitative densitometric analysis

Table C1: Levels of marker set protein expression during standard tissue culture conditions (Serum +).

Protein	Cell Line											
	WHCO1		WHCO3		WHCO5		WHCO6		SNO		MCF-7	
	IOD	% IOD	IOD	% IOD	IOD	% IOD	IOD	% IOD	IOD	% IOD	IOD	% IOD
mTOR	3294	88	1171	31	3310	88	4387	117	3971	106	3727	100
p-RPS6 (Ser 235/236)	2714	69	2226	56	4882	124	4894	124	362	9	3926	100
mATG-13	1095	142	852	110	191	24	623	80	936	121	770	100
ILK	3815	87	3772	86	4472	101	5638	128	5665	129	4385	100

Table C2: Standard error for levels of marker set protein expression expressed as % IOD) during standard tissue culture conditions (Serum +).

Protein	Cell Line					
	WHCO1	WHCO3	WHCO5	WHCO6	SNO	MCF-7
mTOR	1.70	3.77	1.03	4.80	7.75	0.00
p-RPS6 (Ser 235/236)	41.21	41.35	15.91	17.50	3.41	0.00
mATG-13	27.54	29.40	22.85	34.92	22.29	0.00
ILK	3.41	3.41	23.45	2.24	5.07	0.00

Table C3: Comparison of mTOR and mTORβ protein expression levels during standard tissue culture conditions (Serum +).

Protein	Cell Line													
	WHCO1		WHCO3		WHCO5		WHCO6		SNO		MCF-7		HEK-293	
	IOD	% IOD	IOD	% IOD	IOD	% IOD	IOD	% IOD	IOD	% IOD	IOD	% IOD	IOD	% IOD
mTOR	81	1.3	112	1.8	3430	53	3664	56	3226	50	5373	83	6445	100
mTOR β	272	28	949	100	0.0	0.00	0.0	0.0	0.0	0.0	176	18	190	20

Table C4: Standard error for mTORβ protein expression (expressed as % IOD) during standard tissue culture conditions (Serum +).

Protein	Cell Line						
	WHCO1	WHCO3	WHCO5	WHCO6	SNO	MCF-7	HEK-293
mTOR	0.01	0.59	5.22	0.63	7.83	1.70	0.00
mTORβ	51.17	29.10	0.00	0.00	0.00	30.69	0.00

Table C5: Marker set protein expression from the apoptotic cell (A/C) control.

Protein	Tissue Culture Condition	Cell Line	
		WHCO6	
		IOD	% IOD
mTOR	S+	2159	100
	A/C	651	30
p-RPS6 (Ser 235/236)	S+	7914	100
	A/C	0	0
mATG-13	S+	5996	100
	A/C	1427	24
ILK	S+	4629	100
	A/C	3586	77

Table C6: Protein expression levels of marker set proteins after specific inhibition of PI3K with LY294002.

Protein		Cell Line											
		WHCO1		WHCO3		WHCO5		WHCO6		SNO		MCF-7	
		IOD	% IOD	IOD	% IOD	IOD	% IOD	IOD	% IOD	IOD	% IOD	IOD	% IOD
mTOR	L-	1609	75	155	7	1366	63	2159	100	877	41	3232	150
	L+	2212	102	499	23	2053	95	1806	84	1046	48	5445	252
p-RPS6 (Ser 235/236)	L-	453	6	196	2	3751	47	7914	100	3457	44	2755	35
	L+	225	3	2397	30	856	11	3039	38	212	3	184	2
mATG-13	L-	5062	84	7513	125	4153	69	5996	100	7385	123	10277	171
	L+	4918	82	6408	107	6453	108	5138	86	4792	80	3537	59
ILK	L-	3991	86	2541	55	2410	52	4629	100	7091	153	2667	58
	L+	4151	90	2561	55	3284	71	3642	79	4895	106	3245	70

Table C7: Standard error of marker set protein expression (expressed as % IOD) specific inhibition of PI3K with LY294002.

Protein	Treatment	Cell Line					
		WHCO1	WHCO3	WHCO5	WHCO6	SNO	MCF-7
p-RPS6 (Ser 235/236)	L-	0.92	0.22	1.32	0.00	0.00	0.00
	L+	1.48	3.90	8.57	14.00	0.00	0.00
mATG-13	L-	4.50	0.00	22.66	0.00	18.82	25.16
	L+	1.34	34.45	13.58	3.59	8.63	19.07

Table C8: Protein expression levels of marker set proteins during conditions of serum-free tissue culture (Serum -).

Protein	Cell Line											
		WHCO1		WHCO3		WHCO5		WHCO6		SNO		MCF-7	
		IOD	% IOD	IOD	% IOD	IOD	% IOD	IOD	% IOD	IOD	% IOD	IOD	% IOD
mTOR	S+	3156	98	3546	110	4222	130	3237	100	3993	123	4146	128
	S-	4070	126	680	21	2272	70	1765	55	4492	139	2515	78
p-RPS6 (Ser 235/236)	S+	1818	36	4336	85	4528	89	5075	100	3032	60	3934	78
	S-	1176	23	35	1	3304	65	2050	40	2154	42	2957	58
mATG-13	S+	523	38	3048	224	649	48	1359	100	1003	74	1374	101
	S-	747	55	631	46	353	26	1710	126	1010	74	3484	256
ILK	S+	8103	108	5812	77	7323	98	7508	100	7448	99	6900	92
	S-	6582	88	4170	56	6221	83	6528	87	7583	101	5267	70

Table C9: Standard error for protein expression levels expressed as % IOD) of marker set proteins during serum-free tissue culture (Serum -).

Protein	Tissue Culture Condition	Cell Line					
		WHCO1	WHCO3	WHCO5	WHCO6	SNO	MCF-7
mTOR	S+	8.36	18.21	17.01	0.00	7.24	0.84
	S-	20.73	19.33	14.07	17.28	6.27	2.63
p-RPS6 (Ser 235/236)	S+	1.74	5.82	6.10	0.00	3.44	2.48
	S-	0.25	0.18	3.28	6.01	1.96	5.20
mATG-13	S+	20.44	191.97	17.52	0.00	29.58	0.00
	S-	30.15	20.70	6.20	15.31	30.33	0.00
ILK	S+	18.57	8.26	3.81	0.00	2.42	17.86
	S-	8.79	7.38	15.97	2.23	13.94	7.05

Table C10: Expression levels of marker set proteins after specific inhibition of mTOR with rapamycin.

Protein	Rapamycin Treatment Conditions		Cell Line					
			WHCO6		SNO		MCF-7	
	Time (hr)	Concentration (nM)	IOD	% IOD	IOD	% IOD	IOD	% IOD
mTOR	0	0	2167	100	1694	78	2852	132
	6	20	2924	135	1376	63	2410	111
		50	3543	163	950	44	3173	146
		100	4298	198	1445	67	2983	138
	24	20	1733	80	2141	99	2994	138
		50	2055	95	1227	57	2919	135
		100	2124	98	493	23	2641	122
p-RPS6 (Ser 235/236)	0	0	9768	100	8331	85	8197	84
	6	20	3853	39	3722	38	693	7.00
		50	2898	30	3119	32	115	1.00
		100	1864	19	2593	27	87	1.00
	24	20	1405	14.0	100	1.00	195	2.00
		50	731	7.00	142	1.00	168	2.00
		100	189	2.00	324	3.00	320	3.00
mATG-13	0	0	601	100	934	155	151	25
	6	20	393	65	1200	200	234	39
		50	154	26	1394	232	167	28
		100	717	119	787	131	260	43
	24	20	1018	169	1109	184	161	27
		50	94	16	1309	218	117	19
		100	121	20	575	96	602	100
ILK	0	0	3279	100	3511	107	2734	83
	6	20	2855	87	3883	118	4962	151
		50	2148	66	3653	111	3871	118
		100	1444	44	2936	90	4147	127
	24	20	3143	96	2942	90	4145	126
		50	2812	86	4155	127	3421	104
		100	4173	127	3442	105	7672	234

Table C11: Standard error for mTOR protein expression expressed as % IOD) after specific inhibition of mTOR with rapamycin.

Protein	Rapamycin Treatment Conditions		Cell Line		
	Time (hr)	Concentration (nM)	WHCO6	SNO	MCF-7
mTOR	0	0	0.00	7.23	0.00
	6	20	4.23	22.77	0.00
		50	3.92	7.37	0.00
		100	9.62	9.58	0.00
	24	20	1.20	6.84	0.00
		50	8.58	14.48	0.00
		100	9.05	7.60	0.00

Table C12: Protein expression levels of marker set proteins after specific p90RSK inhibition with BI-D1870

Protein	Treatment	Cell Line									
		WHCO5		WHCO6		SNO		MCF-7		HEK-293	
		IOD	% IOD	IOD	% IOD	IOD	% IOD	IOD	% IOD	IOD	% IOD
mTOR	U	970	54	1808	100	1595	88	1342	74	3699	205
	DMSO	1167	65	1850	102	1584	88	1489	82	2270	126
	BI	948	52	1301	72	1237	68	1509	83	2501	138
p-RPS6 (Ser 235/236)	U	3919	46	8439	100	59	58	64	64	5276	84
	DMSO	5997	71	75	75	67	67	50	49	6730	108
	BI	5712	67	65	65	85	85	50	50	2264	36

Table C13: Standard error for key protein intermediates (expressed as % IOD) after specific p90RSK inhibition with BI-D1870

Protein	Treatment	Cell Line	
		WHCO5	HEK-293
mTOR	U	11.21	47.79
	DMSO	2.59	21.70
	BI	23.48	55.43
p-RPS6 (Ser 235/236)	U	5.81	0.00
	DMSO	13.79	0.00
	BI	6.28	0.00

Table C14: Protein expression levels of marker set proteins after growth of HOSCC cells on fibronectin (FN) or collagen (CN).

Protein		Cell Line											
		WHCO1		WHCO3		WHCO5		WHCO6		SNO		MCF-7	
		IOD	% IOD	IOD	% IOD	IOD	% IOD	IOD	% IOD	IOD	% IOD	IOD	% IOD
mTOR	U	541	37	91	6	902	61	1471	100	427	29	105	4
	FN	1032	70	125	8	110	7	1539	105	578	39	817	28
	CN	2251	153	148	10	159	11	81	5	1291	88	288	10
p-RPS6 (Ser 235/236)	U	9195	110	3726	45	3933	47	8353	100	6263	75	8194	98
	FN	8706	104	4189	50	1580	19	10584	127	11156	134	8423	101
	CN	9149	110	5034	60	1646	20	1761	21	10967	131	9118	109

Table C15: Standard error for marker set proteins (expressed as % IOD) after growth of HOSCC cells on fibronectin (FN) or collagen (CN).

Protein		Cell Line					
		WHCO1	WHCO3	WHCO5	WHCO6	SNO	MCF-7
mTOR	U	8.46	0.48	13.43	0.00	0.71	1.19
	FN	18.45	0.67	0.71	7.86	8.87	9.26
	CN	16.31	0.58	0.31	0.86	6.98	3.27
p-RPS6 (Ser 235/236)	U	7.59	1.21	13.22	0.00	3.09	18.37
	FN	8.57	3.10	5.48	2.36	0.90	9.59
	CN	3.02	4.16	5.47	6.19	11.53	2.83

Table C16: Protein expression levels for marker set proteins after combination treatment with fibronectin (FN) and PI3K-specific inhibition LY294002.

Protein	Treatment	Cell Line							
		WHCO 5		WHCO6		SNO		MCF-7	
		IOD	% IOD	IOD	% IOD	IOD	% IOD	IOD	% IOD
mTOR	U	509	60	849	100	334	39	542	64
	FN	713	84	967	114	768	90	553	65
	L+	687	81	129	15	962	113	536	63
	FN & L+	526	62	202	24	489	58	367	43
p-RPS6 (Ser 235/236)	U	2346	71	3319	100	3551	107	2578	78
	FN	3564	107	3454	104	2588	78	3330	100
	L+	1466	44	1644	50	2035	61	876	26
	FN & L+	2134	64	1873	56	2564	77	1018	31

Table C17: Standard error of marker set protein expression (expressed as % IOD) after combination treatment with fibronectin (FN) and PI3K-specific inhibition LY294002.

Protein	Treatment	Cell Line			
		WHCO 5	WHCO 6	SNO	MCF-7
mTOR	U	0.32	0.00	9.36	13.61
	FN	8.91	35.38	23.19	12.18
	L+	25.47	1.98	20.47	12.48
	FN & L+	13.12	2.51	8.55	7.45
p-RPS6 (Ser 235/236)	U	2.95	0.00	15.80	7.38
	FN	15.62	3.77	11.13	13.75
	L+	7.54	2.43	8.55	3.45
	FN & L+	12.51	5.27	10.97	4.51

APPENDIX D

4.1. Statistical analysis of protein expression levels obtained from semi-quantitative densitometry.

Table D1: Student's t-test analysis of the difference in protein expression between cells of the WHCO series and the MCF-7 cell line obtained under standard tissue culture conditions (Serum +).

i)	WHCO1			WHCO3			WHCO5			WHCO6			SNO			MCF-7		
Protein	**Mean**	**SD**	**SEM**	**Mean**	**SD**	**SEM**	**Mean**	**SD**	**SEM**	**Mean**	**SD**	**SEM**	**Mean**	**SD**	**SEM**	**Mean**	**SD**	**SEM**
mTOR	3294.5	727.5	420.0	1171.6	262.2	151.4	3310.9	121.0	69.9	4387.0	0.0	0.0	3971.2	1468.0	847.5	3727.5	899.9	519.6
p-RPS6 (Ser 235/236)	2714.4	2774.0	1961.5	2226.2	2686.4	1899.5	4882.0	84.5	59.7	4894.2	0.0	0.0	362.1	256.0	181.0	3926.5	764.9	540.8
mATG-13	1095.4	1374.1	971.6	852.5	1097.1	775.7	52.853	31.4	22.2	623.5	0.0	0.0	936.0	1012.2	715.7	770.8	899.5	636.1
ILK	3815.5	344.9	199.1	3772.3	2579.2	1489.1	4472.1	2215.8	1279.2	5638.7	0.0	0.0	5665.9	507.4	292.9	4385.8	130.2	75.1

ii)	WHCO1		WHCO3		WHCO5		WHCO6		SNO		MCF-7	
Protein	**t-statistic**	**p value**	**t-statistic**	**p value**	**t-statistic**	**p value**	**t-statistic**	**p value**	**t-statistic**	**p value**	**t-statistic**	**p value**
mTOR	-0.648	0.552	-4.723	0.009	-0.794	0.471	1.269	0.273	0.245	0.818	N.A.	N.A.
p-RPS6 (Ser 235/236)	-0.596	0.612	-0.861	0.480	1.756	0.221	1.789	0.215	-6.249	0.0247	N.A.	N.A.
mATG-13	0.279	0.806	0.0814	0.943	-8.832	0.0126	-0.232	0.838	0.172	0.879	N.A.	N.A.
ILK	2.679	0.0553	-0.411	0.702	0.0673	0.950	16.660	< 0.001	4.232	0.0133	N.A.	N.A.

* Indicates significant difference ($p < 0.05$).

Table D2: Student's t-test analysis comparing mTORβ protein expression under standard tissue culture conditions (Serum +).

i)	WHCO1			WHCO3			MCF-7			HEK-293		
Protein	**Mean**	**SD**	**SEM**	**Mean**	**SD**	**SEM**	**Mean**	**SD**	**SEM**	**Mean**	**SD**	**SEM**
mTORβ	272.1	63.1	44.6	949.0	701.09	495.7	176.1	30.5	21.5	190.8	107.9	76.3

ii)	WHCO1		WHCO3		MCF-7		HEK-293	
Protein	**t-statistic**	**p value**	**t-statistic**	**p value**	**t-statistic**	**p value**	**t-statistic**	**p value**
mTORβ	0.919	0.455	1.512	0.135	-0.185	0.435	N.A.	N.A.

* Indicates significant difference ($p < 0.05$).

Table D3: Paired t-test analysis on the difference in marker set protein expression during conditions of serum withdrawal for 24 hours (Serum -).

i) mTOR	WHCO1		WHCO3		WHCO5		WHCO6		SNO		MCF-7	
	S+	S-	S+	S-	S+	S-	S+	S-	S+	S-	S+	S-
Mean	3156.8	4070.3	3546.0	53.167	4222.7	2272.7	3237.4	1765.6	3993.0	4492.4	4146.4	2515.4
SD	468.8	1445.4	4373.0	3.650	2102.5	788.7	0.0	1220.0	405.6	351.5	1582.2	1922.9
SEM	270.6	834.5	2524.8	2.107	1213.8	455.3	0.0	704.3	234.2	202.9	913.5	1110.1

ii) p-RPS6 (Ser 235/236)	WHCO1		WHCO3		WHCO5		WHCO6		SNO		MCF-7	
	S+	S-	S+	S-	S+	S-	S+	S-	S+	S-	S+	S-
Mean	1818.1	1176.3	4335.7	34.7	4527.5	3303.7	5075.0	2050.4	3031.7	2154.3	3933.6	2957.1
SD	2670.0	1887.9	974.0	15.8	1056.2	288.7	0.0	394.3	1924.5	1836.8	157.6	678.0
SEM	1541.5	1090.0	562.3	9.1	609.8	166.7	0.0	227.6	1111.1	1060.5	91.0	391.4

iii) mATG-13	WHCO1		WHCO3		WHCO5		WHCO6		SNO		MCF-7	
	S+	S-	S+	S-	S+	S-	S+	S-	S-	S+	S-	S+
Mean	522.5	746.6	5048.1	630.7	649.0	352.9	1358.7	1709.8	1002.5	1010.4	6976.9	180.7
SD	392.8	579.3	860.3	397.7	336.5	119.1	0.0	294.1	568.3	582.8	340.6	72.7
SEM	277.7	409.6	608.3	281.2	237.9	84.2	0.0	207.9	401.9	412.1	240.8	51.4

iv) ILK	WHCO1		WHCO3		WHCO5		WHCO6		SNO		MCF-7	
	S+	S-	S+	S-	S+	S-	S+	S-	S+	S-	S+	S-
Mean	8102.7	6581.5	5812.3	4170.1	7322.9	6221.2	7507.8	6528.3	7448.4	7583.4	6899.9	5267.2
SD	2768.0	1072.3	854.0	779.9	2945.9	1971.6	312.3	471.3	0.0	1764.2	3767.3	2898.4
SEM	1598.1	619.1	493.0	450.2	1700.8	1138.3	180.3	272.1	0.0	1018.5	2175.0	1673.4

v)	Table D3 continued											
Protein	**Cell Line**											
	WHCO1		**WHCO3**		**WHCO5**		**WHCO6**		**SNO**		**MCF-7**	
	t-statistic	**p value**	**t-statistic**	**p value**	**t-statistic**	**p value**	**t-statistic**	**P value**	**t-statistic**	**p value**	**t-statistic**	**p value**
mTOR	-0.960	0.438	11.382	0.030	1.214	0.349	2.090	0.172	-7.159	0.0190	0.936	0.448
p-RPS6 (Ser 235/236)	1.418	0.292	7.555	0.0171	2.626	0.120	13.284	0.005	5.307	0.0337	2.272	0.151
mATG-13	-1.700	0.339	13.505	0.0471	1.925	0.305	-1.689	0.340	-0.766	0.584	23.252	0.0274
ILK	1.425	0.290	13.883	0.005	0.753	0.530	6.234	0.024	-0.133	0.907	2.709	0.114

* Indicates significant difference ($p < 0.05$).

Table D4: Paired t-test analysis on the extent fibronectin (FN)- or collagen (CN)-coated substrates effect marker set protein expression.

i)	WHCO1			WHCO3			WHCO5			WHCO6			SNO			MCF-7		
mTOR	**U**	**FN**	**CN**	**U**	**FN**	**CN**	**U**	**FN**	**CN**	**U**	**FN**	**CN**	**U**	**FN**	**CN**	**U**	**FN**	**CN**
Mean	541	1032	2970	91.2	124	147	902.3	109	158	1470	1538	80.6	427.1	578.4	1291.4	N.A.	N.A.	N.A.
SD	528	1150	0.0	29.7	41.7	36.1	837.6	44.5	19.3	0.0	490.5	53.6	44.3	553.4	435.3	N.A.	N.A.	N.A.
SEM	373	813	0.0	21.0	29.4	25.5	592.2	31.4	13.6	0.0	346.8	37.9	31.3	391.3	307.8	N.A.	N.A.	N.A.

ii)	WHCO1			WHCO3			WHCO5			WHCO6			SNO			MCF-7		
p-RPS6 (Ser 235/236)	**U**	**FN**	**CN**	**U**	**FN**	**CN**	**U**	**FN**	**CN**	**U**	**FN**	**CN**	**U**	**FN**	**CN**	**U**	**FN**	**CN**
Mean	9195	8705	9148	3725.8	4188	5034	3933.0	1580	1645	8353.2	10584	1760	6263.2	11155	10967.2	8194	8423	9117
SD	2689	3035	1071	427.1	1098	1473	4685.4	1943	1937	0.0	835.5	2193	1095.6	317.2	4086.7	6511	3399	1001
SEM	1902	2146	757.5	302.0	776	1042	3313.1	1373	1370	0.0	590.8	1550	774.7	224.3	2889.7	4604	2403	708.0

iii)	WHCO1		WHCO3		WHCO5		WHCO6		SNO		MCF-7	
FN	**t-statistic**	**p value**	**t-statistic**	**p value**	**t-statistic**	**p value**	**t-statistic**	**p value**	**t-statistic**	**p value**	**t-statistic**	**p value**
mTOR	-1.115	0.466	-3.991	0.156	1.413	0.392	-0.197	0.876	-0.420	0.747	N.A.	N.A.
p-RPS6	2.005	0.295	-0.975	0.508	1.213	0.439	-3.776	0.165	-8.889	0.0357	-0.104	0.934

iv)	WHCO1		WHCO3		WHCO5		WHCO6		SNO		MCF-7	
CN	**t-statistic**	**p value**	**t-statistic**	**p value**	**t-statistic**	**p value**	**t-statistic**	**p value**	**t-statistic**	**p value**	**t-statistic**	**p value**
mTOR	-6.507	0.0485	-1.213	0.439	1.227	0.435	-6.507	0.0485	-1.213	0.439	1.227	0.435
p-RPS6	0.0407	0.974	-1.768	0.328	1.177	0.448	0.0407	0.974	-1.768	0.328	1.177	0.448

* Indicates significant difference ($p < 0.05$).

Table D5: Paired t-test analysis of mTOR and p-RPS6$^{(Ser\ 235/236)}$ protein expression in response to combined Fibronectin (FN) stimulation and PI3K-specific inhibition with LY294002.

I)	WHCO5				WHCO6				SNO				MCF-7			
mTOR	**U**	**FN**	**L+**	**FN & L+**	**U**	**FN**	**L+**	**FN & L+**	**U**	**FN**	**L+**	**FN & L+**	**U**	**FN**	**L+**	**FN & L+**
Mean	509.0	712.8	188.9	270.6	849.2	967.4	128.5	201.6	333.9	767.8	961.7	488.6	542.3	552.8	535.6	366.7
SD	10.9	302.8	102.3	82.7	0.0	1201.8	67.4	85.1	318.0	787.7	695.2	290.5	462.4	413.7	424.0	253.2
SEM	7.7	214.1	72.3	58.4	0.0	849.8	47.6	60.1	159.0	393.8	347.6	145.2	266.9	238.9	244.8	146.1

ii)	WHCO5				WHCO6				SNO				MCF-7			
p-RPS6 (Ser 235/236)	**U**	**FN**	**L+**	**FN & L+**	**U**	**FN**	**L+**	**FN & L+**	**U**	**FN**	**L+**	**FN & L+**	**U**	**FN**	**L+**	**FN & L+**
Mean	2345.9	2432.2	1034.9	1439.5	3318.5	8073.8	1644.0	1872.9	2393.9	2587.5	1382.9	1741.4	2577.9	2293.3	613.8	698.2
SD	391.9	2073.2	1000.5	1659.9	0.0	8010.4	322.0	699.2	2097.7	1477.2	1135.5	1456.3	979.4	1825.4	458.1	598.2
SEM	226.2	1196.9	577.6	958.3	0.0	4624.8	185.9	403.7	1211.1	852.9	655.6	840.8	565.4	1053.9	264.4	345.3

iii)	WHCO5		WHCO6		SNO		MCF-7	
	t-statistic	**p value**	**t-statistic**	**p value**	**t-statistic**	**p value**	**t-statistic**	**p value**
FN	-0.919	0.527	-0.139	0.912	-1.181	0.323	-0.0826	0.942
L+	3.998	0.156	15.121	0.0420	-1.815	0.167	0.0493	0.965
FN & L+	3.601	0.172	10.759	0.0295	-0.662	0.555	1.402	0.296

iv)	WHCO5		WHCO6		SNO		MCF-7	
	t-statistic	**p value**	**t-statistic**	**p value**	**t-statistic**	**p value**	**t-statistic**	**p value**
FN	-0.0862	0.939	-1.028	0.412	-0.518	0.656	0.485	0.676
L+	2.808	0.107	9.004	0.0121	1.735	0.225	5.581	0.0306
FN & L+	1.080	0.393	3.581	0.0350	1.037	0.409	7.824	0.0159

* Indicates significant difference ($p < 0.05$).

Plagarism analysis by Turnitin Orginality Report Software

Analysis Settings and Procedure:
Turnitin software analyses a string of 20 words with a database comprising of scientific journal articles, peer-reviewed publications and internet-based sources for a specified degree of similarity. During this analysis, a string of twenty (20) words were selected and the overall similarity could not exceed 15 %.

Sumbitted File:
Ari_Nerwich_0604379w_Turn It In Document_Ari Nerwich_MSc_Sep 2012.docx by Ari Nerwich
From MSc Dissertation 2012B (MCB Masters)
Processed on 28-Sep-2012 12:31 PM SAST
ID: 271156785
Word Count: 24624

The above submission included the following sections: abstract, introduction, results and discussion, but excluded figure legends and references in order to minimize the detection of false-positive hits. See next page for an example of the results using the Document Viewer.

Findings:

A. Similarity:

   Overall Similarity Index (OSI): 4%

B. Similarity by Source:
   1. Internet Sources: 1 %
   2. Publications: 3 %
   3. Student Papers: 0 %

A full report of this MSc is available through the following link:
https://api.turnitin.com/dv?s=1&o=271156785&u=1012947287&student_user=1&lang=en_us&session-id=5a45d4d0f2acfce7bb579eb37efa3aaa

Outcome
Acceptable level of source similarity was found in the submitted document (OSI = 4 %). Kindly see an example of the report, which can be found on the next page.

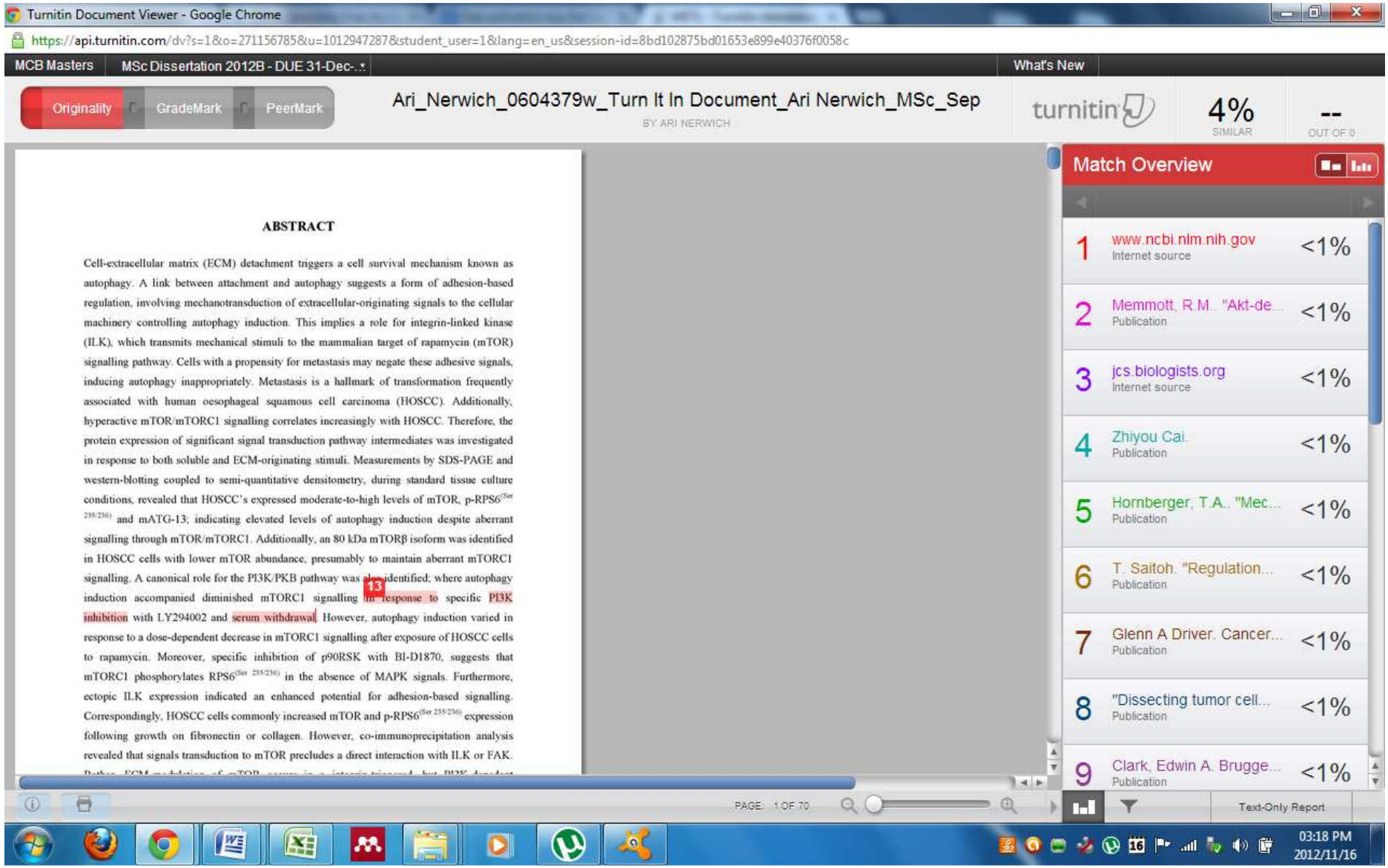
Turnitin Document Viewer - Google Chrome
https://api.turnitin.com/dv?s=1&o=271156785&u=1012947287&student_user=1&lang=en_us&session-id=8bd102875bd01653e899e40376f0058c
MCB Masters
MSc Dissertation 2012B - DUE 31-Dec-...
What's New
Originality
GradeMark
PeerMark
Ari_Nerwich_0604379w_Turn It In Document_Ari Nerwich_MSc_Sep
BY ARI NERWICH
turnitin
4%
SIMILAR
--
OUT OF 0
ABSTRACT
Cell-extracellular matrix (ECM) detachment triggers a cell survival mechanism known as autophagy. A link between attachment and autophagy suggests a form of adhesion-based regulation, involving mechanotransduction of extracellular-originating signals to the cellular machinery controlling autophagy induction. This implies a role for integrin-linked kinase (ILK), which transmits mechanical stimuli to the mammalian target of rapamycin (mTOR) signalling pathway. Cells with a propensity for metastasis may negate these adhesive signals, inducing autophagy inappropriately. Metastasis is a hallmark of transformation frequently associated with human oesophageal squamous cell carcinoma (HOSCC). Additionally, hyperactive mTOR/mTORC1 signalling correlates increasingly with HOSCC. Therefore, the protein expression of significant signal transduction pathway intermediates was investigated in response to both soluble and ECM-originating stimuli. Measurements by SDS-PAGE and western-blotting coupled to semi-quantitative densitometry, during standard tissue culture conditions, revealed that HOSCC's expressed moderate-to-high levels of mTOR, p-RPS6(Ser 235/236) and mATG-13; indicating elevated levels of autophagy induction despite aberrant signalling through mTOR/mTORC1. Additionally, an 80 kDa mTORβ isoform was identified in HOSCC cells with lower mTOR abundance, presumably to maintain aberrant mTORC1 signalling. A canonical role for the PI3K/PKB pathway was also identified; where autophagy induction accompanied diminished mTORC1 signalling in response to specific PI3K inhibition with LY294002 and serum withdrawal. However, autophagy induction varied in response to a dose-dependent decrease in mTORC1 signalling after exposure of HOSCC cells to rapamycin. Moreover, specific inhibition of p90RSK with BI-D1870, suggests that mTORC1 phosphorylates RPS6(Ser 235/236) in the absence of MAPK signals. Furthermore, ectopic ILK expression indicated an enhanced potential for adhesion-based signalling. Correspondingly, HOSCC cells commonly increased mTOR and p-RPS6(Ser 235/236) expression following growth on fibronectin or collagen. However, co-immunoprecipitation analysis revealed that signals transduction to mTOR precludes a direct interaction with ILK or FAK.
Match Overview
1 www.ncbi.nlm.nih.gov Internet source <1%
2 Memmott, R.M.. "Akt-de... Publication <1%
3 jcs.biologists.org Internet source <1%
4 Zhiyou Cai. Publication <1%
5 Hornberger, T.A.. "Mec... Publication <1%
6 T. Saitoh. "Regulation... Publication <1%
7 Glenn A Driver. Cancer... Publication <1%
8 "Dissecting tumor cell... Publication <1%
9 Clark, Edwin A. Brugge... Publication <1%
PAGE: 1 OF 70
Text-Only Report
03:18 PM
2012/11/16